An Investigation into Vibration Based Techniques for Wind Turbine Blades Condition Monitoring

Abdelnasser Abouzid Abouhnik

A thesis submitted in partial fulfilment of the requirements of the Manchester Metropolitan University for the degree of Doctor of Philosophy

Faculty of Science and Engineering
Manchester Metropolitan University
December 2012

Abstract

The rapid expansion of wind power has been accompanied by reported reliability problems and the aim is to provide a means of increasing wind turbine reliability, prevent break downs, increase availability and reduce maintenance costs and power outages.

This research work reports the development of condition monitoring (CM) for early fault detection in wind turbine blades based on vibration measurements. The research started with a background and a survey of methods used for monitoring wind turbines. Then, finite element modelling (FEM) of three bladed horizontal axis wind turbine (HAWT) was developed to understand the nature and mechanism of the induced vibration. A HAWT test rig was constructed and equipped with computerised vibration measuring system for model verification. Statistical and spectral processing parameters then were used to analyse vibration signals that collected in healthy and faulty cases. Results obtained using time and frequency based techniques are not suitable for extracting blades condition related information.

Consequently, empirical mode decomposition method (EMD), principal component analysis method (PCA) and continuous wavelet transform (CWT) are applied for extraction blade condition related features from the measured vibration. The result showed that although these methods generally proved their success in other fields, they have failed to detect small faults or changes in blade structure.

Therefore, new techniques were developed using the above mentioned methods combined with feature intensity level (FIL) and crest factor. Namely, those are EDFIL, RMPCA and wavelet based FIL. The new techniques are found to be reliable, robust and sensitive to the severity of faults.

Those analysis techniques are suitable to be the detection tool for an integrated wind turbine condition monitoring system. Directions for future work are also given at the end of the thesis.

Table of Contents

Abstract II
List of figures VII
List of Tables X
Nomenclature XI
Declaration XIII
Acknowledgements XIV
List of publications: XV
Chapter 1 Introduction 1
1.1 Wind Turbines Background and classification 2
1.2 Condition Monitoring Overview 7
1.3 Problems Setting and Goal of the Study 8
1.3.1 Wind Turbines Failure Modes 8
1.4 Rotating Machinery Conditioning Monitoring Techniques 13
1.4.1 Vibration Analysis 13
1.4.2 Oil Analysis 15
1.4.3 Thermography 17
1.4.4 Physical Condition of Materials 18
1.4.5 Strain Measurement 18
1.4.6 Acoustic Monitoring 18
1.4.7 Electrical Effects 19
1.4.8 Process Parameters 20
1.4.9 Visual Inspection 20
1.4.10 Performance Monitoring 21
1.5 Research Aim and Objectives 21
1.5.1 Aims 21
1.5.2 Objectives 21
1.6 Outline of Thesis 22
Chapter 2 Literature Review 25
2.1 Introduction 26
2.1.1 Blade Failure Modes 29
2.2 Condition Monitoring Technologies 30

2.3 Signal Processing Techniques 42
2.4 Summary 52
Chapter 3 Dynamic Model of Horizontal Axis Wind Turbine 55
3.1 Introduction 56
3.2 Airfoil Characteristics and Blade Design Aspect 57
3.2.1 Blade Shape 57
3.2.2 Lift and Drag and Moment Coefficients 59
3.2.3 Reynolds Number 60
3.2.4 Reading Airfoil Data Charts 61
3.3 Modelling in 3D with Software Packages 64
3.3.1 The Principle Theories Relevant to Modelling 64
3.3.2 Finite Element Method (FEM) 65
3.4 Three-dimensional Wind Turbine Modelling 66
3.4.1 Blade Design 66
3.4.2 Hub Design 68
3.4.3 Helical Gears Design 68
3.4.4 Bearings Design 71
3.4.5 Shaft Design 73
3.5 Vibration Analysis by Finite Element Package ANSYS 76
3.5.1 Modal Analysis 76
3.6 Execution of Computations 77
3.7 Mode Shape Identification 78
3.8 General Trends in Response 78
3.8.1 Healthy Natural Frequency Results 78
3.8.2 Overall Wind Turbine Vibration Simulation 83
3.9 Summary 84
Chapter 4 Experimental Set-up and Fault Simulation 86
4.1 Introduction 87
4.2 Test-Rig Suitability 87
4.3 Design and Fabrication of Wind Turbine Test Rig 88
4.4 Test Rig Safety Precautions 91
4.5 Fault Simulation 91
4.5.1 Piezoelectric Accelerometer 92

4.5.2 Accelerometer Theory 93
4.5.3 Accelerometer Mounting Techniques 95
4.5.4 Sources of Error with Piezoelectric Accelerometers 97
4.6 Charge Amplifier 98
4.7 Data Acquisition System 98
4.8 Processing and Analysing Software 100
4.9 Experimental Procedure 100
Chapter 5 Fundamental Characteristics of Wind Turbine Vibration 101
5.1 Introduction 102
5.2 Time Domain Overview 102
5.2.1 Statistical Parameters: 104
5.3 Frequency Domain Overview 107
5.3.1 Spectrum Analysis 108
5.3.2 Performance of Conventional Techniques on Simulation Vibration Signals 109
5.3.3 Time Domain based Analysis of Vibration Signals 109
5.3.4 Performance of fast Fourier Transform on Experimental Vibration Signals 113
5.4 Summary 119
Chapter 6 Condition Features Extraction Using Empirical Mode Decomposition 120
6.1 Introduction 121
6.2 Modified Hilbert Huang Technique 122
6.3 Empirical Mode Decomposition Description 122
6.4 Empirical Mode Decomposition to obtain IMFs 123
6.5 Numerical Simulation Signal: 126
6.6 The Performance of EMD on Simulation and Experimental Vibration Data 130
6.7 Proposed Novel Condition Index 135
6.8 Validation of the EDFIL: 137
6.9 Summary 138
Chapter 7 Wind Turbine Vibration Analysis Using a Wavelet Technique 140
7.1 Introduction 141
7.1.1 Continuous Wavelet Transforms (CWT) 141
7.1.2 Selection of Analysing Wavelet 143
7.1.3 Properties of the Wavelet Transform 144
7.2 Performance of CWT Method in Detection of Wind Turbine Blade Crack 145

7.3 Summary 150
Chapter 8 Principal Component Analysis Techniques for Signal Enhancement 152
8.1 Introduction 153
8.2 Principal Component Analysis 154
8.3 Implementation of PCA using Single Value Decomposition 157
8.4 Fault Detection Based on the PCA Model – Q and T^2 -Statistics 159
8.5 Performance of PCA Method in Detection of a Wind Turbine Blade Crack 160
8.6 Derivation of Novel Condition Index Based on PCA 164
8.7 Performance of Proposed Method (RMPCA) 166
8.8 Summary 168
Chapter 9 Contribution to Knowledge, Achievements, Conclusions and Future Work 169
9.1 Introduction 170
9.2 Overview of Objectives and Achievements 170
9.3 Contribution to Knowledge 174
9.3.1 Wind Turbine Modelling: 174
9.3.2 The performance of Basic Signal Processing Techniques: 175
9.3.3 The Performance of Empirical Mode Decomposition (EMD) 175
9.3.4 The Performance of Continuous Wavelet Transform (CWT): 176
9.3.5 The Performance of Principle Components Analysis Method (PCA): 176
9.4 Conclusion 176
9.5 Future Work 177
9.5.1 Test Rig Improvement 177
9.5.2 Monitoring Techniques 177
9.5.3 Theoretical Research 178

List of figures

Figure 1.1 Global annual installed wind capacity 1996-2011 5
Figure 1.2 Horizontal Axis Wind turbine (HAWT) 6
Figure 1.3 Vertical Axis Wind turbine (VAWT) (Darrieus design) 6
Figure 1.4 Failures of wind turbine at Swedish power plants during 2000-2004 12
Figure 1.5 Percentage of wind turbine downtime at Swedish power plants during 2000-2004 12
Figure 2.1 Diagram of the floor-mounted fixture used by the infrared camera 34
Figure 2.2 Blade model with damage 35
Figure 3.1 Airfoil geometric parameters 58
Figure 3.2 Profile for NACA 2412 62
Figure 3.3 Lift and Moment coefficients vs. angle of attack at varying Re values 62
Figure 3.4 Lift coefficient vs. Drag coefficient at varying Re values 63
Figure 3.5 Final blade design 67
Figure 3.6 Hub model in SolidWorks 68
Figure 3.7 Nomenclature of helical gear 69
Figure 3.8 Input gear 70
Figure 3.9 Output gear 70
Figure 3.10 Physical parameters of input bearing 72
Figure 3.11 Input bearing 72
Figure 3.12 Output bearing 73
Figure 3.13 Low speed shaft 74
Figure 3.14 High speed shaft 74
Figure 3.15 Wind turbine assembly in SolidWorks 75
Figure 3.16: A 3D finite element model of blade 77
Figure 3.17 The first mode shape 1 at 31.458 Hz 80
Figure 3.18 First mode shape of multi-blades at 34.95 Hz 81
Figure 3.19 Simulated vibration signal for healthy system 83
Figure 3.20 Time domain of simulated healthy vibration signal. 84
Figure 4.1 Wind turbine test rig in MMU Mechanical Engineering Laboratory 90
Figure 4.2 Schematic diagram of the wind turbine monitoring system 90
Figure 4.3 Simulated local faults on one blade 92
Figure 4.4 Schematic of an accelerometer mounted on a structure 93

Figure 4.5 Accelerometer mounting techniques and their effects on the frequency response function 96
Figure 4.6 Proper mounting of accelerometer cable 97
Figure 4.7 Data acquisition card 99
Figure 5.1 Time-domain vibration profile for healthy wind turbine 104
Figure 5.2 Magnitude of Kurtosis; a) simulation signal, b) experimental signal 110
Figure 5.3 Magnitude of RMS; a) simulation signal, b) experimental signal 110
Figure 5.4 Magnitude of Crest Factor; a) simulation signal, b) experimental signal 111
Figure 5.5 Magnitude of Skewness; a) simulation signal, b) experimental signal 111
Figure 5.6 Magnitude of Standard Deviation; a) simulation signal, b) experimental signal 112
Figure 5.7 Frequency- domain for simulation and experimental vibration signatures for healthy wind turbine 114
Figure 5.8 FFT for healthy and faulty simulation signals at 150r/min; 116
Figure 5.9 FFT for healthy and faulty experimental signals at 150r/min; 116
Figure 5.10 FFT for healthy and faulty simulation signals at 250r/min; 117
Figure 5.11 FFT for healthy and faulty experimental signals at 250r/min; 117
Figure 5.12 FFT for healthy and faulty simulation signals at 360r/min; 118
Figure 5.13 FFT for healthy and faulty experimental signals at 360r/min. 118
Figure 6.1 Flowchart of Empirical Mode Decomposition Algorithm [134] 125
Figure 6.2. Five sinusoidal signals; 127
Figure 6.3. The IMFs of Equation 6.9 128
Figure 6.4. Fast Fourier Transforms for IMFs shown in Figure 6.3 129
Figure 6.5 Decomposition of experimental vibration signals for healthy signal 131
Figure 6.6 Decomposition of experimental vibration signals for healthy signal 131
Figure 6.7 Decomposition of experimental vibration signals for healthy signal 132
Figure 6.8 Fast Fourier transform is applied on each (IMF) at speed 150 r/min 133
Figure 6.9 Fast Fourier transform is applied on each (IMF) at speed 250 r/min 134
Figure 6.10 Fast Fourier transform is applied on each (IMF) at speed 360 r/min 134
Figure 6.11 Flowchart of the proposed method EDFIL 136
Figure 6.12 Normalized Feature intensity level contained in simulation signals 137
Figure 6.13 Normalized Feature intensity levels of experimental signals 138
Figure 7.1CWT contour plot for healthy and cracked wind turbine blade. 146
Figure 7.2 CWT contour plot for healthy and cracked wind turbine blade. 147

Figure 7.3 CWT contour plot for healthy and cracked wind turbine blade. 148
Figure 7.4 Normalized energy at rotational speed 150 r/min 149
Figure 7.5 Normalized energy at rotational speed 250 r/min 149
Figure 7.6 Normalized energy at rotational speed 360 r/min 150
Figure 8.1 Principal components in three dimensions 156
Figure 8.2 Eigenvalues for healthy and blade with seeded cracks. 161
Figure 8.3 Score plot for healthy and faulty blade for the first PC 162
Figure 8.4 Residual error plot for healthy and faulty blade. 163
Figure 8.5 Illustration of the RMPCA based proposed technique 165
Figure 8.6 Crest Factor for healthy and faulty turbine blade at 150 r/min. 166
Figure 8.7 Crest Factor for healthy and faulty turbine blade at 250 r/min. 167
Figure 8.8 Crest Factor for healthy and faulty turbine blade at 360 r/min. 167

List of Tables

Table 3.1 NACA 2412 Results for incompressible potential flow (Aerofoil Investigation Database, 2012) 63
Table 3.2 NACA 2412 Airfoil properties in fractions of chord length 63
Table 3.3 the blade angle and chord width values 66
Table 3.4 Equations used in calculating the maximum bending stress for gears 69
Table 3.5 Bearing specifications 71
Table 3.6: Five mode shapes with corresponding natural frequency 78
Table 3.7: Three main mode shapes with natural frequencies 80
Table 3.8 : Natural frequency of first multi-blade mode shape 82
Table 3.9: First mode single blade, natural frequency for healthy blade and blade with four seeded cracks. 82
Table 4.1 Basic dimensions of wind turbine 91
Table 5.1 Values of statistical parameters for healthy and four faulty turbines 113

Nomenclature

Global Wind Energy Council	GWEC
Horizontal Axis Wind turbine	HAWT
Vertical Axis Wind turbine	VAWT
condition monitoring system	CMS
Gauge factor	GF
Acoustic Emission	AE
Non-destructive examination	NDE
Machine Current Signature Analysis	MCSA
Finite element method	FEM
Wigner-Ville Distribution	WVD
continuous wavelet transforms	CWT
Empirical mode decomposition	EMD
Principle component analysis	PCA
Computational Fluid Dynamics method	CFD
National Advisory Committee for Aeronautics	NACA
Condition based maintenance	CBM
Glass fibre reinforced plastic	GFRP
Secondary longitudinal surface acoustic waves	LSAW II
Resonant comparison	RC
Wave propagation methods	WP
Transmittance function	TF
Operational deflection shape	ODS
Scanning laser Doppler micrometer	SLDV
Back propagation neural network	BPNN
Support vector machine	SVM
Fibre Bragg Grating	FBG
Independent Component Analysis	ICA
Crest Factor	CF
Kurtosis	Ku
Root mean square	RMS
Skewness	Sk
kernel principal component analysis	KPCA
Fast Fourier Transform	FFT
Short-Time Fourier Transform	STFT
Singular value decomposition	SVD
Pseudo Wigner-Ville transform	PWVT
Hilbert-Huang transform	HHT
Auto Term Window	ATW
Discrete wavelet transforms	DWT
Bivariate Empirical Mode Decomposition	BEMD
Ensemble empirical mode decomposition	EEMD
Intrinsic mode function	IMF

Instantaneous power spectrum	IPS
Milti-resolution Fourier Transform	MFT
Empirically decomposed feature intensity level	EDFIL
Residual matrix of principal component analysis	RMPCA
Tips speed ratio	TSR
Reynolds numbers	Re
Finite Difference Method	FDM
Finite Volume Method	FVM
Analogue-to-digital converter	ADC
Data acquisition system	DAS
Data acquisition card	DAQ
Standard deviation	*SD*
Noise ratio	S/N
Blade pass frequencies	BPF
Wavelet transform	WT
Digital Fourier Transform	DFT

Declaration

No portion of the work referred in this thesis has been submitted in support of an application for another degree or qualification at this, or any other university, or institute of learning

Date: _____

Signed: _____

Acknowledgements

In these moments I would like to acknowledge the help many of people, and government organizations. I would like to express my gratitude to those people who supported me during doing this research;

First of all, extremely grateful to my director of studies Dr. Alhussein Albarbar for his guidance and continuous support.

Special thanks for my wife and my children, for selflessly gave me their support to get this research done. Great thanks to my parents for their support, patience and their pray for me, since elementary school and up to now.

Then, I would say thanks for my colleagues; Ramadan Shniba and Ghalib Ibrahim for encouraging me and for the help with different problems from the first day at University.

I would like to thank Almergheb University for the financial support.

Finally, I would like to thank Manchester Metropolitan University and all staff for offering ideal place to carry on this research.

List of publications:

1- Characterization of wind turbine to be used for powering a computer Laboratory. In first faculty of science and engineering research and development day at MMU University, Manchester, 2010. (See appendix D)

2- Wind turbine blade fault detection using the empirical mode decomposition method; numerical simulation and experimental testing. In: The Third International Renewable Energy Congress, Hammamet, Tunisia (2011). (See appendix E)

3- Wind turbine blades fault detection based on principal component analysis In: International conference on applications and design in mechanical engineering (icadme 27th - 28th February 2012) Perlis, Malaysia. (See appendix F)

4- Coherence analysis of wind turbine induced air-borne acoustics and vibration signals. In second faculty of science and engineering research and development day at MMU University, Manchester, 2012. (See appendix G)

5- Novel Approach to Rotating Machinery Diagnostics Based on Principal Component and Residual Matrix Analysis. ISRN Mechanical Engineering 2012, Artical ID 715893. , 7 pages, doi:10.5402/2012/715893. (See appendix H)

6- Wind turbine blades condition assessment based on vibration measurements and the level of an empirically decomposed feature. (2012), Energy Conversion and Management 64, 606-613. (See appendix I)

7- Identification of wind turbine blade defects using airborne acoustic measurement and residual matrix of principal component analysis In: The Third International Renewable Energy Congress, Sousa, Tunisia (2012). Accepted for publication.

Chapter 1

Introduction

This chapter gives a brief review of the historical development of wind turbines and describes the most widely used common wind turbines. It also introduces the condition monitoring of rotating machineries that could be adopted for monitoring the condition of wind turbines. The research aims and objectives are given. Finally, the thesis structure is described.

1.1 Wind Turbines Background and classification

Windmills are one of the most used and effective energy resources; they have blades, traditionally referred to as “sails”, which are moved by the wind and generate useable energy. Windmills, especially horizontal–axis windmill, were widely used in most rural areas for grinding grain or pumping water. But were rapidly replaced by fossil-fuelled engines with the advent of steam power and then electricity became widely available[1].Wind energy became a means of battery charging for remote dwellings.

The oldest wind turbine still in use is thought to be the 1250 kW Smith-Putnam constructed in the USA in 1941. This machine is outstanding in its construction. It has a steel rotor 53 m in diameter, full-span pitch control and the load is reduced by flapping blades. It was the largest wind turbine for 40 years even although in 1945 a blade spar catastrophically failed [2].Wind turbine design history is provided by Golding[3] and Shepherd and Divone in Spera [4], including the Balaclava wind turbine, 100 kW 30 m diameter in USSR in 1931 and the Andrea Enfield, 100 KW 24m diameter in UK which was a pneumatic design constructed in early 1950s.The turbine had hollow blades with open tips that helped to draw air up through the tower where another turbine drove the generator. Many inventive and light weight turbines were constructed by Hutterin Germany in 1950s and 1960s.

However, interest in wind generation increased dramatically when oil prices rose steeply in 1973 and a number of research and development programs were funded by Governments in Canada, Germany, Sweden, UK and USA[1].

In the USA, for example a series of sample turbines were constructed beginning in 1975 with the 38 m diameter 100 kW Mod-0 and culminating in the 97.5 m diameter 2.5 MW Mod-5B in 1987. These initial projects showed to create a cost effective and modern turbine considerable development was needed. For the first time a 4 MW vertical-axis Darrieus wind turbine was constructed in Canada and in the USA a 34 m diameter turbine was tested in the Sandia vertical axis test facility. Another development was in UK by Musgrove who created a 500 kW, vertical-axis design using straight blades which gave an 'H' type rotor [1].

Initially multi-megawatt test turbines were constructed only as a result of significant state support and most of the turbines produced for commercial sale by private companies were much smaller. Development of vertical axis and horizontal axis wind turbines was combined with the concept of hydraulic transmission and a suitable process for yaw drive. The turbines developed at that time used a maximum three blades, but this was not on the basis of a full theory which specified an exact number of blades required for each turbine.By the mid-1980s a very large number of quite small (100 kW) wind turbines were produced with Government support. Such numbers provided a good testing ground and many problems were found, but being smaller and relatively simple these turbines were easy to manage and repair.

In Denmark a simple design of windmill was developed which gained in popularity; these had three blades, a rotor regulated by a stall and having a fixed speed, induction machine drive train. These were soon scaled up 60m diameter and 1.5 MW. The concepts of variable speed operation, full-span control of the blades and advanced materials which

were developed and tested at that time are now being used increasingly by designers. For example, the synchronous generator being coupled directly to the aerodynamic rotor to eliminate the need of a gearbox [1].

Other sources of energy were also looked into, like fossil fuel and nuclear power stations. However, environmental considerations have meant that most western governments will prioritise use of nuclear power stations to avoid burning fossil fuels which pollute the environment with harmful discharges [5].

The use of wind turbines has been accelerated by the fact that it has virtually zero CO_2 emission and so could help replace fossil fuel to provide a safer and cleaner environment. Wind energy can provide nations with energy resources to make them more energy independent and advance the economy thus providing jobs[6]**.** As a result the wind energy market grew in different places of the world and in 2009 it was estimated that in the USA wind power generation was more than 25,000 MW [6]. Recently statistics released by the global wind energy council (GWEC) claim that more than 41 GW of wind power was installed throughout the world in 2011,Figure 1.1, shows the global annual installed wind capacity 1996-2011[7].

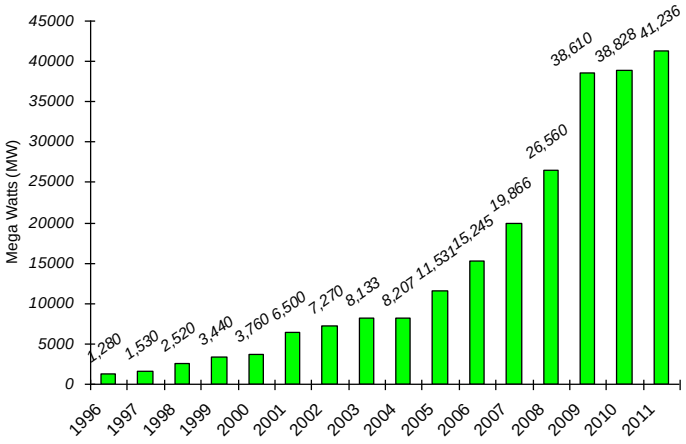

Figure 1.1 Global annual installed wind capacity 1996-2011 [7]

Wind turbines can be classified into two different categories based on the axis about which the turbine rotates: horizontal-axis and vertical-axis. Most windmills are the horizontal-axis type. Vertical-axis machines constitute about five percent of the mills used today. Another way of classification of the wind turbines is the location where they are used such as onshore, offshore or even aerial wind turbines. The design varies according to the location of use. The wind turbines mostly used fall into the following categories, see Figure 1.2 and Figure 1.3;

1. Design on axis Horizontal,
2. Design on axis Vertical

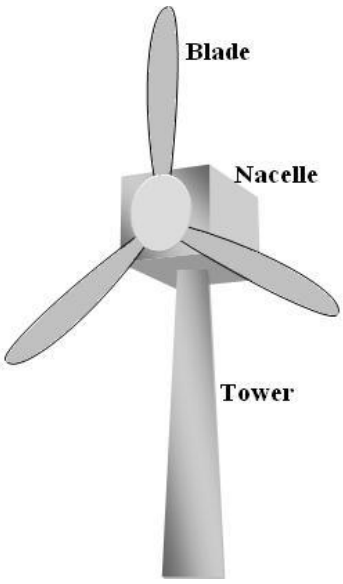

Figure 1.2 Horizontal Axis Wind turbine (HAWT**)**

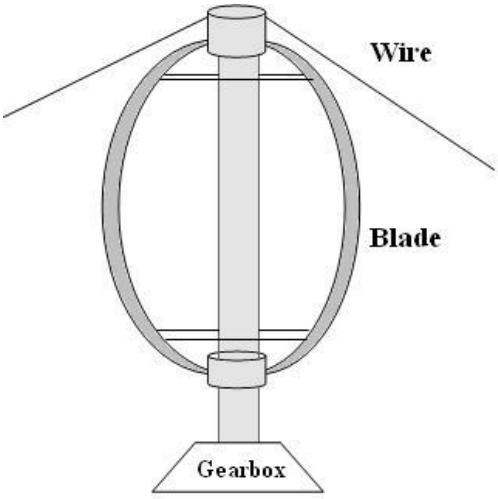

Figure 1.3 Vertical Axis Wind turbine (VAWT) (Darrieus design)

1.2 Condition Monitoring Overview

Thus, for the past twenty years the wind power industry has been giving special attention to improving productivity which has included optimising production by minimising down-time. Due to the requirement of uninterrupted operation one focus has been cost-effective solutions to quality maintenance and this has led to the development of online condition monitoring systems (CMS) [8]. This is particularly true for off-shore applications where the operational overheads are especially high and reliability is a major issue. For the wind turbine industry the direction proactive maintenance strategies have taken is the implementation of online continuous CM systems [9].

The use of CM systems for rotating machinery has a long history especially in management of processing industries and thermal power plants [10]. Because wind farms tend to be located in remote areas and are geographically dispersed CM technology has had to be correspondingly extended. In particular, the strategies to be adopted for the setting-up and application of remote centralised continuous monitoring to a large numbers of identical machines.

It is well known that when a machine component begins to deteriorate its dynamic behaviour changes. Monitoring relevant parameters allows identification of the changes taking place and possible failure modes. The goals of CM are to determine the actual condition of any specified component, to maintain its level of performance, assure machine efficiency, reduce frequency and lengths of down-time and increase productivity. To do this effectively it is necessary to monitor the condition of the wear of the component and determine that point when action should be taken to avoid an

unplanned outage [11]. When using CM or condition based maintenance, staff take action according to when it is needed - or as soon as the machine is available for shutdown to carry out the maintenance work [12].

Experience shows that a major cause of wind turbine failures is in the blades, but with larger turbines gear box failures are increasingly being reported, even with the latest robust designs of gearbox, generator and other wind turbine components[13].

1.3 Problems Setting and Goal of the Study

Pro-active CM is an appropriate maintenance strategy to prevent unplanned outages. Continuous observation of the dynamic behaviour of the wind turbine components will allow wear and incipient faults in the machine to be detected long before it reaches failure. Such an approach not only prevents system break down and interruption of power generated it also prevents expensive damage to other parts of the turbine [14]. The research question has been posed based on these considerations: “For wind turbine blades which vibration based analysis techniques are most suitable for the early detection of incipient faults?”

1.3.1 Wind Turbines Failure Modes

An inspection strategy should provide economic as well as technical advantages, thus the cost of maintenance should not exceed the cost of the whole machine. The historic approach to maintenance of wind turbines was periodic replacement of worn parts or items such as oil filters and lubricant, and then run the turbines to failure. As the cost of machines increased and the turbines grew in capacity this approach was considered no

longer practical. ‘Offline’ condition monitoring requires the system to shut down and properly inspected by machines periodically [15].

Nowadays scheduled maintenance uses skilled technicians to keep a check on every part of the turbines. They use analysis tools and their own human senses and experience to identify if any turbine part needs replacement, oiling or any other maintenance. These inspections are considered a lower limit for the performance of an automated condition monitoring system if also combined with online techniques for identifying, e.g., the level of gearbox oil.

In general maintenance procedures can be classified into three groups:

1. Reactive Maintenance (run to failure),
2. Preventive Maintenance (time-based), and
3. Predicative Maintenance (condition based)

Reactive maintenance or the “run to failure” maintenance mode is where no action is taken to maintain the components and/or machines.

Preventive maintenance is where the machine is regularly tested and checked for errors (including filter and oil checks) according to a pre-determined work schedule. It helps:

- Protect assets and extend the useful life of machinery components,
- Improving the reliability of the system,
- Decrease costs for replacement parts,
- Reduces system downtime, and
- Reducing the risk of injury.

Predictive maintenance is where measurements detect the onset of degradation, allowing the causes to be eliminated or controlled before there is a significant deterioration in the physical state of a component. Predictive differs from preventive maintenance because it is based on the actual condition of the machine rather than on some preset schedule.

Sutherland et al [16]used an almost exclusively offline non-destructive technique for the testing of a wind turbine blade. Finite element simulations of the elastic deformations were checked using accelerometers and/or laser Doppler techniques, and modal analysis of the wind turbine blades. The complexity of these methods meant they are used only when the machine is offline: when designing or certifying new machines. Offline methods are not appropriate while the machine is running and so can't identify or determine the actual working condition of an individual wind machine.

Online technology monitors a machine while it is operating and provides information about various functions of the system. It senses and measures aspects such as strain, vibration, etc., and assesses the present condition. Fluid monitoring (e.g. gear oil) can also be done online, either by obtaining a sample of oil and testing it for various factors or testing the fluid 'inline'. Inline monitoring can be used for all the fluids circulating in the machine

All these monitoring techniques are precautionary measures to maintain the smooth running of the operation but are still uncertain. They give economic advantages by analysing defects and helping smaller parts to be changed rather than shut down the whole plant. CM may completely prevent a disaster and is an important factor in averting most failures but there remains a need for greater reliability, particularly where the

limited access and the size of the component or project makes continuous monitoring important [15].

Wind turbines fault scan result in either temporary or completely shut down of the system. Some faults, such as high temperature of the gear oil, are considered temporary and the system can continue working as the error is fixed or would to be closed only as precautionary measure. All failures are logged by the control unit which registers the significance of the fault. However, wrong failure detection by the system where the fault is due to “noise” could cause the turbine to be stopped. Such a problem would be serious if the system had to be completely shut down and thoroughly checked to avoid potentially serious damage to the turbine. However, mostly a fault indication is due to a malfunctioning of a part which needs to be replaced or repaired. An automatic report is generated to be documented to help avoid of such failures in future. The reports include all details: defining the part, nature and cause of failure (e.g. electrical / mechanical). Figure 1.4 shows the failures that occurred during 2000-2004 in a Swedish wind power plant by Ribrantet. al., [17].The report shows that most were electric system failures, followed by sensors and blade pitch components. Figure 1.5 shows the corresponding distribution of down-time.

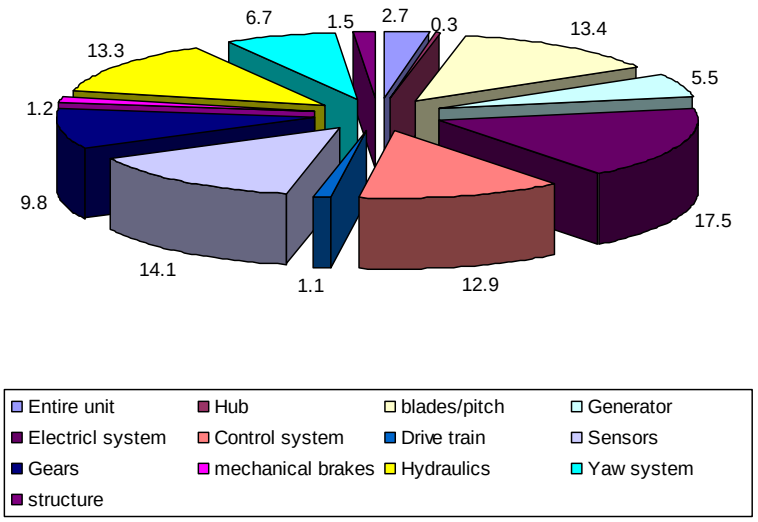

Figure 1.4 Failures of wind turbine at Swedish power plants during 2000-2004[17]

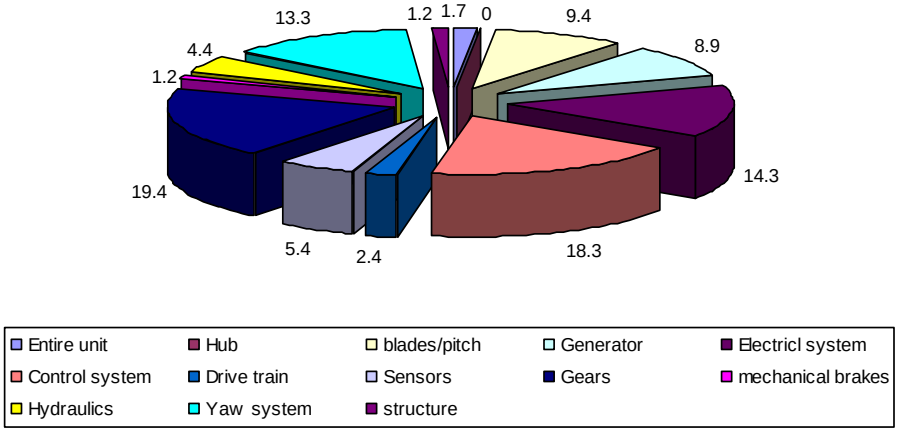

Figure 1.5 Percentage of wind turbine downtime at Swedish power plants during 2000-2004[17]

It is known that heating of the gearbox, lubricant failure, ice on blades and wind turbulence can all be causes of failure. Therefore most failures occur in gearbox, rotor (Hub and Blades) and generator, which means there should be specific techniques for monitoring each of those components.

1.4 Rotating Machinery Conditioning Monitoring Techniques

Different CM techniques are used for monitoring different parameters in machines [18].Widely used techniques in industry to detect changes in material due to defects such as cracks on a drive shaft include: acoustic emission, oil analysis and vibration analysis [19]. Different CM applications which are possibly suitable for use with wind turbines are:

Vibration analysis, oil analysis, thermography, physical condition of materials, strain measurement, acoustic measurements, electrical effects, process parameters, visual inspection and performance monitoring.

1.4.1 Vibration Analysis

Vibration analysis is usually presented as the most effective CM method, especially for rotating equipment because rotating equipment produces vibration which is specific in its behaviour and character. A new rotating machine has a relatively smooth vibration signal during the normal operation but as it gets older degradation as a result of wear will change the characteristics of the signal. The integrity of the machine can be evaluated by detailed comparison of the “new” and “old” vibration spectra. It is well known that the vibration signal carries information about structural resonances and other components in

the machine, thus it can give information on the operating condition and efficiency of the machine. Vibration analysis is a non-destructive test of plant performance and can be used as a tool for quality control. The overall vibration signal is a mixture of a host of components at different frequencies, but on its own cannot yet provide all of the information necessary for a successful condition based maintenance programme[18].

Industrial vibration analysis techniques use vibration transducers with different frequency ranges according to the machine being monitored. The vibration transducers are usually placed at critical locations where the local load is a maximum such as wheel axles, bearings of the gearbox, bearings of the generator and the main bearing. This is also the case for wind turbines.

Traditionally different types of sensor were used for measurement of vibration:

- Displacement sensor (proximity probe) for the low frequency range;
- Velocity sensor (velocity pickup) in the middle frequency area; and
- Acceleration sensor (accelerometer) in the high frequency range.

However, today wide range and sensitive accelerometers are used. If velocity of the vibrating surface is required the acceleration signal is integrated. If displacement is required then the acceleration signal is integrated twice.

Vibration analysis is applicable for wind turbines to monitor the drivetrain including gearbox, rotating components downstream of rotor; shaft, couplings, generator and brakes and the main bearing. High quality signal analysis requires specialized knowledge

as well as special inspectors for such analysis but the costs are compensated by reduction of production losses.

Application of vibration monitoring techniques and working methods for wind turbines differ from other applications with respect to:

- Dynamic load characteristics and low rotational speeds: Wind turbines have more dynamic characteristics and relatively low rotational speed compared to other rotating machines. Importantly the speed does not remain constant which complicates the analysis.
- Investment costs vs. production losses: The production losses in wind turbines are relatively low thus the investment cost is paid back by reduction of maintenance cost and reduced costs of increased damage [20].

1.4.2 Oil Analysis

Gearbox problems can be characterized by changes in the size, number and total mass of particulates generated in the oil of that gearbox. The efficiency of bearings and gears vastly depends on its oil condition, thus lubrication is a key phenomenon of a gearbox. The lubricants used in the wind turbines have the specific function of keeping the rotor running. It is exposed to high temperatures, varying load and contamination. Under such conditions it is necessary to monitor using oil analysis. This has two purposes:

- Safeguarding the oil quality (contamination by parts, water content)
- Safeguarding the components involved (characterisation of parts)

Oil analysis is done offline. A sample of the oil is taken from the machine and undergoes various tests to check its condition. The oil is tested for five conditions [21]:

- Viscosity.
- Oxidation.
- Water content.
- Particle count.
- Machine wear.

The oil should be free from hard particles (which might be the result of machine wear) that could scratch the surfaces of the gears and bearings. Viscosity analysis is important to reduce the friction to allow smooth function of the bearings and the gears, the greater the water content the less effective the lubricant. Metal to metal contact occurs due to too thin a lubricant and increases friction and surface wear.

Although the offline analysis provides detailed information, still the need remains for the online diagnosis. Commercially online systems are widely used. Such systems monitoring gear conditions by checking the number of particles present. The systems offer optical and electromagnetic counters and sensors to assess the number of particles present.

The pressure drop across oil filters is widely used as an indicator of machine condition: a sudden increase in pressure drop indicates that many particles have been released in the oil which is a sign of machine distress. Helicopter gearboxes use similar sensors [5]. The related technologies such as in aviation can also be applied to wind turbines. Such as wear site sensors (WSS) from Smiths Aerospace higher resolution counters which use

Fraunhofer diffraction and particle counters that use capacitance or electrostatic charge. However, as non-ferrous and hybrid bearings, such as silicon nitride balls in a steel race, become more common, particle counters and analyzers that rely on the debris to be magnetic or electrically conducting will become less useful [15].

1.4.3 Thermography

Thermography, also known as thermal inspection or infrared inspection, is one of the most common non-destructive testing or inspection methods and considered as a quick observation approach to monitor the general condition of a machine. This approach is usually applied for monitoring and failure identification of electronic and electric components. The infrared images diagnose the heat conditions from a thermal profile of the machinery and determine leaks, cracks, corrosion, poor electrical wiring and contacts. This procedure is widely used in industry where it has been found that to give best results if used offline.

Composite materials are used in manufacturing wind turbine blades, which are large and highly stressed structures. This has led to the need for a suitable CM technique and thermography is a satisfactory method for monitoring a structure in two distinct ways depending on whether or not heat energy is applied from outside the body. In the first case, external heat is applied to the surface and conducts into the body; the presence of a flaw is revealed due to the difference between the thermal conductivity of the flaw and the base material, giving rise to a temperature difference at the surface which can be detected using an infra-red imaging system. Alternatively, if the body is cyclically stressed then heat may be generated at a flaw within the body due to a combination of

thermo-elastic effects, hysteresis heating (due to the viscoelastic nature of the composite material) and frictional heating between free crack surfaces[22].

1.4.4 Physical Condition of Materials

This method depends on the well-known fact that the molecules of materials which undergo a transition under the influence of physical phenomenon such as temperature, pressure and stress, remain unbroken[21]. This technique is normally offline and helps in physical condition detection of cracks (nucleation and growth) detection [23].

1.4.5 Strain Measurement

Strain measurement is a common technique and calculates the level of stress in any system i.e. turbine blades. In CM this is accomplished using strain gauges which undergo a change resistance in response to their surface strain. The relationship between strain and resistance is expressed by the gauge factor (GF) of the strain gage foil, which can range from 2.0 to 4.0. The most common foil material is constantan alloy (55% copper and 45% nickel) having a GF of 2.0. The changes in resistance are converted into voltage changes by passive circuit networks. The voltage is then amplified for signal transmission or display [24].

1.4.6 Acoustic Monitoring

The surface vibration of a machine is often the most important factor in generating the airborne acoustic signal from the machine. Thus there is a close relation between the acoustic and vibration signals. The basic difference is that the vibration sensors are rigidly mounted on the component involved and register the local motion while the

acoustic sensors (microphones) sum up the sound from many sources on the machine. This technique is not appropriate with online testing. Airborne acoustic signals get contaminated by background noise of the machinery if used in online conditions.

Today, increasingly Acoustic Emission (AE) is used for CM, some of these are widely known by their trade names. Amongst these are the Spectral Emitted Energy sensors promoted by SKF.

AE is a non-destructive examination (NDE) method. AE is the production of high-frequency elastic waves (in the approximate range 100 kHz to 1000 kHz) due to the rapid release of accumulated strain energy from a localised source within a material such as a crack or fracture. The energy released by the change of condition travels through the material and causes elastic vibrations. The AE signals can be detected and measured at the surface of a structure using a suitable sensor (e.g. loosely attached to a turbine blade by flexible glue) and the signal can be analysed to give information on the condition of the structure. There are two types of acoustic monitoring. The first one is the passive type performs by the component itself whereas the second type, the excitation is externally applied[20]. Due to high cost of the monitoring equipment it is not recommended for high cost structures. This method is primarily used for bearing defect detection and gear box fault detection and is not appropriate for differential machine faults.

1.4.7 Electrical Effects

Electrical effects are used for CM of electrical machines. Machine Current Signature Analysis (MCSA) is used to detect any and all unusual occurrence in electrical machines,

and for accumulators the impedance can be measured to establish the condition and capacity. For medium and high voltage grids, a number of techniques are available:

- Discharge measurements,

- Velocity measurements for switches,

- Contact force measurements for switches, and

- Oil analysis for transformers.

Cabling isolation faults can be detected through inspection measurements but these techniques don't have a direct impact on the operation of the wind turbine [20].

1.4.8 Process Parameters

For wind turbines, safeguarding based on process parameters is common practice. As the control systems become more sophisticated, so the diagnostic capabilities improve. However, safeguarding is still largely based on level detection or comparison of signals. When the signal goes above a predefined limit value an alarm is raised. At present, with wind turbines this is usually the most intelligent usage of signals based on parameter estimation and trending.

1.4.9 Visual Inspection

Visual inspection is a type of predictive maintenance which has historic importance. Specialised inspectors performed routine checks by just "looking" and observing the machine. In fact, of course, most of the human senses were used: did the machine sound right, was it too warm to the touch, was there a smell of burning, did the fingers sense excessive vibration, was there a pool of oil on the floor, etc. This was usually done on

industrial sites. No other analysis was involved. A “visual” inspection is widely used in industries as a routine daily checks but will fail to detect faults in the early stages[25].

1.4.10 Performance Monitoring

Performance detection involves monitoring of power, wind velocity, rotor speed and blade angle and the relationship between them can be used for safeguarding purposes. Detection margins are set; if any of the variables deviates outside its margins an alarm is generated. These margins are kept large to prevent false alarm. This method is not widely used in case of wind turbines [20].

1.5 Research Aim and Objectives

1.5.1 Aims

The project aims at developing an effective and reliable monitoring technique for wind turbine blades based on real-time vibration signal analysis:

(i) to extract from the vibration signature, a description of the fault and its level of severity, and

(ii) to provide a condition monitoring technique that uses complex signal multivariate classification of parameters.

1.5.2 Objectives

To achieve the project’s aims; the following research objectives have been identified:

1- To understand the working principles and related parameters of wind turbines.

2- To determine and describe the common failure modes of the key components of a wind turbine.

3- To review current rotating machinery monitoring and vibration analysis techniques, and examine them on monitoring the condition of wind turbine blades.

4- To simulate a 3-D model of a wind turbine with three air foil blades using ANSYS and SolidWorks packages, For the purpose of understanding induced vibration signals under different operating conditions including healthy and faulty blades.

5- To build a test rig for data collection and analysis; 3 bladed horizontal wind turbine with the necessary instrumentations and data acquisition system.

6- To collect vibration baseline data; under different rotation speed; 150, 250 and 350 r/min.

7- To experimentally seed quantified faults by removal of small slivers from one blade face; 10mm, 20mm, 30mm and 40mm length, all with a consistent 3 mm width and 2 mm depth.

8- To detect the seeded faults and evaluate their severity using conventional and advanced signal processing analysis techniques (principal components, empirical mode decomposition, and time frequency domain methods).

9- To use the knowledge and results gained from the objectives above to develop signal processing that suits wind turbine blade CM vibration based schemes.

1.6 Outline of Thesis

The thesis is presented in nine chapters and organised in the following way:

Chapter 2: in this chapter recent developments in the CM of wind turbine are described and reviewed. The literature review explores the dominant themes of the project including the common failure modes of the wind turbine.

Chapter 3: deals with wind turbine simulation using 3D FEM package, airfoil characteristics and blade design aspect and the vibration analysis by finite element package ANSYS followed by modal analysis of the simulated blades.

Chapter 4: explains the motivation of this work, presents the test rig and describes the instrumentation and failure mode of blade.

Chapter 5: describes conventional CM methods and their performance in detection of a wind turbine crack for simulation and experimental works.

Chapter 6: explains the mathematical principle of the empirical mode decomposition method followed by numerical signal example. It also, presents EMD performance in detecting faults in blade for both simulation and experimental and then introduces a novel method that developed in this research.

Chapter 7: gives an introduction for wavelet transform followed by description of continuous wavelet transforms (CWT). It presents CWT performance in detection of a wind turbine blade crack followed by applying the proposed method on CWT.

Chapter 8: introduces the theory of PCA followed by the performance of PCA in detection of a wind turbine blade crack. It also, explains novel method based on PCA for detecting cracks in wind turbine blade.

Chapter 9: gives overview of objectives and achievements, contribution to knowledge and conclusion. Finally, the future work is presented and divided into three parts; test rig improvement, technology and theoretical research.

Chapter 2

Literature Review

This chapter reviews current literature reporting improvements in wind turbine monitoring techniques and fault finding methods. The review is limited to an introduction to the specific problem of the condition monitoring of wind turbines and methods and techniques used to resolve that problem. This chapter is a summary of research into efficient problem solving and concentrates on the type of faults found in wind turbine blades and techniques for detecting and identifying them.

2.1 Introduction

To meet the economic efficiency demands of the wind energy industry, the scale of wind turbines has increased substantially in the last two decades and current wind turbines are larger than any previous wind turbines, and are generally fitted with two or three bladed rotors. These turbines are mounted atop 60m to 80m high towers because wind speed increases with height above the ground. Particularly for lower wind speeds turbines with longer blades which incorporate modern blade design harvest more energy [26].

Unfortunately, there are many problems linked with wind turbines that reduce their effectiveness and stop them from producing more power from wind energy, such problems can be overcome by, amongst other things [27]:

- Selection of wind farm sites on which to establish wind turbines,
- Selecting a suitable electric generator for the wind turbine,
- Increase machine availability by employing an enhanced maintenance procedure for the wind turbine,
- Using high capacity machines,
- Using turbines that respond well to low wind speeds,
- Increase tower height,
- Better aerodynamic and structural design,
- Increasing the power factor,
- Wider swept area of rotor blade,
- More government support for research and development, and
- Construction of several wind monitoring stations.

Different of technologies can form the basis of comprehensive condition based maintenance programmes with the different technologies limited to specific types of machinery and particular classes of problems [28]. Thus it is important to determine which condition monitoring (CM) technologies will be most useful and cost effective for monitoring wind turbine blades. Each technique will give different relative long and short term economic benefits.

Wind energy converters depend on rotational components which produce complex non-stationary and non-linear vibration signals when the wind turbine is working. Such signals have long been used to monitor the condition of machines and gearboxes.

The peaks in the vibration spectra of rotating machines are directly related with the structure of the machine, its geometry and speed. The causes of problems and remaining useful life of components can be estimated from changes in the relative magnitudes of the frequency peaks. Of course when determining the health of a machine and its remaining useful life the history of the machine, the trend in measured vibration levels and previous degradation patterns are vitally important [29]. Vibration analysis is a powerful CM and diagnostic tool and can be used to determine final state failures or identify faults at an early stage of their development (this is the emphasis in this thesis). It is important to use appropriate method for each specific item of equipment, though the most common technique is to use trend analysis based on RMS vibration amplitude.

As wind turbines become larger, more complex and more expensive the online monitoring of wind turbines became more costly [30]. Stimulation methods are used to

assess likely life cycle maintenance costs using different maintenance strategies such as online CM.

Mohamed *et. al.,* [31] simulated the aerodynamics of steady low-speed flow past 2-D profiles of S-series wind turbine blades. They used a Computational Fluid Dynamics (CFD) method based on a finite-volume approach to determine the lift and drag forces on various sections of the wind turbine blades. They found that an S826 blade profile was the most efficient of the S-series at 0^0angle of attack and is suitable for low and high wind speeds. The study showed that the CFD code they used could accurately predict aerodynamic loads along the blade profile.

El Amine *et. al*.[32] used a lattice Boltzmann method to investigate 2-D incompressible flow around an arrangement of two wind turbine blades. Staggered and tandem arrangements of the NACA 23015 and NACA 4412 wind turbine blades were modelled and good agreement was found between the study results and those available in the literature. The authors concluded that the Boltzmann method was extremely useful in simulating fluid dynamics problems.

Studies of wind turbines focus mainly on fault detection in the blades after manufacturing in factories, whilst many defects occur during the transformation and assimilation of turbine blades on the spot. Such studies have led to important observations on the nature of blade design that will help in avoiding early malfunction of blades. Even though methods of designing blades have developed a lot in the last decade, more improvement is needed in the area of dynamic load control and cost reduction.

Early detection of faults minimizes downtime and maximizes productivity so extensive numerical and experimental investigations have been made into wind turbine maintenance which has resulted in reduction of failures of wind turbines.

2.1.1 Blade Failure Modes

Fatigue is a frequent cause of failure in composites. When the local applied force exceeds the local yield stress microscopic cracks may form and grow and act as a source of fatigue failure. Crack propagation in brittle materials is largely because local stress is magnified at the tip of the crack. A major difference between regular and composite brittle materials is that the presence of resin around the fibres acts as a barrier to stress concentration being transmitted directly to adjacent fibres. The presence of the resin reduces the stress concentration because it is not as brittle as the fibre and so will yield to an extent.

Common fatigue failures in composite blades include: delamination due to an excessive compression load; the fibre breaking due to an excessive tension load; and debonding of the top and bottom skins of a composite blade due to adhesion failure. The progress of each of these failures should change the natural frequency of the blade. Another common failure is due to extreme weather or lightning strikes will cause cracks in the gel coat which exposes the composites below to moisture and water and significantly reduces the life of the wind turbine blades [33].

2.2 Condition Monitoring Technologies

Machinery diagnostics, such as predictive or condition based maintenance (CBM), will use a wide variety of measurements including vibration, acoustic emission (AE), oil debris analysis, etc., to monitor the condition of the machine. For the system to be efficient and effective the measurements must be good indicators of the condition of the machine, should be cost-effective and practical and obtained on a regular and frequent basis. Today, vibration acceleration is extensively used as a measure for the detection of machinery faults. Other parameters that are widely used to monitor machine condition include AE, airborne sound, lubricant analysis, motor current, thermography and ultrasonic measurement.

Besnard and Bertling [34] have recently developed an approach in which degradation is classified based on the severity of the damage. A model was developed to optimize the maintenance of blades for a 5MW offshore wind turbine by considering distinct maintenance strategies, such as inspection with situation monitoring techniques, visual inspection and online CM. Such approaches were used to modify the maintenance outcomes for every strategy and then to consider them in a combined framework.

Lu and Chu [35] examined a number of algorithms and methods based on vibration, noise and AE signals used to diagnose faults in wind turbines. It was established that morphological undecimated wavelet decomposition is more efficient and appropriate for online diagnostics of bearings in rotating machines. It was also established that the time wavelet energy spectrum is efficient in extracting impulse features created by localised gear damage. In identifying and locating gear faults vibration - AE based methods are

capable of recognising the type of fault that has occurred and to implement precise diagnostics.

Zhiqiang *et al.*,[36] have presented a new method for damage diagnosis of wind turbine blades by measuring the vibration response at one fixed point on the turbine. Subsequently, the blade fault can be evaluated based on the degree of shift in the characteristic frequencies in the signal. They stated that the results of these studies show that the method can be applied in engineering practice as well as developing a process for structural health monitoring techniques for wind turbine blades.

Park et al. [37] analysed the vibration of a rotating wind turbine blade to obtain its characteristic vibratory features. The equations of motion for the blades were found and vibration features of the rotating blade extracted. This study indicated that the stiffness of the blade changes when the blade is rotating since it is stretched by centrifugal forces. A computational algorithm of blade stiffness variations resulting from centrifugal forces was proposed.

Jundert [38] used two distinct acoustic techniques for wind turbine blade inspection: gently tapping the blade with a small hammer and the excited sound picked up using a microphone - changes in internal structure are detected by changes in the excited sound. The second method was to transmit ultrasound pulses into the material and internal flaws detected from the reflections. The ultrasound echoes were used to assess the condition of bonded areas under thick glass fibre reinforced plastic (GFRP) laminates.

Sajauskas *et al*., [39] utilized secondary longitudinal surface acoustic waves (LSAW II) to locate surface defects on the inaccessible inner surfaces of sheet products. The method

was found to be effective for discovering general shape defects with predictable orientation, for example, along welded joint. **Raisutis, *et al.*,** [40] used a 290 kHz ultrasonic air coupled system to locate internal defects in wind turbine blades. The transducers were mounted in a pitch and catch configuration for generation and reception of guided ultrasonic waves. These were able to define the size and geometry of internal defect of the main spar in the wind turbine.

Yang, *et al.*, [41] recently used an avideometric technique to assess deformations of large-scale composite wind turbine blades. This was a non-contact optical method to measure non-rigid motion of large turbine. The results showed that the accuracy of the measurement is high, better than 0.1 mm per meter.

Borum, *et al.*, [42] used AE to monitor damage development during a full scale test of a 25m epoxy glass fibre wind turbine blade. Information on the internal condition of the blade was obtained from the AE signals generated by damage initiation and its progress until a failure under increasing loading of the blade. The sensors were attached to the surface of the blade in areas where bending moment calculations predicted critical stresses. Two AE sampling systems were used both using a frequency of 150 kHz; one was commercial, the Spartan AT, and the other was a customised system. It was claimed that AE has shown itself to be a technique that can be successfully used to examine defect development in full scale tests for wind turbines. It was also claimed that this method is more reliable than other methods currently available and can be used to predict the occurrence of damage that would lead to a malfunction.

AE was used by **Beattie** [43] over a decade ago to monitor 20 m long wind turbine blades**.** Using materials to hand, e.g. the coupling cement was GE silicone II household cement, and AE sensors with peak sensitivity at 60 kHz it was found that the system revealed that the peak load was too high and continuing to run the turbine would have done significant damage to the blade. This was later confirmed when the blade was run to destruction. The results indicated that that fatigue tests of large wind turbine blades can be monitored by AE techniques and that the monitoring can produce useful information.

Ghoshal, *et al*.,[44] used an 2.44 m (eight foot) long section of fibreglass wind turbine blade to test four algorithms used in detecting damage to wind turbine blades: Resonant comparison (RC), Wave propagation methods (WP), Transmittance function (TF) and Operational deflection shape (ODS). Such methods depend on measuring the vibration response of the blade using a scanning laser Doppler micrometer (SLDV) or piezoceramic patch sensor, and exciting the structure with piezoceramic patch actuators. The blade section is supported by an elastic cord and rope to avoid rigid body motion and to establish free-free boundary conditions. The experiments established the feasibility of applying piezoceramic patches for excitation and SLDV or piezoceramic patches to evaluate vibration to find damage.

Beattie and Rumsey [45] used an infrared digital camera as a non-destructive measurement tool with two different blade fatigue tests: the first was of part of a 13.1 m wood epoxy composite blade, and the second was of a section of a 4.25 m pultruded fibre glass blade driven at a number of its mechanical resonant frequencies. The

arrangement was as shown in Figure 2.1. As camera is mounted horizontally on the floor, under the blade, a front surface mirror held at an angle of 45° to the floor.

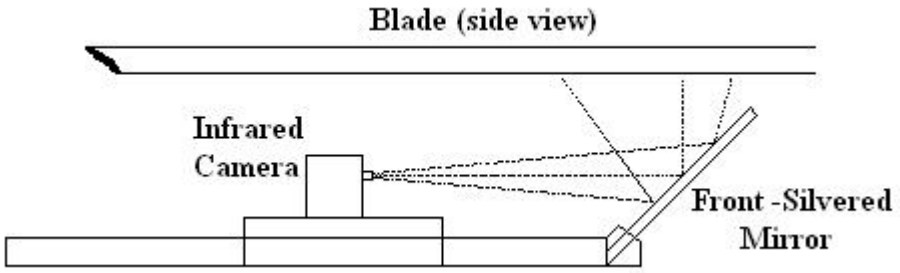

Figure 2.1 Diagram of the floor-mounted fixture used by the infrared camera[45]

It is claimed that that the dynamic temperature distribution provides a summation of principles stresses at every stage on the blade surface and that with the wood epoxy composite blade fatigue test, the section of vital failure was observed before the failure appeared. An important amount of data was obtained from the digital infrared thermograph camera relating to the steady state thermal and thermo elastic stress impacts on small and large areas of blade.

Laren, *et al.*, [46] used wavelet transforms to observe and localize damage in the composite coat of wind turbine blades. The mode shapes were determined by experiment which used a laser vibrometer and ANSYS and MatLab simulation programs in which a finite element model of a 3-D wind turbine blade was created to simulate the real blade.

The simulation results were tested using a real blade set up on a steel table with an electromechanical shaker as a vibration excitation source. Blade mass was 2 kg, the natural of the undamaged blade was estimated and then a 2 mm wide crack was

simulated. The crack had one of four lengths from 5% to 30% of the blade width and was positioned at three locations. The damage site and blade model are shown in Figure 2.2.

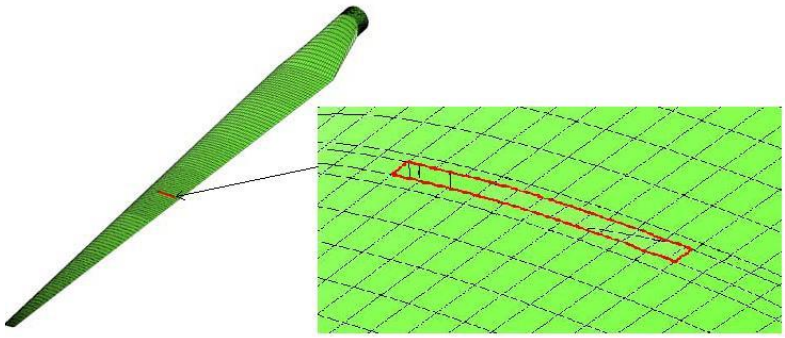

Figure 2.2 Blade model with damage (red line)[46]

In experimental work a laser scanning vibrometer was used to evaluate blade vibration and blade mode shapes for various blade conditions.

The measurements were carried out for three values of additional mass at different locations and the damage cases (values of additional mass) were taken as 2 %, 6 % and 12 % of the total mass. Wavelet transform techniques were used to examine the mode shapes of damaged plates and beam and in all damage cases it was possible to locate even relatively small damage (crack).

Xueli, *et al*.,[47] has proposed a back propagation neural network (BPNN) model for fault diagnosis of a direct-drive wind turbine based on the measured vertical and horizontal vibration. The experiments were carried out for various conditions; wind wheel mass imbalance, blade brake, normal condition, yaw and wind wheel aerodynamic imbalance. The time domain vertical and horizontal vibration data for the main shaft were

gathered. Using this data, the BPNN fault diagnosis model was shown to be suitable for wind turbine fault diagnosis in complex conditions.

Li, *el al*., [48] introduced an approach to the fault diagnosis direct drive wind turbines that depends on certain chosen features and a support vector machine (SVM). Certain parameters from the time domain of the main shaft displacement signal in both the vertical and horizontal directions were selected using a developed distance evaluation technique. This research investigated five conditions: normal; wind wheel mass imbalance fault generated by fixing a mass to a blade; aerodynamic imbalance generated by fixing a light cardboard to a blade; a yaw fault caused by varying wind turbine axle line to wind flow direction by 20°; and a blade airfoil fault by covering the blade from the tip to the root. Based on the results, it was concluded that this method is efficient in recognizing wind turbine faults. This has better organization capability and robustness to diagnose the faults in direct drive wind turbines in complicated conditions.

Bazilevs *et al*.,[49] claimed to have developed a single computational framework for the superior simulation of wind turbines and to have successfully applied it to the full scale NREL 5MW offshore baseline wind turbine. The work was divided into two parts. The first part concerned modelling of the wind turbine geometry and numerical simulation in which the rotor was assumed to be constant. The second part investigated structural discretization for wind turbine blades and the details of the computation of fluid–structure interaction. In addition, the computational framework was extended to coupling of flow with rotating rigid body, and was successfully applied to the simulation of wind turbine rotor over-spinning under high wind speed inlet conditions**.**

In recent years there have been significant developments in wind energy conversion systems using variable speed doubly fed induction generators. Unfortunately, induction motors exhibit highly non-linear behaviour, rapid dynamics and complex control. Predictive control has been shown to be a valuable tool for use with linear systems. Recently, there have been many researchers attempting to adapt predictive control to non-linear systems.

Kamel, *et al*., [50] applied non-linear predictive control to control the rotor speed of a doubly fed induction generator. It was stated that the control system was equivalent to a non-linear PID controller. Simulation results showed satisfactory performance tracking trajectories with rejection of disturbances by the non-linear generalized predictive controller.

Amirat *et al*.,[51] carried out a study of mechanical and electrical fault diagnosis in a double-fed induction generator wind turbine. A single-component signal (the first intrinsic mode function) that examined amplitude demodulation was extracted using empirical mode decomposition through a stator current signal that was analyzed to find bearing failures. The results of experiments indicate that the method works under various conditions and can be used to diagnose different bearing failures.

Distortion or unbalance in rotating machines is general source of vibration excitation, with mass distortion the main cause of vibration excitation of the rotor shaft in a transverse direction. Rotor imbalance of a wind turbine can be detected at an early stage because of its impact on the operation time of wind turbines.

In this regard **Niebsch, *et al*.**,[52] proposed a method to evaluate inhomogeneous mass distributions of rotors and deviations in pitch angles of rotor blades from vibration data. A mathematical model related the imbalance to the effect of resulting vibrations was established and a vibration equation was derived and solved analytically after discretization, and numerical simulations were also performed using artificial vibration data.

Muztagh, *et al*., [53] investigated the feasibility of applying dampers to wind turbines and used a tuned mass damper, a passive control device, to reduce wind induced vibrations in a three bladed wind turbine situated on top of a uniform tower. The free vibration properties of the rotating blades and tower were obtained using a discrete parameter approach. A tuned mass damper was placed at the top of the tower and was successful in solving the displacement of the tower. It was claimed that the use of the tuned mass damper had the significant advantages of ease of use, low cost and no need for an external power source.

Besnard *et. al*.,[54] presented a life cycle cost model, which can be used to analyze economic benefits gained from implementing CM systems. The study used two approaches to analyse how the random behaviour of failures can affect life cycle cost and what are the critical parameters (subject to uncertainty) that influence the value of a CM system. There was a clear result showing the benefit of enhanced reliability of a gearbox.

Xiukun Wei [55] considered fault detection and fault estimation issues of blade root moment sensors and pitch angle actuators for a three bladed wind turbine. The fault detection system was applied for underlying faults and the proposed approach was

demonstrated by simulation studies on a linearized wind turbine model at a rated operation point for several scenarios of blade moment sensor and pitch actuator faults. The proposed approach provides a useful alternative for practical application.

Chang-Hwan Kim *et al.*,[56] calculated the approximate deflection mode shapes of a FRP wind turbine blade. The system was basically a cantilever consisting of a wind turbine blade connected to the hub at its root and directly fitted by six bolts. The length of the blade used was 960mm, whilst the diameter was 44.5 mm. Seven fibre bragg grating (FBG) sensors and seven strain gauges were used to extract static and dynamic responses of the blade. Sensors were being located on the blade. The distance between two adjacent sensors was fixed to be 100 mm. The results showed that the mode shapes obtained from FBG sensors and strain gages were very similar. However the Fourier spectra obtained showed more peaks in the FBG signals than in the signals from the strain gages.

Al-Bedoor, *et al.*, [57] developed a mathematical model to study the feasibility of extracting information on rotating blade vibration from shaft torsional vibration for a shaft-disk-blades system rotating at constant speed. The model considered n-blades which were attached radially to a rigid disk, the disk was driven at constant speed by a flexible shaft. Simulation results showed that the shaft torsional vibration signal carried the blades vibration signatures at their respective natural frequencies which suggest rotating blade vibration can be measured using the shaft torsional vibration measurement.

Fadaeinedjad, *et al.*,[58] used three simulation programs; TurbSim, FAST and Simulink to model both the mechanical and electrical systems of a wind turbine and its controllers in detail. The main aim of this study was to investigate the consequence of voltage sag on

vibration of the wind turbine tower. This study also considered such power system characteristics as short circuit levels and X/R ratio and mechanical parameters such as wind turbine operating conditions and mechanical damping of the tower. The results showed that disturbance of the power system (e.g. voltage sag) can impact on the electrical dynamics and mechanical performance of the wind turbine, including tower vibration. The model predicted that voltage sag can cause severe tower vibration and the tower oscillations can affect rotation speed and interact with the pitch control system. The result showed that the effect of voltage sag will depend on a complex interaction between the frequency at which the voltage sag occurs and the natural frequencies of the tower, so that higher tower vibrations occur for certain voltage sag durations, on the other hand for the electrical system of the wind turbine the longer the voltage sags the more severe the consequences.

Al-Ghamd, *et al.*, [59] used vibration measurement and AE to identify bearing defects and to estimate the magnitude of the defect. The tests were performed at rotational speeds between 10 and 4000 rpm and defects of different sizes were seeded onto the outer race of the test bearing. Comparison of vibration and AE results showed that AE enabled earlier detection of the fault, had better identification capabilities and was more able to quantify the size of defect.

Tan and Mba [60] studied the application of AE to the detection and identification of defects seeded into a spur gearbox arrangement with two identical oil bath lubricated gear boxes connected in a back-to-back arrangement. The results showed that the level of the

AE signal was not influenced by the load and the source of AE activity was due to asperity contact.

Bouaziz, *et al.*, [61] investigated the effects of shaft misalignment in a test rig which consisted of a rotor and two hydrodynamic journal bearings mounted in such a way as to have two degrees of freedom. A theoretical model was developed for the dynamic behaviour of the system including the effect of angular misalignment. It was found that the vibration level of the angular misalignment decreases with the increase of relative eccentricity and the increasing when the imposed angle increases. Comparison of hydrodynamic journal and roller bearings revealed that the hydrodynamic journal bearing gave greater attenuation of vibration resulting from the misalignment.

Radoslaw, *et al*., [62] presented a novel method of classifying data obtained from online monitoring systems using a technique based on long term trends of such parameters as the RMS of the time domain of the vibration signal and power variation. They claim to have shown that analysis of data separately for several sub-ranges of load is much better than classical analysis. The study showed that by decomposing data into several sub-ranges can provide better fault recognition than when all the data is taken together. It is claimed that this method could improve automatic decision making algorithms in vibration based CM systems.

Siores and Negro [63] explored the use of AE techniques to identify possible failure modes in a gearbox during its useful life. The test rig included a gearbox with input and output gear sets, a DC shunt motor and a variable speed motor. The AE sensor with resonant frequency 175 kHz was mounted on the gearbox casing. Prior to the test, the

gearbox was run-in for four one-hour intervals at 1200 rpm and full load. Common gear faults such as worn and broken teeth, shaft misalignment and excessive backlash were seeded into the test gears. The RMS and standard deviation of the time domain of the AE signal were measured and it was concluded that these AE parameters could identify the failure modes.

Singh, *et. al.*, [64] used AE to investigate detection of the growth of a gear tooth crack but no information was given regarding the type of gear, applied load, sensors used, or the data sampling rate. A single tooth bending machine was used where the load on the tooth varied sinusoidally at a frequency of 40 Hz. An accelerometer and AE transducer were mounted on a spur gear close to the loaded tooth. The test showed that the vibration level did not change significantly during crack initiation and the initial stages of crack growth, but did increase substantially during the final stage of failure. On the other hand the AE had detected the presence of a fault by the time the gear reached 90% of its final life. Generally the amplitude of the AE signal increased as the crack progressed. A high amplitude AE signal was obtained during the final stage of gear tooth fracture. It was concluded that AE method was superior to the vibration monitoring technique.

2.3 Signal Processing Techniques

To reduce operational and maintenance costs it is necessary to continuously improve the CM of wind energy conversion systems. The condition of the wind turbines can be estimated using approaches which vary from simple measurement techniques to sophisticated signal processing. This section seeks to provide a brief summary of the common fault detection techniques; time domain analysis, frequency domain analysis,

cepstrum analysis and time-frequency analysis, applied to vibration signals obtained from rotating machinery,

One approach is to extract statistical properties of the time domain signals; the most common of these are *RMS, standard deviation, Kurtosis, mean, skewness, crest factor, impulse factor, ... etc*. Applications are given in [65, 66]. When using this approach is it usual to perform time domain averaging to minimise the random element of the vibration signal [65, 67]. Some of these factors such as Crest factor can be sensitive indicators of the presence of a fault, but as the damage progresses and becomes well advanced their values decreases and may well fall to that the undamaged bearings [68].

Fraser and King [69] used kurtosis to assess when a gearbox component was severely damaged. Kurtosis is a measure of the peakedness of a signal, and a slightly damaged gear for example will exhibit multiple impulses in the time domain which increase the value of the kurtosis. As the damage progresses and the rate at which the peaks appear increases and the peaks begin to merge one with another and the magnitude of the kurtosis decreases.

Residual analysis, where major frequency components are removed from the averaged vibration signal can also be used to detect gear faults. The simplest characterisation of the signals is to use an index of central tendency such as the mean to indicate the point where the signal is centred on a scale of measures [70, 71].

Another approach is cepstrum analysis which attempts to condense the frequency domain information into an easier to interpret form, thus providing a practical system for routine prognostic monitoring.

Principle Component Analysis (PCA) is a popular tool in multivariate statistical analysis because it can be used to reduce the number of variables with a minimal loss of information. PCA is a statistical technique which can be used for early indication of any irregularity in the data structure (small fault) and can determine which features of a system are most important in regulating its behaviour. PCA can be used to reduce the dimensionality of a data matrix and then Independent Component Analysis (ICA) can be applied to identify the independent components among the data and correlate them to faults in, e.g., a gearbox[72].

Makinezhad [73] used PCA to analyse raw AE data from a faulty ignition system of an automobile. The sampled dataset was heavily contaminated by unwanted noise from nearby automobile engines and other sources of sound found in an engineering workshop. Parameters such as Crest Factor, Kurtosis, RMS, Skewness, Maximum count, Minimum count and Zero count were calculated from the sound signals and PCA was used for dimension reduction. They were used for classifying the signal. It was claimed that the accuracy of this AE based method was greater than 70%.

Hu [74] proposed a novel non-linear method for feature extraction from the time-domain signal using wavelet packet pre-processing and from the corresponding frequency-domain of the signal using the kernel principal component analysis (KPCA), to characterize the condition of a gearbox. Experimental tests on an automobile gearbox showed that KPCA outperformed PCA in terms of clustering capability, and both the two KPCA-based subspace methods were effectively applied to gearbox CM.

Spectral analysis is a widely used technique in vibration analysis. The development of the fast Fourier transform (FFT) [75] made a huge contribution to its almost universal use in transforming time domain signals to their corresponding frequency domains.

Hamid and Kabiri [76] used the FFT to extract useful features for fault detection from the time domain of airborne acoustic signals. The variations in the frequency spectrum were used to distinguish between healthy and faulty operating conditions of four different automobile engines with a fault the ignition system. The FFT coefficients of the acoustic signal for the different frequency bands were taken as representative features.

The standard FT decomposes a time domain signal into its frequency spectrum but it represents the spectrum of a stationary signal with no time information. If the time domain signal is non-stationary the spectral content will change with time and the FT cannot fully describe the signal. If a fault is progressing its vibration signal is non-stationary and some method other than the FT is required. Time-frequency distributions can be performed with constant or varying time-frequency resolution and thus are an ideal method for describing the change in spectral content of a signal with time.

Secil *et al.*, [77] used the STFT method to analysis signals for healthy and faulty turbine blades. They investigated electro-mechanical systems in wind turbine, particularly the variation in generator rotor speed, gear and generator torque resulting from a possible wind turbine blade fault. Analysis and comparison of healthy and faulty signals proved to be able to determine the fault and successfully identified changes in blade structure.

Chin-Shun *et al.*, [78] proclaimed a signal processing approach using the STFT to enhance inspection of wind turbine blades. It is claimed that with this approach the test

signals received from sensors distinguished a damaged structure from a healthy one under a number of process scenarios. **Fitzgerald, *et al*.**,[79] investigated the use of time-frequency methods and the STFT to detect defects in wind turbine blades using the blade vibration signal. A model was developed and used for simulation studies of the behaviour of the wind turbine blade and nacelle with change in rotational speed and stiffness of the blades. This study emphasised structural dynamics of the turbine including interaction between the blades and with the tower.

Kelley *et al.*, [80] decomposed and analyised turbulence/rotor interaction. Both wavelet and Short-Time Fourier Transforms (STFTs) were applied to the inflow turbulence (Reynolds stresses) and a turbine key rotor response parameter (root flapwise loads). Those techniques were applied to both observed and simulated turbulence and turbine response. By comparing results, it was found that STFT did not give as much information as obtained from continuous and discrete wavelet transforms.

The Wigner-Ville Distribution (WVD) is a time-frequency method which has been widely used in machine diagnostics, indeed the earliest application of time-frequency methods was of STFT and WVD by Forrester to detection of gear faults [81, 82]. The work of Forester [83] demonstrated that time-frequency techniques, such as the WVD provide a framework for robust detection and classification schemes that describe how the spectral content of a signal changes with time.

Al-Ahmar *et al*.,[84, 85] discovered a particular transient technique suitable for mechanical and electrical fault diagnosis in double fed induction generator (DFIG) wind turbines. This technique is a combination of statistical variance and energy analysis using

wavelet decomposition of the stator current signals, and was found to be useful for CM and failure diagnosis in wind generators. The test rig was a 1.1 kW induction generator, DC motor and gearbox. The sensors used were: two speed sensors (drum and shaft speeds); three current sensors (supply currents) two torque sensors (torque instantaneous value and lifting torque) and multiple vibration sensors positioned on the generator.

Jiang *et al.*, [86] investigated feature extraction from the vibration signals of wind turbines using an adaptive Morlet wavelet and singular value decomposition (SVD). The Shannon wavelet entropy was adapted to optimise the central frequency and bandwidth parameter of the Morlet wavelet to maximise matching with the impulsive components. Improved matrix methods were used to obtain the wavelet coefficient and appropriate transform scale after which the SVD was used to obtain the most appropriate transform scale. Experimental results showed that the adaptive Morlet wavelet combined with the SVD performed better than the Donoho's "soft-thresholding denoising" method for extracting the features associated with impulsive components contained in the time domain vibration signals.

Lardies and Gouttebroze [87] adapted the Morlet wavelet to better extract modal parameters such as natural frequencies and damping ratios of a vibrating system. These researchers used the son wavelet function to obtain results which were claimed to be better than those obtained with the traditional Morlet wavelet function. The technique was tested quantitatively using a turbine tower subject to ambient winds and it is claimed that the results demonstrate that this particular wavelet transform is well suited to the analysis of mechanical systems excited by random forces.

Bouchikhi *et al.*, [88] carried out a comparative study of the performance of the STFT, the Continuous Wavelet Transform (CWT), the Pseudo Wigner-Ville transform (PWVT) and the Hilbert-Huang transform (HHT) for detection of a broken-rotor bar fault in non-stationary conditions. The comparison was based on a number of criteria which included computational complexity and ease of interpretation of the representation. It was demonstrated that each technique could be used for detection of this particular fault and the advantages and disadvantages are given.

Tang *et al.*, [89] attempted to compensate for the two major weaknesses of the WVD in the detection of incipient faults in wind turbine gearboxes. The WVD is sensitive to background noise and this was reduced by applying the CWT in the form of a Morlet wavelet to the time domain of the vibration signal. The WVD is also sensitive to internally generated cross-terms which were suppressed using an Auto Term Window (ATW) function based on the Smoothed Pseudo Wigner-Ville Distribution (SPWVD). It was claimed that the method was effective in suppressing cross-terms and background noise, gave high time-frequency resolution and good energy aggregation and the fault features extracted were clear.

According to **Yang *et al.***, [90] the wavelet transform is an appropriate and efficient technique to analyse and monitor electrical generators and drive trains for mechanical faults. Information was gathered using a number of transducers to evaluate vibration, generator voltage, DC load current, shaft rotational speed and torque. Drive signals are rich in noise which it is hard to remove using of conventional filters with fixed cut-off frequencies. However, discrete wavelet transforms (DWT) can be used for noise deletion

and CWTs for character extraction. The electric signals from generator can be monitored and analysed to find drive train mechanical faults and those experiments showed that it is feasible and relatively easy to gather electrical signals from a wind turbine generator rather than torque, proximity or vibration measurements. Tsai *et al.*,[91] proposed a complex CWT based on signal entropy to differentiate between a healthy structure and an impaired turbine blade, for improvement of damage detection ability of wind turbine blades.

Abouel-seoud and Elmorsy [92] proposed wavelet fault feature extraction method based on the CWT for diagnosis of faults such as cracks in gear teeth and the main bearing inner race in planetary gearboxes. The time domain vibration signal was filtered to indicate the presence and progression of the fault. These researchers claimed that de-noising the vibration signals is a useful technique for enhancing fault detection hence determining the type of fault accurately and quickly.

Wenxian *et al.*,[93] have a proposed a versatile method of CM which will diagnose both mechanical and electrical faults in a wind turbine. The test rig used was built to simulate wind turbines working under different conditions and consisted of a 50 kW DC variable speed drive controlled motor, a two-stage gearbox with gear ratio 11.14:1, and a three-phase synchronous permanent-magnet generator. Voltage and current signals were accessed through the terminals of the generator, vibration transducers were fixed to the test rig, and shaft torque and rotational speed were measured. Induced mechanical faults included rotor imbalance which was simulated by attaching a mass to the outer surface of the generator rotor. The drive train mechanical fault was simulated through an

eccentricity fault in the gearbox. The electrical faults were generator stator winding faults simulated by simultaneous shorting of the load bank to ground, and a full short circuit fault simulated by connecting one of the phase terminals of the generator and resistance bank to ground. The data measured from the terminal generator was analyzed using empirical mode decomposition (EMD) which can remove variations in the signals due to such factors as variable wind and was able to detect both the mechanical and electrical faults.

Parey *et al.*, [94] developed a 6-degree-of-freedom dynamic model for a real gear system consisting of a spur gear pair, two shafts, two inertial loads a prime mover and bearings. A localised tooth defect (pitting) was then introduced into the model. The simulated and measured vibration signals were compared and EMD was used to "break down" the time domain vibration signal. Early detection of the pitting fault was obtained by decomposing the gear vibration signal into a number of intrinsic mode functions (IMFs) and then calculating the Crest Factor and Kurtosis for each IMF. Unfortunately these researchers restricted their work to pitting and did not consider other gear faults such as cracks and/or breakages in gear teeth.

Yang *et al.*, [95] developed a new technique, Bivariate Empirical Mode Decomposition (BEMD), for use with wind turbine condition monitoring for incipient mechanical and electrical faults. The authors recognise the efficiency and effectiveness of the EMD technique, but point out that it was developed for one dimensional signals which can be a severe limitation when wanting to fuse data to obtain a more rounded assessment of a fault condition. BEMD using a recently developed wavelet-based 'energy tracking'

technique was proposed as a method of overcoming this disadvantage. Experimental results showed that the BEMD-based technique was better than EMD for assessing shaft vibrations, and more powerful than EMD and wavelet-based techniques when processing non-stationary and nonlinear signals.

An *et al.*, [96] applied ensemble empirical mode decomposition (EEMD) and Hilbert transform to the time domain vibration signal to investigate a loose bearing pedestal in a direct-drive wind turbine. IMFs were extracted very effectively from the measured vibration signals using the combination of EEMD and Hilbert transform. The authors claim that the efficiency of this method was verified by information extracted from experimental signals for the loose bearing pedestal.

Feng *et. al.*, [97] proposed a joint amplitude and frequency demodulation analysis method based on EEMD and an energy separation algorithm to monitor and diagnose planetary gearbox faults. Vibration signals from the planetary gearbox of a test rig representing a wind turbine drive train were decomposed into a finite set of IMFs using EEMD. Each IMF represented a different vibration source. The energy separation algorithm was used to approximate the amplitude of the envelope and the instantaneous frequency of the modulated signals ready for further demodulation analysis. The authors claim that this method is sensitive to both wear and chipping damage of the gears, and by using these methods, these faults can be diagnosed and located.

Tsai *et al.*,[98] applied a wavelet transform approach using a Meyer basis function for enhancing the damage-detection capability of wind turbine blades to distinguish

between damaged and undamaged structures of a turbine blade. The test results showed successful discrimination in blade-damage detection in different conditions.

Baydar and Ball [99] utilized the instantaneous power spectrum (IPS) for detecting local of faults in helical gears and assessing fault severity. The study showed that changes in the IPS can provide useful information on the presence and progression of faults in a gear. The IPS can be used locate a defect by noting the frequencies of the peaks in the spectrum even under varying loads and speeds.

Kar and Mohanty [100] carried out an experimental investigation to determine the presence of faults in a multistage gearbox under transient loading. The experimental work investigated three defects under three transient loads. The DWT and a milti-resolution Fourier Transform (MFT) were used to investigate the transient vibration signal from an accelerometer sited on the tail-end bearing of the gearbox, and transient current signals drawn by the induction motor. The RMS values of the MFT coefficient of vibration transient were calculated at various discrete frequencies to facilitate distinguish various faults in gears undergoing fluctuation in loads.

2.4 Summary

Monitoring of wind turbines assists in avoiding unplanned downtime and can be an aid to prevent damage of the wind turbine. Recently, CM methods for rotating machinery have been also applied for monitoring wind turbines. Most of those methods have been carried out offline and the focus was other wind turbine components e.g. gearbox and generator. It is also noted that only a few studies investigated blades health monitoring and no online monitoring methods were reported in the literature. Different condition monitoring

technologies are widely used to monitor wind turbines condition such as: vibration, acoustic emission, lubricant analysis, motor current, thermography and ultrasonic measurement. Vibration analysis, acoustic emission and ultrasonic methods are often used to monitor blades after the manufacturing process. Vibration is the most effective method to monitor wind turbine blades online to avoid breakdown. Therefore, this research project focuses on detecting and diagnosing faults of wind turbine blades using vibration analysis techniques and possibility of real-time monitoring. The review revealed that various methods of analysing information have been used for monitoring the condition of rotating machinery, including simple statistical parameters such as: RMS, Standard Deviation, Kurtosis, Mean, Skewness, Crest Factor, and Impulse Factor which were used to extract statistical properties of the time domain signals. Beside that Fast Fourier Transform FFT and Short-Time Fourier Transform (STFT) are commonly used for condition monitoring purposes in rotating machineries. Moreover, Principle Component Analysis (PCA), Independent Component Analysis (ICA) and kernel principal component analysis (KPCA) are used to characterize the condition of a gearbox. Other techniques such as Wigner-Ville Distribution (WVD), Pseudo Wigner-Ville transform (PWVT) and Continuous Wavelet Transform (CWT), are a time-frequency method which has been widely used in machine diagnostics. The discrete wavelet transforms (DWT) were used for noise deletion and CWTs for character extraction. Another technique, Empirical mode decomposition (EMD), is used to remove variations in the signals due to such factors as variable wind and was able to detect both the mechanical and electrical faults. Bivariate Empirical Mode Decomposition (BEMD) is used with wind turbine condition monitoring for incipient mechanical and electrical

faults. Also, Ensemble empirical mode decomposition (EEMD) and Hilbert transform is used to investigate a loose bearing pedestal in a direct-drive wind turbine.

The above mentioned techniques have been used for rotating machinery condition monitoring including wind turbine gearbox and generator and have proved their success in detecting wind turbine electrical and mechanical faults. Thus, based on results that have been obtained after applying those methods, developing an inexpensive, flexible and innovative method to actively monitor the behavior of wind turbines is necessary.

Due to wind turbine vibration complexity, modulation and the number of free degrees of freedom, empirical mode decomposition (EMD), continuous wavelet transform (CWT) and principle component analysis (PCA) are suitable analysis techniques for extracting blades condition related features.

Chapter 3

Dynamic Model of Horizontal Axis Wind Turbine

This chapter introduces the software packages used, then blade design and aerodynamic characteristics are given followed by the finite element simulation method and the work on component design. Model analysis and vibration characteristics of the blade are explained in detail followed by a chapter summary.

3.1 Introduction

During service life wind turbine blades are exposed to conditions which excite severe vibrations and which can have an adverse effect on dynamic behavior and even lead to structural damage. Much theoretical and laboratory research has been carried out in an attempt to improve overall wind turbine efficiency, with an emphasis on reducing condition monitoring (CM) and maintenance costs and, in particular, techniques for the CM of turbine blades[101].

This project has designed a horizontal wind turbine, using the SolidWorks and ANSYS software packages version11.0, to study blade vibration characteristics of a simulated wind turbine in order to predict blade behaviour and assess whether nacelle vibration carries useful information about the health of the wind turbine blades and other components. Such an approach is relatively inexpensive and gives the possibility of simulating faults, such as cracks in the blades, into the system. The results were used to develop a wind turbine test rig to confirm experimentally whether this method can be developed into a wind turbine CM system.

From known parameters (e.g. Reynolds number) the software calculated dimensionless lift, drag and pitching moment coefficients for a selected blade, and their optimum values were found from lift/drag polar curves and moment modelling data. The results were used to select the aerofoil with best overall aerodynamic performance on the basis of a 3D model.

Here, a National Advisory Committee for Aeronautics (NACA 2412) blade profile was selected and the pitch-line velocity and gear bearing specifications (e.g. tooth bending stress) were determined. Then the SolidWorks software was used to generate a 3-D model of a horizontal axis wind-turbine with three airfoil blades. Cracks were simulated in one of the three blades. The cracks had one of four lengths: 10 mm, 20 mm, 30 mm and 40 mm. Every crack

was 3 mm wide and 2 mm deep. Cracks were seeded on the blade 5 cm close to the root, where the stresses due to bending are greatest. ANSYS software was then used to study the natural frequencies of vibration for healthy and faulty blades so that their behaviour could be predicted at different rotational speeds when in situ in the wind turbine. The simulated and experimental results were compared and the vibration signals generated by the model were used in the study of the effects of real cracks in the blade.

3.2 Airfoil Characteristics and Blade Design Aspect

3.2.1 Blade Shape

The shape and orientation of an airfoil are key in creating the differences in velocities and pressures which generate the aerodynamic forces on the airfoil, its boundary layer profiles and separation characteristics. Designers take great care determining the optimum shape for the airfoil for a particular design. Today computer programs generate and optimise these airfoils, but many initial airfoil shapes are chosen from published data. Airfoils are often classified into families or groups of similar shapes, each member differing from the next by a gradual change in one or other of its shape parameters. Figure 3.1 shows a typical airfoil and the parameters which describe it.

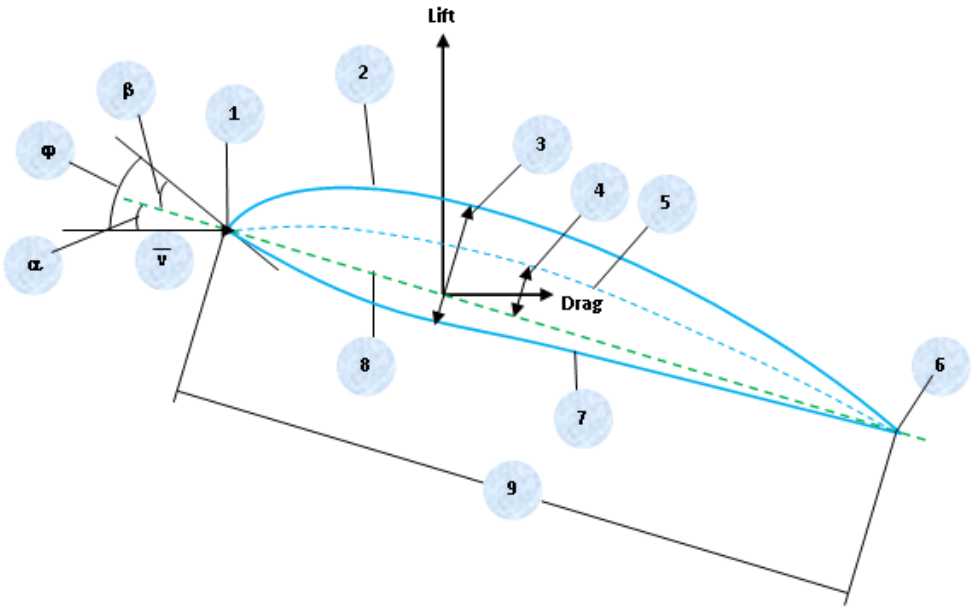

1-	Leading edge	2-	Upper surface	3-	Maximum thickness
4-	Maximum camber	5.	Camber line	6-	Trailing edge
7-	Lower surface	8-	Chord line	9-	Chord length

Figure 3.1 Airfoil geometric parameters

From general considerations we can say that the blade angle β should be set to give this angle of attack (α), whilst the angle φ must be known. In practice, most airfoil sections produce their best lift when the angle of attack is about 4^0 or 5^0. The angle of attack is the angle between the airfoil chord line and the relative air wind - direction of airflow in relation to the airfoil.

$$\beta = \varphi - 5 \qquad 3.1$$

Thus,

$$\varphi = \tan^{-1}\left[\frac{2}{3\left(\frac{r}{R}\right)}\right] \qquad 3.2$$

And

$$\beta=\tan^{-1}\left[\frac{2}{3(r/R)}\right]-5 \quad 3.3$$

The blade profile for each station along a turbine blade is determined by blade angle, β, and C the chord width;

$$C=\frac{5.6*R^2}{NC_l\lambda^2 r} \quad 3.4$$

Where λ is the tip speed ratio (TSR = ratio of speed of the tips of the turbine blade to the wind speed), r is the local radius at point of computation, R is the radius of the blade at tip, C_l is the lift coefficient and N is the number of blades.

Up to a certain value the lift increases with increase in angle of attack but if the angle of attack exceeds a certain value (called the critical angle of attack), the airflow over the top of the airfoil breaks away to form eddies, the airfoil loses lift and stalls [102].

3.2.2 Lift and Drag and Moment Coefficients

Wind tunnel measurements are usually used to evaluate lift and drag generated by an airfoil. The results are reported as dimensionless coefficients which are defined as follows:

Lift coefficient: $c_l=\frac{l}{1/2\rho V^2 S}$ 3.5

Drag coefficient: $c_d=\frac{d}{1/2\,\rho V^2 S}$ 3.6

Where *l* and *d* are the measured lift and drag forces for the particular airfoil, *S* is the area swept by the rotor blades (m²), sometimes denoted by the chord length, ρ is the local density of air and V is the velocity of the air(m/s). The pitching moment, M, is important for the stability of a

blade. NACA has shown both theoretically and experimentally that on most low speed airfoils the aerodynamic force acts at a location a distance of about ¼ the chord length back from the leading edge, and the magnitude of the turning moment (called the pitching moment) produced on the airfoil by this force remains nearly constant with angle of attack. The pitching moment acts to rotate the airfoil leading edge, where a "nose-up" moment is defined as positive. The dimensionless pitching moment coefficient, C_m, is given by:

$$C_m = \frac{m}{\frac{1}{2}\rho V^2 SC} \tag{3.7}$$

Where m is the turning moment and *C* is the airfoil chord length.

It is usual in airfoil simulations to set the centre of the pitching moment a distance of one quarter the chord length as a first approximate value [103]. Table 3.1 shows lift coefficient, pitching moment and estimated critical Mach number values that used in this study.

3.2.3 Reynolds Number

The Reynolds number (Re) is the non-dimensional ratio of inertial to viscous forces:

$$Re = \frac{\rho V^2/L}{\mu V/L^2} = \frac{\rho VL}{\mu} \tag{3.8}$$

In this study the Reynolds number is estimated as 68500 x chord length x wind speed. Here Re is between 25000 and 55000 so lift coefficient is estimated as close to zero. Aerofoil behaviour can be described into three flow regimes [1]: Attached flow regime; in this situation, lift increases with the angle of attack.

High lift/stall development regime; the lift coefficient peaks at the critical angle of attack and above this angle (which depends the Reynolds number) the airfoil becomes increasingly stalled. Stall occurs when boundary layer on the upper surface separates from the airfoil.

Flat plate/fully stalled regime; airflow over the airfoil is turbulent. Airfoil behaviour and aerodynamic performance will depend on aerofoil geometry so choosing an aerofoil applicable for a wind turbine blade (low wind speeds) will improve its efficiency [103].

3.2.4 Reading Airfoil Data Charts

As stated above, in this study a NACA 2412 blade profile was chosen because it has a well-defined critical angle of attack. NACA uses codes of 4, 5 or more digits to classify and define the airfoil shapes that they have tested. In the four digit series:

(i) The first digit gives the airfoil's maximum camber as a percentage of the chord length, so here this airfoil has a 2% camber, see Table 3.2.

(ii) The second digit gives the position of maximum camber behind the leading edge in tenths of the chord length, so here the maximum camber is 40% of the chord length behind the leading edge.

(iii) The third and fourth digits comprise a single number which gives the airfoil maximum thickness as a percentage of chord length, so here the maximum thickness of the airfoil is 12% of its chord length [104]. Figure 3.2 shows the profile of the NACA 2412.

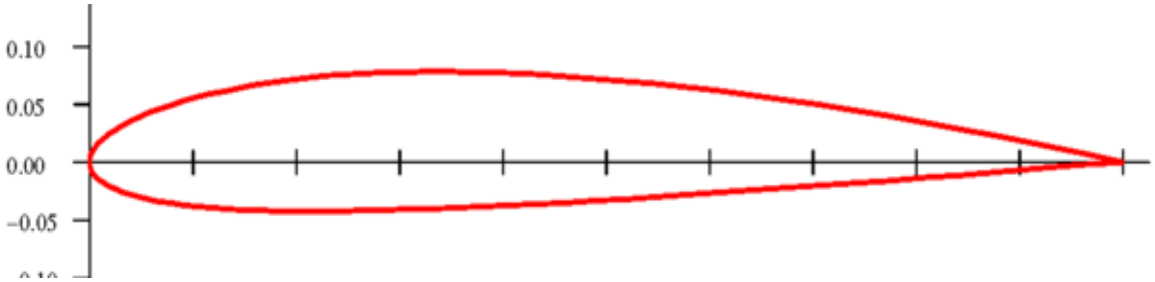

Figure 3.2 Profile for NACA 2412

Figure 3.3 shows the lift and moment coefficients of the airfoil section as functions of the angle of attack at four different Reynolds numbers (Re). The drag and lift forces for the airfoil were measured experimentally and the results are shown in Figure 3.4[105].

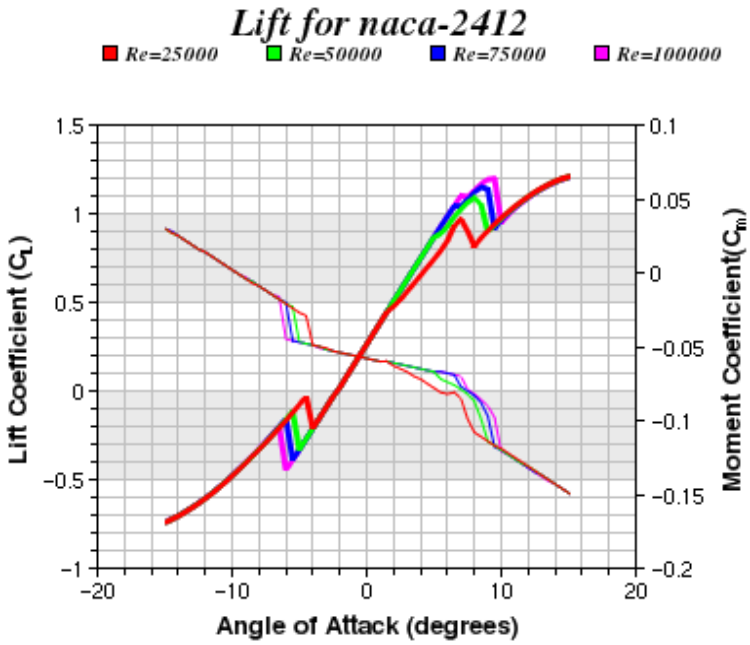

Figure 3.3 Lift and Moment coefficients vs. angle of attack at varying Re values

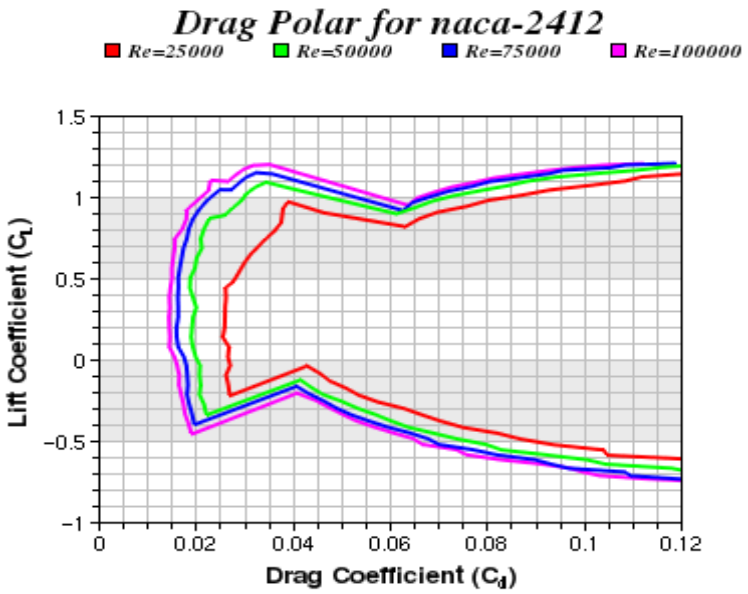

Figure 3.4 Lift coefficient vs. Drag coefficient at varying Re values

Table 3.1 NACA 2412 Results for incompressible potential flow (Aerofoil Investigation Database, 2012)

Parameters	Values
lift coefficient	0.847
leading edge pitching moment coefficient	-0.271
estimated critical Mach number	0.504

Table 3.2 NACA 2412 Airfoil properties in fractions of chord length

Parameters	Values
centre of pressure	0.184
maximum camber	0.02
maximum camber location from leading	0.4

3.3 Modelling in 3D with Software Packages

Many commercial software packages are used in engineering as mechanical analysis tools which assess the relative merits of different designs. They are often used to assess machine performance and reliability from concept through design and development to finished product. These programs offer modal analysis and shape, structural and thermal optimization studies. This project used the SolidWorks software package to design the components of the wind turbine and then to assemble them into a 3D three bladed horizontal wind turbine. The ANSYS software package was used to investigate the dynamic behaviour of the blades and to simulate vibration for healthy and faulty conditions at different rotational speeds. The use of these packages in the design of the wind turbine and simulation of its performance accelerated development and provide feedback on multiple fault scenarios which could reduce maintenance costs. It also allowed simulated machine behaviour to be monitored under different condition modelling real conditions.

3.3.1 The Principle Theories Relevant to Modelling

Deriving the governing equations (e.g. mass, momentum and energy) is a necessary precondition for accurate modelling. Initial and boundary conditions are also essential. For meshing models the next step is to create a mesh of cells which places the discretized equations and boundary conditions into a single grid. 2D unstructured grids have basic elements which are triangular or quadrilateral cells, but for structured grids rectangular cells are more common. In 3D simulations unstructured grids tend to use cells which are tetrahedra and/or pentahedra, and in structured grids the hexahedra cell is used. Good mesh quality is essential to obtain a reasonably accurate physical solution, traditionally selection of a suitable mesh was a measure

of the ability of the simulation engineer, but modern packages have remeshing built into them. Generally, the finer the mesh the larger the number of nodes and the greater the computational time needed to solve the problem. So selecting an efficient mesh was indispensable. Today however, the package automatically adapts the mesh size to the problem, making changes as the simulation proceeds. One of three numerical methods is used to discretize equations: finite element method (FEM), finite difference method (FDM) and finite volume method (FVM). With FVM and FEM problems are relatively easily formulated compared to FDM, and have the advantage that they can cope with unstructured meshes, have greater flexibility and so can be applied to a variety of geometries.

3.3.2 Finite Element Method (FEM)

The FEM is a numerical method to solve engineering problems defined by the user [106]. First applied to stress analysis problems it has since been used to solve problems in fluid dynamics, material behaviour, thermal analysis, and many more. The researchers attempt to determine the behaviour of a field variable such as displacement in material behaviour or the temperature in thermal analysis, and so on.

The FEM attempts to find a close approximation of the solution numerically, when it is difficult or impossible to obtain an analytical solution. This is achieved by dividing the domain of interest into many elements which usually have a relatively simple geometry. Known physical, chemical and/or biological laws are then applied to each small element. The field variable – which is a continuous function - is approximated using a straight line function in each element formed by the nodes. The shorter these “lines” the more exactly they approximate the continuous function. The discrete values of the field variable at the nodes are then the

unknowns. The known equations are used to determine the equations for these "lines", after which they are joined to each other. This process gives a set of simultaneous equations which define the entire system and can be solved to give the desired field variable [107].

Here the FEM used for modal, static, and dynamic analysis is a commercially available software package called ANSYS version11.0. Modal analysis determines such parameters as natural frequencies and mode shapes of a structure. Static solutions are suitable for steady state loading on a structure in equilibrium. Dynamic or time-transient analysis determines the time response of a structure to e.g. a displacement or applied force [108].

3.4 Three-dimensional Wind Turbine Modelling

3.4.1 Blade Design

Inserting the equations from 3.1 to 3.8 into Microsoft Excel and using logic commands, the blade angle and chord width were calculated as shown in Table 3.3:

Table 3.3 the blade angle and chord width values

	A	B	C	D	E	F	G
1	**Blade design spreadsheet**						
2							
3							
4	Tip speed ratio	λ		5			
5	Diameter (m)	D		0.44			
6	number of blades ?	B		3			
7	angle of attack (degrees)	α		5			
8	Lift coefficient	Cl		0.8			
9	No. of stations	STN		5			
10							
11							
12	station	Local radius	ϕ	β	β	Chord width	
13		(r) meters		(radians)	(degrees)	C (meters)	
14	1	0.0440	33.6925	0.5007	28.6925	0.0711	
15	2	0.0880	18.4363	0.2345	13.4363	0.0462	
16	3	0.1320	12.5297	0.1314	7.5297	0.0326	
17	4	0.1760	9.4630	0.0779	4.4630	0.0250	
18	5	0.2200	7.5952	0.0453	2.5952	0.0202	
19							
20	All dimensions in metres.	[0.001m=1mm.]					
21							

Each station on the blade is defined by three variables: local radius (the distance from blade root to the individual station), chord width and blade angle (the angle of twist of the blade). NACA defines aerofoil profiles using Cartesian x,y and z coordinates for each station of the aerofoil as a percentage of the the total chord length. To obtain the coordinates for the blade chords shown in, the NACA 2412 station coordinates in percentages are multiplied by the chord widths. For example, at station 1.25% the coordinate for the chord of length 0.0711 m is: $1.25*0.0711/100 = 8.888x10^{-4}$ m = 0.8888 mm (conversion to millimeters makes for easier plotting in SolidWorks). Very large turbine airfoils will require as many as 120 points on each of the upper and lower surfaces of the blade, but for this project 18 points are sufficient to define the blade geometry accurately. Five Sketch planes were created and offset 44 mm apart. The coordinates were converted to Notepad files and imported into SolidWorks as spline curves which were then converted to sketches as specified in the Blade design spreedsheet. Using the loft command to join the profiles at the local radi, a well engineered wind turbine blade was created and modelled as can be seen in Figure 3.5.

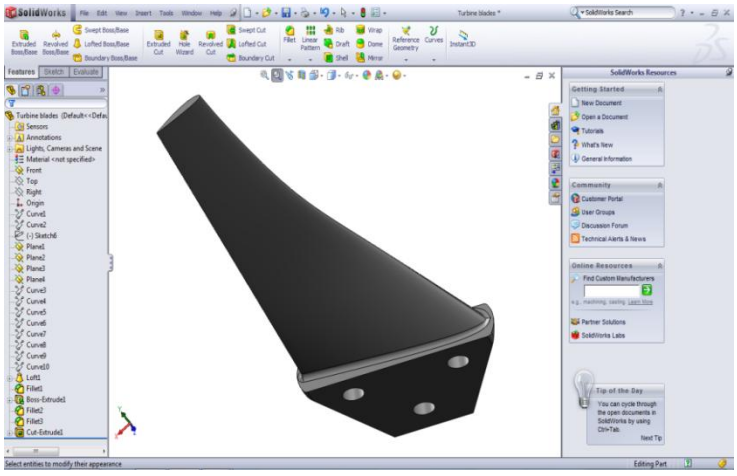

Figure 3.5 Final blade design

3.4.2 Hub Design

After designing the blade the hub is the next most important part of the design: to make it as lightweight as possible but with the strength to ensure mechanical integrity. The blades of a wind turbine are joined to the hub which, in turn, is connected to the drive shaft. Being wind driven this shaft will operate at low speeds and the hub was a circular block (150.7 mm diameter and 16 mm width, see Figure 3.6) of Nylon 6; a tough plastic material that is easily machined

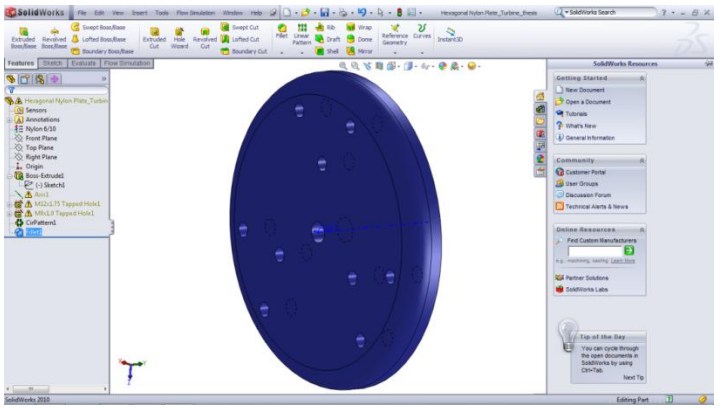

Figure 3.6 Hub model in SolidWorks

3.4.3 Helical Gears Design

Helical gears were selected for this project after thorough research. Figure 3.7 labels the various elements of a helical gear. In a pair of gears, the larger is the gear and the smaller is the pinion. Helical gears have their teeth inclined to the axis of rotation and this produces a more gradual engagement of the teeth than occurs with spur gears which generates less noise and vibration. An important feature of helical gears is that they can be used to transmit motion between non-parallel shafts. The most important part of the gear is the tooth and the use of

gears must ensure maximum tooth bending stress is not exceeded. The pitch-line velocity and maximum tooth bending stress were calculated, see Table 3.4.

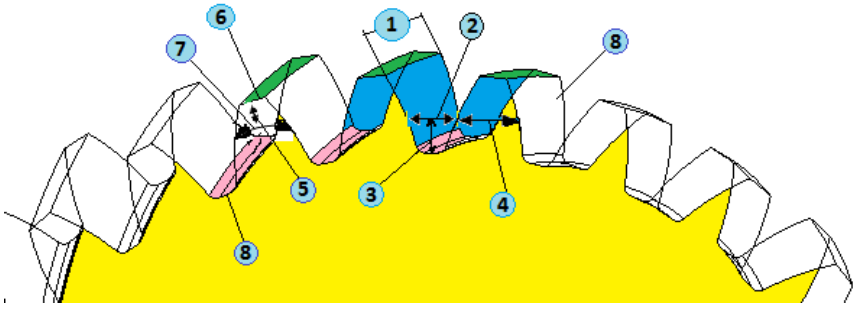

Figure 3.7 Nomenclature of helical gear

1- Face width	2- Space width	3- Dedendum	4 Circular Thickness
5 -Addendum	6 -Addendum Circle	7 -Pitch Circle	8 Face

Table 3.4 Equations used in calculating the maximum bending stress for gears.

Pitch line velocity (v)	$v = \frac{\pi * d * N}{6 * 10^4}$	where N is the rotation speed, d is the pitch diameter	6.82 m/s
Dynamic factor (Kv)	$K_v = \frac{6.1}{6.1 + v}$	where v is the pitch line velocity	0.47
Module (m)	$m = {}^{d}/_{x}$	d is pitch circle, x is the number of teeth.	2
Transmitted load (Wt)	$W_t = \frac{power}{v}$	where v is the pitch line velocity	5.61 N
Tooth bending stress (σ)	$\sigma = \frac{W_t}{mk_vYF}$	where Y=0.355 is the Lewis form factor, the number of teeth is 30, F is the face width	935.04 Nm-2

Using the formulae above the required factors were calculated and SolidWorks used to simulate the helical gears, see Figure 3.8 and Figure 3.9.

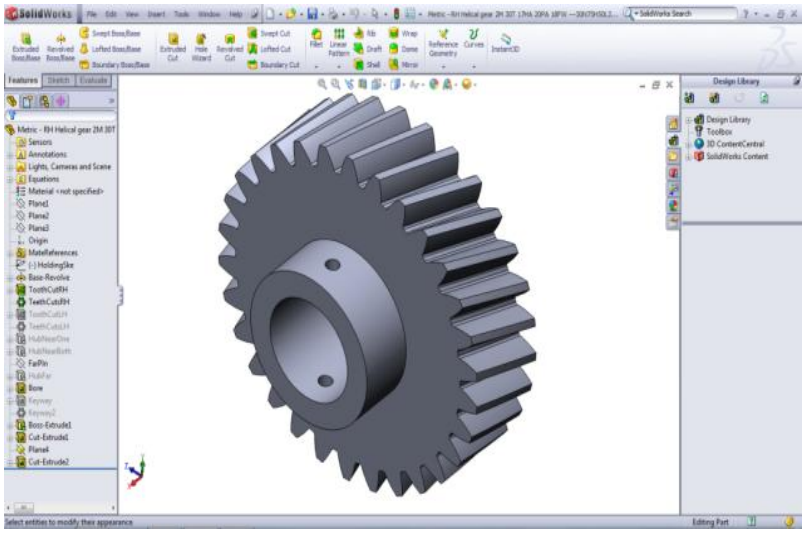

Figure 3.8 Input gear

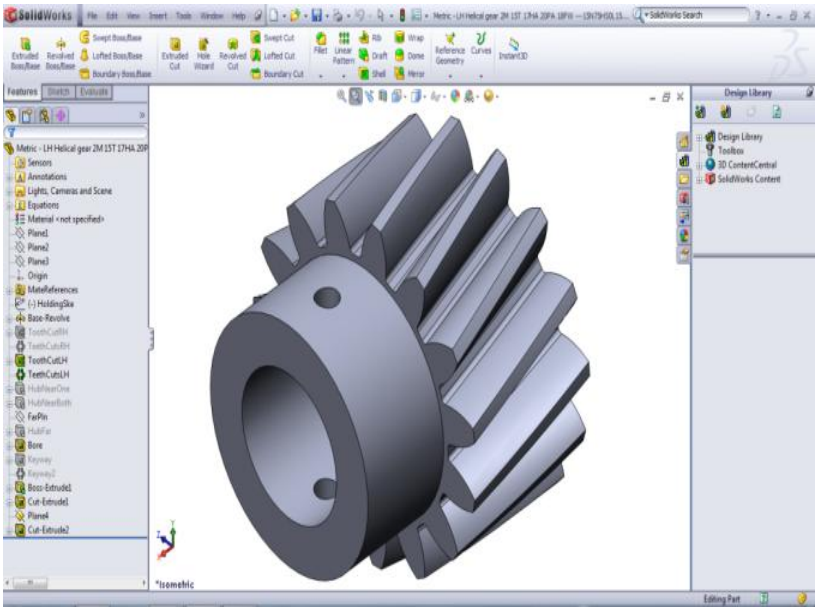

Figure 3.9 Output gear

3.4.4 Bearings Design

Bearings were used to transmit loads efficiently from the superstructure to the substructure and to provide for expansion, contraction, and rotation of the superstructure. Their main purpose was to allow a shaft to spin smoothly and to bear loads.

Table 3.5 shows the bearing specifications calculated and verified for this project. Figure 3.10 illustrates the physical parameters of the bearings, while Figure 3.11and Figure 3.12 show the SolidWorks bearing model.

Table 3.5 Bearing specifications

Basic bearings	Inner diameter d, mm	Outer diameter D, mm	Width mm	Basic load Rating KN		Reference speed	Limiting speed	Radius , mm	Ball complement		Weight, kg
				Dynamic load	Static load				Number of balls	Size, mm	
Input bearing	20	32	7	13.5	6.55	32000	17000	0.3	12	4	0.018
Input bearing	15	28	7	4.36	2.24	56000	16000		12	4	0.016

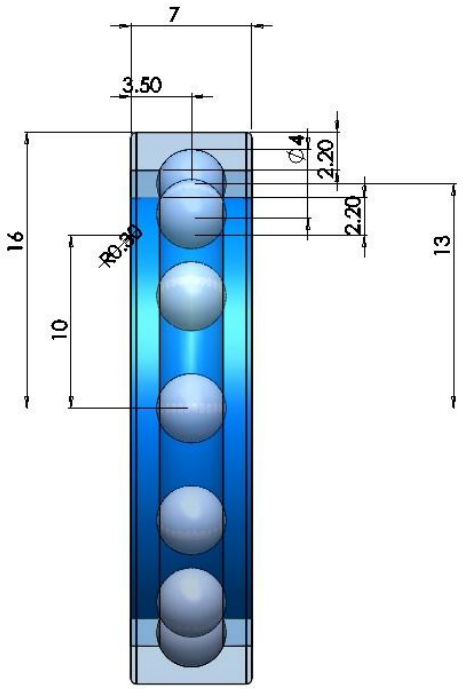

Figure 3.10 Physical parameters of input bearing

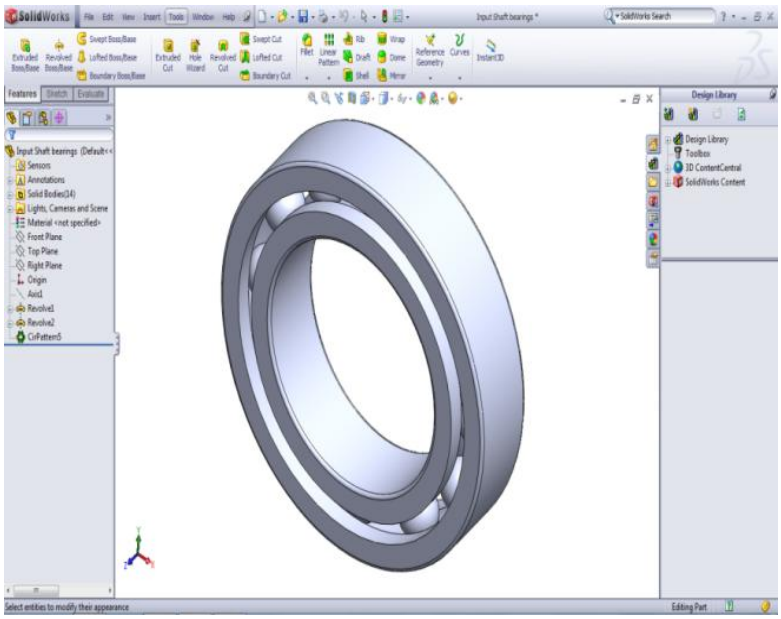

Figure 3.11 Input bearing

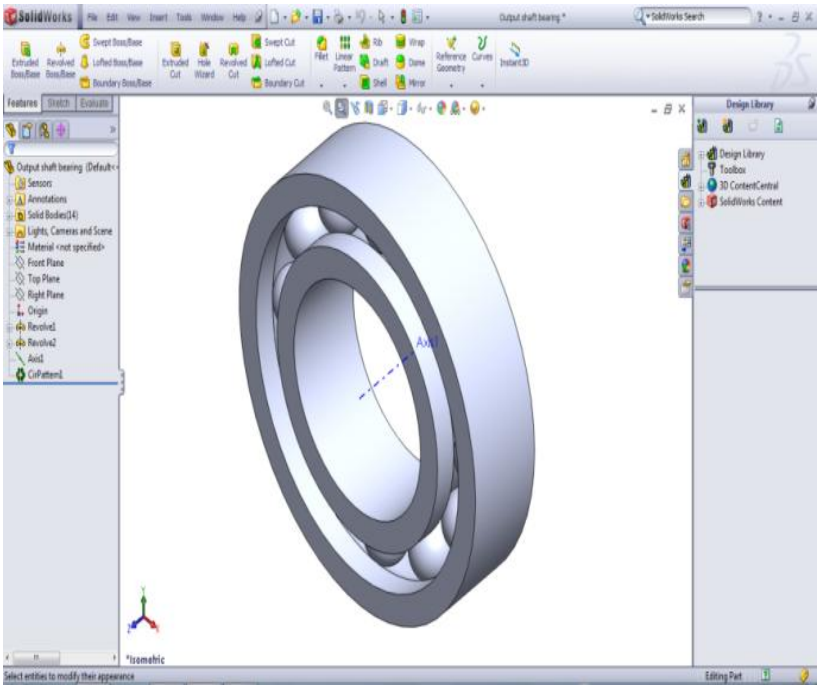

Figure 3.12 Output bearing

3.4.5 Shaft Design

Shafts invariably have a circular cross-section because they rotate and are used to transmit power or motion. By virtue of its function the shaft acts as the axis of rotation of such elements as gears, flywheels and cranks and controls their motion. In this study two shafts were created, see Figure 3.13 and Figure 3.14. The low speed shaft was 156.2 mm long and the high speed shaft was 88.3 mm long.

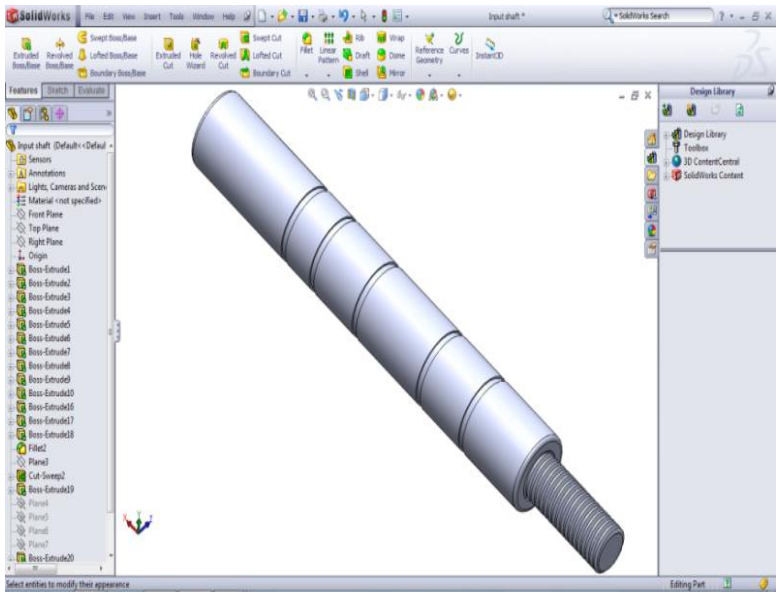

Figure 3.13 Low speed shaft

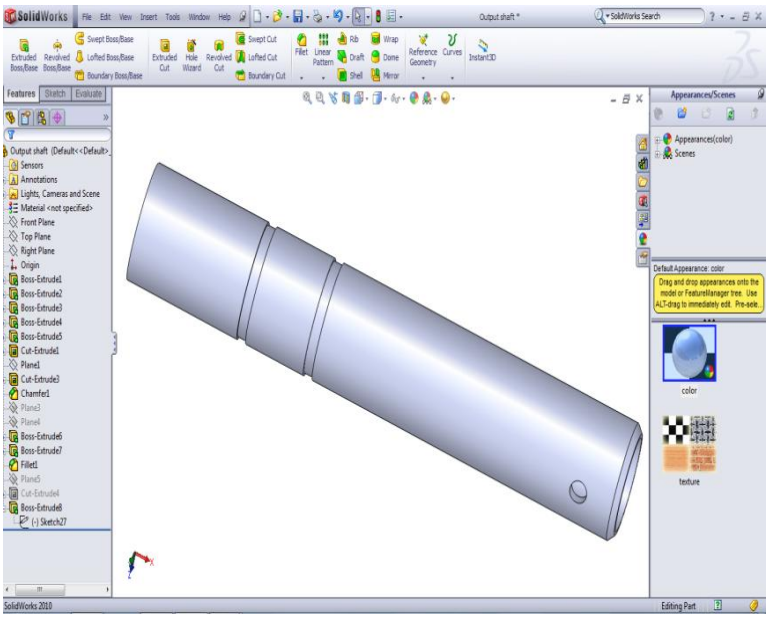

Figure 3.14 High speed shaft

3.1.6 Nacelle and Tower Design

The nacelle protects the bearings, gears and generator from the local environment, and humans from any parts that break off. The nacelle was 280 mm long, 150 mm wide and 150 mm high. Aluminium was chosen as the material for the nacelle because it is reasonably strong, can be made corrosion resistant relatively easily, is non-magnetic and, in the given circumstances, non-combustible. The nacelle can be opened from above (lid), and can also be opened from the left and right sides for repairs. The tower is an important parts of a wind turbine. It supports the rotor and the blades at an appropriate height for efficient operation. Generally the tower is a structural item of large mass and high initial cost. They tend to be manufactured from steel (truss or tubular) or reinforced concrete. The tower used here was made from steel and had a height of 900 mm and 50 mm diameter. All the assembly drawings of the wind turbine components including the tower were produced using SolidWorks software, see Figure 3.15.

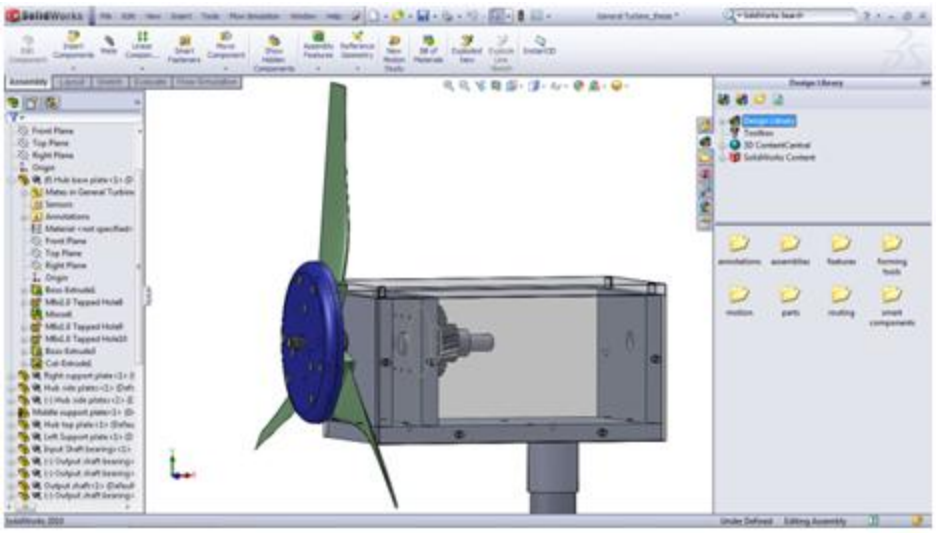

Figure 3.15 Wind turbine assembly in SolidWorks

3.5 Vibration Analysis by Finite Element Package ANSYS

3.5.1 Modal Analysis

Each component of the wind turbine including the airfoil blades were simulated, using the measured dimensions and actual material properties and subjected to modal analysis to determine the natural frequencies of the system so that the frequencies of excitation of the system did not coincide with system resonances.

This section focuses on the modal analysis procedure used in the experiment with a horizontal axis wind turbine. The aim is to give an overview of the theory and then to extract natural frequencies. The formulation of a mathematical model of a wind turbine blade first requires the idealization of the structure. Then, the equations of motion governing the natural vibrations of the model may be found. For harmonic vibration these have the following form:

$$([k] - \omega^2[m])\{X\} = \{0\} \qquad 3.9$$

Where k is the stiffness matrix, m is the mass matrix, X is the displacement amplitude vector and ω is the frequency of vibration. Equation 3.9 which may be solved by standard techniques to give the natural frequencies (ω_i) of the system and the corresponding mode shapes (Φ_i). The generalized mass [M] and generalized stiffness [K] can be obtained from:

$$[M] = [\Phi]^T[m][\Phi] \qquad 3.10$$

$$[K] = [\Phi]^T[k][\Phi] \qquad 3.11$$

Equations 3.10 and 3.11 allow the free vibration equations to be written as uncoupled differential equations:

$$[M]\{\ddot{Y}\} + [K]\{Y\} = \{0\} \qquad 3.12$$

Equation 3.12 may be solved for any given applied force, and the total response may be obtained by superposition [101].

3.6 Execution of Computations

Structural analysis is carried out using the FEA package ANSYS. This required meshing the model into a FEM as shown in Figure 3.16. The root of blade was assumed fixed (no displacement) and material properties were defined. The material used was a glass reinforced plastic. The generated model had 260 elements with 1554 nodes. A free vibration simulation was performed for a healthy blade and blade suffering from a crack. The analysis took between 6 to 10 seconds to determine the first 5 mode shapes.

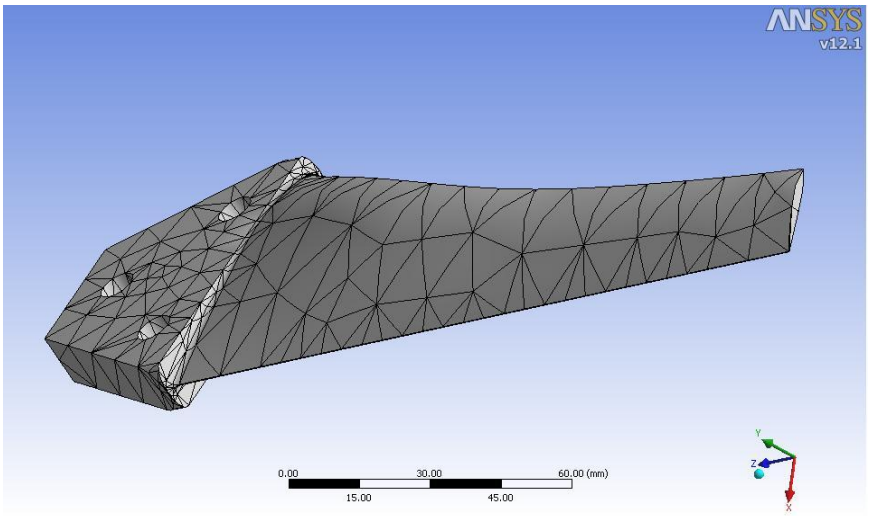

Figure 3.16: A 3D finite element model of blade

3.7 Mode Shape Identification

Vibration analysis is necessary in order that excitation of the natural frequencies and therefore resonance phenomenon can be avoided. It is also possible to detect areas of excessive movement which could weaken the material and possibly cause failure of the blade [101]. With rotational symmetry, natural frequencies can superimpose and identification of mode shape can be difficult. However, this turbine blade was sufficiently asymmetric that every mode shapes was clearly discernible and there was no confusion about which mode was associated with which natural frequency. For this analysis it was assumed that the mode shapes are the same for every blade.

3.8 General Trends in Response

3.8.1 Healthy Natural Frequency Results

The wind turbine blade was clamped at the root. The frequencies of each mode can be seen in Table 3.6.

Table 3.6: Five mode shapes with corresponding natural frequency

Mode	Natural frequency
1	31.458 Hz
2	166.04 Hz
3	340.40Hz
4	437.28 Hz
5	481.49 Hz

In Table 3.6 the first mode shape corresponds to first order of bending (these are transverse vibrations similar to those of a cantilever beam fixed at one end), second mode shape represents the second order of bending, third mode shape shows first order of bending in the x direction (the force applied transverse), the fourth mode shape gives the third order of the bending in *y* direction and fifth mode shape is the torsional vibration.

3.8.1.1 First Mode Shape

Figure 3.17 shows the first mode of vibration, it is a bending mode in the perpendicular *y* - direction about the root. The natural frequency was 31.458 Hz. The parameters affecting root stiffness have a substantial impact on the frequency of the first mode. This frequency is also influenced by tip mass but section stiffness has very little impact. In this mode shape, the airfoil is tending to bend around the root section's minimum moment of inertia.

3.8.1.2 Second Mode Shape

This is also a bending mode but in the *x*-direction, and again the airfoil is tending to bend around the root. The natural frequency was 340.40 Hz. This frequency is higher because of the greater stiffness in this direction. The greater chord length of the airfoil root section also increase stiffness for this mode thus increasing its frequency. Tip mass affects this frequency in a similar manner to the first mode frequency.

3.8.1.3 Third Mode Shape

The third mode is torsional with a natural frequency of 481.49 Hz. The vibration is characterized by the twisting of the airfoil tip. The 481.49 Hz is a function of torsional stiffness of both root and midsection of the airfoil and tip rotational moment of inertia. There is very

little displacement in the root area. If we focus on only the first order of each mode we will have the Table 3.7 :

Table 3.7: Three main mode shapes with natural frequencies

First Mode	**Natural frequency, (Hz)**
***y*-direction**	31.458
***x* –direction**	340.40
Torsional	481.49

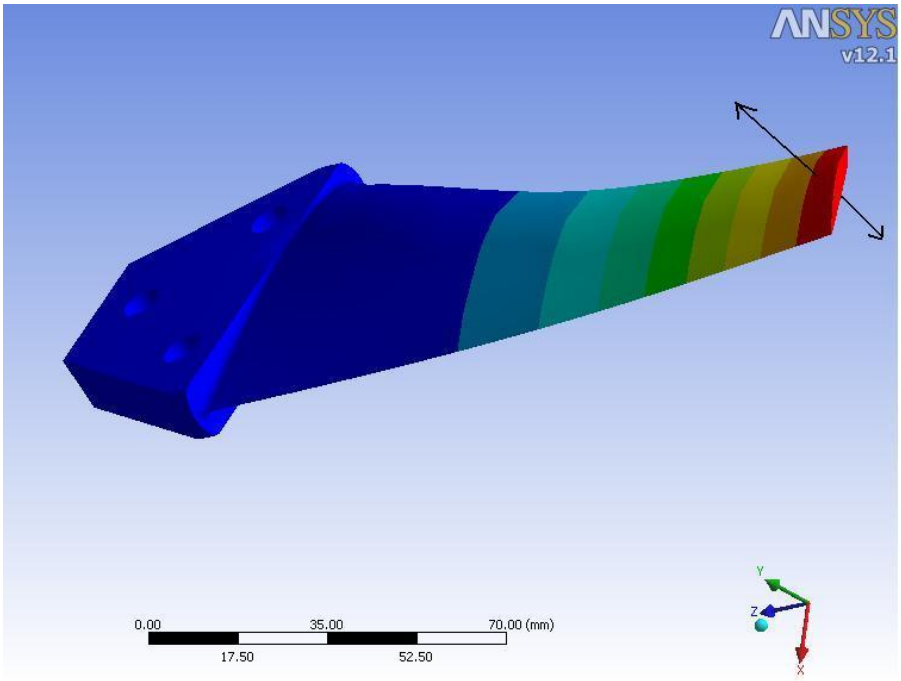

Figure 3.17 The first mode shape 1 at 31.458 Hz

3.8.1.4 Multi-blade Natural Frequencies

The natural frequency of three blades is different from the natural frequency of a single blade because the three blades are part of a system which includes the hub and shaft. Thus having a number of blades will change the natural frequencies and the modes. Determining the natural frequency for wind turbine blades as group coupled to the hub, may explain many blade failures and help designers and engineers to better understand blade behavior and to build more reliable blades. A finite element program was used to simulate a structure consisting of a group of three blades attached to a common hub, and evaluate the eigenvalues for the healthy case, see Figure 3.18.

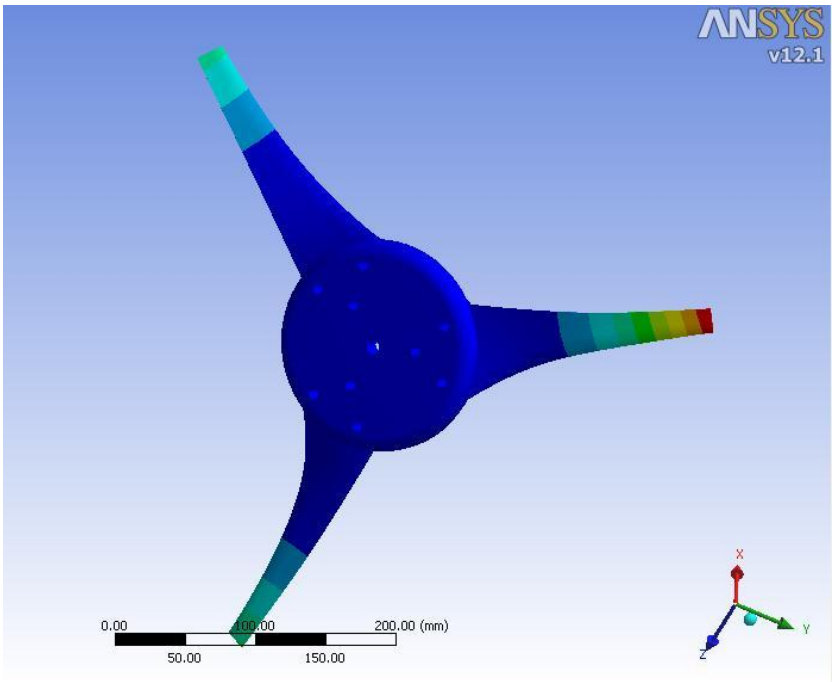

Figure 3.18 First mode shape of multi-blades at 34.95 Hz

Table 3.8 shows that the number of blades affected the magnitude of frequencies. By comparing the first mode of a single blade and multi-blades the effect on the natural frequency can be seen.

Table 3.8 Natural frequency of first multi-blade mode shape

First Mode	Natural frequency (Hz)
y-direction	34.950

3.8.1.5 Natural Frequencies for Healthy and Faulty Blades

The simulation work was carried out on a healthy blade and a blade suffering from the cracks specified in Section 4.1. For the healthy blade the first mode had a frequency of 31.458 Hz, with crack of length 10 mm the natural frequency fell very slightly to 31.441 Hz; with the 20 mm crack the natural frequency was 31.368 Hz, for the 30 mm crack - 31.231 Hz, and for the 40 mm crack - 31.101 Hz. Table 3.9 shows the first mode frequency for a single blade suffering from the four different length cracks.

Table 3.9: First mode single blade, natural frequency for healthy blade and blade with four seeded cracks**.**

Natural frequency, Hz	Condition of blade
31.458	Healthy
31.441	Fault 1
31.368	Fault 2
31.231	Fault 3
31.101	Fault 4

It can be seen from Table 3.9 that with increase in crack length [(all cracks with same depth (2 mm) and thickness (3 mm)] there was a slight decrease in resonant frequency. The introduction of the 40 mm long crack reduced the resonant frequency of this particular mode by only about 1%.

3.8.2 Overall Wind Turbine Vibration Simulation

ANSYS software was used to simulate the vibration signals produced by a wind turbine with three healthy blades, see Figure 3.19. The time domain of the simulated vibration signal for the healthy case and speed of 250 r/ min is shown in Figure 3.20.

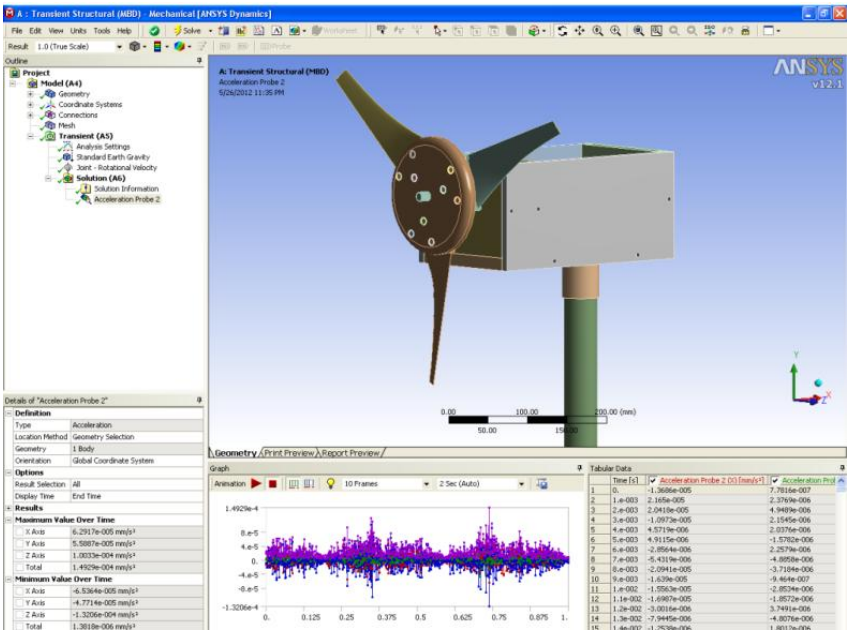

Figure 3.19 Simulated vibration signal for healthy system

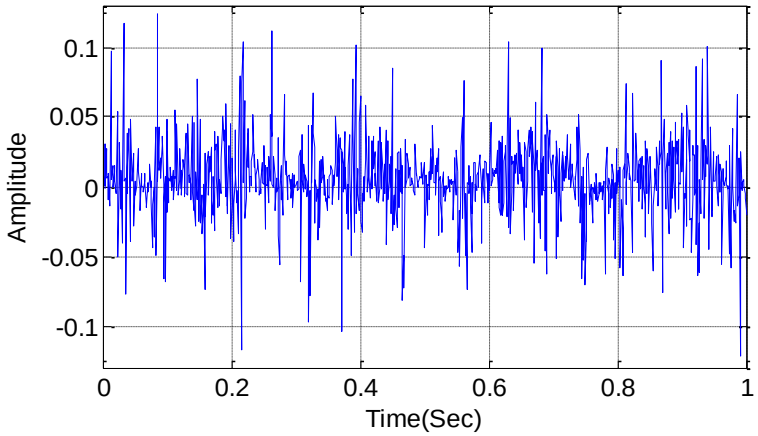

Figure 3.20 Time domain of simulated healthy vibration signal**.**

3.9 Summary

The aims and objectives of this chapter have been achieved. A 3D wind turbine simulation model has been developed using the SolidWorks software package and then imported into the ANSYS software package. Comparisons between the ANSYS results and experimental data for different conditions, presented in the next chapters, show ANSYS is a reliable benchmark.

Simulation has the capability of modelling the system over a wider range of rotational speeds than can be achieved experimentally. Also an analysis of the natural modes of the blades was performed very quickly using ANSYS so that unwanted resonances could be avoided. In this regard three analyses were performed: (i) an analysis of a single healthy blade, (ii) analysis of a single faulty blade, and (iii) an analysis of three healthy blades on the hub.

The results confirm that the ANSYS software package offers a quick and accurate method of investigating resonance phenomena in wind turbines, and subsequently ANSYS was used to

simulate vibration data for different conditions of blades. The simulated outcomes will be compared with real-time vibration measurements in the next chapters.

The results obtained show that using such numerical simulation software can improve product quality, in particular, by helping to create the wind turbine in the most cost-effective manner, simplifying the overall design process, possibly decreasing manufacturing costs by enabling the investigation of the use of lower-priced raw materials. Moreover such software packages help researchers to understand wind turbines working principles and devise ways of increasing efficiency, reliability and reducing the cost of maintenance.

Chapter 4

Experimental Set-up and Fault Simulation

This chapter introduces the test rig and gives a complete description of test rig design and construction and makes an assessment of test rig suitability including safety precautions. A description of fault simulation is given. The equipment and sensors used in the test rig to collect data are described. The accelerometer (including sources of errors inherent in piezoelectric sensors and due to mounting), the amplifier, the data acquisition system, processing and analyzing software are explained. Finally the experimental procedure is described.

4.1 Introduction

Over the past decade many techniques and instruments have been used for fault detection and identification in complex rotating machinery such as wind turbines which has confirmed the necessity of comprehensive an on-line condition monitoring system for analysing and enhancing rotating machine performance

In this project a test rig was designed and purpose-built to simulate the behaviour of a real wind turbine. When faults were seeded into the rig it imitated the response of a real wind turbine and could be used to investigate methods for the detection and diagnosis of the seeded faults. All moving mechanical components in the system will generate vibration to some level, including; bearings, gears, shafts, unbalanced rotor of wind turbine (due to a cracked blade) and the supporting tower. Each of these will have a resonant frequency and if the frequency of an unbalanced driving force were to match any one of these then large amplitude vibrations would be expected, with possible structural damage. This study focuses on vibration and will investigate the use of vibration measurements induced by wind turbine blades, both healthy and faulty, for fault detection and fault severity evaluation.

4.2 Test-Rig Suitability

A three aerofoil bladed wind turbine was designed in advanced industrial diagnostics centre (AID) at Manchester metropolitan University (MMU) by the author and introduced as a key component of the test rig. Studies were conducted on the wind turbine with healthy blades to determine:

- The efficiency and overall performance of the test rig at different wind speeds,

- The experimental turbine performance curves and how power generation varied with wind speed,
- Whether the wind generator was performing correctly and how the performance of the test wind turbine comparing with the electricity power obtained from other wind turbines available in the laboratory,
- Typical wind speeds for the test rig with different electrical loads,
- The vibration behaviour of the wind turbine test rig at different rotational speeds for the healthy condition, and
- Whether the wind turbine test rig was safe, because the work with a wind turbine must be considered as potentially dangerous.
- Balanced turbine was assured by performing laser based alignment before data was collected.

4.3 Design and Fabrication of Wind Turbine Test Rig

The test-rig had to be capable of simulating the behaviour of a real wind turbine, of having representational faults seeded into it and for its behaviour to be monitored. Thus horizontal and vertical accelerometers were incorporated in the rig to be used to detect blade faults and monitor the condition of the wind turbine. The blades of the turbine (type were NACA 2412) were chosen to represent a typical wind turbine.

The design and construction of the wind turbine test-rig took one year to complete and was divided into three stages:

1st stage: Design and fabrication blades and other wind turbine components using SolidWorks software package.

2nd stage: fabricate the entire wind turbine rig in the mechanical engineering laboratory workshops at MMU. The wind turbine consisted of three airfoil blades; each blade was 32 cm long. The basic dimensions of wind turbine components are as listed in Table 4.1.

3rd stage: installation of the test rig in the wind tunnel laboratory at MMU, addition of measurement sensors (accelerometers and amplifiers) and equipment (including speed controller, data acquisition system, PC, and supporting tower). The wind turbine, supported by the tower, was placed 1 meter directly in front of the wind tunnel with the plane of the propeller normal to the air flow, see Figure 4.1 and schematic diagram of the test-rig shown in Figure 4.2.

The vibration signals were collected by two accelerometers (B&K type 4371) mounted on the nacelle of the wind turbine: one vertical and the other horizontal. The accelerometers had sensitivity of 10 mV/g and a frequency range of 1 Hz to 12 kHz. Their signals were fed to a B&K type 2635 charge amplifier which was used to condition the signal and to convert the low charge output signal of the accelerometer (pico-coulomb) to a low impedance and high voltage (in the range of mV) signal. The cut-off frequency for the initialising filter was set to 10 kHz. Data acquisition card (NI USB 9233) was connected between a PC and the charge amplifier to collect data.

Figure 4.1 Wind turbine test rig in MMU Mechanical Engineering Laboratory

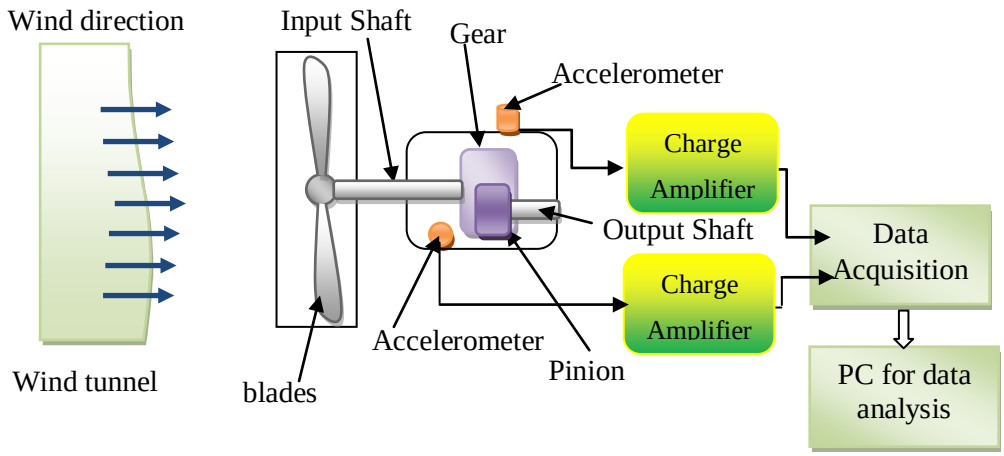

Figure 4.2 Schematic diagram of the wind turbine monitoring system

Table 4.1 Basic dimensions of wind turbine

Components	**Dimensions**
shaft length	22 cm
shaft diameter	3 cm
Hub diameter	14 cm
Blades length	32 cm
Input gear teeth	30
output pinion teeth	15
Input bearing inner diameter	20 mm
Input bearing outer diameter	32 mm
Input bearing width	7 mm
Output bearing inner diameter	15 mm
Output bearing outer diameter	28 mm
Output bearing width	7 mm
Nacelle of wind turbine	28X15X15cm

4.4 Test Rig Safety Precautions

The nacelle of the wind turbine enclosed the gearbox and generator and thus protected the surroundings from any debris or parts that may have flown off in case of breaking and failure. Data acquisition system, amplifiers and PC were situated away from the test rig for safety. Steel wires restraints were fitted to the tower and attached to the stanchions in the ground to provide greater safety.

4.5 Fault Simulation

The experimental work was performed using a three bladed wind turbine with either three healthy blades or two healthy blades and one blade with a crack seeded into it. The cracks were of four length: (10 mm, 20 mm, 30 mm and 40 mm) referred to as f1, f2, f3 and f4 respectively), all were 2 mm deep and 3 mm wide, see Figure 4.3. The cracks were introduced

by removing part of the blade face using drill. The tests were carried out for three rotation speeds; 150, 250 and 360 r/min and with a constant 100 Ω load.

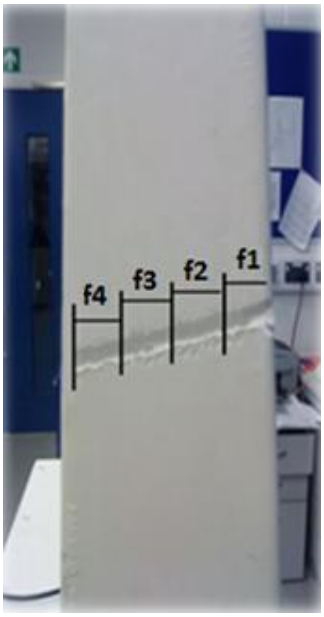

Figure 4.3 Simulated local faults on one blade

4.5.1 Piezoelectric Accelerometer

Accelerometers are widely used because of their accuracy, robustness and sensitivity as well as being easier to mount, lighter and smaller than other motion transducers. Accelerometers are inertial electromechanical devices which convert mechanical motion into an electrical output in accordance with Newton's second law of motion: $F = ma$.

A piezoelectric accelerometer contains a mass which generates an inertial force and a piezoelectric crystal which convert the force to an electric charge, see Figure 4.4 [109].

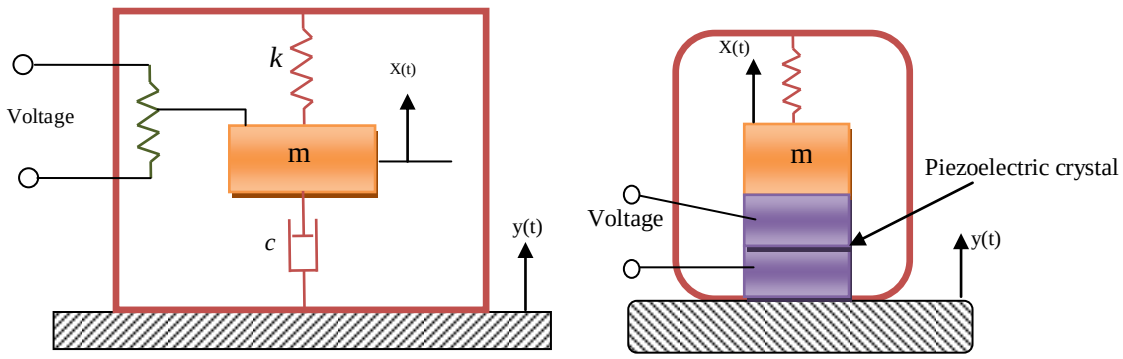

Figure 4.4 Schematic of an accelerometer mounted on a structure

4.5.2 Accelerometer Theory

The standard model of the accelerometer is well established and well known. The model is based on the damped mass-spring system. The equation of motion for the mass is:

$$m\ddot{x} + c(\dot{x} - \dot{y}) + k(x - y) = 0 \qquad 4.1$$

Where m is the mass, c is the damping constant of the system assumed proportional to the relative velocity between mass and base, k is the stiffness of the system and $x(t)$ and $y(t)$ are the displacements of mass and structure, respectively.

If the relative displacement between mass and base is $z(t) = x(t) - y(t)$, and the base undergoes a sinusoidal motion, $y = Ycos(\omega t)$ - there is little loss of generality in this assumption as most repeated waveforms can be written as the sum of a series of sinusoids. The equation of motion then becomes [110].

$$m\ddot{z} + c\dot{z} + kz = m\omega^2 Ycos(\omega t) \qquad 4.2$$

The steady state solution for Equation 4.2 is:

$$z(t) = \frac{\omega^2 Y}{\sqrt{\left(\omega_n^2 - \omega^2\right)^2 + (2\zeta\omega_n\omega)^2}} cos\left[\omega t + \left(-\tan^{-1}\frac{2\zeta\omega_n\omega}{\omega_n^2 - \omega^2}\right)\right] \quad 4.3$$

Where ω is the driving frequency, ω_n is natural frequency of the accelerometer spring-mass system, and ζ is its damping ratio (= $c/2\sqrt{(km)}$).

For linear systems *z(t)* has the same frequency as the base but with a phase shift between the two movements. The amplitude of *z(t)* will depend on the relationship between driving frequency and natural or resonant frequency of the system. For systems with little damping, such as accelerometers, $\omega_n = \sqrt{(k/m)}$. From Equation 4.3 it can be seen that the maximum amplitude of *z(t)* will be zero for a stationary system (ω = 0) and will gradually increase as ω increases. However when ω approached ω_n the denominator in equation 4.3, $\sqrt{(\omega_n^2 - \omega^2)^2 + (2\zeta\omega_n\omega)^2}$, approaches its minimum value and of *z(t)* will approach its maximum value, the system will be in resonance. This maximum value can be very large for systems with little damping. As ω gets progressively larger than ω_n the value of *z(t)* decreases and asymptotically approaches Y the larger ω becomes. In practice the upper frequency limit of the working range of an accelerometer is well below its resonant frequency.

Today accelerometers are preferred to velocity and displacement sensors because [111]:

1- Small accelerometers have a very wide working frequency range much greater then alternative sensors.
2- Systems respond to applied forces and so acceleration is more directly relevant than velocity or displacement.
3- Measurements of shock and transient responses can be readily made, more easily than with velocity or displacement sensors.

4- Direct integration of the output of the accelerometer will provide velocity and displacement.

5- Today accelerometers can be made much smaller than velocity or displacement sensors, and the less the mass of the transducer the less it will affect the system on which it is mounted.

4.5.3 Accelerometer Mounting Techniques

Correct mounting of the accelerometer is essential [112]. There are four commonly accepted mounting techniques used for attaching accelerometers to accurately measure vibration signals, these are shown in Figure 4.5. The major requirement is for close mechanical contact between the base of the accelerometer and the surface to which it is to be attached [4].

- *Stud mounting* – a stud is attached to the machine surface by tapping and screwing. Once the stud is in position the accelerometer is screwed onto it, but care must be taken not so generate stresses in the piezoelectric material. This gives the best frequency response and is the best technique for permanent mounting.
- *Adhesive mounting* – for permanent fixing accelerometers can be glued to the machine surface if an appropriate adhesive is used. Traditionally Araldite was used but increasingly today superglue is replacing it. In wet environments dental adhesive is preferred.
- *Magnet, beeswax or double-sided adhesive tape* – only suitable for temporary measurements such as spot checks. Their frequency responses are relatively poor even when attached by an expert.

- *Handheld probes* are used for spot checks only and have a poor frequency response probably less than 5 kHz.

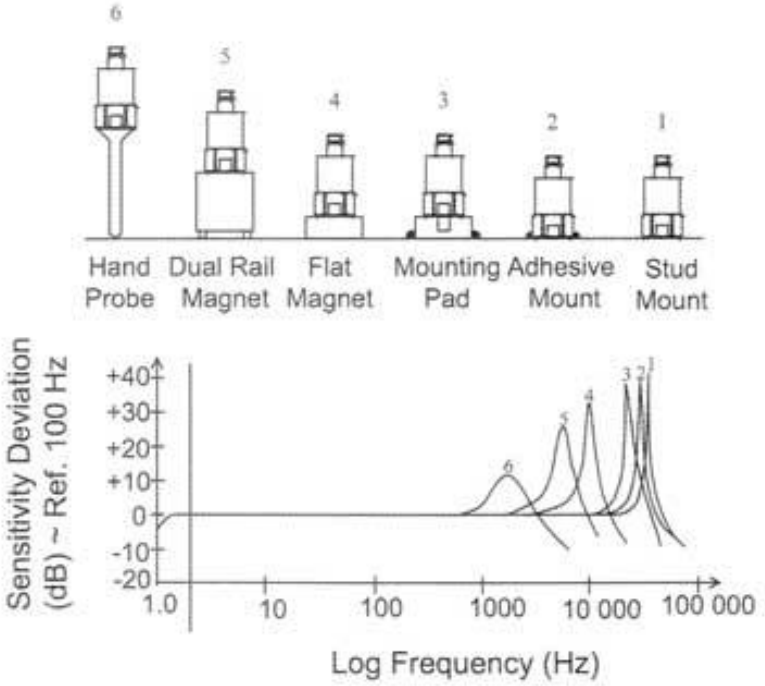

Figure 4.5 Accelerometer mounting techniques and their effects on the frequency response function [113]

Moreover, Figure 4.5 shows typical frequency ranges for expertly mounted accelerometers. This is the best that can be expected, bad mounting will adversely affect vibration measurements by seriously reducing the usable frequency range. More information and details about accelerometers used in this research is outlined in appendix B.

4.5.4 Sources of Error with Piezoelectric Accelerometers

The precision of accelerometer measurements made in the laboratory depends on many factors including; accelerometer mounting, sensitivity, temperature of surface, transducer mass, and fixing and length of cables. Accelerometer mounting has been discussed above.

The sensitivity of the accelerometer must be such that it provides a measurable output over the range of vibration levels being investigated. This will be decided when the transducer is purchased. Temperature is rarely a problem for laboratory experiments but in industry sensitivity can be affected by the local temperature.

The mass of the accelerometer must be at least ten times less than that of the surface being monitored so that it does not significantly affect the motion of the surface. Larger accelerometers will usually be more sensitive than small ones but this is unlikely to be a problem in practice.

When a charge amplifier is connected to an accelerometer by a cable, triboelectric effects contaminate the vibration signal. Triboelectric noise is due to rubbing between adjacent layers of insulating material and conductors. To minimized this source of noise cables should be as short as possible and fixed to the vibrating structure using adhesive tape or epoxy glue, as shown in Figure 4.6 [114].

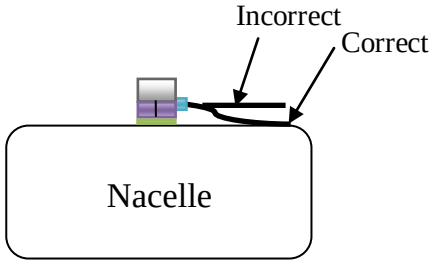

Figure 4.6 Proper mounting of accelerometer cable

4.6 Charge Amplifier

Signal conditioning units are important when transforming analogue data to a digital form. For example, the magnitude of the incoming voltage signals must be compatible with the input range of the data acquisition board. Signal conditioning units will amplify low amplitude signals, and filter-out unwanted high-frequency (and low-frequency) signals to give a more accurate measurement. This is the role of the B&K type 2635 charge amplifier used in this work, see appendix C.

The optimum amplification to achieve the highest clarity, to maximise the resolution of low level signals and distinguish them from background noise, should be such that the maximum voltage range of the conditioned signal equals the maximum input range of the analogue-to-digital converter (ADC). On the test-rig, both vibration and acoustics signals were amplified before reaching the ADC.

4.7 Data Acquisition System

The data acquisition system (DAS) was a general system designed to interface any test rig to any PC in order to measure and monitor variables such as temperature and vibration. The DAS consists of hardware and software.

The hardware is the accelerometers, PC and data acquisition card (DAQ) which was a National Instruments type USB NI9233, see Figure 4.7. The card was used to transmit signals from the accelerometer to the PC and has the following features; ±5 V input range, 102 dB dynamic range, 24-bit resolution, 50 KS/s maximum sampling rate per channel and anti-aliasing filters.

The full scale supply voltage (E_{FSR}) and the resolution of this DAQ card and limit settings determine the smallest detectable change in the input voltage. The resolution can be determined using the following formula [115];

$$V_{cw} = \frac{E_{FSR}}{2^{24}} \quad 4.4$$

For this DAQ the resolution is in the range of few microvolts.

The software, designed for a Windows operating system, provided the interface between the ADC and the user. The DAQ software was USB NI9233 using LabVIEW to control the PCI boards, saving of data to the hard drive and viewing the recorded data. Interfacing between user and the ADC board allowed changes to be made to such operating parameters as sampling frequency.

The interfacing software could process the data from the accelerometer online, which made possible to view the vibration spectrum at any time this is one of MatLab's many strengths it is excellent for visualizing data. It could also display such operational parameters as wind turbine speed and power generated.

Figure 4.7 Data acquisition card

4.8 Processing and Analysing Software

Fault detection and diagnosis are fundamentally dependent on the software used to gather and process data. MatLab was chosen for this study, because it is highly interactive with an excellent library of applications backed by a good support literature. The application sub-routines range from simple spectral analysis to complex wavelet functions, which can be simply drawn down for use as required. MatLab thus has the ability to extend and creat new commands and functions [116]. The writing and development of the MatLab codes used in this project for processing and analysis of the acquired data was an important part of this research work. The results obtained using these codes are presented in Chapters 5, 6, 7 and 8.

4.9 Experimental Procedure

- The DAQ card, amplifier, accelerometers and cables were connected and their performance verified.
- The mounting locations for the transducers were cleaned of dirt, oil and paint and the accelerometers were then glued to the surface using an appropriate adhesive.
- LabVIEW software was used to interface with the DAQ and to set: signal input range, samples to read and sampling frequency.
- LabVIEW was used to build a suitable graphical user interface which was then used to monitor the test rig and to save the collected data for further analysis using MatLab.

Chapter 5

Fundamental Characteristics of Wind Turbine Vibration

In this chapter, some of commonly used conventional descriptors of vibration signals and their basic principles are summarized. The description focuses on: time domain and frequency domain analyses. The application of these techniques and their performance is explained using local faults seeded into one of the wind turbine blades. Experimental and simulation signals analysed and summary is given.

5.1 Introduction

Conventional techniques used to monitor the condition of rotating machinery are not widely used in the condition monitoring (CM) of wind turbines due to the complex, non-linear and non-stationary nature of the signals. Vibration analysis is the best known technology for CM of rotating equipment including bearings and wind turbines and features extracted from the vibration signals can accurately reflect the condition of the machine. Such a system is indispensable for the effective CM of machinery.

Most traditional methods for CM are simple to use and easy to understand; the two that will be introduced here and applied to CM of a wind turbine using vibration data are:

- Statistical parameters, and
- Spectrum analysis.

Vibration analysis involves the collection of relevant data from a machine which can then be displayed as a time domain plot or transformed using standard techniques into the frequency domain [117].

5.2 Time Domain Overview

Before digital signal processing made spectral analyses widely available and relatively cheap most CM using vibration analysis extracted statistical measures from the time-domain. The time domain is a plot of amplitude versus time and time-domain approaches are appropriate where periodic vibration (which may take the form of impulses) occurs [118]. The most common such statistical indicators for machinery are Kurtosis (*Ku*), Root mean square (*RMS*), Crest factor (*CF*), Skewness (*Sk*) and Standard deviation (*SD*) [119,

120]. A commonly used term for these indicators is “condition indices” and according to their value the condition of a gearbox, for example, would be judged acceptable or not, as the case might be.

As the value of the statistical parameter, such as the RMS increased that would be taken as an indication of the gearbox’s deteriorating condition. The assumption is that measured values for a damaged gear would be greater than the corresponding values for a healthy gear, and by comparing like with like, e.g. RMS values of a given vibration signal from a healthy gear with measured RMS values for the same gear the presence of a fault and its severity can be detected. The RMS is a measure of energy in the signal but *Ku* and *CF* of a signal are measures of its “spikiness”, which can be of great use in detecting the early stages of gear damage. , *Ku* and *CF* both increase with increase in vibration but beyond a certain stage, as the damage increases and the defect spreads, the vibration becomes more random in nature and *Ku* and *CF* reduce to more normal levels. Thus, statistical analysis based on *Ku* and *CF* of a signal is not used to detect well-developed gear defects. Figure 5.1shows the time domain of the vibration data from a healthy wind turbine

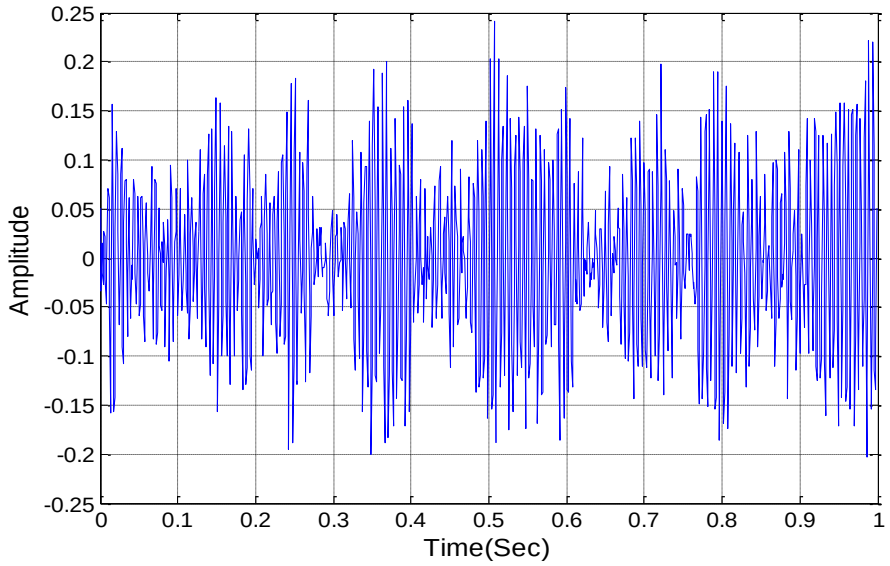

Figure 5.1 Time-domain vibration profile for healthy wind turbine

5.2.1 Statistical Parameters:

Periodical excitation forces are present in and affect all rotating machinery including wind turbines. These forces arise mainly from the natural action of the machine, in particular rotational and translational forces as the machine performs its specified functions. However, such forces are complemented by forces from mechanical defects such as shaft imbalance or bearing defects or faulty gears. A fault, then, will generate a signature impulse in each revolution of the machine.

Statistical measures such as *Ku*, *RMS*, *CF*, *Sk* and *SD* obtained from the time-domain signal are widely used with vibration signals of rotating machines to assess the level of wear and possible damage. [121]. *Ku*, *RMS*, *CF Sk* and *SD* were used to evaluate a

healthy wind turbine blades and one blade suffering from different faults as described earlier. A brief review of these parameters is given below.

5.2.1.1 Kurtosis

Ku is the normalised fourth moment of the signal *x* [122] and is a measure of how spiky the signal is, the higher the value of *Ku* the more pointed and sharper the peaks and the longer the tails of the signal, the lower the value of *Ku* the more rounded the peak. Equation 5.1 gives the non-normalised value of *Ku*:

$$Ku = \frac{\frac{1}{N}\sum_{n=1}^{N}\left(x(n)-\bar{x}\right)^4}{\left[\frac{1}{N}\sum_{i=1}^{N}\left(x(n)-\bar{x}\right)^2\right]^2} \qquad 5.1$$

If the *Ku* for a distribution which closely followed the Gaussian was calculated its value would be 3. A flatter curve would have $Ku < 3$, and a sharper peak would have $Ku > 3$.

5.2.1.2 The Root Mean Square

The *RMS* is defined as "the square root of the average of the sum of the squares of an infinite number of samples of the signal" [6]. This parameter is intensively used in electrical engineering and for signal analysis:

$$RMS_x = \sqrt{\frac{1}{N}\left[\sum_{i=1}^{N}(x_i)^2\right]} \qquad 5.2$$

Where *x* is the time signal, *N* is the number of samples and *i* refers to the i^{th} sample.

RMS is the simplest and most commonly used measure in vibration monitoring for assessing the overall intensity of a (wide-band) vibration signal. Because it is an average it reduces the influence of one-off vibration impulses.

5.2.1.3 The Crest Factor

CF is defined as "the ratio of the maximum positive peak value of the signal *x* divided by the *RMS* value of the signal *x*" [7]. *CF* is this normalised measure of the signal peak amplitude. *CF* can be considered a measure of either the smoothness of a signal or its impulsiveness, increasing in value as problems become more severe [123]:

$$CF = \frac{x_{pk}}{RMS_x} \tag{5.3}$$

Where x_{pk} is the maximum value of *x*.

5.2.1.4 Skewness

Sk is a measure of the asymmetry of a signal, whether an amplitude distribution curve is skewed to the right or left of the Gaussian. If *Sk* < 1 most of the data appear to the left of the average – the distribution will have a tail or pointed end extending towards lower or more negative values. If *Sk* > 1 most of the data appear to the right of the average. *Sk* is the normalised third central moment;

$$SK = \frac{\boldsymbol{E[(x_i - \bar{x})^3]}}{\boldsymbol{RMS^3}} \tag{5.4}$$

Where *E* is the expected value of the function.

5.2.1.5 Standard Deviation

The *SD* is the square root of the variance. It indicates the spread of the data, the larger the *SD* the more widely the data are spread out. Although influenced by extreme values, the *SD* is important in many tests of statistical significance:

$$SD = \sqrt{\left(\frac{\sum_{i=1}^{N}(x_i-\bar{x})^2}{N}\right)} \qquad 5.5$$

Where x_i a set of samples, N is the total number of samples, and $\bar{x}$ is the mean value of the samples.

5.3 Frequency Domain Overview

The spectral content of the measured vibration signal could be more useful than the time domain for determining turbine condition. This approach transforms the time domain signal into the frequency domain using fast Fourier transformation (FFT). Strictly the FFT should be used only for linear and stationary signals [1], but here it is assumed that once the crack fault is seeded into the blade conditions are stationary over the measurement period.

Using this technique it is possible to identify eccentricity by noting the increase in the magnitude of modulation sidebands in the spectrum. Local defects such as fatigue cracks are another defect/fault which can be found by detecting the presence of sidebands on both sides of the gear meshing frequency (and its harmonics). These sidebands are separated from the gear meshing frequency by integer multiples of the frequency of gear rotation. Useful information on the health of the gear is often provided by sidebands generated by either amplitude or frequency modulation in the vibration signal. Randall

has claimed that successful gear fault identification can be achieved by analysis of the first three gear meshing harmonics and their sidebands [124]. Tracking the changes in amplitude of the sidebands of a particular frequency in a vibration signal can often provide a reliable indicator of gear failure.

When looking for incipient faults the signal to noise ratio (S/N) is very low, simultaneously the healthy vibration spectrum will have a multitude of peaks and using only an FFT it becomes impossible to distinguish the fault peaks. This is the most difficult problem associated with FFT based fault detection. This also applies to the side bands which depend on periodic nature of the exciting force and on the transmission path.

5.3.1 Spectrum Analysis

Nevertheless most CM of rotating machinery is still performed on frequency-domain vibration data using the FFT despite its limitations. However, an additional and major limitation of the FFT is that the spectral analysis provides only frequency information and cannot provide information of spectrum changes that take place with respect to time.

Spectral analysis is a commonly and widely used method for interrogating the vibration signal of rotating machines for detection and diagnosis of faults, and assessment of fault severity. The spectral components of the vibration signal are closely related to the dynamics of a machine and its condition. In particular, for example, detection of the characteristic frequencies of bearings which are well defined theoretically can be very useful in the early detection of bearing faults.

This study will detect faults in the mechanical condition of the wind turbine as reflected by changes in the vibration signal [125].

5.3.2 Performance of Conventional Techniques on Simulation Vibration Signals

Vibration data collected from simulated wind turbine as shown in chapter 3 and vibration data collected from experimental work analysed using time and frequency domain methods. The result for statistical parameters for Ku, RMS, CF, Sk and SD are explained in section 5.3.3.

5.3.3 Time Domain based Analysis of Vibration Signals

These statistical parameters were applied to the both vibration signals (simulation and experimental work) obtained for a wind turbine with three healthy blades and four cases where one of the blades had an increasingly severe crack fault seeded into it. Using the five statistical quantities simultaneously may provide the basis for a more reliable decision than relying on the value of a single parameter. The results can be seen in Figures 5.2 to 5.6. Table 5.1lists the statistical parameters with increase in crack length and rotational speed. Clearly there is so much fluctuation in the values that individually none of them is suitable for fault diagnosis used on its own.

Figure 5.2 shows the Ku values for the simulation and experimental vibration signals obtained for the healthy condition and for one blade with different crack lengths (10 mm, 20 mm, 30 mm and 40 mm) at rotational speeds 150 rpm, 250 rpm and 360 rpm.

Figures 5.3, to 5.6 show the RMS, CF, Sk and SD values, respectively for the same signals. The data for the healthy wind turbine are used as guide to the faulty cases with

seeded cracks. Obvious these parameters vary with crack length but not in a consistent way, they also vary with speed of rotation.

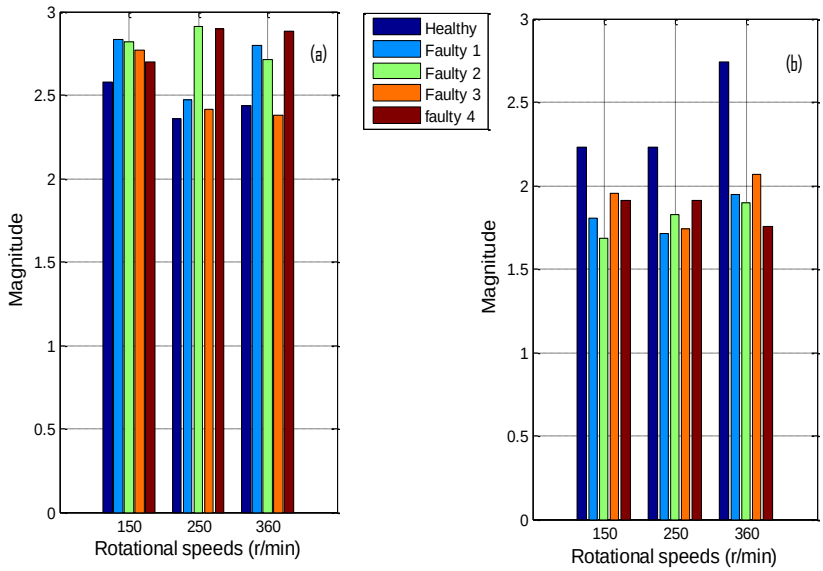

Figure 5.2 Magnitude of Kurtosis; a) simulation signal, b) experimental signal

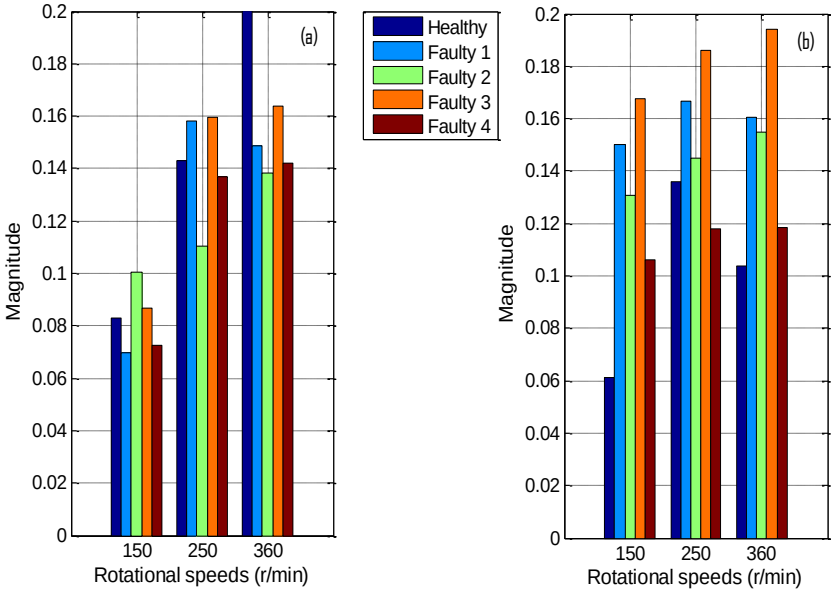

Figure 5.3 Magnitude of RMS; a) simulation signal, b) experimental signal

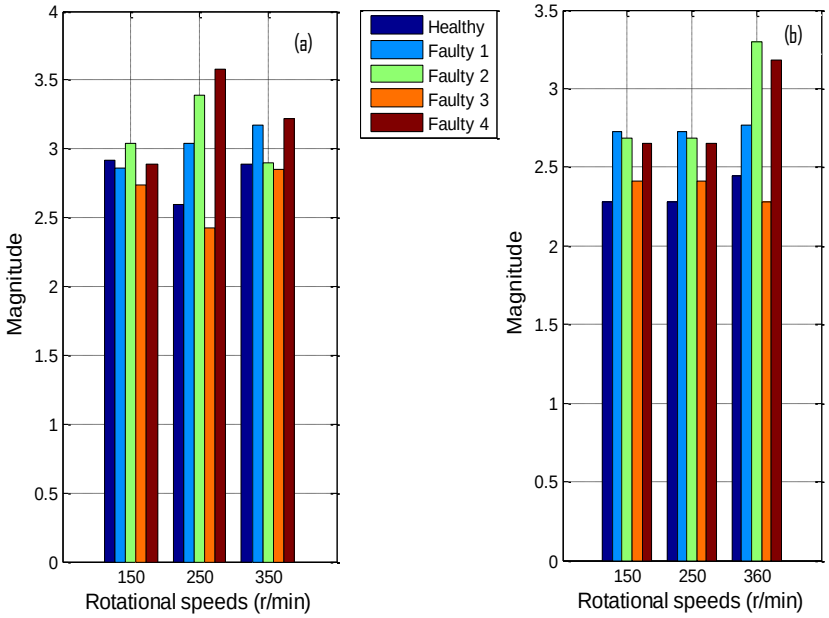

Figure 5.4 Magnitude of Crest Factor; a) simulation signal, b) experimental signal

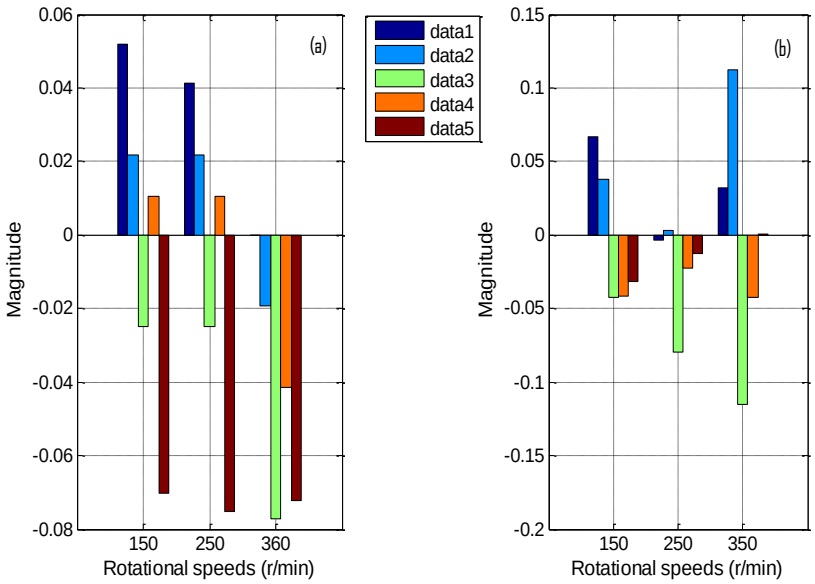

Figure 5.5 Magnitude of Skewness; a) simulation signal, b) experimental signal

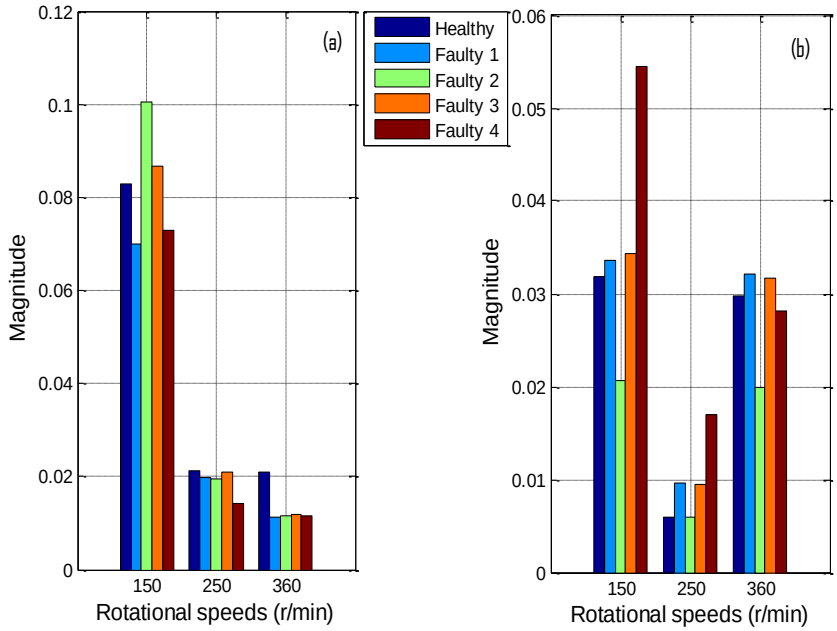

Figure 5.6 Magnitude of Standard Deviation; a) simulation signal, b) experimental signal

It can be seen that these five statistical measures of the vibration signal when applied to a wind turbine are not sensitive enough to detect particular type of fault because they show no consistent of significant change with presence or severity of the blade crack.

Table 5.1 Values of statistical parameters for healthy and four faulty turbines

	Blade fault severity (mm)	Rotational speeds		
		150 rpm	250 rpm	360 rpm
Kurtosis	Healthy	2.5791	2.3568	2.4377
	10	2.8324	2.4682	2.7958
	20	2.8225	2.9146	2.7118
	30	2.7702	2.4183	2.3776
	40	2.6991	2.8988	2.8823
Root mean square	Healthy	0.0829	0.1428	0.2001
	10	0.0700	0.1581	0.1486
	20	0.1005	0.1103	0.1383
	30	0.0865	0.1593	0.1638
	40	0.0728	0.1371	0.1420
Crest factor	Healthy	2.9156	2.5984	2.8922
	10	2.8612	3.0416	3.1713
	20	3.0372	3.3875	2.8944
	30	2.7363	2.4208	2.8473
	40	2.8849	3.5798	3.2162
Skewness	Healthy	0.0670	-0.0034	0.0318
	10	0.0375	0.0030	0.1121
	20	-0.0425	-0.0797	-0.1149
	30	-0.0417	-0.0225	-0.0425
	40	-0.0313	-0.0128	0.0003
Standard Deviation	Healthy	0.0829	0.0214	0.0211
	10	0.0700	0.0199	0.0112
	20	0.1005	0.0195	0.0115
	30	0.0866	0.0209	0.0120
	40	0.0728	0.0143	0.0116

5.3.4 Performance of fast Fourier Transform on Experimental Vibration Signals

5.3.4.1 Baseline Spectrum Analysis

The chosen vibration method depends is baseline spectrum analysis; comparing a healthy baseline spectrum with that of the wind turbine under seeded fault conditions. Thus

acquiring, analysing and saving of data sets from the healthy wind turbine is the first step in establishing a maintenance program [126]. All the frequency peaks in the baseline spectrum should be identified and examined for different operating conditions. Normally the reference data set for all future measurement should be compiled when the wind turbine is first installed or after a scheduled maintenance. To obtain a baseline spectrum data sets from a healthy wind turbine were obtained and stored for three different rotational speeds (150, 250 and 360 rpm), see Figure 5.7.

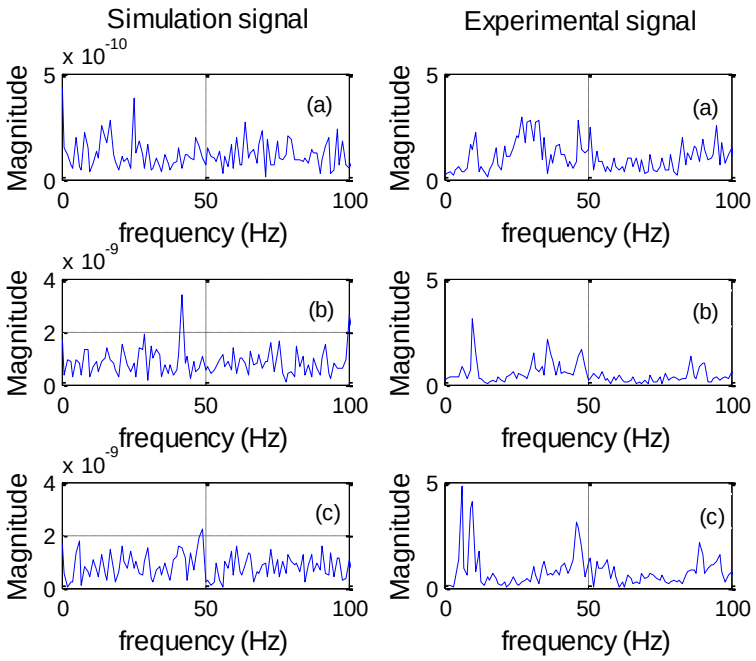

Figure 5.7 Frequency- domain for simulation and experimental vibration signatures for healthy wind turbine, a) at 150 r/min, b) at 250 r/min and c) at 360 r/min.

5.3.4.2 Spectral Analysis for Non-baseline Operating Conditions

Frequency analysis of the simulation and experimental vibration signals collected from the wind turbine under four fault conditions of increasing severity (seeded cracks as described above) and at different rotational speed was carried out using the FFT, as shown in Figures 5.8 to 5.13, respectively.

Unfortunately from these figures although there are changes to the frequency spectrum with the presence of a crack fault the changes did not appear consistent and significant. The reason is that the collected signals are non-stationary and their statistic characteristics vary with time as well as the low frequency. The signals are contaminated with noise. Sources of vibration are, for example, the gear box, the generator as well as the fan pass frequency. The vibration generated from gear box and the generator contains more or less prominent tones, whose amplitude and sometimes also frequency fluctuate slightly in rhythm with the blade passing frequency of the rotor [12].

The results show that the FFT is not suitable for analysing these signals and it has not provided consistent blade's condition related information.

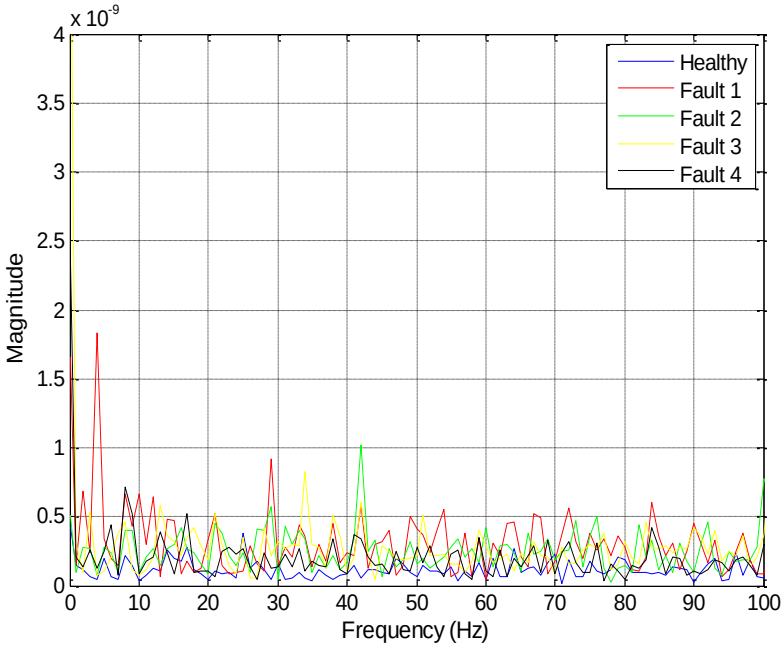

Figure 5.8 FFT for healthy and faulty simulation signals at 150r/min**;**

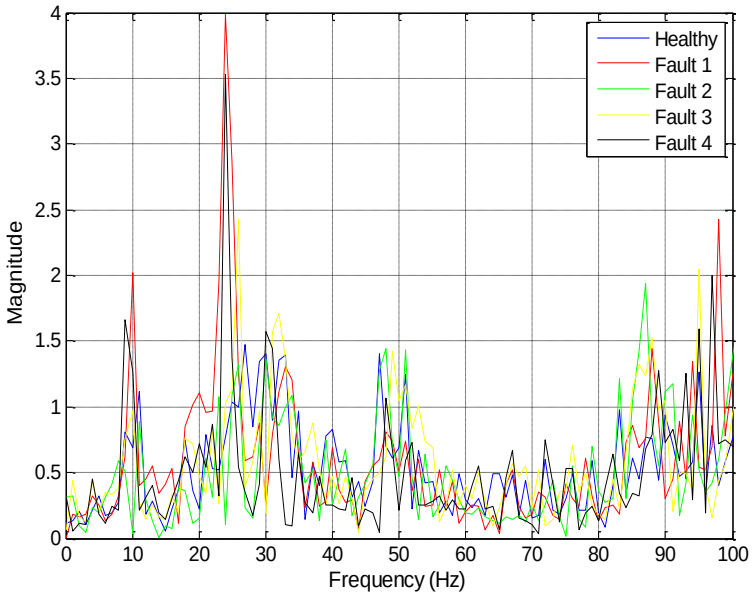

Figure 5.9 FFT for healthy and faulty experimental signals at 150r/min;

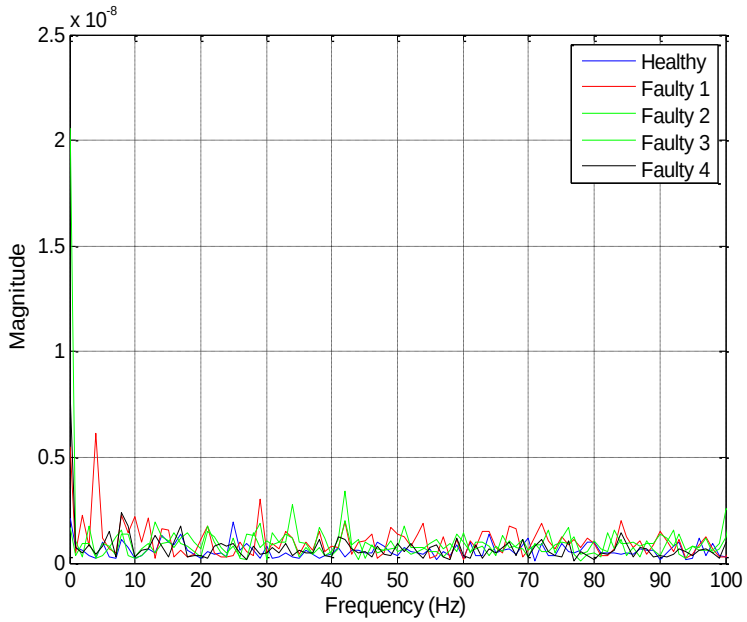

Figure 5.10 FFT for healthy and faulty simulation signals at 250r/min;

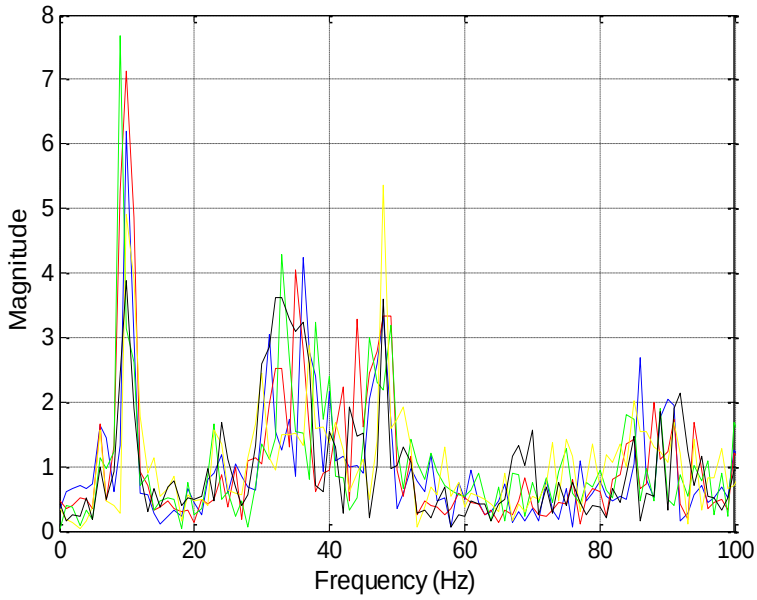

Figure 5.11 FFT for healthy and faulty experimental signals at 250r/min;

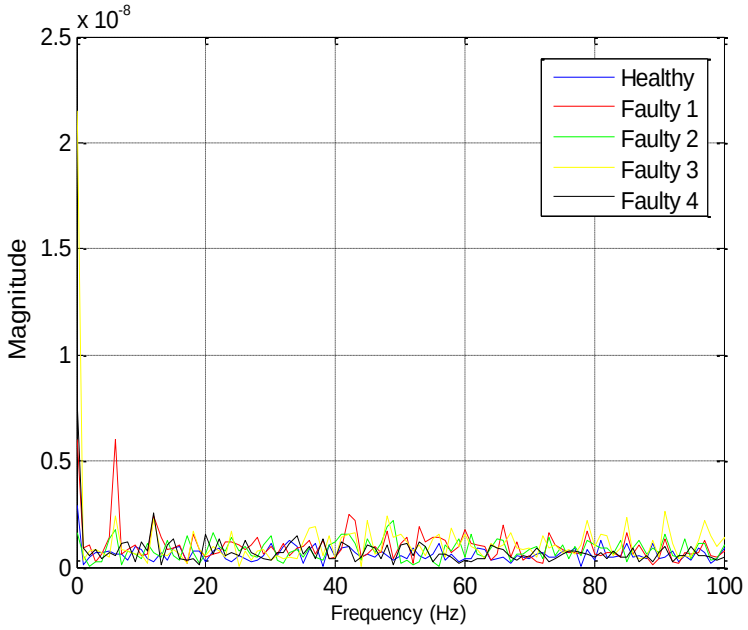

Figure 5.12 FFT for healthy and faulty simulation signals at 360r/min;

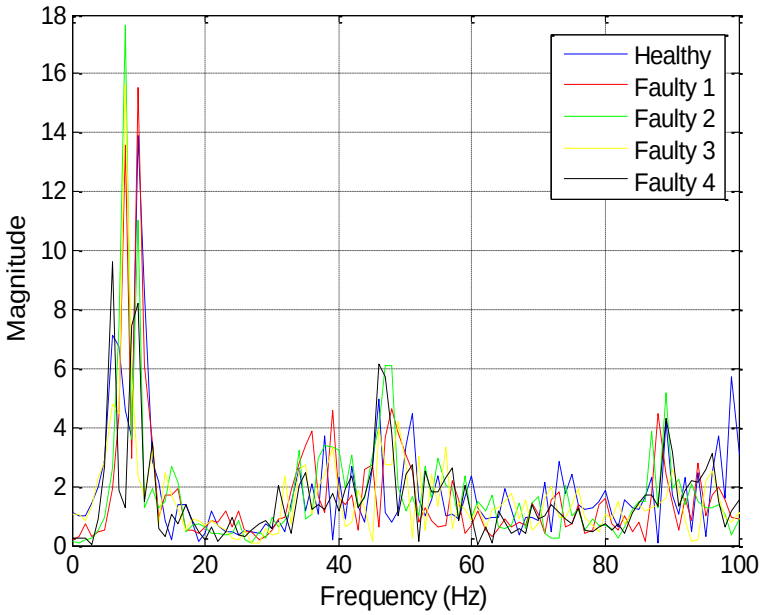

Figure 5.13 FFT for healthy and faulty experimental signals at 360r/min.

There remain important advantages to using the FFT with stationary signals. But there are inherent performance limitations with non-stationary signals; in particular the FFT

approach may not to be able to distinguish the spectral responses of healthy and faulty signals. Moreover due to energy leakage of the data that occurs when processing with the FFT is other limitation [14].

5.4 Summary

The statistical analysis of the time-domain signal from healthy and faulty wind turbine blades shows that – at least for the statistical parameters used - there is limited information that could be extracted about the wind turbine blades' condition from the vibration signal time domain wave form. From results, Figures from 5.2, to 5.6 showed that the values of Ku, RMS, CF, Sk and SD, fluctuate around the initial values for the healthy case and it is not possible to reliably determine whether there is any fault present even if they are used simultaneously.

In general, failure detection using frequency domain analysis can be achieved by monitoring two parameters in the spectrum. The first is variation in the amplitude of a particular frequency – such as the appearance of the characteristic frequencies associated with bearing faults - and the second are changes in the structure of sidebands in the spectrum. As can be seen from Figures 5.8 to 5.13, the Results showed the presence of abnormalities in wind turbine structure with crack severity. But the amplitude of the shaft frequency did not changed considerably, although the increase in the number of sidebands had been observed under severe fault situations. Thus the signals analysis is still limited to provide enough information about the crack condition at this stage.

Chapter 6

Condition Features Extraction Using Empirical Mode Decomposition

This chapter begins by introducing methods of analysis of non-linear and non-stationary signal. Then it provides a brief description of the mathematical characteristics of empirical mode decomposition (EMD) followed by a description of the principles of application of EMD to the analysis of numerical data, after which EMD is applied to simulation and experimental data obtained in this research project. The chapter then introduces the feature intensity level "EDFIL", as a new method of fault diagnosis for wind turbines blades, and its basic principles. The chapter concludes with a summary.

6.1 Introduction

Data analysis is an essential part of the transition from pure research to application. Theory usually begins with linear and stationary processes which are relatively easy to analyse, but many real world problems, particularly in condition monitoring, non-linear and non-stationary. For the past sixty years the transformation of the time-domain signal to its frequency spectrum has been dominated by the FFT (initially analogue and then digital fast Fourier transform). But as shown in chapter five, the FFT has a severe limitation it is, strictly, applicable only to stationary signals but today – as in this thesis – it is non-stationary signals that are of interest.

A recent transform pioneered by Huang et al [127] for analysing non-stationary and non-linear signals is the Hilbert Huang transform (HHT). This combines empirical mode decomposition (EMD), and the Hilbert transform (HT). The HT has been known for some time; what Huang did that was new was to introduce EMD and decompose the original signal into its intrinsic modes (known as the intrinsic mode functions, IMFs) each of which will have its own frequency characteristic and identifies the instantaneous frequencies contained in the signal. Huang describes the "EMD as a data-adaptive decomposition method with which any complicated data set can be decomposed into zero mean oscillating components, named intrinsic mode functions (IMFs)"[128]. Thus the use of IMFs reduce the problem associated with sharp changes in frequency content of the original signal and so are very compatible with the HT. Once the IMFs are obtained the HT is applied to each IMF to obtain the time-frequency representation.

6.2 Modified Hilbert Huang Technique

Details of the HHT together with some later improvements and variations are given in[129, 130]. The HHT has two parts:

First, the EMD is used to decompose the signal waveform into multiple intrinsic mode functions (IMFs) that possess well-behaved HTs. Each IMF has two principal properties – (a) it has a zero mean, and (b) in the full data set, the number of extrema and number of zero-crossing must either be equal or differ at most by one. (A local extremum is any point on the waveform where the first derivative is zero and the second derivative is non-zero). Second, the HT is applied to obtain the instantaneous amplitudes and frequencies of the individual IMFs.

6.3 Empirical Mode Decomposition Description

This section briefly outlines the EMD method. Recently EMD methods have been applied to many different types of time domain decompose them into IMFs, each of which is taken to be generated by a separate physical source with its own time characteristics [131]. Huang et al. [129, 132] and Wu et al. [133] have used EMD methods to identify oscillatory modes in data sets using local maxima and minima, and based on the following three assumptions:

1- The data set contains at least one maximum and one minimum (two extrema);
2- The time intervals between two consecutive extrema defines the characteristic local time scale; and

3- If the data contained no extrema but did contain inflections, then the signal can be obtained by integration of the components.

6.4 Empirical Mode Decomposition to obtain IMFs

In elementary vector notation a signal with one component can be represented as a vector rotating round a point, and its instantaneous frequency is given by the time derivative of the signal's phase. This is the principle underlying Huang's EMD method[133]. However, real signals will contain many modes of oscillation and so will not have a single instantaneous frequency. Thus, real signals must be decomposed into their constituent mono-component parts before applying the HT to determine the instantaneous frequencies.

The heart of the EMD is the recognition of those oscillatory modes which exist in the periods between local extrema. Several local extrema may occur within an observation window. The major advantage of EMD is that the basic functions are derived directly from the signal itself.

The EMD is defined by a process called sifting. It decomposes a given signal x(t) into a set of IMF. K modes $d_K(t)$ and a residual term r(t) are obtained and expressed as:

$$X(t) = \sum_{k=1}^{K} d_K(t) + r(t), \qquad 6.1$$

k=1, 2, …….. K

The EMD algorithm is summarised by the following steps:

1. Commence with the signal $d_1(t)$, $K = 1$ .Sifting process $h_j(t) = d_K(t), j = 0$.

2. Identify all local extrema of $h_j(t)$.

3. Compute the upper (*EnvMax*) and the lower envelopes (*EnvMin*) by cubic spline lines: interpolation of the maxima and the minima.

4. Calculate the mean of the lower and upper envelopes,

$$m(t) = {}^{1}/_{2}\,[EnvMin(t) + EnvMax(t)] \qquad 6.2$$

5. Extract the detail $h_{j+1}(t) = h_j(t) - m(t)$,

6. If $h_{j+1}(t)$ is an IMF, go to step 7, otherwise iterate steps 2 to 5 upon the signal

$h_{j+1}(t), j = j + 1,$ (4)

7. Extract the mode $d_k(t) = h_{j+1}(t)$

8. Calculate the residual $r_k(t) = X(t) - d_k(t)$ 6.3

9. If $r_k(t)$ has less than 2 minima or 2 extrema, the extraction is complete$r(t) = r_k(t)$. Otherwise iterate the algorithm from step 1 upon the residual$r_k(t), K = K + 1$. Figure 6.1 shows the flowchart of the EMD algorithm.

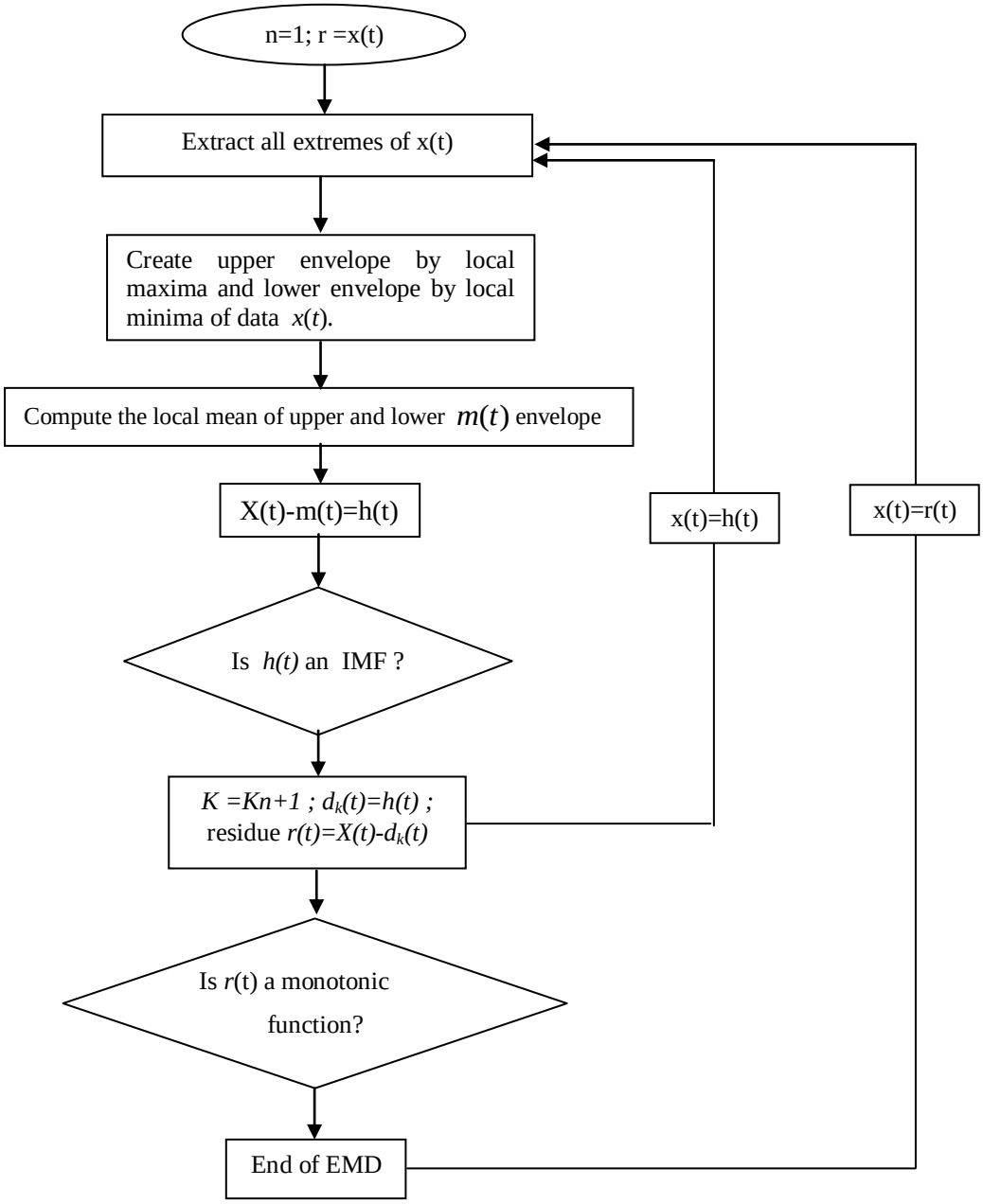

Figure 6.1 Flowchart of Empirical Mode Decomposition Algorithm [134]

6.5 Numerical Simulation Signal:

Bladed rotating machinery generates complex vibration from such different sources such as blades, shaft, gears and bearings with most of data non-stationary and non-linear. The frequency of the signal changes within a characteristic period so that Fourier Methods are of limited use.

To demonstrate the efficiency and performance of EMD methods in analysing non-stationary and non-linear signals, consider the following signals:

$$x_1(t) = 0.3 * \sin(2\pi * f_1 * t) \quad 6.4$$

$$x_2(t) = 0.3 * \sin(2\pi * f_2 * t) \quad 6.5$$

$$x_3(t) = 0.3 * sin(2\pi * f_3 * t) \quad 6.6$$

$$x_4(t) = 0.3 * sin(2\pi * f_4 * t) \quad 6.7$$

$$x_5(t) = randn\big(size(t)\big) \quad 6.8$$

Where f_1 =4.16 Hz, f_2 =12.5 Hz, f_3 = 25 Hz and f_4 =125 Hz. These frequencies are analogy to the shaft frequency, fan pass frequency, second harmonic of the fan pass frequency and meshing frequency, respectively. The signals including the noise are shown in Figure 6.2

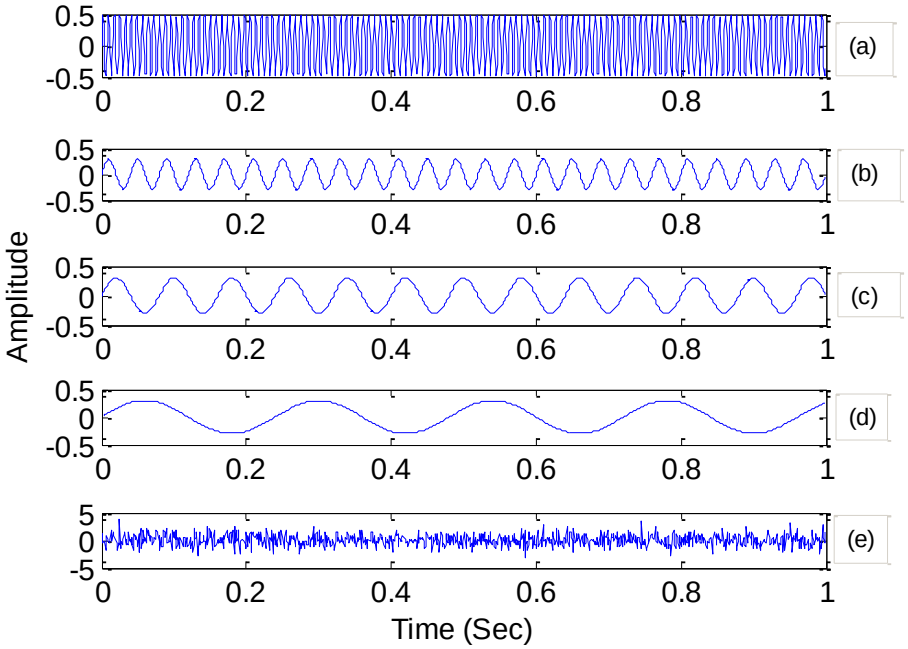

Figure 6.2. Five sinusoidal signals; a) generated by Eq. 6.7, b) generated by Eq. 6.6, c) generated by Eq. 6.5, d) generated by Eq. 6.4, e) generated by Eq. 6.8

The following is example that shows how the EMD algorithm works. Although the process is not non-stationary, however, the example illustrates the basic concepts of EMD:

$$x_T(t) = 0.3 * \sin(2\pi * 4.16 * t) + 0.3 * \sin(2\pi * 12.5 * t) + 0.3 * \sin(2\pi * 25 * t) + 0.3 * sin(2\pi * 125 * t) + randn\big(size(t)\big) \quad 6.9$$

Suppose a time domain signal is given by Equation 6.9 .We might say the signal $x_T(t)$ is the sum of four sinusoids corrupted with zero-mean random noise. Figure 6.3a show the signal $x_T(t)$ in time domain of total duration 1 second. The EMD is decomposes the

signal into its IMFs, with the first IMF having the highest frequency (contained in the noise due to Equation 6.8 and subsequent components will have lower frequencies as shown on Figure (6.3b, 6.3c, 6.3e, 6.3f and 6.3g. The decomposition is "polluted" by the presence of more than one mode and random noise.

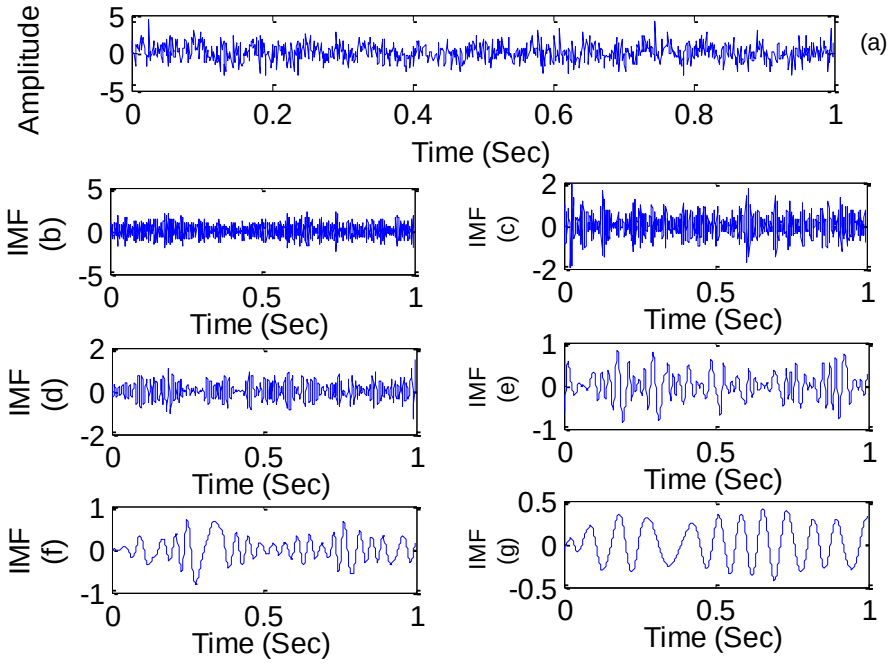

Figure 6.3. The IMFs of Equation 6.9

The fact there are numerous (4) modes mean that oscillations of different time scales will coexist in individual IMFs, or that oscillations with the same time scale could be assigned to different IMFs because the EMD is not band pass filtered. The frequency-domain analysis presented in Figure 6.4 is for numerical signal as a result of applying fast Fourier transform on each IMF – this is done here for comparison because the sinusoids are linear and stationary so the use of the FFT is acceptable.

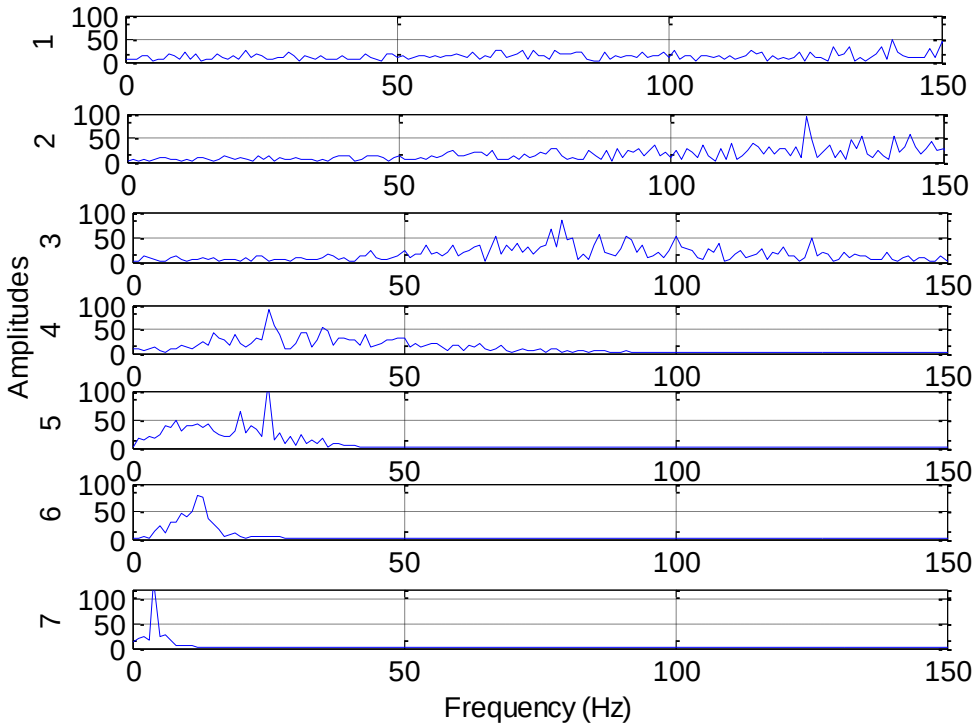

Figure 6.4. Fast Fourier Transforms for IMFs shown in Figure 6.3

After applying FFT on IMFs modes in Figure 6.3, the first spectra shown in first trace in Figure 6.4, gives the highest frequencies because these are contained within the noise generated by Equation 6.8; The second trace contains the frequency 125 Hz corresponding to mode IMF2 from Figure 6.3 that generated by Equation 6.7. The fourth trace contains a peak at frequency 25 Hz and corresponds to mode IMF4 which is generated by Equation 6.6, which simulate second harmonic of the fan pass frequency. The 6^{th} trace corresponds to modes IMF6 contain peaks at frequencies 12.5 Hz that simulate the fan pass frequency generated by Equation 6.5. Finally, the 7^{th} trace is the spectra produced from mode IMF7 and it is associated to signal generated by Equation 6.4 that simulate shaft frequency at 4.16 Hz.

Not all IMFs are physically significant as there will always be some degree of noise contamination in real samples: e.g. EMD applied to the measured signals from wind turbines.

6.6 The Performance of EMD on Simulation and Experimental Vibration Data

Empirical mode decomposition method applied used to decompose vibration signals collected from simulation and experimental work into a finite set of signals. The decomposition of the simulation vibration signals for the healthy case at different rotational speeds its spectra is shown in Appendix A, whilst the decomposition of the experimental vibration signals for the healthy cases at different rotational speeds are considered in this chapter.

The test runs were dynamic analysis was performed and the fundamental vibration characteristics were extracted for a three bladed propeller with two healthy blades and one blade with one of four cracks introduced. The cracks were of lengths 10 mm, 20 mm, 30 mm and 40 mm, all had a consistent 3 mm width and 2 mm depth. The tests were carried out for three rotation speeds; 150, 250 and 360 r/min. The measured vibration signal for the healthy case was decomposed for rotation speeds; 150, 250 and 360 r/min as shown in Figures 6.5, 6.6 and 6.7, respectively and the sampling rate was 3 KHz .

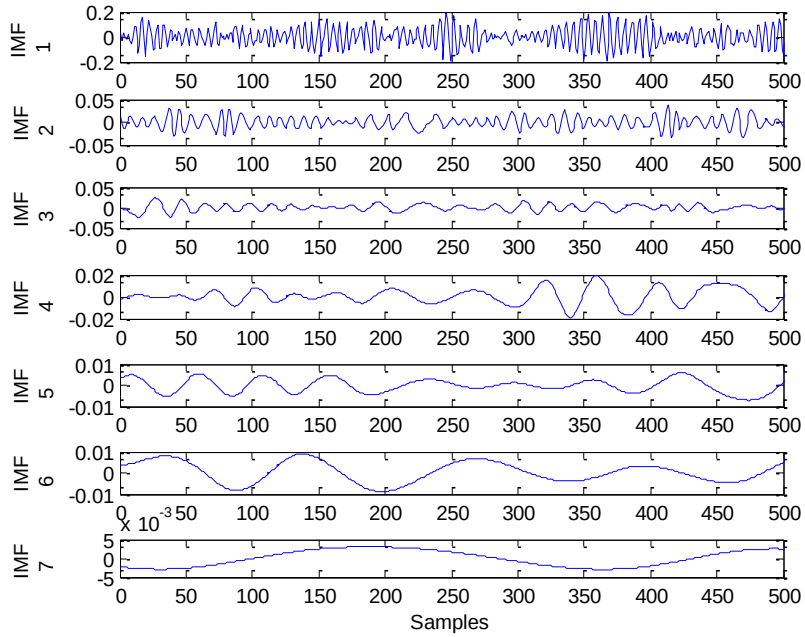

Figure 6.5 Decomposition of experimental vibration signals for healthy signal at 150 r/min

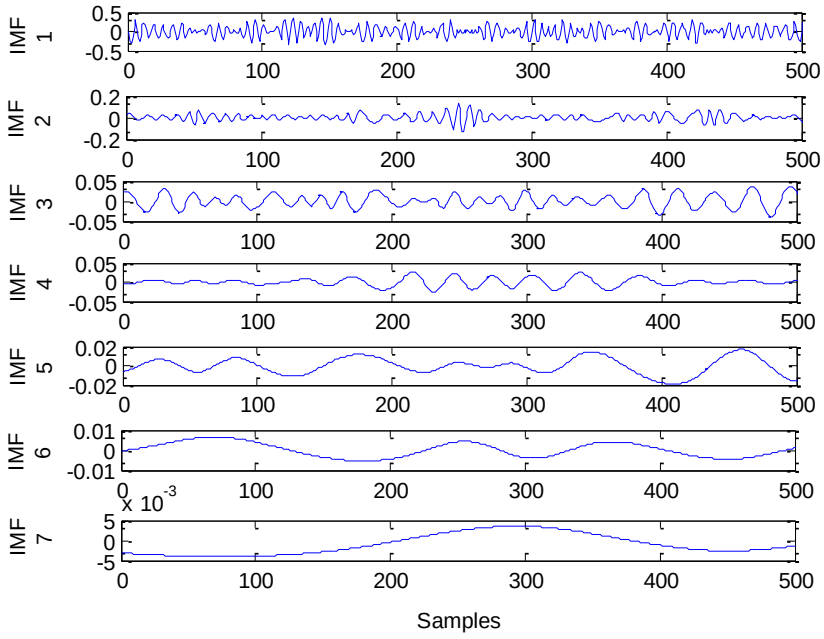

Figure 6.6 Decomposition of experimental vibration signals for healthy signal at 250 r/min

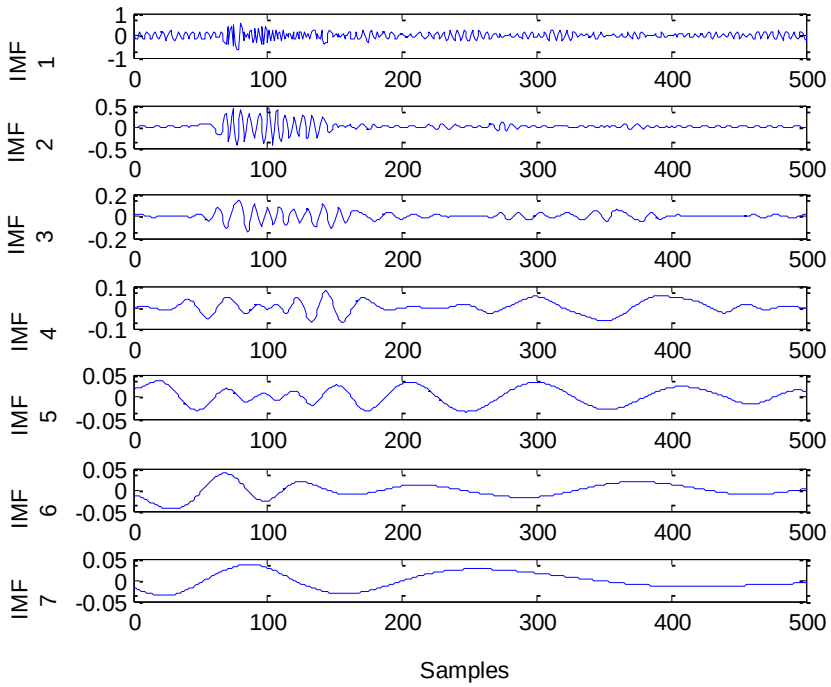

Figure 6.7 Decomposition of experimental vibration signals for healthy signal at 360 r/min

The decomposition separates modes high frequencies from low frequencies and it is assumed that the results shown in first IMF are completely corrupted by noise, whilst low frequency modes is usually related with components such as gears, bearings and shafts. The FFT was applied on each IMF for Figures 6.5, 6.6 and 6.7 in turn to produce the spectra shown in Figures 6.8, 6.9 and 6.10, respectively.

From these figures, the signals show different frequencies; high and low frequencies are produced from different sources such as gears, bearings, fan pass frequency and the shafts. By analysing the spectra shown in Figure 6.9 produced at 250 rpm, the first mode IMF1 contains a noise-contaminated signal. The second mode IMF2 is associated with meshing frequency (125 Hz), which is can be calculated as follows:

$$f_m = \omega_p N_P = \omega_g N_g \quad = \frac{250}{60} * 30 = 4.16 * 30 = 125\ Hz \qquad 6.10$$

Where Np, Ng = number of teeth on pinion and gear respectively. ω_p, ω_g are rotational speeds of the pinion and gear respectively.

The wind turbines blade pass frequencies (BPF) vary with number of blades (x) and rotational speed and can be expressed as:

$$\text{BPF} = \frac{\text{nx}}{60} \quad = 250 * \frac{3}{60} = 12.5\ \text{Hz} \qquad 6.11$$

Thus, the third mode IMF3 is associated with third harmonic of the fan pass frequency (50 Hz). The fourth mode IMF4 is associated second harmonic of the fan pass frequency (25.0 Hz), while the fifth mode IMF5 contains blade pass frequency (12.5 Hz).

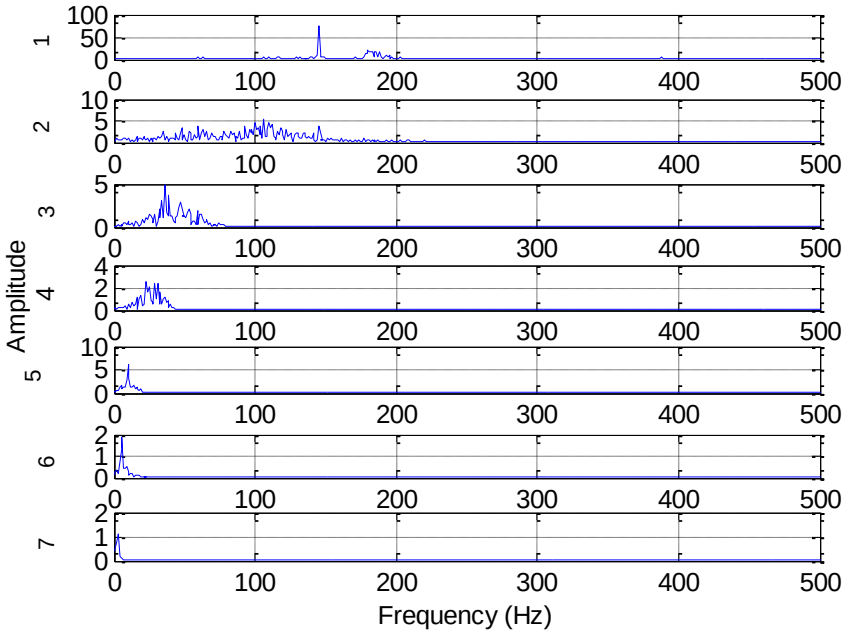

Figure 6.8 Fast Fourier transform is applied on each (IMF) at speed 150 r/min

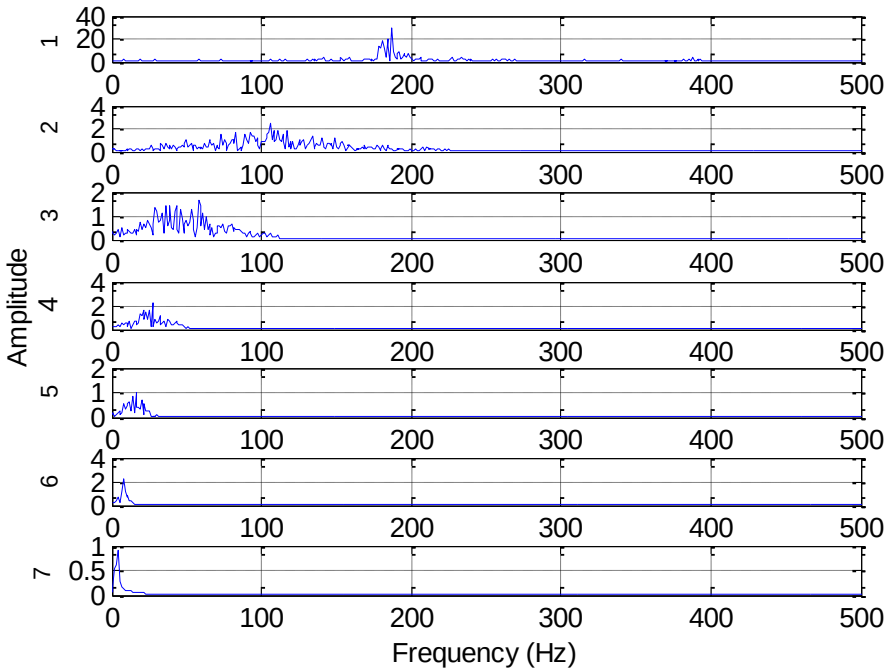

Figure 6.9 Fast Fourier transform is applied on each (IMF) at speed 250 r/min

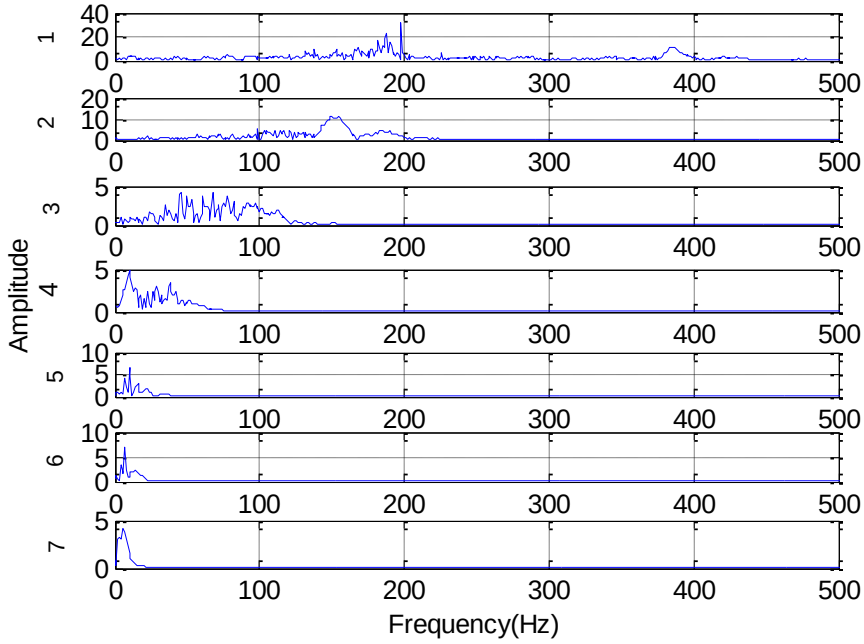

Figure 6.10 Fast Fourier transform is applied on each (IMF) at speed 360 r/min

In Figure 6.8, 6.9 and 6.10 the spectra corresponding to Mode IMF7 contains a spectral peak in the region of the shaft frequency. Thus for these cases, mode IMF7 was adopted to compute feature intensity level at different rotational speeds; 150, 250 and 360 r/min as explained below.

6.7 Proposed Novel Condition Index

The proposed method starts by measuring the wind turbine nacelle vibration, decomposes the measured signal into its fundamental frequency components and calculates the shaft speed signal intensity level. It then compares this level with the threshold amplitude of the baseline data for each speed. It uses curve fitting for the FFT spectrum in the region of the shaft frequency and its sideband zones.

If the fitted curve for the signal is p(f) the feature intensity level (FIL) of the signal in the frequency band from f_1 to f_2, can be expressed as:

$$\mathrm{FIL} = \int_{f_1}^{f_2} \mathrm{p(f)df} \qquad 6.12$$

Where, f_1 and f_2 are upper and lower frequencies of the frequency band.

Digitally using the discrete FFT, the feature intensity level (FIL) of the signal in the frequency band from f_1 to f_2, can be expressed as:

$$FIL = \sum_{f_1}^{f_2} \frac{1}{2}\left[p(f_i) + p\left(f_{(i+1)}\right)\right]df \qquad 6.13$$

Where $df = f_{(i+1)} - f_i$, $p(f_i)$. $p(f_i)$ = Amplitude of signal at f_i , and $p(f_{(i+1)})$ = amplitude of signal at $f_{(i+1)}$. The integration may be done for the whole range of frequencies obtained using the FFT. In this study the area contained between adjacent points on the spectral

envelope was calculated using the trapezoidal rule via MatLab. Figure 6.11shows the flowchart of algorithm proposed for the EDFIL.

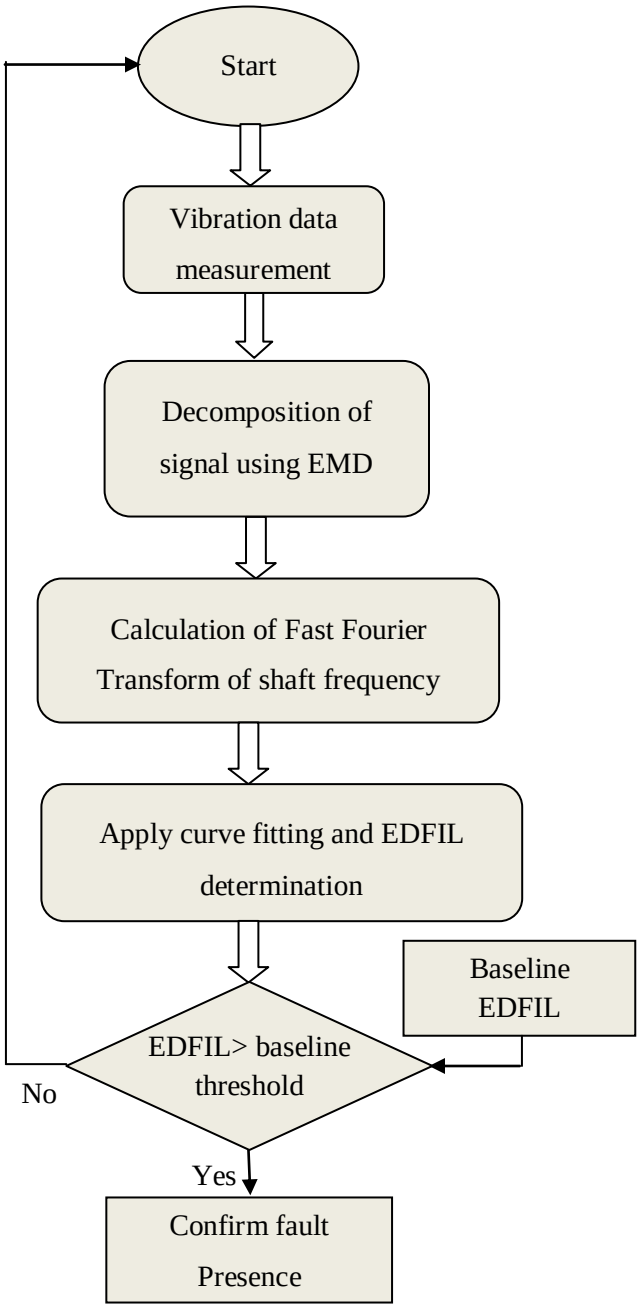

Figure 6.11 Flowchart of the proposed method EDFIL

6.8 Validation of the EDFIL:

Figures 6.12 and 6.13 represent feature intensity level for three healthy blades (h- healthy condition) and two healthy blades and third suffering from a crack (f1=10 mm, , f2= 20 mm, f3=30 mm, and f4=40 mm length) at three rotation speeds 150 r/min, 250 r/min and 360 r/min for both simulation and experimental signals, respectively.

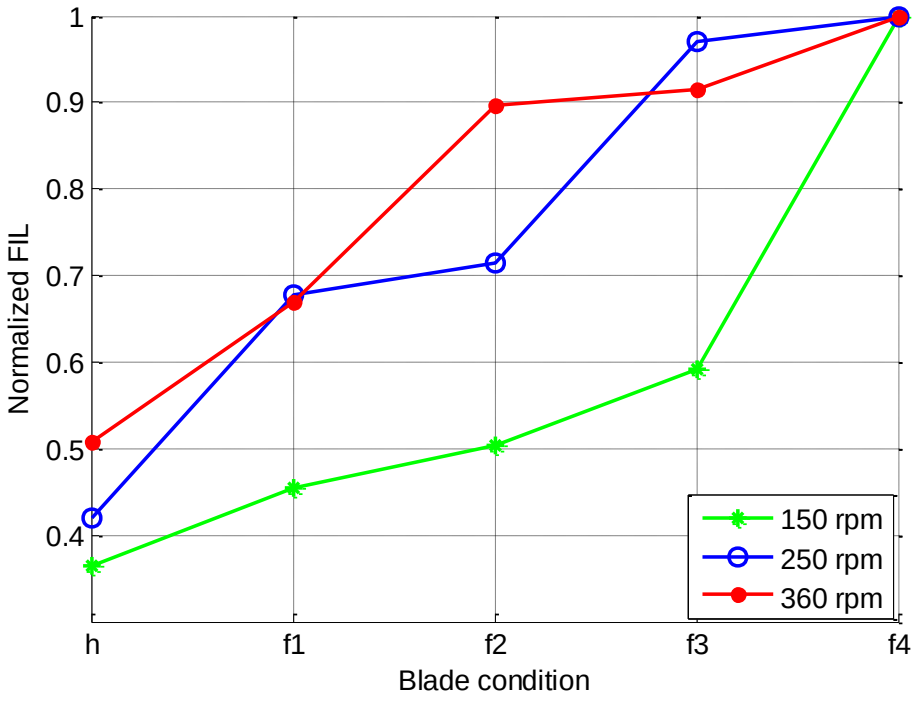

Figure 6.12 Normalized Feature intensity level contained in simulation signals

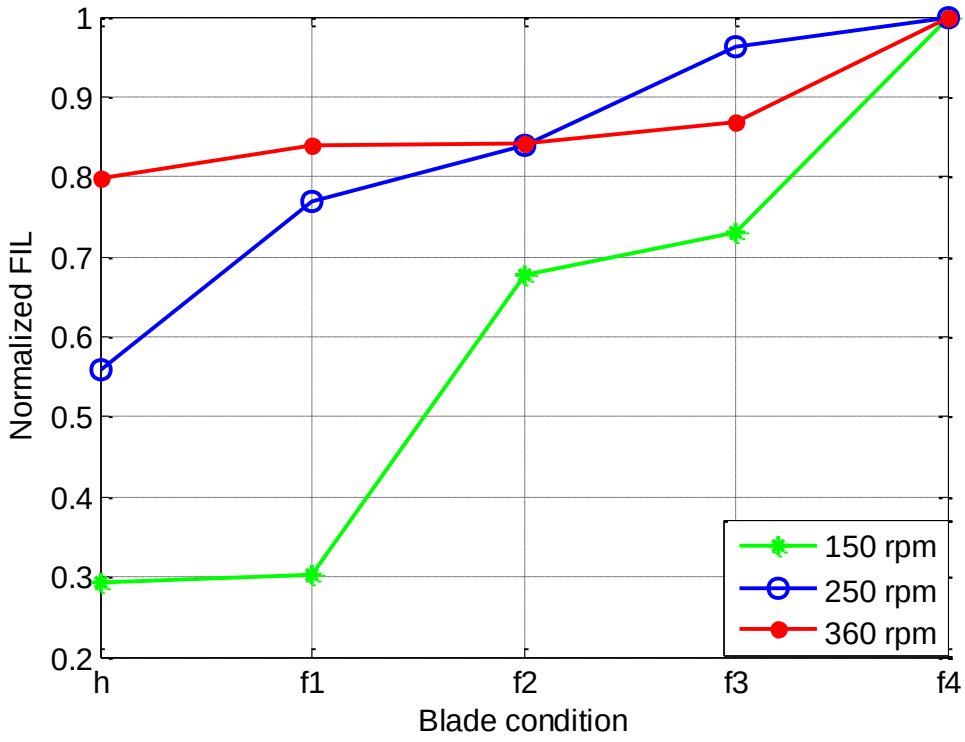

Figure 6.13 Normalized Feature intensity levels of experimental signals

For the experimental and simulation results it is noticeable that the normalized FIL increases both with shaft speed and with the severity of the fault. This is a promising result because it suggests that the rate of increase of normalized FIL could be significant for practical applications.

6.9 Summary

Empirical mode decomposition (EMD) is a powerful technique for improving signal to noise ratio of the measured corrupted vibration. EMD is an adaptive technique for signal decomposition with which complex signals can be decomposed into finite set of signals called intrinsic mode functions (IMF). Each IMF represents different frequency component from the whole frequency spectrum of the signal. Because of this ability, the

EMD is far better than the usual Fourier spectral analysis techniques and suits non-linear and non-stationary signals. .

This chapter has shown that with EMD it is possible to successfully identify the wind turbine vibration sources from the IMFs of a contaminated vibration signal. The FFT is applied on each IMF in turn to produce the spectra of those components. A new condition index has been proposed to increase the efficiency of EMD method when applied to practical situations. The new method seeks to combine feature intensity level and EMD for predictive maintenance and CM of wind turbine blades, in particular. The combination of feature intensity level and EMD were used to detect the presence and severity of cracks in a wind turbine blade. The EDFIL approach can indicate change in the running condition of a wind turbine and to provide the possibility of online CM of wind turbines which could be an optimal condition indicator especially for detecting crack initiation.

With further development EDFIL approach should be suitable and sensitive for both detecting and diagnosing the severity of crack faults.

Chapter 7

Wind Turbine Vibration Analysis Using a Wavelet Technique

This chapter introduces the wavelet analysis techniques and then gives the theory of the continuous wavelet transform (CWT). The CWT method is applied to the wind turbine vibration signal. The blades condition related feature intensity levels based on CWT were calculated for healthy and faulty signals fallowed by discussions and a summary of the results obtained.

7.1 Introduction

The increasing popularity of wavelet transform has meant that today its use rivals that of the Fourier Transform (FT) or Fourier series particularly for time varying signals. Comparing the two, the wavelet transform (WT) uses a so-called mother wavelet instead of the exponential scaling of the FT and translation replaces frequency shift. The essential difference is that a two-dimensional (surface) wavelet coefficient replaces the single dimension Fourier coefficient. The consequent advantage of the WT is that it can provide an analysis that contains information in both the time and frequency domains. Wavelets used to analyze signals are mathematical functions which are limited with definite end points along their axis – unlike the sine and cosine functions of the FT they do not repeat to infinity. This makes wavelets different from other transformations because not only can they divide time domain signals into their component frequencies, they can also be expand or compress the (time) scale over which the frequencies are analyzed[135]. This allows the scale to be matched to the required resolution of the signal and gives the WTs the ability to treat non-stationary signals. Thus the WT is used increasingly used for condition monitoring of rotating machinery, to diagnose the presence of faults such as bearing defects, rotor cracks, rotor misalignment and unbalance, etc. Recently WTs have also been applied to detect stable and propagating cracks.

7.1.1 Continuous Wavelet Transforms (CWT)

Once the window function has been selected the commonly used fast Fourier transform (FFT) and digital Fourier transform (DFT) are constrained to fixed resolutions in both the time and frequency domains. The WT of a time signal is an expansion of the signal in

terms of family of functions, which are generated from a mother wavelet which may contain one or more wavelet kernels[136]. The classical FT transforms data from the time to the frequency domain using sinusoids as the basis functions, which give the time-averaged characteristics of the signal. The WT moves data from a space to a scale (or time-frequency) domain with the chosen wavelet as the basis function retaining local features of the original signal. An important characteristic of the WT is that the duration of the time window can be changed depending on whether the signal has a high or low frequency content. This is a crucial difference between WT methods and traditional time-frequency methods because it means the WT can resolve transient phenomena making it suitable for analysing non-stationary signals such as early detection of faults in gearboxes.

In this section, the continuous wavelet transform (CWT) is introduced and used to detect wind turbine blade faults. Wavelets occur in sets or families of functions defined by the mother function; the position of the wavelet in time (where on the signal the daughter wavelet is placed) is controlled by the *translation* or *shift*, the scaling parameter (which determines the time and frequency resolution) is defined by a *dilation*. Mathematically, the CWT of the continuous signal *x(t)* is defined [137, 138]:

$$CWT_x(a,b) = W_\psi(a,b) = \frac{1}{\sqrt{a}}\int_{-\infty}^{+\infty} x(t)\psi^*\left(\frac{t-b}{a}\right)dt \qquad 7.1$$

Where a (a>0) is dilation/contraction factor, b is the translation factor, $\psi(t)$ is the mother wavelet and the factor $1/\sqrt{a}$ is included for energy normalisation. The mother wavelet is translated and dilated into the daughter wavelet ($\psi_{ab}(t)$) as:

$$\psi_{ab}(t) = \frac{1}{\sqrt{a}}\,\psi(\frac{t-b}{a}) \qquad 7.2$$

Where $\psi(\frac{t-b}{a})$ is the mother wavelet translated by a factor of *b* and dilated by *a*. The daughter wavelet, $\psi_{ab}(t)$, changes continuously due to varying the scaling parameter and changing *a* and *b*. When a low frequency wavelet is required (one spread out in time) large scales are selected, and *vice versa*. CWT is defined as the sum over all time of the signal, and is one of the best transforms for singularity detection.

7.1.2 Selection of Analysing Wavelet

There are a number of functions that can be used as analysing wavelets and each will have its own properties. Some of the most widely used wavelets are; Daubechies, Haar, Meyer and Morlet, see [139, 140]. Window function in L^2(IR) should have a localisation property.

The size of the time-frequency window determines the localisation property of the Short Time Fourier Transform (STFT), and is defined in terms of its frequency bandwidth Δf and duration Δt. For good time-frequency localisation the window must have a sufficiently small area, but the resolution is restricted by the uncertainty principle [137]:

$$\Delta t\,\Delta f \geq \frac{1}{4\pi} \qquad 7.3$$

The greatest precision is with equality in Equation 7.3, a condition which is reached if the window is the Gaussian function [137]:

$$g_{\alpha}(t) = \frac{1}{2\sqrt{\pi\alpha}}\,e^{\left(\frac{-t^2}{4\alpha}\right)} \qquad 7.4$$

Where $\alpha > 0$. Such a window is called the Gabor Transform and is given by:

$$G(f) = \int_{-\infty}^{\infty} x(t)e^{iwt}\, g_t(t-b)dt = \int_{-\infty}^{\infty} x(t)\overline{G(t)}dt \qquad 7.5$$

Where *x(t)* is the signal being transformed and *G(t)* is taken as a windowing function. In this study, Equation 7.5 is used as an analysing wavelet by setting [137]:

$$G(t) = \psi(t) = ce^{iat}\, g_{\infty}(t-b) \qquad 7.6$$

Where $c \neq 0$, $\alpha > 0$.

Analysing wavelets with fast decay rates usually possess a good localisation capability. An advantage of the wavelet in Equation 7.5 is that the decay rate can be controlled not only the scale parameter *a* but also by selection of α. This provides additional flexibility when attempting to obtain good time-frequency resolution.

7.1.3 Properties of the Wavelet Transform

The four most important properties of the WT transform are [137, 140, 141]:

Conservation of Signal Energy: A WT preserves the energy of a signal so that the total energy of the signal can be expressed in terms of the WT [142]:

$$E_x = \int_{-\infty}^{\infty} |x(t)|^2 dt = \iint |CWT_x(a,b)|^2 \frac{dadb}{a^2} \qquad 7.7$$

Thus the square of the modulus of the CWT is an energy density distribution of the signal in the time-scale plane.

Linearity: In most time-frequency distributions bilinearity is undesirable because it causes interference when multi-component signals are analysed. The WT is suitable for

the analysis of multi-component signals because it is a linear representation of a signal and so does not generate interference.

Resolution: The *uncertainty principle*, Equation 7.3, expresses an unavoidable relationship between time and frequency which imposes a limit on their resolution. In contrast the WT offers a local resolution in time and frequency as [143]:

$$\Delta t = a\Delta t_g \qquad 7.8$$

$$\Delta f = \frac{\Delta f_g}{a} \qquad 7.9$$

Where Δf_g and Δt_g are the bandwidth and duration of the analysing wavelet, respectively. From Equations 7.8 and 7.9, it can be seen that the time resolution becomes arbitrarily good at high frequencies, while the frequency resolution becomes arbitrarily good at low frequencies. The wavelet is suitable for the detection of transients in signals because of this high resolution characteristic.

Localisation in the frequency and time domains: Generally, the value of the CWT at any particular (a, b) in Equation 7.2 will be *non-local* and depend on the analysed signal at all instances of time.

7.2 Performance of CWT Method in Detection of Wind Turbine Blade Crack

Important practical parameters that have substantial impact on the quality of analysis by WT are the sampling frequencies of the signal and of the wavelet function. The sampling frequency of the signal determines the accuracy of the time resolution and the sampling frequency of the wavelet function determines the frequency bandwidth of the analysis.

In this chapter the CWT was used to distinguish between wind turbine conditions and detect faults. Figures 7.1 to 7.3 show the CWT plots for the healthy and faulty wind turbine at 150, 250 and 360 rpm respectively. The results are displayed as time-frequency distributions with the colours representing the intensity (magnitude) of the signal.

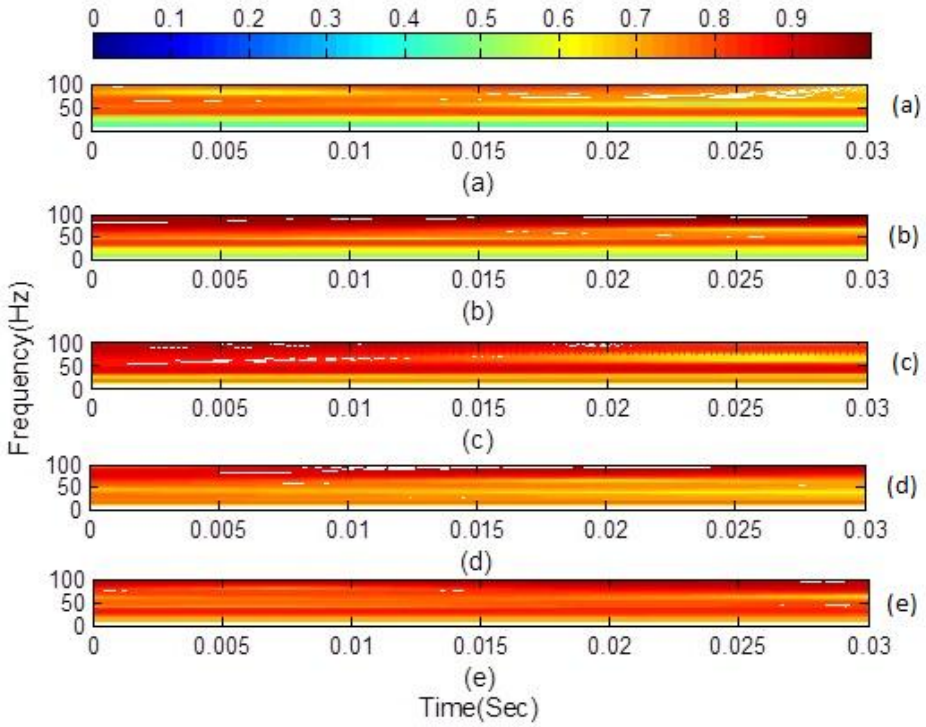

Figure 7.1 Wavelet transform (CWT contour plot) for healthy and cracked wind turbine blade at 150 r/min a) healthy, b) fault 1 (10 mm), c) fault 2 (20 mm), d) fault 3 (30 mm) and e) fault 4 (40 mm).

Figure 7.1a shows the contour plot for the healthy wind turbine and it can be seen that the energy distribution varies with time, and this is more clearly observable at higher frequencies. Figures 7.1b, 7.1c, 7.1d and 7.1e present the CWT plots for increasing fault severity and show that the vibration energy around the fundamental shaft frequency 2.5

Hz and its 2nd and 3rd harmonics 5.0 Hz and 7.5 Hz, respectively are affected significantly and gradually increase with growth in the fault. Figure 7.2a, presents the plot for the healthy wind turbine at a rotational speed 250 rpm, while 7.2b, 7.2c,7.2d and 7.2e show the CWT plots for increasing fault severity around the fundamental shaft frequency 4.1 Hz.

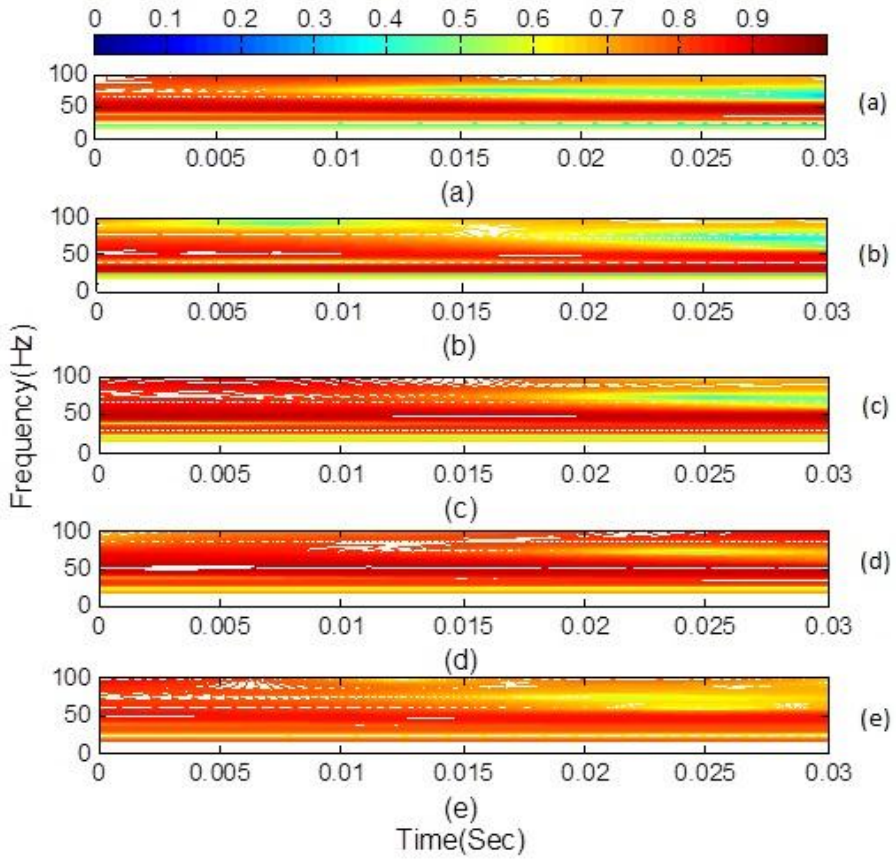

Figure 7.2 Wavelet transform (CWT contour plot) for healthy and cracked wind turbine blade at 250 r/min. a) healthy, b) fault 1 (10 mm), c) fault 2 (20 mm), d) fault 3 (30 mm) and e) fault 4 (40 mm).

Finally, Figure 7.3 show the CWT plots for wind turbine healthy and with seeded cracks at a rotation speed 360 r/min. As can be seen the energy distribution increases around the fundamental shaft frequency and its multiples as the severity of the fault increases.

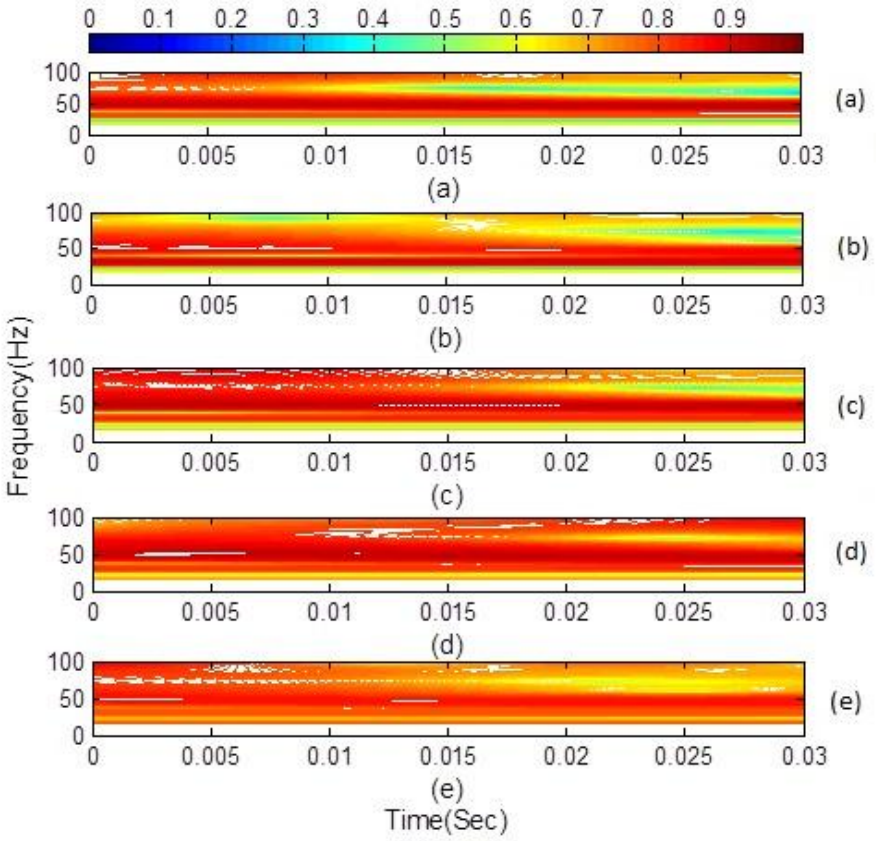

Figure 7.3 Wavelet transform (CWT contour plot) for healthy and cracked wind turbine blade at 360 r/min a) healthy, b) fault 1 (10 mm), c) fault 2 (20 mm), d) fault 3 (30 mm) and e) fault 4 (40 mm)

Figures 7.4, 7.5 and 7.6 represent the feature intensity level for three healthy blades (h - healthy condition) and two healthy blades and third suffering from a crack (f1=10 mm, , f2= 20 mm, f3=30 mm, and f4=40 mm length) at three rotation speeds 150 r/min, 250 r/min and 360 r/min for experimental signals, respectively.

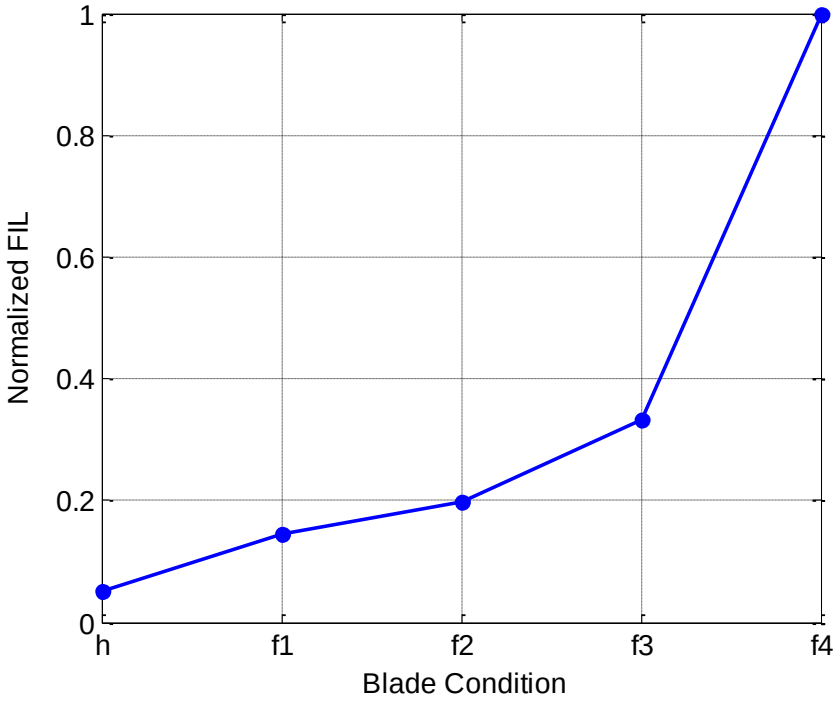

Figure 7.4 Normalized FIL at rotational speed 150 r/min

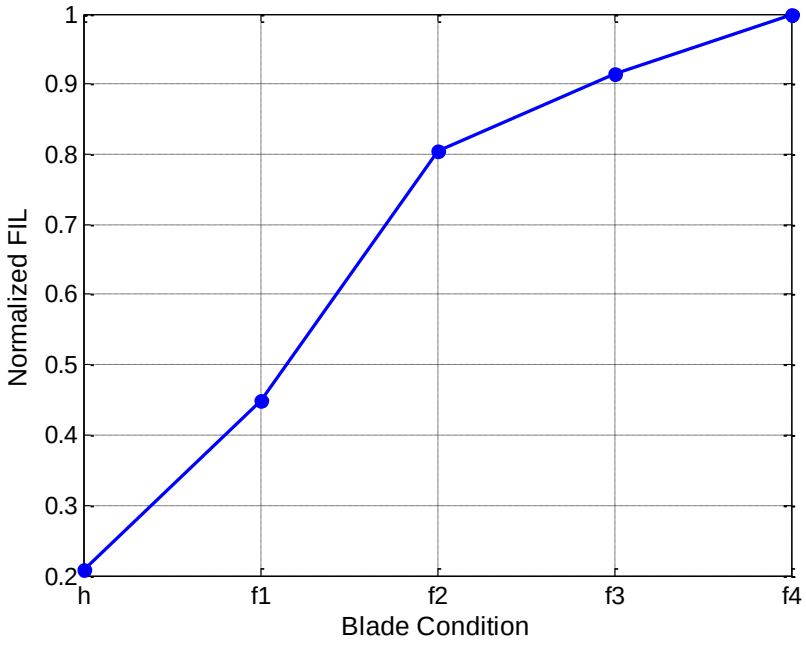

Figure 7.5 Normalized FIL at rotational speed 250 r/min

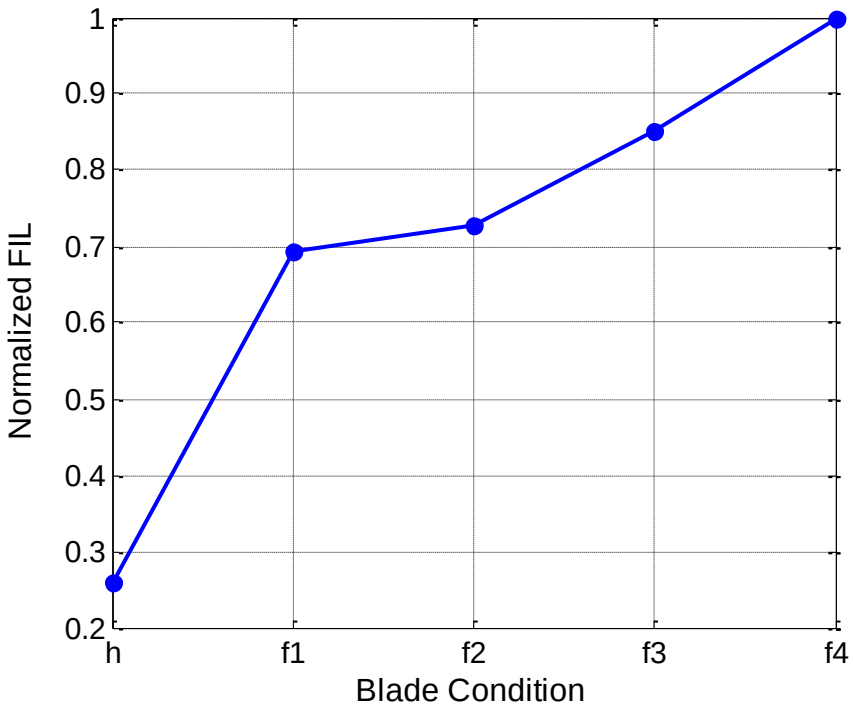

Figure 7.6 Normalized FIL at rotational speed 360 r/min

Form the results; it is noticeable that the normalized FIL increases both with shaft speed and with the severity of the fault. This is a promising result because it suggests that the rate of increase of normalized FIL could be significant for practical applications.

7.3 Summary

This work has introduced wavelet analysis as a time-frequency analysis tool and has used the CWT algorithm to analyse noisy, non-stationary and nonlinear vibration data from a wind turbine.

Wavelet based analysis techniques have advantages over traditional Fourier transforms for revealing the random and non-stationary components within the signals of interest. This kind of analysis is suitable for signals composed of high frequency components with

short duration and low frequency components with long duration, which is often the case in practical situations. Moreover, CWT is an excellent denoising signal tool in joint time and frequency domain. In this chapter, the mathematical background of the CWT technique was briefly explained and a MatLab code was developed for analysing wind turbine vibrations.

The CWT representation produces an interpretable contour plot of the vibration signals when applied to detect the presence of cracks in the wind turbine blades. From Figures 7.1a, 7.2a, 7.3a, the energy of the signal appears predominantly around the fundamental shaft frequencies 2.5 Hz, 4.2 Hz and 6 Hz for the healthy blade at 150 r/min, 250 r/min and 360 r/min, respectively. When the cracks are seeded into one of the blades, see Figure 7.1(b, c, d and e), Figure 7.2 (b, c, d and e) and Figure 7.3(b, c, d and e) some of the energy of vibration can be seen to concentrate around fundamental shaft frequency.

Thus, it has clearly shown that the energy content of the CWT is proportional to the blade's crack severity. Moreover, calculation of FIL offers a more effective way to detect faults than these statistical measures. The technique has been successfully applied for detection of cracked blade.

Chapter 8

Principal Component Analysis Techniques for Signal Enhancement

This chapter introduces principal component analysis (PCA) its underlying concepts and the background before discussing the application of PCA to data collected from a wind turbine. Finally, the Crest Factor (CF) is applied to the residual matrix as an approach for the detection of cracks in wind turbine blades. This is followed by a summary of the results obtained.

8.1 Introduction

Detection of faults in complex rotating machinery, particularly wind turbines, remains an ongoing challenge. It has long been established both experimentally and theoretically that many machine faults are directly related to machine vibrations [144]. Over the past decade there have been substantial advances in both sensing and signal processing but many difficulties remain to the successful detection of incipient faults [145, 146]. The emphasis has tended to be on the development and application of new signal processing techniques because it is believed that modern sensors are sufficiently sensitive that their output signals contain sufficient information to detect faults in their early stages, and what is required is a method to extract that information. Signal processing methods to obtain suitable statistical measures may involve:

- Identification of a suitable statistical model/process,
- Cluster analysis and classification,
- Data compression to reduce data dimensionality, and
- Other data manipulation techniques.

Wind turbine vibration even for a healthy machine will be contaminated by noise, and for faulty machines will be a non-stationary and nonlinear process. It has been found that Principal Component Analysis (PCA) is well suited to analysing such a problem.

PCA is a method used for identifying those features of a system, which are most important in regulating its behaviour. Statistically this means establishing the most informative features in the data sat. PCA is used to reduce the complexity of a large data

set that contains information from a numerous variables all of whose behaviour influences the system. The starting point might be the peaks in the vibration spectrum of, say, a faulty wind turbine. PCA uses matrix analysis to reduce the original data set to a much smaller set of variables which represent the original data with minimum loss of information. The technical problem here is to gain sufficient simplicity to make the process worthwhile but ensure the information lost in the process does not contain essential information about the system behaviour. In the condition monitoring (CM) of wind turbines, PCA can be looked at as a method of selecting the most important features to monitor [147].

PCA is a popular tool in multivariate statistical analysis and is based on an orthogonal decomposition of the covariance matrix of the process variables along the directions that explain the maximum variation of the data.

8.2 Principal Component Analysis

Potentially important uses for PCA in the CM of, say rotating machinery, is the classification of the relative importance of variables, early detection and identification of any abnormality arising in the data set and the detection of outliers in the data set. In CM there can be a very large number of measured variables, and multivariate statistical techniques are used to reduce data dimensionality (number of variables) so that only the more essential information is retained which can then be analyzed relatively easily.

Johnson and Wichern [148] have described how multivariate techniques, by considering all possible relevant variables simultaneously, have extended traditional single variable univariate methods to process variation. Kourti [149-151]has explained that PCs can be

extracted using a linear combination of the original input variables. He has shown that if, for example, there are six relevant variables in a process: and of these *v*1, *v*3 and *v*4 demonstrate the same trend – that is they are correlated (could be positive or negative correlation) with each other over the specified time period – then a weighted average of *v*1, *v*3 and *v*4, can be used as a single PC. If there were also a correlation between of *v*2, *v*5 and *v*6 then a weighted average of these three variables would be a second PC. The initial six variables are reduced to two PCs which because of the correlations between the variables can still adequately represent the major trends contained the original data set. According to Kourti [151] PCA methods when applied to steady state conditions can invariably reduce the original number of variables to a two-dimensional matrix. In practice, of course, such steady state conditions may not prevail but relevant PCA methods have been developed for use in such real conditions

Before generalising let us consider the three dimensional data set of *n* points shown in Figure 8.1.This represents three variables contributing to the data set. For simplicity the n-points lie on a plane. Here, the first PC axis will be the line on which the projections of the *n* points have maximum variance. It can be seen that this is the line PC-1. The second PC will be orthogonal to the first and will be the line on which the projections of the *n* points have maximum variance; this is the line PC-2, and so on if there were more dimensions.

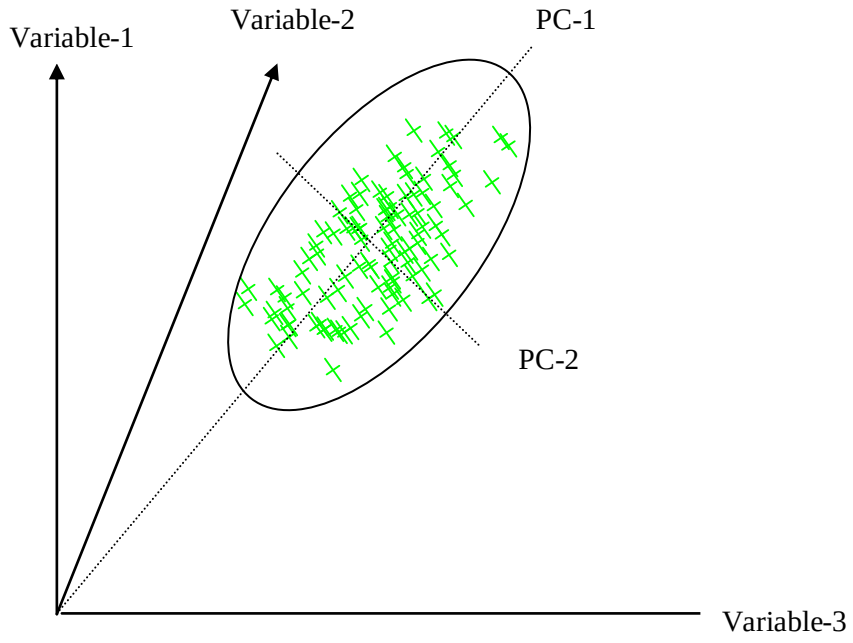

Figure 8.1 Principal components in three dimensions

More generally, PCA explains the spread of a sample set of *m* points in *s*-dimensional space in terms of a set of orthogonal linear coordinates so that the variance of the sample with respect to these new co-ordinates is in decreasing order of magnitude.

$Let\ X = x1, x2, x3, \ldots xm$ be a data set in m-dimensions describing the behaviour of a wind turbine under consideration. PCA decomposes vector, X, as [152]:

$$X = TP^T = t_1 p_1^T + t_2 p_2^T + \cdots .. + t_m p_m^T = \sum_{i=1}^{m} t_i p_i^T \qquad 8.1$$

Where pi is an eigenvector of the covariance matrix of X. T is defined as the *score* matrix of the PCs, and P is defined as the PC *loading* matrix. Information on which variables contribute most to the PCs is given by the loading and information on how the data set is clustered is obtained from the score – as is identification of transitions between different operating conditions.

The PCA transforms take the groups of correlated variables in the original data set and uses the covariance matrix to transform them into a new set of uncorrelated variables. The general expectation is that there is a sufficiently large correlation among the original data set that the first few PCs account for most of the variance. If this is true then no important information or insights are lost by using only the first few PCs for further analysis. Thus it is often both possible and desirable to omit higher order PCs and retain only the first few lower order PCs. In that case Equation 8.1 can be expressed as [153]:

$$X = TP^T + E = \sum_{i=1}^{K} t_i p_i^T + E \qquad 8.2$$

Where E is the residual error matrix; the error due to omitting the higher order PCs. For example, if the first two PCs represent most of the total variance, the residual error matrix will be:

$$E = X - [t_1 p_1^T + t_2 p_2^T] \qquad 8.3$$

It is common to find in the literature claims that the first few PCs contain all of the necessary information. This may be the case for most CM but in some process monitoring applications when a plant suddenly malfunctions it is the higher order PCs which dominate. Analysis of these higher order components may provide valuable diagnostic information on sudden failures in process engineering [152].

8.3 Implementation of PCA using Single Value Decomposition

With process machinery a common first step in implementing PCA is to obtain a correlation matrix or covariance matrix. For m-variables$(X = x1, x2, x3, \ldots xm)$, the correlation matrix is:

$$S = \begin{bmatrix} s_{11}^{\ 2} & s_{12} & \dots & s_{1m} \\ s_{21} & s_{22}^{\ 2} & \dots & s_{2m} \\ : & : & \dots & : \\ s_{m1} & s_{m2} & \dots & s_{mm}^{\ 2} \end{bmatrix} \quad 8.4$$

Where s_i^2 is the variance of the i_{th} variable, $x_{i,}$, and s_{ij} is the covariance between the i_{th} and j_{th} variables. The method of PCs is to calculate the *eigenvectors* and *eigenvalues* of matrix *S*. The covariance of matrix *S* will be a symmetric, non-singular, *m x m* matrix, and such a matrix can be reduced to a diagonal matrix *L* by suitable matrix manipulation:

$$U^T SU = L \quad 8.5$$

Where U is an orthogonal, unit matrix.

The eigenvalues of *S* are the diagonal elements of *L*, (l_1, l_2, $\dots l_m$). The eigenvectors of S are the column vectors of *U*, $(u1, u2, \dots um)$. The eigenvalues can be obtained by solving the following determinantal equation:

$$|S - lI| = 0 \quad 8.6$$

Where *I* is the identity matrix.

Equation 8.6 represents an m^{th} degree polynomial in *l* which can be solved for the Eigenvalues and eigenvectors using, e.g., an iterative technique [154].

Singular value decomposition (SVD) is used to implement PCA In SVD, a data matrix *X* is decomposed into products using [155-157]:

$$X = U\lambda P^T \quad 8.7$$

Where U are eigenvectors and λ eigenvalues of XX^T and P^T is a loading matrix.

The major advantage of SVD is that all three matrices can be found in a single operation without the need to find a covariance matrix. MatLab can be used to implement PCA by SVD.

8.4 Fault Detection Based on the PCA Model – Q and T^2 -Statistics

Once a PCA model is established it can be used as a basis to which the behaviour of the machine can be referred. Suppose a new event occurs (a fault say) which was not present in the data used to develop the PCA model, the new observation(s) will be outside the space defined by the PCA model and as such will indicate an abnormality. One technique to detect such events is to compute the square prediction error (SPE) of the residuals of the new observations [158]. The SPE is found by finding taking the differences between the observed values and values predicted for the normal condition, squaring and summing them as:

$$SPE = \sum_{I=1}^{K}(x_{ij} - \bar{x}_{ij})^2 \quad 8.8$$

Where, x_{ij} and $\bar{x}_{ij}$ are the observed values and values predicted by the PCA model respectively.

This statistic is known as the Q-statistic or "distance to the model" [159] It represents the square of the perpendicular distance of the new observation from the plane. When the machinery operates normally, the SPE is relatively small, but when there is a deviation from the normal condition, such the introduction of a fault, the value of the SPE will

increase and may fluctuate depending on the nature and severity of the fault. An unusual event that produces a change in the covariance of X will be detected as a high value of the SPE which means that the normal PCA model is no longer valid. Thus the Q-statistic can be used as a measure of a parameter varying outside of the normal PCA model. Upper control limits for the SPE can be determined from normal/historical data [158]. Because the T^2-statistic measures the overall variability of the data it can be used to detect unusual variations beyond the norm.

The T^2-statistic focuses directly on the PCs rather than the residual. Hotelling's T^2-statistic is simply the sum of squares of the PCs that are retained. Thus, if the u_i represents the principal components, then T^2 can be calculated [154]:

$$T^2 = u_1^2 + u_2^2 + \cdots \ldots + u_K^2 \ (i = 1,2,3, \ldots k \text{ retained PCs}) \qquad 8.9$$

8.5 Performance of PCA Method in Detection of a Wind Turbine Blade Crack

In this section we apply the PCA method to real data and consider it as a method for reducing what may be considered a contaminated signal into a series of manageable data sets. Every set contains its PCs, which are interpretations of the original data.

The experimental work was carried out with two healthy blades and a single blade with a crack introduced. The seeded cracks were all 3 mm wide and 2 mm deep, and of four lengths 10mm, 20mm, 30mm and 40mm, as shown in Figure 4.3. The tests were carried out for three rotation speeds; 150, 250 and 360 r/min and then analyzed using the PCA method.

Figure 8.2 shows eigenvalues plotted against PCs at rotational speed 150 r/min. From theory each PC contains a proportion of the total variance and the eigenvalues represent the amount of variance. Thus the eigenvalues are a measure the relative importance of each PC in reconstructing the real signal. It can be seen the shape of the eigenvalue plot changes with significantly once a crack fault is introduced into the blade but the change in shape of the curves is not sufficiently clear to detect and identify the seeded faults.

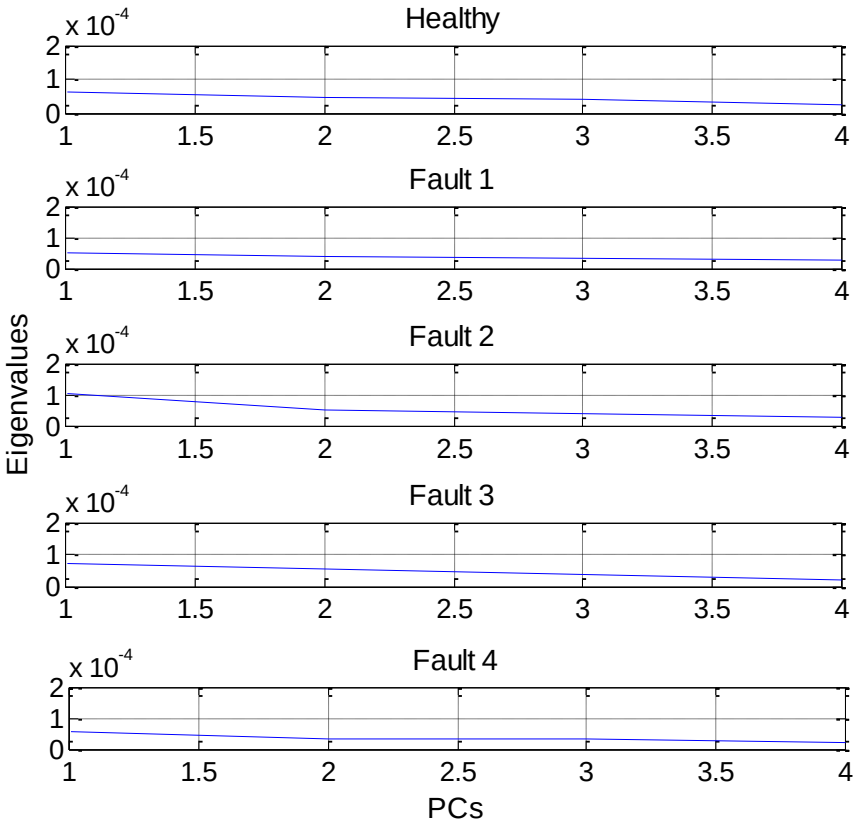

Figure 8.2 Eigenvalues for healthy and blade with seeded cracks.

Figure 8.3 shows score plot for healthy and four faulty cases. This plot presents such characteristics as size, spread and clusters in the data. From the plot there is no clear difference between healthy and faulty cases, which means that this method is certainly not sensitive enough to small changes in the vibration signal to detect initial faults.

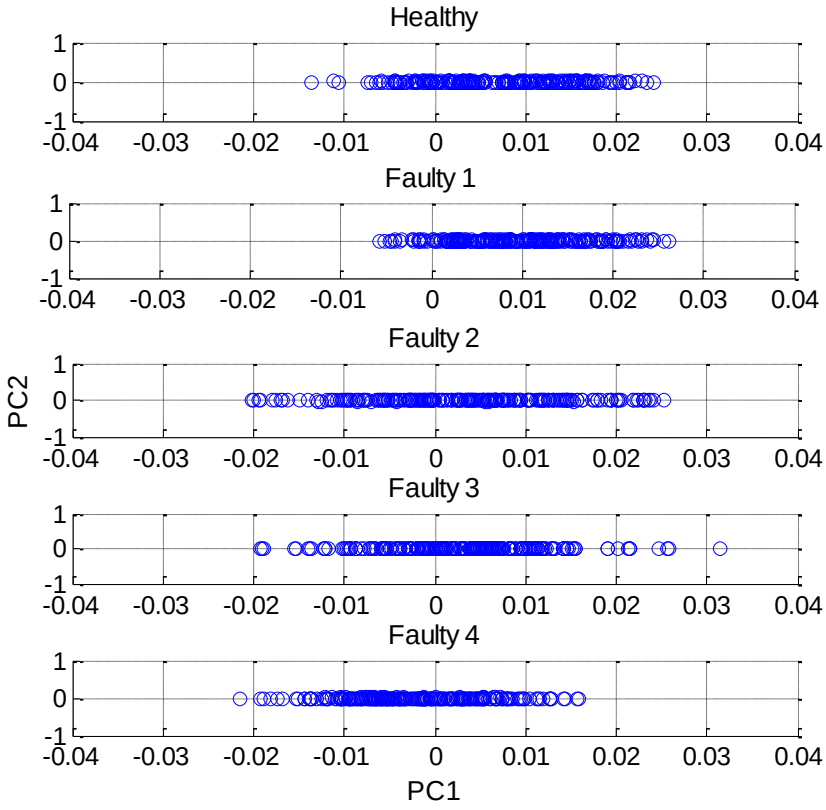

Figure 8.3 Score plot for healthy and faulty blade for the first PC

The main use of PCA is to reduce the dimensionality of a data set and it is assumed that the first few PCs contain most of not all the necessary relevant information contained in the original data. Thus it follows that the remaining PCs should contain mostly noise from the original data. According to PCA theory these PCs can be placed in a separate matrix called the residual matrix, which is constructed in the same way as the original

data matrix except it contains only the so-called irrelevant PCs and their respective weightings.

In fact, the relevant scores (PCs) are used to calculate the Residual Matrix. The Residual Matrix contains the information which has been removed from the analysis and the residual errors are found using this matrix. Here the sum of the error in each column of the matrix is squared to give a positive result which is plotted. The residual errors plots for healthy and faulty cases are showed in Figure 8.4. From this figure, there appears to be a noticeable difference between healthy and faulty cases. But to differentiate the cases between healthy and faulty was difficult.

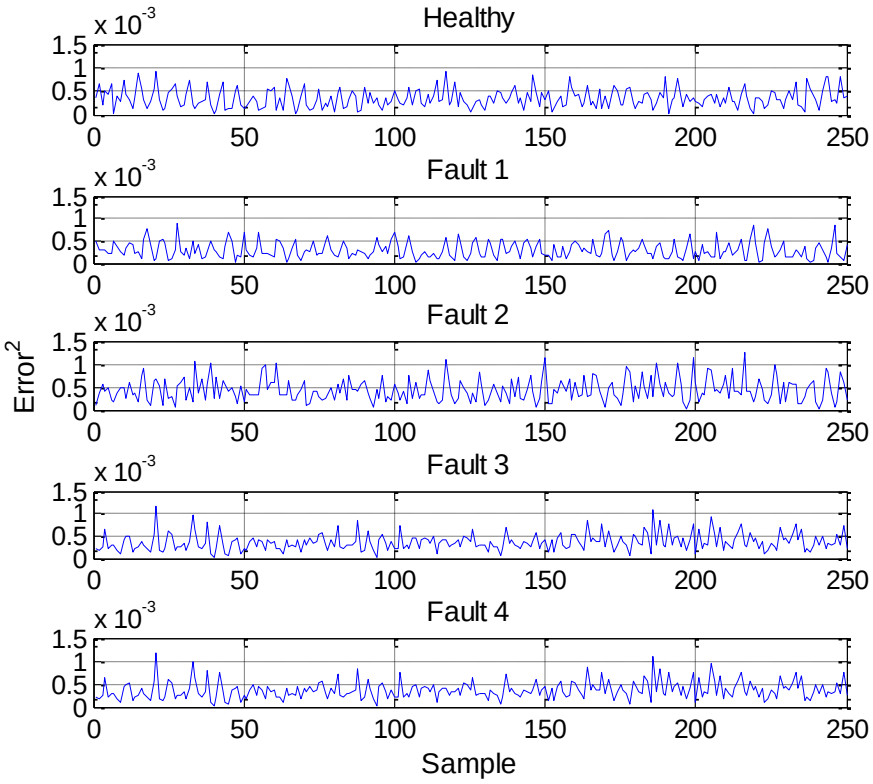

Figure 8.4 Residual error plot for healthy and faulty blade**.**

Developing a new way of thinking about this analysis could provide an effective PCA method of evaluating the signals obtained from CM to determine incipient faults. It was decided to calculate the Crest Factor (CF) for the residual signal for each fault seeded into the system and this has led to a novel condition index ‘’indicator’’.

8.6 Derivation of Novel Condition Index Based on PCA

A PCA-based technique was applied to the measured data collected form wind turbine under different condition. According to equation 8.3 the residual error matrix is E, it extracted for healthy and faulty signals, thus CF was calculated for the residual signal for healthy and for each fault seeded into the wind turbine blade. As known to calculate CF, the root mean square (RMS) is required. It is defined as the square root of the average of the sum of the squares of N samples of the signal and is given by;

$$RMS_x = \sqrt{\frac{1}{N}[\sum_{i=1}^{N}(E_i)^2]} \qquad 8.10$$

Where E_i is the prediction error vector of the residual error matrix sampled time signal, N is the number of samples and subscript i represents the value of the i^{th} sample. The CF is defined as the maximum positive peak value of the matrix E divided by the RMS value of the residual error matrix E:

$$CF = \frac{E_{0-pk}}{RMS_x} \qquad 8.11$$

Healthy and damaged blade, with different size of cracks is set up and vibration signals are collected and processed in order to properly detect a fault as explained in chapter 4

that continue experimental setup. The proposed novel technique is to determine wind turbine faults based on the RMPCA algorithm shown graphically in Figure 8.5.

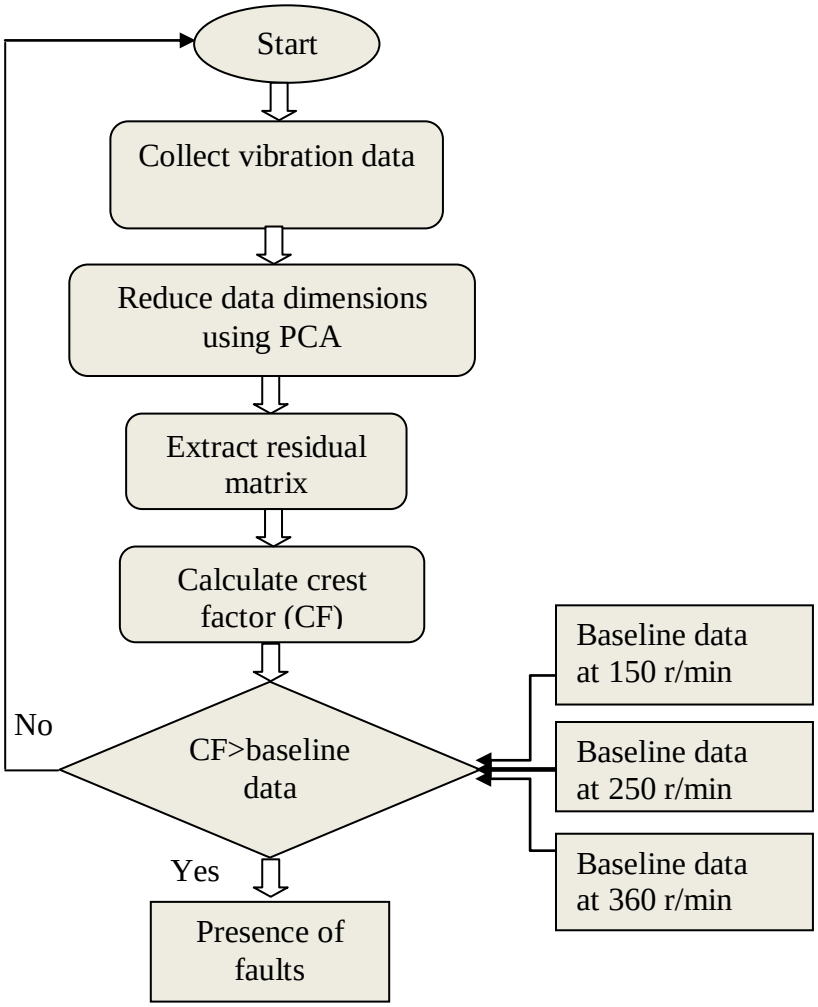

Figure 8.5 Illustration of the RMPCA based proposed technique

8.7 Performance of Proposed Method (RMPCA)

The proposed technique was applied on the residual matrix for the three healthy blades and blade with faults seeded into it. Figures 8.6, 8.7 and 8.8 represent CF values for the residual matrix for the wind turbine blade signal at three rotational speeds. It can be seen that the value of CF increased with fault level which suggest that the proposed method may have advantages over the other statistical techniques when used with PCA.

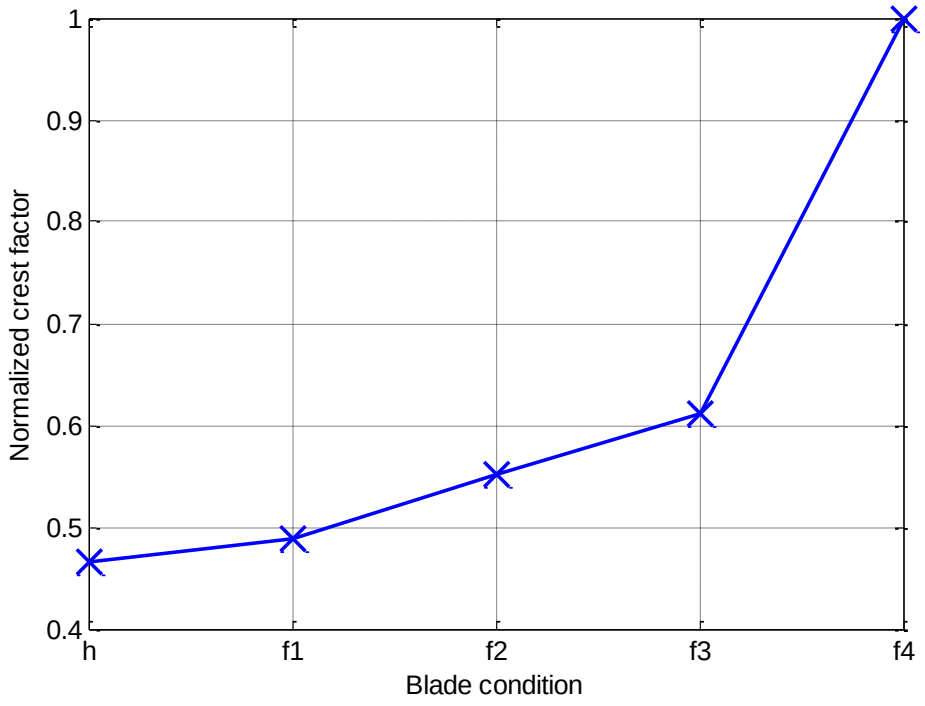

Figure 8.6 Crest factor value for healthy and faulty wind turbine blade at 150 r/min**.**

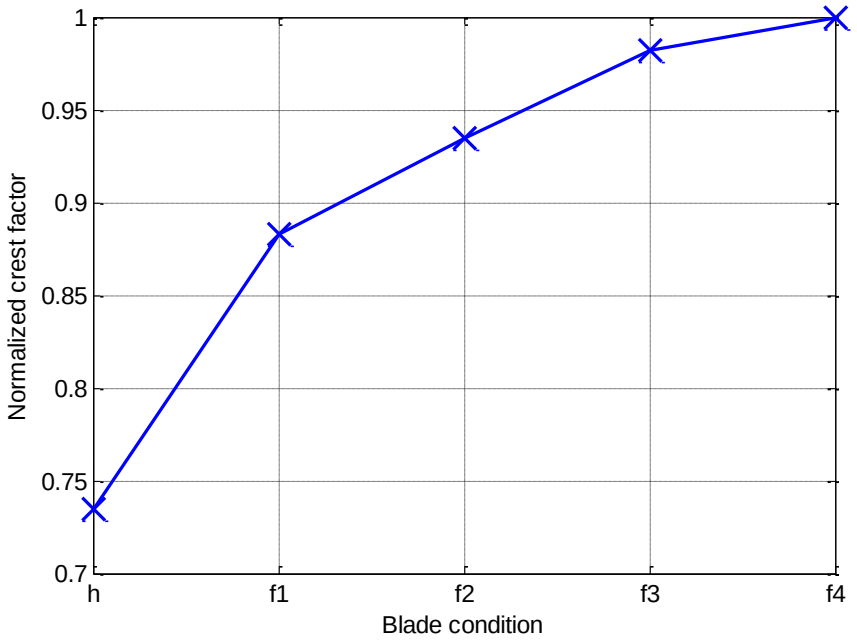

Figure 8.7 Crest factor value for healthy and faulty wind turbine blade at 250 r/min**.**

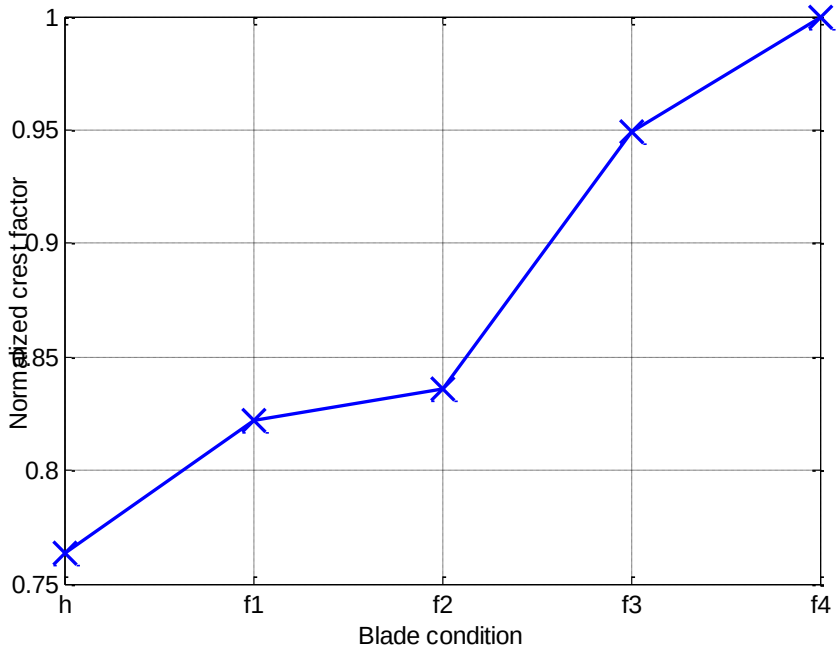

Figure 8.8 Crest factor value for healthy and faulty wind turbine blade at 360 r/min.

8.8 Summary

Principle component analysis (PCA) is a statistical technique and a powerful tool for finding hidden patterns in data of high dimensions. It can be used to reduce the number of dimensions of data set while retaining the variability in the data. The above mentioned capabilities of the PCA indicates that this technique suits wind turbine vibration data where dimensionality, noise content and the number of components are very high.

However, its application to vibration data for healthy and faulty turbine blades could not distinguish between healthy and faulty signals. The PCA was then developed into a new approach for analysing such signals, with the statistical analysis of the residual error matrix to determine its CF.

The residual matrix contains the information removed from the analysis as not usefully contributing to the PCA. When the CF was applied to the residual matrix it was found great promise in detecting cracked blades with all four cracks and at all rotational speeds used.

The vibration signals collected from wind turbine are often so contaminated that simple statistical parameters are not sufficient for fault detection. This study has introduced a promising new approach to detect cracks in wind turbine blades.

Chapter 9

Contribution to Knowledge, Achievements, Conclusions and Future Work

This chapter presents the contribution to knowledge made by this research project. It summarises the achievements of the research and explains how the objectives stated in Section 1.6 were achieved. The chapter concludes the study and suggests further work in this area of condition monitoring of wind turbines.

9.1 Introduction

Changes in blade structure cause rotor imbalance and generate vibration so that the vibration signature carries useful information about the health of the turbine blades and was used in this project to identify defects in the wind turbine blades. The vibration signal will also contain information concerning structural (tower) resonances, possible electrical faults, bearings and gear meshing frequencies.

Different analytical techniques were used to detect blade faults in their early stages. The techniques used were;

(i) Time domain methods including time series analysis,

(ii) Frequency domain techniques including Fourier analysis, and

(iii) Time-frequency methods such as wavelets.

This project included the design and construction of a test rig that allowed the simulation of different severities of a given defect in a turbine blade. Signals from this test rig were analysed using time and frequency domain tools. The signal characteristics were also evaluated using non-linear techniques which demonstrated their relative abilities to analyse the increased signal complexity of machines with defects.

9.2 Overview of Objectives and Achievements

The main achievements of this work are described below and matched with the original objectives in Section 1.5.2

Objective 1:

Understand the working principles and related parameters of wind turbines.

Achievement 1:

The working principles of wind turbine were studied under varying wind speeds, different loads and different condition including the number of blades**,** see appendix B.

Objective 2:

Determine and describe the common failure modes of the key components of a wind turbine.

Achievement 2:

Wind turbine failure modes including blade failure were determined and described in Chapter 1.

Objective 3:

Review current rotating machinery monitoring and vibration analysis techniques, and examine them for monitoring the condition of wind turbine blades.

Achievement 3:

Different technologies for monitoring purposes including vibration monitoring, acoustic monitoring, electrical effects, oil analysis, strain measurement, thermography, visual inspection and performance monitoring were outlined in Chapter 1.Condition monitoring techniques used for rotating machinery were reviewed in Chapter 2.

Objective 4:

Simulate a 3-D model of a wind turbine with three airfoil blades using SolidWorks and ANSYS packages for the purpose of understanding induced vibration signals under different operating conditions including healthy and faulty blades.

Achievement 4:

A 3-D model of a wind turbine with three airfoil blades was created using the SolidWorks package and then imported into the ANSYS package to study blade natural frequencies and to extract induced vibration signals, see Chapter 3. Data was collected under different blade condition and different rotational speeds.

Objective 5:

Build a test rig for data collection and analysis; using a three-bladed horizontal wind turbine with the necessary instrumentations and data acquisition system.

Achievement 5:

The experimental wind turbine test rig is described in Chapter 4. It consisted of a three-bladed wind turbine with simple gearbox, connected to a generator. Blade faults were simulated on one of the three blades.

Objective 6:

Collect vibration baseline data for three rotation speed; 150, 250 and 360 r/min.

Achievement 6:

Baseline data was collected at the three rotational speeds and stored for comparison with the faulty signals, see Chapter 4.

Objective 7:

Experimentally seed quantified faults into one of the blades by removal of small slivers from one blade face; 10mm, 20mm, 30mm and 40mm length, all with a consistent 3 mm width and 2 mm depth.

Achievement 7:

This objective delivered in Chapter 4. The four faults were seeded into one of the three blades. The same faults were also modelled in the simulation work, see Chapter 3.

Objective 8:

Detect the seeded faults and evaluate their severity using conventional and advanced signal processing analysis including Principal Components Analysis (PCA), Empirical Mode Decomposition (EMD), and Continuous Wavelet Transform (CWT).

Achievement 8:

Statistical analysis of the time and frequency domain signals and PCA, EMD and CWT were applied to the collected data. The results obtained from the statistical techniques for time and frequency domain analysis are presented in Chapter 5 and the performance of EMD is presented in Chapter 6. The results obtained from the CWT are presented in Chapter 7 and the performance of the PCA is presented in Chapter 8.

Objective 9:

Use the knowledge and results gained from the objectives above to develop signal processing that suits wind turbine blade CM vibration based schemes.

Achievement 9:

To achieve the goal of this study, of effectively monitoring the condition of wind turbine blades, different techniques have been borrowed from other fields. Those techniques have been reviewed and applied to datasets collected from simulation and experimental work. This led to two new approaches being developed for monitoring wind turbine blades:

- To calculate the feature intensity level (FIL) using curve fitting for the FFT spectrum in the region of the shaft frequency and its sideband zones based on the EMD method and to calculate the FIL using a waveform based on the CWT.
- To calculate the crest factor of waveform based on PCA.

These proposed approaches have shown great promise in detecting cracked blades on a wind turbine.

9.3 Contribution to Knowledge

This research work has made the following contributions to knowledge

9.3.1 Wind Turbine Modelling:

A finite element model of a three bladed wind turbine was created to simulate the real wind turbine used in the experimental work, see chapter three. This was done using the SolidWorks software package and imported into the ANSYS software package which extracted the fundamental vibration characteristics of key components of the wind

turbine. Vibration signals were extracted using dynamic analysis for three healthy blades and with one blade with one of four cracks introduced. Simulation and experimental results were compared.

9.3.2 The performance of Basic Signal Processing Techniques:

Wind turbines are complex machines that emit non-stationary signals. Conventional techniques using statistical measures of the time domain signal (such as kurtosis, root mean square, crest factor, skewness and standard division) and frequency analysis using the fast Fourier transform (FFT) were used to analyse vibration data collected from wind turbine under different blade conditions for three different rotational speeds, see chapter five. Results showed conventional techniques failed to identify the presence of cracks in the wind turbine blade. Other methods are necessary.

9.3.3 The Performance of Empirical Mode Decomposition (EMD)

EMD was applied to analyse the vibration data collected from the wind turbine under different blade conditions and for the three different rotational speeds based on FIL calculation for detecting the faults in the blades, see chapter six. Thus the proposed method based on EMD is the combination of EMD and FIL called EDFIL which gave a good indication of change in the wind turbine running condition and is suitable and sensitive for diagnosing the given faults. It was successfully applied to determine component signatures including the shaft frequency signature.

9.3.4 The Performance of Continuous Wavelet Transform (CWT):

The CWT was used to distinguish between different conditions of the wind turbine blade and detect faults. This technique was successfully applied to the detection of a cracked blade by calculating the FIL of the waveform, see chapter seven. The results showed that the scalogram produced was a more easily interpretable contour plot of the vibration signals to detect the presence of cracks in the wind turbine blades.

9.3.5 The Performance of Principle Components Analysis Method (PCA):

PCA is considered a statistical technique and was used here to extract the residual matrix which contains information not included in the analysis and the errors from the vibration signal. Results showed that the residual matrix contains useful information relating to changes in the condition of the wind turbine blades, information which appears in its residual error plot. However, the residual error plot itself does not show any clear trend to increase or decrease with faults severity rather it requires a statistical analysis of the residual error matrix to determine its crest factor, see chapter eight. The results obtained show that the proposed method has great promise for detecting cracked blades.

9.4 Conclusion

It can be concluded that this study has demonstrated the applicability of vibration measurement for detecting and locating incipient cracks whilst the wind turbine was in operation. The results showed that vibration parameters such as the FIL based on EMD and CWT, or crest factor based on PCA are reliable, robust and sensitive to the detection

of incipient cracks at different rotational speeds. These results have opened the possibility of developing a universal method for wind turbine condition monitoring.

9.5 Future Work

This section describes possible future works that could improve condition monitoring and fault diagnosis of wind turbine systems. The suggestions are:

9.5.1 Test Rig Improvement

- The test rig was built in a laboratory and a wind tunnel was used to produce wind flow, it might be better to build the rig outdoors.
- Additional faults may be designed and introduced into the blades including delamination, fibre breakage, de-bonding of the top and bottom skins of a composite blade and icing up of the blade.
- The focus of the research could be extended to include all wind turbine parts which could include studying gearbox failure modes.

9.5.2 Monitoring Techniques

- To investigate condition monitoring of turbine blades using parameters other than vibration, these could include air-borne acoustic and acoustic emission signals. The efficiency of these methods could be compared with vibration technology with the aim of reducing the cost of maintenance.

9.5.3 Theoretical Research

- Neural networks could be developed to analyse the signals collected and determine the presence of faults and then classify the fault according to type and severity.
- Wavelet analysis has been successfully applied for blade fault detection. It could be developed and combined with other techniques for the monitoring of wind turbines including the gearbox and combined not only with vibration methods but also air-borne acoustic and acoustic emission.
- Filters should be also introduced to reduce noise in the signals.

Theoretical work should develop a numerical simulation (software packages) that can improve product quality, in particular, by helping to create the wind turbine in the most cost-effective manner, simplifying the overall design process, possibly decreasing manufacturing costs by enabling the investigation of the use of lower-priced raw materials. Moreover numerical simulation helps researchers to understand wind turbines working principle and devise ways of increasing efficiency, reliability and reducing the cost of maintenance.

Finally, although, this study has contributed to the development of monitoring techniques for turbine blades there needs to be a universally accepted technique for monitoring all wind turbine components, and its development remains a big challenge. To meet this challenge and to develop a universal condition monitoring technique there is a crucial need to ensure the proposed method is suitable for detecting faults in components such as bearings, gears …etc. The problem is made more difficult because

the faults need to be detected as early as possible. Implementing a condition monitoring system for a wind turbine system is challenging, therefore requires more attention and focus in different areas of the wind turbine.

References

1. Tony Burton, D.S., Nick Jenkins, Ervin Bossanyi. (2001) Wind energy handbook John Wiley & Sons, Ltd, Baffins Lane, Chichester, West Sussex, PO19 1UD, England.
2. Putnam, G.C. (1948) Power from the wind. Van Nostrand Rheinhold, New York, USA.
3. Golding. (1955) The generation of electricity from wind power. E. W. . E. & F. N. Spon (reprinted R. I. Harris, 1976).
4. Spera, D.A. (1994) Wind-turbine technology, fundamental concepts of wind-turbine engineering. ASME Press, New York, US.
5. Park, J., Kim, J., Shin, Y., Lee, J., and Park, J. (2009) 3 MW class offshore wind turbine development. Current Applied Physics 10, S307-S310.
6. Mikail Suleiman, M.S. (2010) A Statistical Analysis and Fuzzy Logic Approach in Assessing the Performance of Wind Turbine in Ohio. In: Civil Engineering: Ohio State University, p. 160.
7. (GWEC), G.W.E.C. (2012) global wind statistics 2011. http://www.gwec.net/fileadmin/images/News/Press/GWEC_-_Global_Wind_Statistics_2011.pdf ed.
8. Adolfo Crespo Márquez. (2007) The Maintenance Management Framework: Models and Methods for system maintenance. Technology & Engineering; Springer.
9. Andrawus, J.A. (2008) "Maintenance Optimization for wind turbines", Ph.D. dissertation. Robert Gordon University.
10. Tejedor, D.T.A. (2007) "Advanced Gas Turbine Asset and Performance Management at Endesa". In: GE Energy, Spain.Tech. Rep. Vol.27 No.2.
11. McGowan, C. (2006) "Condition Monitoring of Wind Turbines" Technology Overview, Seeded-Fault Testing, and Cost-Benefit Analysis, Electric Power Research Institute (EPRI), California, USA, Technical Rep. 1010419.
12. Tadele, T. (2007) "Improvement of Maintenance Management system". Addais Raba University, Scholl of Graduates studies, faculty of Technology. 2007.
13. Ribrant, J. (2006) "Reliability performance and maintenance", A survey of failures in wind power systems. In: Master Thesis, KTH School of Electrical Engineering, .
14. P.Caselitz, J.G., T.Kruger and M. Mevenkamp. (1996) "Development of fault detection system for wind energy converters". Institute of solar energy Technik (ISET), Kassel Germany, Presented at EWEC, Göteborg, Sweden.

15. Hyers, R.W., Mcgowan, J.G., Sullivan, K.L., Manwell, J.F., Syrett, B.C. (2006) Condition monitoring and prognosis of utility scale wind turbines Energy Materials: Materials Science and Engineering for Energy Systems Vol. 1, No. 3, pp. 187-203
16. H. Sutherland, A.B., B. Hansche, W. Musial, J. Allread, J. Johnson and M. Summers (1994) The application of non-destructive techniques to the testing of a wind turbine blade. Sandia National Laboratories, Sandia Report SAND93-1380, Livermore, CA,USA.
17. Ribrant, J., and Bertling, L. (2007) Survey of failures in wind power systems with focus on Swedish wind power plants during 1997-2005. In: Power Engineering Society General Meeting, 2007. IEEE, pp. 1-8.
18. Saeed, A. (2008) Online Condition Monitoring System for Wind Turbine. In: Applied Signal Processing Karlskrona, Sweden Blekinge Institute of Technology, School of Engineering, p. 79
19. A.Davies. (1998) Handbook of condition monitoring techniques and methodology. Chapman&Hall. ISBN 0 412 61320 4 pp. 1- 50.
20. Verbruggen, T.W. (2003) Wind turbine operation & maintenance based on condition monitoring. Final report,. ECN-C—03-047.Energy Research Centre of the Netherlands Petten, T.N. ed.
21. Elforjani, M.A. (2010) Condition Monitoring of Slow Speed Rotating Machinery Using Acoustic Emission Technology. school of engineering, cranfield university.
22. AG, D. (1996) Flaw detection in composite materials using infra-red thermography by the method of external heating proceedings of the institution of mechanical engineers part c-journal of mechanical engineering science 210, 399-407.
23. Liu, W.T., Baoping. Jiang, Yonghua. (2010) Status and problems of wind turbine structural health monitoring techniques in China. Renewable Energy 35, 1414-1418.
24. M. Hilal Muftah, S.M.H. (November 30-December 2, 2010) A Strain Gauge Based Torque Transducer (Sensor) for Measuring Dynamical Load In-Rotation. In: international conference on development, energy, environment, economics (DEEE '10): Published by WSEAS Press ISSN: 1792-6653 www.wseas.org.
25. R.Keith Mobley (2002) An introduction to predictive maintenance 2nd Edition. Butter worth & Heinemann Ltd ISBN 0-7506-7531-4 pp 1-100.
26. R. Thresher, M.R., Paul Veers. (2008) Wind Energy Technology: Current Status and R&D Future. Laboratory, N.R.E. ed.: University of California at Berkeley, p. 24.

27. Joselin Herbert, G.M., Iniyan, S., Sreevalsan, E., and Rajapandian, S. (2007) A review of wind energy technologies. Renewable and Sustainable Energy Reviews 11, 1117-1145.
28. Pusey, H.C. (2007) Turbo machinery Condition Monitoring and Failure Prognosis. SAVIAC /Hi-Test Laboratories, Winchester, Virginia. Available at: http://www.sandv.com/downloads/0703puse.pdf. [Accessed:July, 2012].
29. International. Atomic Energy Agency (2007) Implementation Strategies and Tools for Condition Based Maintenance at Nuclear Power Plants, Nuclear Power Engineering Section International Atomic Energy Agency, Vienna, Austria, Tech Rep. May.
30. Joon-Young Park, J.-K.L., Ki-Yong Oh, Jun-Shin Lee and Beom-Joo Kim. (2010) Design of Simulator for 3MW Wind Turbine and Its Condition Monitoring System. In: International multiconference of engineers and computer scientists(IMECS) Hong Kong.
31. Mohamed A. Sayed, H.A.K., Ahmed A. Shaltot. (2011) Aerodynamic analysis of different wind-turbine-blade profiles using finite-volume method. In: In: The Third International Renewable Energy Congress Hammamet, Tunisia.
32. Ben Amara Mohamed El Amine, K.C., Ben Nasrallah Sassi. (2011) Computational fluid dynamics study of flow interaction between two wind turbine airfoils. In: In: The Third International Renewable Energy Congress Hammamet, Tunisia.
33. CHEUNG, C.K. (Sep 2011) Small Wind Turbine Blade Sensor for Condition Based Maintenance.MSc thesis. In: the Faculty of California Polytechnic University San Luis Obispo.
34. Besnard, M.P., and Bertling F.B. . (2010) An Approach for Condition-Based Maintenance Optimization Applied to Wind Turbine Blades. Sustainable Energy, IEEE Transactions on 1, 77-83.
35. Wenxiu, L., and Fulei, C. Condition monitoring and fault diagnostics of wind turbines. In: Prognostics and Health Management Conference, 2010. PHM '10., pp. 1-11.
36. Zhiqiang, W.Y., Xu Yuanying, Mei. (2009) Damage Diagnosis for Wind Turbine Blades Based on the Shifting Distance of Characteristic Frequency. In: Image and Signal Processing. CISP '09. 2nd International Congress on, pp. 1-3.
37. Jung- Hun Park, H.-Y.P., Seok- Yong Jeong, Sang-II leee, Yoyng-Ho Shin, Jong-Po Park. (2009) Linear vibration analysis of rotating wind-turbine blade. current Applied Physics 3.
38. Jüngert, A. (2008) Damage Detection in wind turbine blades using two different acoustic techniques. The NDT Database & Journal (NDT).

39. Sajauskas, S., Valinevičius, A., and Miežutavičiūtė, L. (2005) Non-destructive testing of sheet product inner surfaces using longitudinal surface acoustic waves. Ultrasound, P. 12–16.
40. Raisutis, R., Jasiuniene, E., and Zukauskas, E. (2008) Ultrasonic NDT of wind turbine blades using guided waves. Ultrasound . Kaunas: Technologija 63, 1.p.7-11.
41. Jinshui Yang, C.P., Jiayu Xiao, Jingcheng Zeng, YunYuan,. (2012) Application of videometric technique to deformation measurement for large-scale composite wind turbine blade. Applied Energy.
42. Borum, K., K., Mc Gugan, M., and Brondsted, P. (Denmark 2006) Condition monitoring of wind turbine blades. Proceedings of the 27th Riso International Symposium on Materials science : Polymer composite materials for wind power turbines, P. 139-145.
43. Beattie, A.G. (1997) Acoustic Emission Monitoring of a Wind Turbine Blade during a Fatigue Test. The 35th Aerospace Science Meeting, Reno, Nevada.
44. Ghoshal, A., Sundaresan, M.J., Schulz, M.J., and Frank Pai, P. (2000) Structural health monitoring techniques for wind turbine blades. Journal of Wind Engineering and Industrial Aerodynamics 85, 309-324.
45. Beattie, A.G.R., M. (1999) Non-Destructive Evaluation of Wind Turbine Blades Using an Infrared Camera. ASME Wind Energy Symposium, 18th, Aerospace Sciences Meeting and Exhibit, 37th, Reno, Nevada.
46. Ł Doliński , M.K. (2009) Damage detection in turbine wind blades by vibration based methods. Physics (http://iopscience.iop.org/1742-6596/181/1/012086).
47. Xueli, A., Dongxiang, J., and Shaohua, L. Application of back propagation neural network to fault diagnosis of direct-drive wind turbine. In: World Non-Grid-Connected Wind Power and Energy Conference (WNWEC), 2010, pp. 1-5.
48. Li, S.H.C., J. An, X. L. Jiang, D. X. (2011) Fault diagnosis of direct-drive wind turbine based on support vector machine. Journal of Physics: Conference Series 305, 12030-12035.
49. Bazilevs, Y.H., M. C. Akkerman, I. Wright, S. Takizawa, K. Henicke, B. Spielman, T. Tezduyar, T. E. (2011) 3D simulation of wind turbine rotors at full scale. Part I: Geometry modeling and aerodynamics. International Journal for Numerical Methods in Fluids 65, 207-235.
50. Ouari Kamel, R.T., Ouhrouche Mohand. (2011) Tow cascaded nonlinear predictive control of wind energy conversion system. In: In: The Third International Renewable Energy Congress Hammamet, Tunisia.

51. Amirat, Y., Choqueuse, V., Benbouzid, M.E.H., and Charpentier, J.F. Bearing fault detection in DFIG-based wind turbines using the first Intrinsic Mode Function. In: Electrical Machines (ICEM), 2010 XIX International Conference on, pp. 1-6.
52. Jenny Niebsch , R.R.a.T.T.N. (2010) Mass and Aerodynamic Imbalance Estimates of Wind Turbines. Energies 696-710;doi:610.3390/en3040696
53. Murtagh, P.J., Ghosh, A., Basu, B., and Broderick, B.M. (2008) Passive control of wind turbine vibrations including blade/tower interaction and rotationally sampled turbulence. Wind Energy 11, 305-317.
54. Besnard, F., Nilsson, J., and Bertling, L. On the economic benefits of using Condition Monitoring Systems for maintenance management of wind power systems. In: Probabilistic Methods Applied to Power Systems (PMAPS), 2010 IEEE 11th International Conference on, pp. 160-165.
55. Xiukun, W., and Lihua, L. Fault detection of large scale wind turbine systems. In: Computer Science and Education (ICCSE), 2010 5th International Conference on, pp. 1299-1304.
56. Chang-Hwan Kim, I.P., Neungsoo Yoo. (2010) Monitoring of small wind turbine blade using FBG sensors. In: International Conference on Control, Automation and Systems 2010 in KINTEX, Gyeonggi-do, Korea.
57. B.O. Al-Bedoor, S.A., Y. Al-Nassar. (2006) Blades condition monitoring using shaft torsional vibration signals. Journal of Quality in Maintenance Engineering Vol. 12 Iss: 3, pp. 275 - 293.
58. Fadaeinedjad, R., Moschopoulos, G., and Moallem, M. (2008) Investigation of voltage sag impact on wind turbine tower vibrations. Wind Energy 11, 351-375.
59. Al-Ghamd, A.M., and Mba, D. (2006) A comparative experimental study on the use of acoustic emission and vibration analysis for bearing defect identification and estimation of defect size. Mechanical Systems and Signal Processing 20, 1537-1571.
60. Tan, C.K.M., David. (2005) Identification of the acoustic emission source during a comparative study on diagnosis of a spur gearbox. Tribology International 38, 469-480.
61. Bouaziz, S., Attia Hili, M., Mataar, M., Fakhfakh, T., and Haddar, M. (2009) Dynamic behaviour of hydrodynamic journal bearings in presence of rotor spatial angular misalignment. Mechanism and Machine Theory 44, 1548-1559.
62. Radoslaw, Z.W., Bartelmus. Tomasz, Barszcz. and Jacek, Urbanek. Statistical data processing for wind turbine generator bearing diagnostics. Internet access July 2012.

63. Siores, E.a.N., A.A. . (1997) Condition Monitoring of a Gear Box Using Acoustic Emission Testing. Material Evaluation. 183-187.
64. Singh, A., Houser, D. R., and Vijayakar, S. . (1999) Detecting Gear Tooth Breakage Using Acoustic Emission. A Feasibility and Sensor Placement Study. Journal of Mechanical Design. 121. 587-593.
65. Stewart, R.M. (1977) Some useful data analysis techniques for gearbox diagnostics. Institute of Sound and Vibration Research, Southampton University.
66. Pachaud, C., Salvetat, R., and Fray, C. (1997) crest factor and kurtosis contributions to identify defects inducing periodical impulsive forces. Mechanical Systems and Signal Processing 11, 903-916.
67. McFadden, P.D. (1987) Examination of a technique for the early detection of failure in gears by signal processing of the time domain average of the meshing vibration. Mechanical Systems and Signal Processing 1, 173-183.
68. Norton, M.P., and Karczub, D.G. (2003) Fundamentals of Noise and Vibration Analysis for Engineers. Cambridge University Press.
69. Fraser, K.F., and King, C.N. (1986) Helicopter gearbox condition monitoring for the Australian Navy. In: Detection, Diagnosis, and Prognosis of Rotating Machinery to Improve Reliability, Maintainability, and Readiness Through the Application of New and Innovative Techniques, (Woodbury, New York), pp. 49-58. Mertaugh, e.b.T.R.S.a.L.J. ed.
70. Stephen B, R.B. (1999) schaum's outline of theory and problems of elements of statistics, Descriptive Statistics and Probability. New York, USA: McGraw-Hill. Ref Type: Book, Whole.
71. National Institute of Standards and Technology. NIST/SEMATECH e-Handbook of Statistical Methods, U.S. Commerce Department's,Technology Administration,. In: http://www.itl.nist.gov/div898/handbook/. Accessed:July, 2012. Ref Type: Online Source
72. Loutas, T.H., Roulias, D., Pauly, E., Kostopoulos, V. . (2010) The combined use of vibration, acoustic emission and oil debris on-line monitoring towards a more effective condition monitoring of rotating machinery. Mechanical Systems and Signal Processing, 25, 1339-1352.
73. Makinezhad, P.K.a.A. (2010) Using PCA in Acoustic Emission Condition Monitoring to Detect Faults in an Automobile Engine. In: 29th European Conference on Acoustic Emission Testing (EWGAE2010), Vienna.

74. Hu, Q., He, Z., Zhang, Z., and Zi, Y. (2007) Fault diagnosis of rotating machinery based on improved wavelet package transform and SVMs ensemble. Mechanical Systems and Signal Processing 21, 688-705.
75. Brigham, E.O. (1974) The Fast Fourier Transform. Prentice-Hall, Englewood Cliffs, New Jersey, USA.
76. KABIRI, H.G.a.P. (3-4 November 2011) Automobile Independent Fault Detection based on Acoustic Emission Using FFT. In: SINCE2011, Singapore International NDT Conference & Exhibition.
77. Secil, V.N.O., Kilic. Tahir, Cetin Akinci. (2012) Analysis of wind turbine blade deformation with STFT method. Energy Education Science and Technology Part A: Energy Science and Research Volume (issues) 29(1): 679-686.
78. Chin-Shun, T., Shyh-Jier, H., and Cheng-Tao, H. (2009) Inspection enhancement of wind turbine blades using novel signal-processing approaches. In: Power Systems Conference and Exposition, 2009. PSCE '09. IEEE/PES, pp. 1-7.
79. Fitzgerald, B., Arrigan, J., and Basu, B. Damage detection in wind turbine blades using time-frequency analysis of vibration signals. In: Neural Networks (IJCNN), The 2010 International Joint Conference on, pp. 1-5.
80. Kelley, N.D., Osgood, R.M., Bialasiewicz, J.T, and Jakubowski, A. (2000) Using Time-Frequency and Wavelet Analysis to Assess Turbulence/Rotor Interactions. AIAA Aerospace Sciences Meeting and Exhibit, Reno, NV, A Collection of the 2000 ASME Wind Energy Symposium Technical Papers pp.130-149
81. Forrester, B.D. (1989) Use of the Wigner-Ville Distribution in Helicopter Transmission Fault Detection. In: Proceeding of the Australian Symposium on Signal Processing and Applications ASSPA-89, Adelaide, Australia, p.77-82.
82. Forrester, B.D. (1989) Analysis of Gear Vibration in the Time-frequency Domain. In: Proceeding of the 44th Meeting of the Mechanical Failures Prevention Group of the Vibration Institute Virginia Beach, Virginia, p.225-234.
83. Forrester, B.D. (1990) Analysis of gear vibration in the time-frequency domain. In: in Current Practices and Trends in Mechanical Failure Prevention, pp. 225-234. Pussy, e.b.H.C.P.a.S.C. ed. (Vibration Institute, Willowbrook,IL), .
84. E. Al-Ahmar, M.E.H.B.a.Y.A., ". (September 2008) DFIG-Based Wind Turbine Fault Diagnosis Using a Specific Discrete Wavelet Transform In: International Conference on Electrical. ICEM'08 ed. Machines, Vilamoura (Portugal).

85. Amirat, Y., Benbouzid, M.E.H., Al-Ahmar, E., Bensaker, B., and Turri, S. (2009) A brief status on condition monitoring and fault diagnosis in wind energy conversion systems. Renewable and Sustainable Energy Reviews 13, 2629-2636.
86. Jiang, Y., Tang, B., Qin, Y., and Liu, W. Feature extraction method of wind turbine based on adaptive Morlet wavelet and SVD. Renewable Energy 36, 2146-2153.
87. Lardies, J., and Gouttebroze, S.p. (2002) Identification of modal parameters using the wavelet transform. International Journal of Mechanical Sciences 44, 2263-2283.
88. Bouchikhi, E.H., Choqueuse, V., Benbouzid, M.E.H., Charpentier, J.F., and Barakat, G. A comparative study of time-frequency representations for fault detection in wind turbine. In: IECON 2011 - 37th Annual Conference on IEEE Industrial Electronics Society, pp. 3584-3589.
89. Tang, B., Liu, W., and Song, T. Wind turbine fault diagnosis based on Morlet wavelet transformation and Wigner-Ville distribution. Renewable Energy 35, 2862-2866.
90. Yang, W., Tavner, P.J., and Wilkinson, M.R. (2009) Condition monitoring and fault diagnosis of a wind turbine synchronous generator drive train. Renewable Power Generation, IET 3, 1-11.
91. Tsai, C.S., Hsieh, C.T., and Lew, K.L. (2009) Detection of wind turbine blades damage by spectrum-recognition using gaussian wavelet-entropy. In: Anti-counterfeiting, Security, and Identification in Communication, 2009. ASID 2009. 3rd International Conference on, pp. 108-113.
92. Shawki A. Abouel-seoud, a.M.S.E. (2012) enhancement of signal denoising and fault detection in wind turbine planetary gearbox using wavelet transform. International Journal of Science and Advanced Technology.Volume 2. (ISSN 2221-8386). .
93. Wenxian, Y., Tavner, P.J., and Wilkinson, M. (2008) Wind turbine condition monitoring and fault diagnosis using both mechanical and electrical signatures. In: Advanced Intelligent Mechatronics, 2008. AIM 2008. IEEE/ASME International Conference on, pp. 1296-1301.
94. Parey, A., El Badaoui, M., Guillet, F., and Tandon, N. (2006) Dynamic modelling of spur gear pair and application of empirical mode decomposition-based statistical analysis for early detection of localized tooth defect. Journal of Sound and Vibration 294, 547-561.
95. Yang, W.C., Richard Tavner, Peter J. Crabtree, Christopher J. Bivariate empirical mode decomposition and its contribution to wind turbine condition monitoring. Journal of Sound and Vibration 330, 3766-3782.

96. An, X., Jiang, D., Li, S., and Zhao, M. Application of the ensemble empirical mode decomposition and Hilbert transform to pedestal looseness study of direct-drive wind turbine. Energy 36, 5508-5520.
97. Feng, Z., Liang, M., Zhang, Y., and Hou, S. (2012) Fault diagnosis for wind turbine planetary gearboxes via demodulation analysis based on ensemble empirical mode decomposition and energy separation. Renewable Energy 47, 112-126.
98. Tsai, C.-s., Hsieh, Cheng-Tao. Shyh-Jier. Huang,. (2006) Enhancement of damage-detection of wind turbine blades via CWT-based approaches. Energy Conversion, IEEE Transactions on 21, 776-781.
99. Baydar, N., and Ball, A. (2000) detection of gear deterioration under varying load conditions by using the instantaneous power spectrum. Mechanical Systems and Signal Processing 14, 907-921.
100. Kar, C., and Mohanty, A.R. (2008) Vibration and current transient monitoring for gearbox fault detection using multiresolution Fourier transform. Journal of Sound and Vibration 311, 109-132.
101. Attaf, B. (2010) Vibrational analyses of fibre-reinforced composite wind turbine blades. In: EFEEA'10 International Symposium on Environment Friendly Energies in Electrical Applications Ghardaïa, Algeria.
102. Defense, D. (1991) Fundamentals of rotor and power train maintenance techniques and procedures, FM 1-514. Headquarters, D.o.t.a. ed. Washington, DC.
103. Cao, H. (2011) Aerodynamics analysis of small horizontal axis wind turbine blades by using 2D and 3D CFD modelling. In: University of the Central Lancashire, School of Computing, Engineering and Physical Sciences Preston, England.
104. Brandt, S.A. (2004) Introduction to aeronautics: a design perspective. American Institute of Aeronautics and Astronautics.
105. NACA. (Access: May-2012) Airfoil Investigation Database - http://www.worldofkrauss.com/foils/1152.
106. JUNG, H.-C. (2006) Thesis, Study on laser forming processes with finite element analysis In: Mechanical Engineering Christchurch, New Zealand: University of Canterbury.
107. Liu, G.R., and Quek, S.S. (2003) The Finite Element Method: A Practical Course. Butterworth-Heinemann.

108. Jeremy Lee Ferguson, B.S.M.E. (2008) thesis, A moving load finite element-based approach to determining blade tip forces during a blade-on-casing incursion in a gas turbine engine In: Mechanical Engineering: Ohio State University.
109. J. Dally, W.R.a.K.M. (1984) Instrumentation for engineering measurements. USA John Wiley &Sons,Inc., ISBN 0471600040.
110. Inman, D. (ISBN 013726142X) Engineering vibrations.
111. Webster, J.G. (1999) The measurement, instrumentation, and sensors handbook. CRC Press LLC. ISBN:3-540-64830-5.
112. Girdhar, P., and Scheffer, C. (2004 UK.Oxford) In: Practical Machinery Vibration Analysis and Predictive Maintenance ISBN 0750662751.
113. http://www.modalshop.com/calibration.asp?ID=200. Accessed Sep. 2012.
114. Hill, J.T.a.M. (1999) Instrumention for engineers and scientists. USA,Oxford University Press, ISBN-10: 0198565186.
115. http://www.engr.sjsu.edu/bjfurman/courses/ME120/me120pdf/DAQslides.pdf .Accessed May 2011.
116. Ingle, V.K.a.J.G.P. (2000) Digital Signal Processing using Matlab. London: BookWare Companion series.
117. Reilly, T.a.T.P. (2011) A Review of Signal Processing and Analysis Tools for Comprehensive Rotating Machinery Diagnostics. Rotating Machinery, Structural Health Monitoring, Shock and Vibration Volume 5, Springer New York. p. 463-479.
118. Stevens, P., W., Hall, D., L. and Smith, E., C. (1996) A Multidisciplinary Research Approach To Rototcraft Health and Usage Monitoring. American Helicopter Society 52nd Annual Forum, Washington, D.C., pp. 1732-1751.
119. Forrester, B.B. (1996) Advanced Vibration Analysis Techniques for Fault Detection and Diagnosis in Gear Transmission Systems, PhD thesis,. Swinburne University of Technology.
120. Mitchell, L.e., al,. (2000) Review of Vibration Analysis Methods for Gearbox Diagnostics and Prognostics. Proc. 54th Meeting of the Society for Machinery Failure Prevention Technology, May 1-4 pp. 623-634.
121. Lu, Y., Tang, J. and Luo, H. (2011) Wind turbine gearbox fault detection using multiple sensors with feature level data fusion. In: Proceedings of ASME Turbo Expo Vancouver, British Columbia, Canada: GT2011-46538.

122. Jüngert, A. (2008) Damage Detection in wind turbine blades using two different acoustic techniques. The NDT Database & Journal (NDT)
123. Lihui W, R.X., Pham DT. . (2006) Condition Monitoring and Control for Intelligent Manufacturing. (Springer Series in Advanced Manufacturing). London, UK: Springer-Verlag London Limited.
124. Lin, S.A.M., P. . (1997) Gear Vibration Analysis by B-spline Wavelet-based Linear Wavelet Transform, . Mechanical Systems and Signal Processing, 25, 1339-1352. 11(4), pp. 603-609.
125. A.K. Jardine, D.L., and D. Banjevic. . (2005) A review on machinery diagnostics and prognostics implementing condition-based maintenance. Technical report.CBM Lab, Department ofMechanical and Industrial Engineering, University of Toronto.
126. Mobley, R.K. (1999) Vibration Fundamentals. Boston: Elsevier.
127. Huang, N.E., Long, S.R., Shen, Z., and John, W.H.a.T.Y.W. (1996) The Mechanism for Frequency Downshift in Nonlinear Wave Evolution. In: Advances in Applied Mechanics: Elsevier, pp. 59-117C.
128. Huang, N.E.Z.S., S. R. Long, M. C. Wu, H. H. Shih, Q. Zheng, N. C. Yen, C. C. Tung, and H. H. Liu, . (1998) The empirical mode decomposition and the Hilbert spectrum for nonlinear and non-stationary time series analysis. Proc. R. Soc. Lond, vol. 454, pp. 903-995.
129. Huang, N.E.a.S.S.P.S. (2005) Hilbert-Huang Transform and Its Applications. Singapore: World Scientific.
130. Rilling, G.P.F., and P. Goncalves (2003) On empirical decomposition and its algorithms,. in IEEE-EURASIP Workshop on Nonlinear Signal Image Process Grado, Italy.
131. J. Sol´e, A.T., and J. E. Llebot. (2007) Using empirical mode decomposition to correlate paleoclimatic time-series. Natural Hazards and Earth System Science 7, 299–307.
132. Huang, N., Wu, M., Long, S., Shen, S., Qu, W., Gloersen, P., and Fan, K. (2003) A confidence limit for the empirical mode decomposition and Hilbert spectral analysis. Proc. R. Soc. London 459 2317-2345.
133. Wu, Z.a.H., N. . (2003) A study of the characteristics of white noise using the empirical mode decomposition method. Proc. R. Soc. London 460, 1597–1611.
134. Trnka, P., Hofreiter, M. . (2011) The Empirical Mode Decomposition in Real-Time. In: Proceedings of the 18th International Conference on Process Control. Editors: Fikar, M., Kvasnica, M ed. Tatranská Lomnica, Slovakia, 284-289.

135. Steeb, W.H. (2005) Chaos, Fractals, Cellular Automata, Genetic Algorithms, Gene Expression Programming, Wavelets, Hidden Markov Models, Fuzzy Logic with C++, Java and SymbolicC++ Programs World Scientific Publishing, CO. Pte. Ltd.
136. Smith, J. (2011) Spectral Audio Signal Processing. WK3 Publishing, Stanford University.
137. Chui, C.K. (1992) Wavelet Analysis and Its Applications –Volume-1, Introduction to Wavelets,. Academic Press.
138. Rioul, O., and Duhamel, P. (1992) Fast algorithms for discrete and continuous wavelet transforms. Information Theory, IEEE Transactions on 38, 569-586.
139. Mallat, S. (1998) A Wavelet Tour of Signal Processing. Academic Press.
140. Forge, M. (1992) Wavelet Transforms and their Application to Turbulence. Annual Rev. Fluid Mechanics, 24, p.395-457, 1.
141. Grossmann, A.a.M., K. R. and Morlet, J. (1992) Reading and Understanding Continuous Wavelet Transforms, Time-frequency Methods and Phase Space. In: Springer- Verlag, Berlin.
142. Rioul, O., and Vetterli, M. (1991) Wavelets and signal processing. Signal Processing Magazine, IEEE 8, 14-38.
143. Gram-Hansen, K.a.D., C. . (1989) On the Choice of Parameters for Time-frequency Analysis. In: Wavelet Applications Proceeding of International Conference, Maseille, France. In Meyar Y, e. ed.
144. Singh G., S.A.A.S. (2003) Induction Machine drive condition monitoring and diagnostic research- a survey. Electric Power systems Research 64,145-158.
145. Reilly, T., and Proulx, T. A Review of Signal Processing and Analysis Tools for Comprehensive Rotating Machinery Diagnostics ,Rotating Machinery, Structural Health Monitoring, Shock and Vibration, Volume 5. Springer New York, pp. 463-479.
146. Lu, Y., Tang, J. and Luo, H. . (2011) Wind turbine gearbox fault detection using multiple sensors with feature level data fusion,. In: Proceedings of ASME Turbo Expo, GT2011-46538.
147. Chiang, L.H., E. L. Russell and R. D. Braatz (2001) Fault Detection and Diagnosis in Industrial Systems. Nueva York.
148. Johnson, R.A., and Wichern, D.W. (1992) Applied multivariate statistical analysis. Prentice Hall, New Jersey.
149. Kourti, T. (2004) Process analytical technology and multivariate statistical control. Part 1: Process Anal. Technol, 1, 13-19.

150. Kourti, T. (2005) Process analytical technology and multivariate statistical control. Part 2: Process Anal. Technol. 2, 24-28. .
151. Kourti, T. (2006) Process analytical technology and multivariate statistical control. Part 3: Process Anal. Technol. 3, 18-24.
152. MacGregor, J.F., and Kourti, T. (1995) Statistical process control of multivariate processes. Control Engineering Practice 3, 403-414.
153. Wise, B.M., and Gallagher, N.B. (1996) The process chemometrics approach to process monitoring and fault detection. Journal of Process Control 6, 329-348.
154. Jackson, J.E. (1991) A User's Guide to Principal Components. USA: A Wiley-Interscience Publication.
155. Noble, B.D., J. W. . (1977) Applied Linear Algebra. Englewood Cliffs, NJ: Prentice-Hall.
156. Goldberg, J.L. (1991) Matrix Theory with Applications. New York, NY, USA: McGraw-Hill.
157. Barnet, S. (1990) Matrices Methods and Applications. Oxford: Clarenton Press.
158. Kresta, J.V., Macgregor, J.F., and Marlin, T.E. (1991) Multivariate statistical monitoring of process operating performance. The Canadian Journal of Chemical Engineering 69, 35-47.
159. Kresta, J., MacGregor, J., and Marlin, T. (1991) Multivariate statistical monitoring of process operating performance. . Canadian J. Chem. Eng. 69 35– 47.

Appendix A: Simulation results

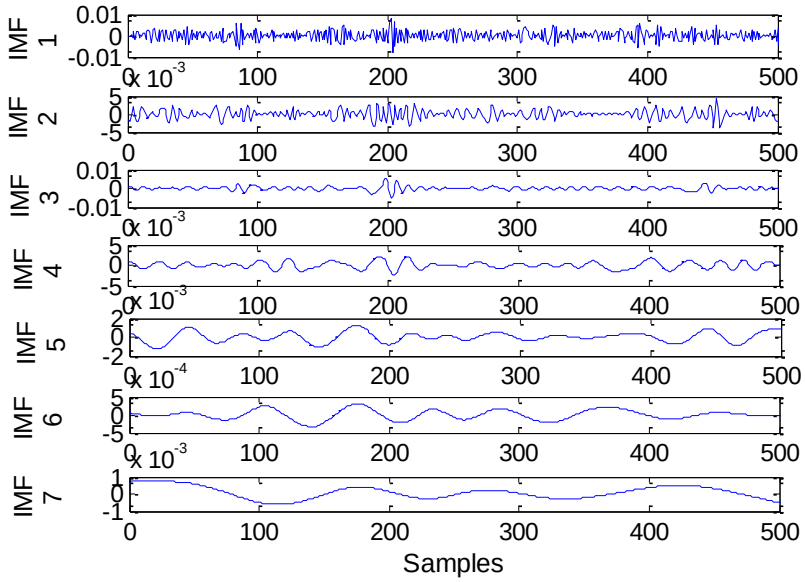

Figure A1 Decomposition of simulated vibration signals for healthy turbine at 150 r/min

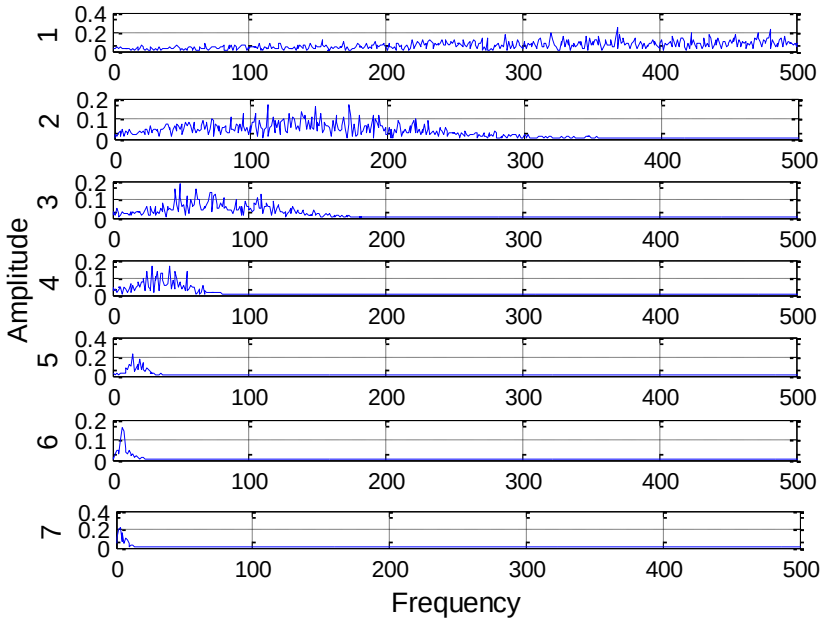

Figure A2 Fast Fourier spectra from the IMFs obtained from simulation signal at 150 r/min

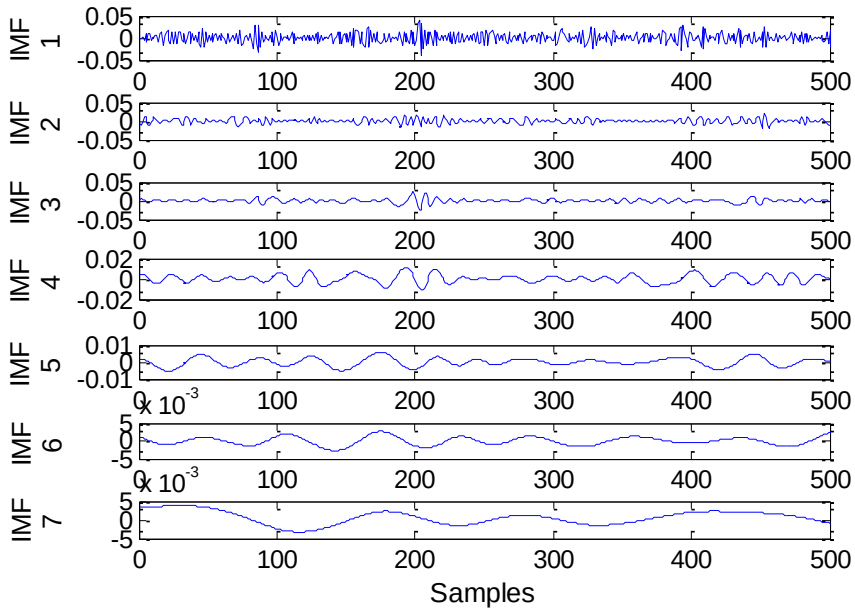

Figure A3 Decomposition of simulated vibration signals for healthy turbine at 250 r/min

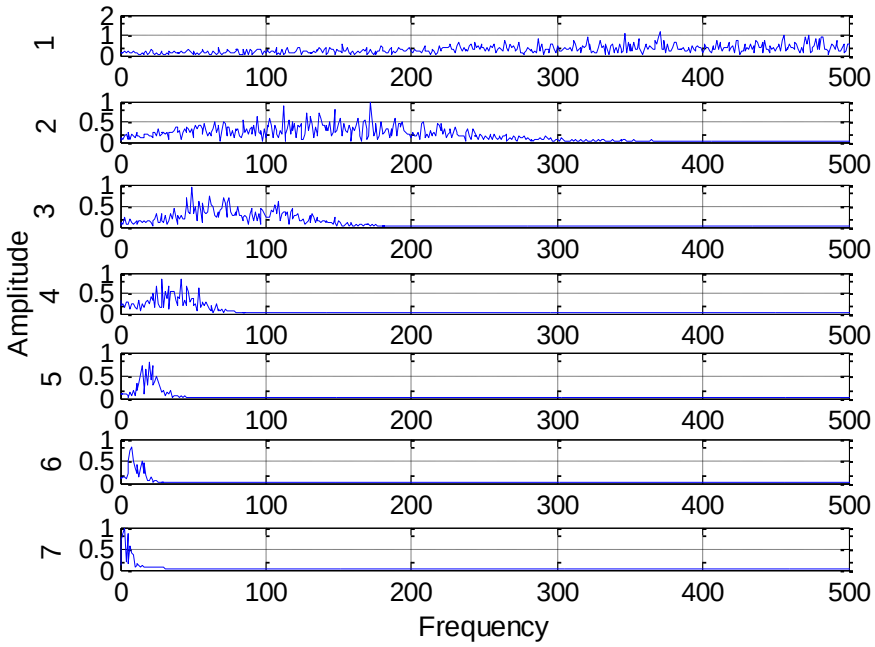

Figure A4 Fast Fourier spectra from the IMFs obtained from simulation signal at 250 r/min

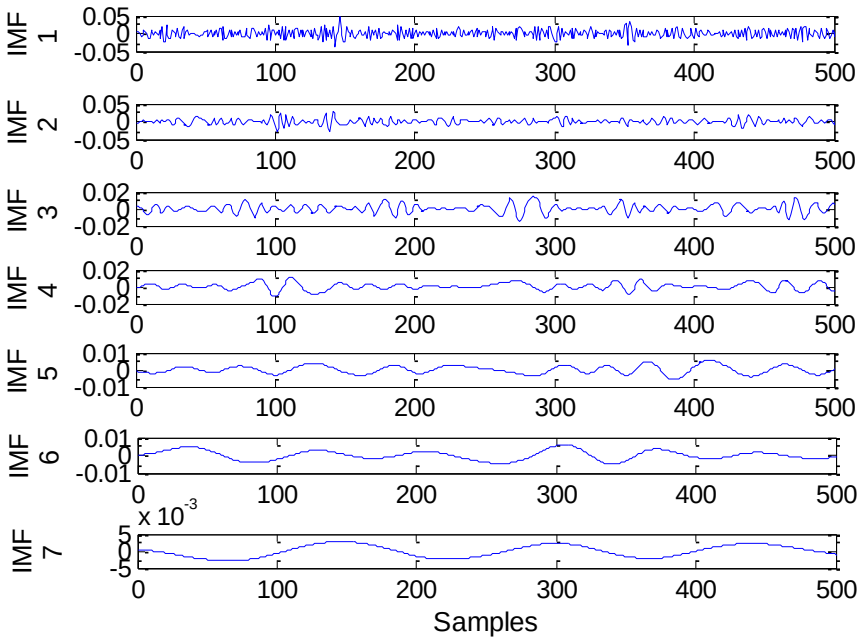

Figure A5 Decomposition of simulated vibration signals for healthy turbine at 360 r/min

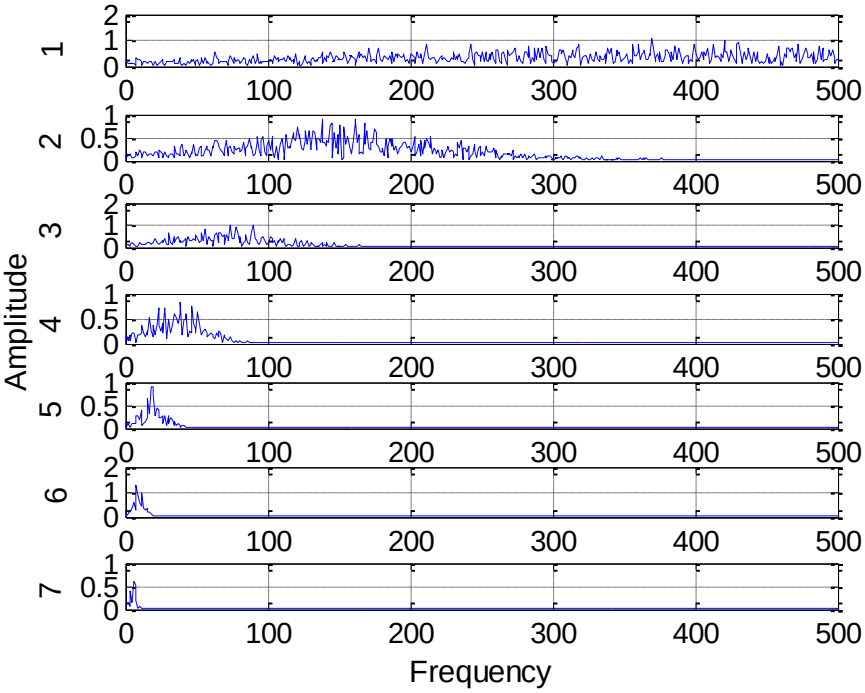

Figure A6 Fast Fourier spectra from the IMFs obtained from simulation signal at 360 r/min

Appendix B:Specifications– Charge Accelerometer Type 4371, 4371 S and 4371 V

	Units	4371/4371 S	437 1 V
Dynamic Characteristics			
Charge Sensitivity (@ 159.2 Hz)	pC/g	9.8 ± 2%	9.8 ± 15%
Frequency Response		See typical Amplitude Response	
Mounted Resonance Frequency	kHz	42	
Amplitude Response ±10% [1]	Hz	0.1 to 12600	
Transverse Sensitivity	%	<4	
Transverse Resonance Frequency	kHz	15	
Electrical Characteristics			
Min. Leakage Resistance @ 20°C	GΩ	≥20	
Capacitance	PF	1200	
Grounding		Signal ground connected to case	
Environmental Characteristics			
Temperature Range	°C (°F)	–55 to 250 (–67 to 482)	
Humidity		Welded, sealed	
Max. Operational Sinusoidal Vibration (peak)	g pk	6000	
Max. Operational Shock (± peak)	g pk	20000	
Base Strain Sensitivity	Equiv. g/µ strain	0.002	
Thermal Transient Sensitivity	Equiv. g/°C (g/°F)	0.004 (0.022)	
Magnetic Sensitivity (50 Hz – 0.03 Tesla)	g/T	0.4	
Physical Characteristics			
Dimensions		See outline drawing	
Weight	gram (oz.)	11 (0.39)	
Case Material		Titanium	
Connector		10 – 32 UNF	
Mounting		10–32 UNF ≍ 3.2 mm threaded hole	

Appendix C:Charge Amplifier — Type 2635

FEATURES:

- Charge Input
- 3 digit conditioning to transducer sensitivity
- Unified output ratings for simplified system calibration
- High sensitivity up to 10 V/pC
- Built-in integrators for displacement and velocity
- Switchable low and high frequency limits
- Built-in test oscillator

Description

The 2635 is a four stage amplifier consisting of an input amplifier; low- pass filter-amplifier, integrator amplifier, and output amplifier (see Figure C1). An overload detector, test oscillator and power supply unit are also included.

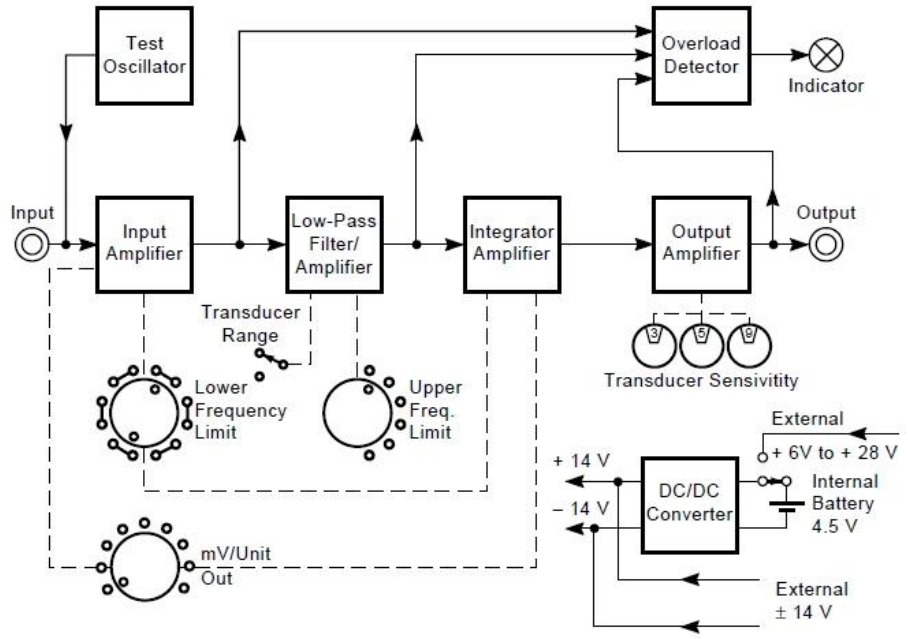

Block diagram charge amplifier-type 2635

Appendix D: Paper1

Characterization of wind turbine to be used for powering a computer laboratory

A. Abouhnik, A. Albarbar
Department of Engineering & Technology,
Manchester Metropolitan University,
Manchester, M1 1GD UK

Abstract:

Fossil fuels pollute the environment and alternative energy sources have recently become much more necessary due to growing awareness of climate change, which has become one out of the greatest challenges of this century. Wind energy is one of the most cost effective among the available renewable energy sources and has attracted considerable attention.

The main purpose of this work is to supply and operate a typical lab using electricity generated from a wind turbine and stored using battery banks. In this paper design details and experimental findings of a new generation of small horizontal axis wind turbines (SHAWT) are presented. The wind turbine blades are attached to a permanent magnet (PM) three phase induction generator; which charges a battery bank trough an AC-DC rectifier and regulator.

The converted wind energy is used to power a typical lab with standard equipment. The behavior of the batteries used in this work has been studied, and battery charge and discharge characteristics investigated. Battery cycle life and system capacity calculations are presented.

The research findings are promising and show potential applications of such renewable power systems.

Keywords: Environment; sustainable development; battery characteristics; green power.

1. Introduction

Renewable energy sources have become very important due to growing awareness of climate change and associated legislation. Wind power is a very promising source of environmentally safe renewable energy; it gained importance and priority in many countries in the latter half of the last century. In Germany about 40% of electricity gained by renewable energies is generated by wind power, and it is expected that 10% of the world's electricity will be wind generated by 2020 [1]. Many countries around the globe are exploiting renewable energy, and wind energy in particular, for the following reasons:

1. Wind energy produces no carbon dioxide.
2. Wind is a clean fuel with no harmful by-products.
3. Wind is free and a huge energy resource which can relatively easily be converted to electricity.

4. Today the cost of this source has become competitive compared with traditional energy sources.

Ref. [2] presents the results of a study to investigate the performance of 1.5kW wind turbine system, while a simple mathematical approach to simulate the lead–acid battery behavior of stand-alone hybrid solar-wind power generation systems was studied in ref [3].

Generally, the site wind characteristics (the availability and persistence of the wind speed) must be taken into account when selecting a wind turbine or wind farm site. This will ensure maximum power from the wind to provide widely available low-cost energy. It is common practice to represent site wind characteristics using Weibull probability density functions. Weibull shape and scale parameters should be calculated to determine wind energy potential available for utilization [4]. Wind data from 10 coastal meteorological stations along the Mediterranean coast of Egypt have been statistically analysed to determine wind characteristics and wind energy potential, and found to be quite promising [5].

In this paper the characteristics and performance of a new generation of wind turbines is investigated. The paper explains all design aspects and the calculations when using the examined wind turbine with a battery bank to deliver and secure the required power for a typical computer laboratory.

2. Theoretical wind power

Estimating power generation is an extremely complicated task, governed by many physical laws. Wind is made up of moving air molecules which has mass of about 1.23kg/m^3 at stp. Figure 1 represents the actual horizontal wind turbine and wind behavior.

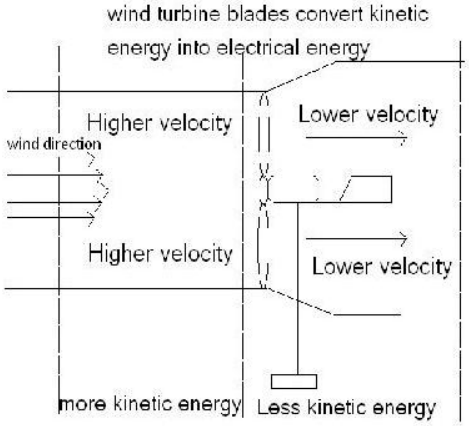

Fig.1. physical wind turbine system

Any moving object with mass possesses an amount of kinetic energy which is given by the equation:

$$E = \tfrac{1}{2} mV^2 \text{.....(1)}$$

Where m the mass in kg, V is its the velocity in m/s, and the energy is in Watts.

The mass of air hitting a wind turbine which sweeps an area A m^2 each second is given by the following equation:

$$\dot{m} = \rho A V \text{.....(2)}$$

Where ρ is the density of the air,

$\dot{m} = \frac{dm}{dt}$, Mass flow rate (kg/s)

But the power is produced by the wind depends on the difference between upstream and downstream wind speed, and the equation (1) above becomes:

$$P = \frac{1}{2}\dot{m}\left[V^2 - V_o^2\right] \quad \text{.....(3)}$$

Where V is upstream wind speed, and Vo is downstream speed.

$$\dot{m} \cong \rho A \frac{V^2 + V_0^2}{2} \quad \text{.....(4)}$$

$$P = \frac{1}{2}\rho A\left[\frac{V + V_0}{2}\right]\left[V^2 - V_0^2\right] \quad \text{.....(5)}$$

$$P = \frac{1}{2}\rho A C_p V^3 \quad \text{.....(6)}$$

$$C_p = \frac{\left[1 + \left(V_0/V\right)\right] + \left[1 - \left(V_0/V\right)^2\right]}{2} \quad \text{.....(7)}$$

C_p is the rotor power coefficient and, as will be shown in the next section, could have a maximum magnitude of about 0.59. This means only about 50% of the wind power can be converted into mechanical power; most modern wind turbines have efficiencies of up to 30 or 40%.

3. Experimental setup

The test rig, Figure 2, consists of:

a) Wind turbine with six blades.

b) Charge regulator: a voltage regulator allows the user to switch between different output modes, e.g., if the battery charge mode is selected the regulator will regulate the voltage to allow the battery to be correctly charged, different types of battery require different settings on the charge controller.

c) Storage batteries: two lead acid batteries were used to investigate the battery characteristics and determine battery capacity.

d) Wind tunnel: acts as a controllable wind source; its cross sectional area is 0.16m^2.

e) AC generator and dc conversion: the rotor will directly turn a 3-phase AC generator similar to a conventional induction motor. The generated AC voltage is then converted to DC within the generator by using full bridge rectifier and mechanical commutators.

f) Decade resistance box: used to simulate different resistance loads on the wind turbine.

h) Two multimeters: measure the generated current, voltage and power.

i) Anemometer: measures upstream and downstream wind speeds.

Fig.2. Test rig and instrumentation

4. Experimental Results

The wind turbine was located 2m away from the wind tunnel. The first experiment was to evaluate the power

generated at different of loads and under different wind speeds. The wind speed from the tunnel was varied from 3 to 9m/s in increments of 2m/s. The connected loads were increased from 10 to 500Ω in increments of 10Ω. Currents and voltages were measured and the generated power was calculated in each case; see Figure 3.

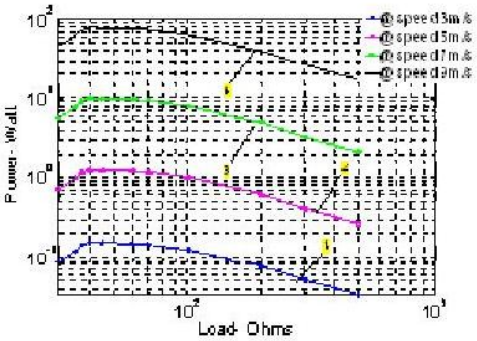

Fig.3. Generated power at different loads and speeds.

As shown in Figure 3, curve (1) wind speed 3m/s, the power increase gradually from that at the cut-in speed to maximum power at a load of 40Ω, after which the curve decreases with increased load to near zero at 400Ω. Curves (2,3,4) represent wind speeds of 5m/s, 7m/s and 9m/s respectively. In each case maximum power is obtained for a load of about 40Ω. Clearly this is the optimum load for all wind speeds tested and turbine efficiency is at its optimum at 40Ω. The maximum power was 80W with a 40Ω load for a wind speed of 9m/s. The maximum power delivered varied with the cube of wind speed for the range of speeds tested.

At 3m/s and maximum power output of 0.156W, C_p = 0.589, then at 5m/s and maximum power output of 1.250W, at 7m/s and maximum power output of about 10W, and finally at 9m/s we see about 80 watts dissipated via the load of 40 Ohms and C_p = 0.589.

The relation between speed ratio and rotor power coefficient C_p was experimentally examined. Up-stream and downstream wind speeds were measured and the C_p was calculated in each case; this was done at three different wind speeds, see Figure 4.

The power coefficient curves obtained are clearly typical and confirm the Betz law that it is not possible to extract more than 59% of the wind's kinetic energy.

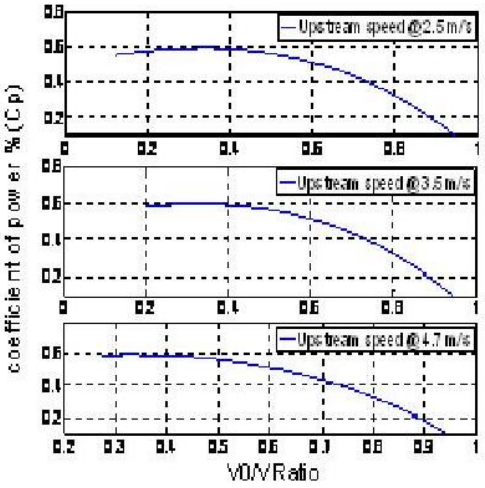

Fig. 4. Power coefficient C_p at different wind speeds

It is desirable that the wind turbine is operated at the highest possible C_p values. The power captured by the

wind turbine rotor may be written as the equation (6). As predicted in Figure 4 the optimum C_p value was achieved when the upstream and downstream wind ratio (V_o/V_{in}) was 0.3.

For this example, the theoretical maximum electrical output power (assuming zero losses in generation) is:

$$P_{out} = (P_{in})(C_p)$$

$$P_{out} = 135.89 \quad x\,0.5887 \quad \approx 79.9\,watts$$

Optimal efficiency is given by:

$$= \frac{P_{out}}{P_{in}}$$

In other studies the problem of output power maximization for low-power wind energy conversion systems operated on partial load was investigated and the results showed that the steady-state performance of the conversion system is strongly determined by generator behavior [6].

4.1 Battery characteristics

Batteries are used as an electrical energy storing medium and so it is essential to understand their characteristics and physical properties. One very important parameter is battery cycle; discharge and recharge. Battery life is determined by the number of cycles a battery can provide and thus the application of a battery can be proscribed. Ref [7] studied the effect on battery performance of a new glass microfibre separator material, capable of minimizing acid stratification inside the battery, and its implementation in a PV/wind demonstration system.

The battery used in this study was charged and discharged five times using the wind turbine system presented in the previous section, see Figure 5. The obtained results are presented in Figures 6 and 7.

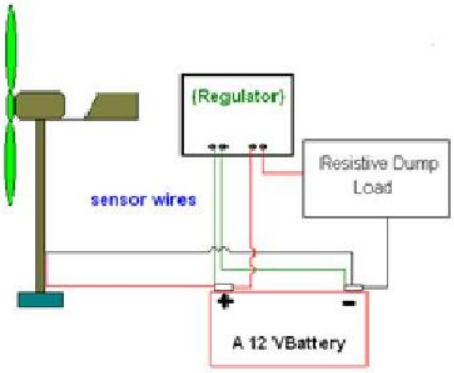

Fig.5. Block diagram of the experimental system

Figure 6 shows the voltage and current discharge curves for the 70Ah battery used in this study at constant discharge load of 10Ω. As can be seen the voltage is relatively high, between 12 and 4 V for a rather long proportion of the discharge time, more than an hour and a half. The lead acid battery which was used converts chemical energy into electrical. As the reaction slows down the voltage will drop and electrolyte's conductivity changes. From other side the lead acid batteries which were charged by wind turbine read fully

charge at around 12.21V but when starting to discharge, the voltage will drop to between 9.4 -11.8 volts.

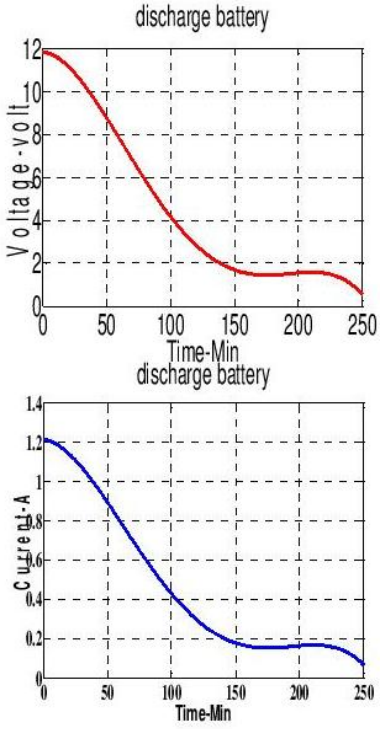

Fig.6. Battery voltage and current

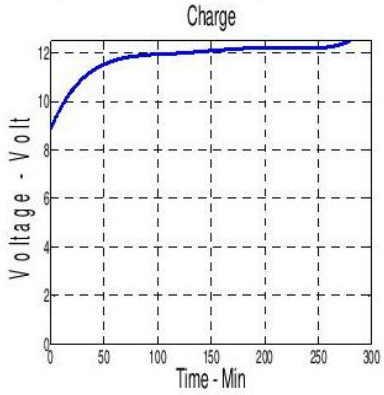

discharge with 10 Ω load

Fig.7. Battery voltage charging process with constant current

4.2 The required battery size

In this section the power required from the turbine is determined and what battery bank size is required. This mainly depends on the laboratory facilities and their power consumption rates.

First of all we need to calculate how much power is needed to supply the scientific equipment in the laboratory, including how many devices will be supplied at any one time.

Total power consumed load in one day =

Number of devices x Rate of power consumption of each device x Time in hours each device is on.

There are 20 similar devices, each consuming 18W and each is on for 12 hours a day.

20 x 18 x 12 = 4320 = 4.32kWh

Therefore, the required battery size for 5 days operation supplying 12V with an overall efficiency of 0.8 would be determined as follows:

$$Battery \quad \text{size required} = \frac{(4320)x(5)}{(12)x(0.8)} = \frac{21600}{9.6} = 2250 \ Ah$$

Assuming the capacity of the batteries is 375 Ah, the number of batteries required to supply 20 laboratory computers for 5 days will be:

$$Number\ of\ batteries\ required = \frac{\text{Batterysize required}}{\text{standardsize(i.e375Ah)}}$$

$$Number\ of\ batteries\ required = \frac{2250}{375\text{Ah}} = 6\ batteries\ .$$

Battery capacity is determined by the amount of electrical energy the battery can deliver at a constant rate over a certain period of time and is measured in Ampere hours (Ah). Amp-hour battery rating is commonly used on sealed lead acid batteries used in wind system.

Because losses in energy occur during charging and discharging batteries and storage systems are not ideal, we need to take into account the total energy required which is expressed as the ratio between the output and input energy as [2]:

$$\zeta_{bat} = \frac{E_{out}}{E_{in}} x100\%$$

5. Conclusions

Wind energy is one of the alternative energy sources and the current developments of technology help to improve systems efficiently in capturing energy storage systems. The main purpose of this work was to supply and operate a typical laboratory using electricity generated from wind energy and stored using battery banks. The aim was achieved and the following conclusions were drawn:

1) The wind turbine was installed and mounted in the laboratory about 2m away from the exit of a wind tunnel to investigate the performance and feasibility of the small wind turbine to supply a computer laboratory using green power. The results show that this wind turbine can be used to supply 20 computers depending on a capacity of the storage batteries. The generated electricity is three phase AC current which means it can be connected to the national grid.

2) The batteries used in this study were two lead acid batteries with capacity of 70Ah at 12 V. They were discharged at constant load of 10Ω for a period of about four hours by which time the voltage had dropped to 1.4 Volt (the deep-discharge protection point), after that they were charged at a constant current of 0.32A to 12.21V (overcharge – protection voltage). By choosing a suitable capacity of battery 400Ah or more we can reduce number of batteries to power any system.

3) The cost is not expensive for a small wind turbine and batteries which have a life warranty of more than seven years.

References

1. Joselin Herbert Gm I S, Sreevalsan E, Rajapandian S. 2007. A review of wind energy technologies. *Renew Sustain Energy Rev*, 11(16) 1117–1145.

2. Ozgener O. 2006. A small wind turbine system (SWTS) application and its performance analysis. *Energy Conversion and Management* 47, 1326-1337.

3. Zhou W, Yang H X and Fang Z H. 2008. Battery behavior prediction and battery working states analysis of a hybrid solar-wind power generation

system. *Renewable Energy* 33, 1413-1423.

4. A.N.M. Mominul Islam Mukut M Q I M M A 2008. Analysis of Wind Characteristics in Coastal Areas of Bangladesh. Journal of Mechanical Engineering. *Journal of Mechanical Engineering* ME39,N0 1.

5. Shata S A and Hanitsch R. 2006. Evaluation of wind energy potential and electricity generation on the coast of Mediterranean Sea in Egypt. *Renewable Energy* 31, 1183-1202.

6. Vlad C, Munteanu I, Bratcu I and Ceanga E. 2010. Output power maximization of low-power wind energy conversion systems revisited: Possible control solutions. *Energy Conversion and Management* 51, 305-310.

7. Fernandez M, Ruddell J, Vast N, Esteban J and Estela F. 2001. Development of a VRLA battery with improved separators, and a charge controller, for low cost photovoltaic and wind powered installations. *Journal of Power Sources* 95, 135-140.

Appendix E: Paper2

The Third International Renewable Energy Congress
December 20-22, 2011 – Hammamet, Tunisia
ID73/©IREC2011-WHE

Wind turbine blade fault detection using the empirical mode decomposition method; numerical simulation and experimental testing

A. Abouhnik, Ghalib R. Ibrahim, R. Shnibha, A. Albarbar

School of Engineering, Manchester Metropolitan University
ManchesterM1 5GD, UK
Emails: abouhnik@yahoo.com, ghalib_ibrahim@hotmail.com ,
rshnibh@yahoo.com, a.albarbar@mmu.ac.uk

Abstract *- In this paper assessment of the condition of the wind turbine blades is based on vibration analysis. The experimental work was carried out using a six bladed turbine with five healthy blades and one blade with one of three cracks introduced. The cracks were of length 15, 25 and 40 mm, all had a consistent 3 mm width and 2 mm depth. The tests were carried out for two rotation speeds; 250 and 360 rpm. The dynamic analysis was performed with a full 3–D finite element method (ANSYS) and the fundamental vibration characteristics were extracted. Simulation outcomes were compared with real-time vibration measurements using a purpose designed and fabricated permanent magnet wind turbine test rig.*
This study presents the total energy method applied to empirical mode decomposition (EMD) for signals collected from experimental and simulation work. The results showed that the total energy method was more sensitive to the presence of a fault than conventional techniques such as kurtosis, RMS and crest factor (CF).

Keywords *- Empirical mode decomposition method (EMD), crack, finite element method, wind turbine blades, total energy.*

1. Introduction

Recognition of the need to increase the use of renewable energy sources has recently become widespread due to growing awareness of climate change. Among such sources wind energy is gaining importance and it is expected that 10% of world electricity could be supplied by wind power by 2020 [1]. Hence, availability and reliability of wind turbines is essential. Although damage can occur to any component or part of the wind turbine, the most common type is rotor or blade damage and tower damage. Thus, special attention should be given to the structural health of blades because they are the elements of a wind power generation system most likely to be damaged and the cost of the blades can account for 15–20% of the total turbine [2]. Blade failure can be caused by excessive stress, fatigue, material properties, load and environmental factors.
Toft et al. [3] have recently presented a framework for modelling defects in wind turbine blades with emphasis given to distribution of defects in the blades and reliability of the blades. Park at al. [4] have studied a rotating wind turbine blade to obtain its vibratory characteristics, they derived a computational algorithm based on blade stiffness variation due to centrifugal inertia forces. Jundert [5] used two different acoustic techniques for wind turbine blade inspection; local resonance spectroscopy and audible sound. Both methods were found to give information about the internal structure of the area being inspected. Ultrasound has also been used to check the bonding areas beneath thick glass fibre reinforced plastics (GFRP) laminates. An ultrasonic air-coupled technique (non-contact and frequency 290 kHz) was applied to detect two different sizes of internal defects (19 mm and 49 mm) in the wind turbine blade by Raišutis et al. [6]. Acoustic emission has successfully been used for monitoring damage development and fault location during a full scale test of a 25 m long wind turbine blade [7]. Sajauskas et al. [8] used secondary longitudinal surface acoustic waves (LSAW II) to detect surface defects on the inaccessible inner surface of sheet products and showed that this method was particularly efficient in the investigation of regular shape defects (cracks) with predictable orientation. Ghoshal et. al. [9] studied four different algorithms for detecting damage on a wind turbine blade based on the vibration response of the blade: transmittance function, resonant comparison, operational deflection shape and wave propagation.
The method reported here is based on applying EMD to the measured signal and then calculating the energy contained within certain frequency bands; particularly the rotor frequency and its sideband zones. This total energy calculation was carried out

for two different rotor speeds (250 and 360 rpm) and three crack lengths (15 mm, 25 mm and 40 mm) each of 3 mm width and 2 mm depth.

Email: abouhnik@yahoo.com

2. Experimental test rig

The experimental work was carried out in the Manchester Metropolitan University Mechanical Engineering Laboratory using the wind turbine in Figure 1. The rig comprises a wind turbine which consists of a six airfoil blades; each blade has 32 cm length. The wind turbine was placed about 1 meter in front of the wind tunnel. The accelerometers were B&K type 4371 with sensitivity of 10mV/g and mounted on the nacelle of the wind turbine. A B&K type 2635 charge amplifier was used to convert the output of accelerometer (Pico-coulomb) to mV. Data acquisition card (NI USB 9233) was connected between a PC and the charge amplifier to collect data.

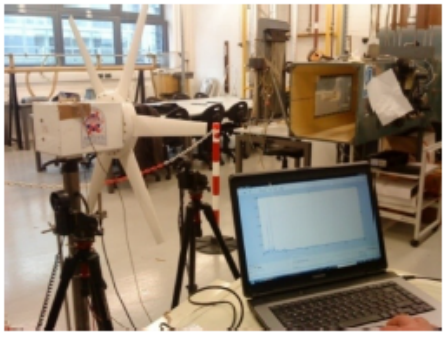

Figure 1. Experimental test rig

3. Simulation work

A finite element model of a wind turbine with six blades was created using 3ANSYS software to build a 3D finite element model of wind turbine as shown in Figure 2. The model simulated healthy blades and a blade suffering from a crack.

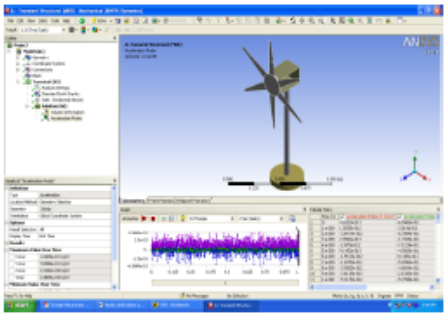

Figure 2. Simulation of wind turbine

Figure 3 represents the time-domain of the experimental vibration signal for the healthy case. Each signal for both the healthy and faulty conditions was analyzed using EMD, see Section 5.

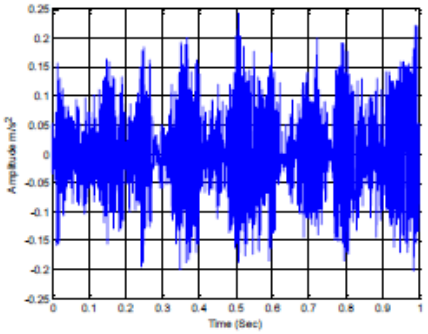

Figure 3. Experimental vibration signals from accelerometer attached to nacelle

4. Vibration analysis technique

Vibration analysis is probably the most widely used technology for condition monitoring, especially for rotating equipment such as gearboxes, bearings and wind turbines. Features extracted from signals which can sensitively reflect the characteristics of machinery conditions are very much sought after. Statistical methods which, for example, extract kurtosis, RMS and CF from the time-domain of vibration signal are commonly used to assess the severity of any damage. However, previous studies have shown that such measures are not suitable for non-stationary signals. So that wind turbines require more advancing monitoring techniques such as EMD, short time Fourier transform (STFT), Winger-Ville distribution (WVD) and the continuous wavelet transform (CWT). This study focus on Empirical Modal Decomposition.

5. Empirical Modal Decomposition description

The EMD is defined by a process called sifting. It decomposes a given signal *X(t)* into a set of AM–FM components, called Intrinsic Mode Functions (IMF) to give K modes $d_K(t)$ and a residual term *r(t)*[10]:

$$X(t) = \sum_{k=1}^{K} d_k(t) + r(t), \qquad (1)$$

$$k = 1, 2, \ldots \ldots \ldots K$$

The EMD algorithm is summarized by the following steps:

1. Start with the signal $d_1(t)$, $k = 1$. Sifting process $h_j(t) = d_K(t), j = 0$.

2. Identify all local extrema of $h_j(t)$.

3. Compute the upper and the lower envelopes ((EnvMax and EnvMin respectively) by cubic spline line interpolation of the maxima and the minima.

4. Calculate the mean of the lower and upper envelopes,

$$m(t) = {}^{1}/_{2}\,(EnvMin(t) + EnvMax(t)) \qquad (2)$$

5. Extract the detail $h_{j+1}(t) = h_j(t) - m(t)$

6. If $h_{j+1}(t)$ is an IMF, go to step 7, else, iterate steps 2 to 5 upon the signal $h_{j+1}(t), j = j + 1$

7. Extract the mode $d_k(t) = h_{j+1}(t)$.

8. Calculate the residual. $r_k(t) = X(t) - d_k(t)$

9. If $r_k(t)$ has less than 2 minima or 2 extrema, the extraction is finished $r(t) = r_k(t)$. Else iterate the algorithm from step 1 upon the residual $r_k(t)$, $k = k + 1$.

6. Result and discussion

The aim of this study is to detect and diagnose the crack defect in the wind turbine blades.
The time-domain vibration signals collected from wind turbine as analyzed using EMD and then the energy contained within certain frequency bands of interest were calculated. These bands were around the rotor frequency and its sideband zones. The total energy calculation was applied the six cases described above - two different rotation speeds and blades suffering from three cracks of different lengths. The decomposition of the experimental and simulation vibration signals for the healthy case at rotation speed 360 rpm was as shown in Figures 4 and 5.

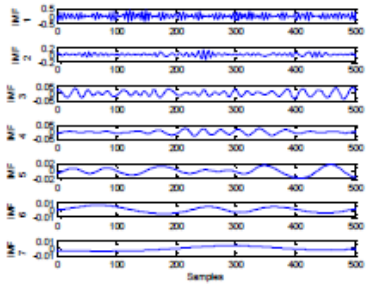

Figure 4. Decomposition of experimental vibration signals for healthy turbine at 360 rpm

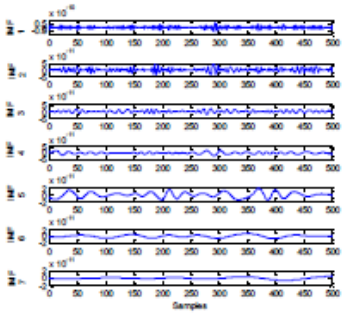

Figure 5. Decomposition of simulated vibration signals for healthy turbine at 360 rpm

Each IMF represents a different vibration source. A fast Fourier transform was applied to each IMF in turn to produce the spectra shown in Figures 6 and 7. The spectra corresponding to Mode IMF6 contains a spectral peak in the region to the shaft frequency. The amplitudes of the modes above IMF6 are very low and this is why they are not shown. The spectra corresponding to the first IMFs are relatively high frequency and come from sources such as the bearing and gears. The shaft frequency for the simulation work also appears in mode IMF6. Thus for these cases, mode IMF6 was adopted to compute total energy.

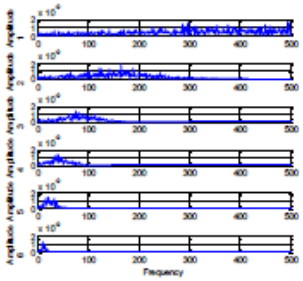

Figure6. Fast Fourier spectra (Experimental) obtained from the IMFs shown in Figure 4

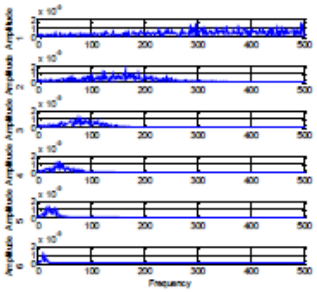

Figure7. Fast Fourier spectra (simulation) obtained from the IMFs shown in Figure 5

Figures 8 and 9 represent total energy for healthy blades and blades suffering from a crack of length 15 mm, 25 mm and 40 mm for the two rotation speeds 250 and 360 rpm respectively of experimental and simulation work.

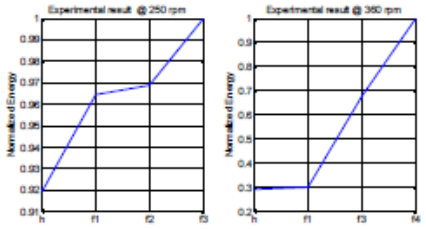

Figure 8. Experimental total energy

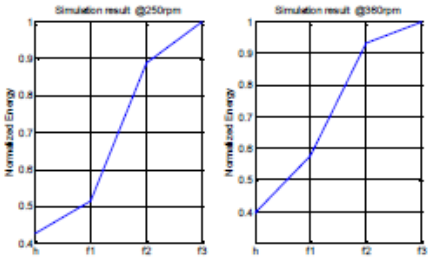

Figure 9. Simulation total energy

The energy levels were calculated for the wind turbine running frequency. It can be seen that there is a clear relationship between the fault severity and the energy levels at different speeds. The curve gradually rises as crack length increased because of rotor imbalance increased.

7. Conclusion

This paper has proposed the combination of total energy and EMD as a useful approach to predictive maintenance and condition monitoring of wind turbine blades. Total energy and EMD was used to detect the presence and severity of a crack in a wind turbine blade and so help avoid catastrophic damage to the blade and structure. This method appears to provide the possibility of online condition monitoring of wind turbines which could be an optimal maintenance strategy for detecting crack initiation. The results showed that the total energy and EMD is suitable and sensitive for diagnosing the given faults.

8. References:

[1] Herbert GM, Iniyan S, Sreevalsan E, Rajapandian S., "A review of wind energy technologies". Renew Sustain Energy Rev **11** (6), pp. 1117–1145. 2007

[2]. Ciang CC, Lee JR, Bang HJ., "Structural health monitoring for a wind turbine system: a review of damage detection methods". Meas. Sci. Technol. 19 122001. 2008.

[3]. Toft HS, Branner K, Berring P, Sørensen J D. , "Distribution of Defects in Wind Turbine Blades & Reliability Assessment of Blades Containing Defects", 2009. www.vbn.aau.dk; accessed in Jan. 2010.

[4]. Park JH, Park HY, Jeong SY, Lee SI, ShinYH, Park JP., "Linear vibration analysis of rotating wind-turbine blade".Current Applied Physics 10(2, Supplement): p. S332-S334.2009.

[5]. Jüngert A.,"Damage Detection in wind turbine blades using two different acoustic techniques". The NDT Database & Journal (NDT). 2008.

[6]. Raisutis R, Jasiuniene E, Zukauskas E. "Ultrasonic NDT of wind turbine blades using guided waves". Ultrasound. Kaunas: Technologija 63, 1.p.7-11. 2008.

[7]. Borum K, Mc Gugan M, Brondsted P., "Condition monitoring of wind turbine blades". Proceedings of the 27th Riso International Symposium on Materials science : Polymer composite materials for wind power turbines, Denmark, 2006 , P.139-145.

[8]. Sajauskas S, Valinevičius A, Miežutavičiūtė L., "Non-destructive testing of sheet product inner surfaces using longitudinal surface acoustic waves". Ultrasound, P. 12–16. 2005.

[9]. Ghoshal A, Sundaresan MJ, Schulz MJ, Pai P. "Structural health monitoring techniques for wind turbine blades". Journal of Wind Engineering and Industrial Aerodynamics 85, 309-324. 2000.

[10]. N.E. Huang, Z. Shen, S.R. Long, M.L. Wu, H.H. Shih, Q. Zheng, N.C. Yen, C.C. Tung and H.H. Liu, "The empirical mode decomposition and Hilbert spectrum for nonlinear and non-stationary time series analysis," Proc. Roy. Soc. London A, Vol. 454, pp. 903–995 1998.

Appendix F:Paper3

International Conference on Applications and Design in Mechanical Engineering 2012 (ICADME 2012)
27-28 February 2012, Penang, Malaysia.

WIND TURBINE BLADES FAULT DETECTION BASED ON PRINCIPAL COMPONENT ANALYSIS

Abdelnasser. Abouhnik, Ghalib R. Ibrahim, A. Albarbar
School of Science & Engineering
Manchester Metropolitan University, (MMU)
Manchester, UK
Emails: abouhnik@yahoo.com,
ghalib_ibrahim@hotmail.com, a.albarbar@mmu.ac.uk

Mohammed sh-eldin
National University of Malaysia
Malaysia
mashema69@gmail.com

Abstract— **This paper presents a new approach to detect faults in wind turbine blades. This approach is based on Principal Component Analysis (PCA) of the vibration signal. The residual matrix signals for healthy and faulty system were compared by applying the crest factor. It contains information extracted from the PCA and the faults were found from the comparisons. The experimental work was carried out using three bladed wind turbine. The cracks were simulated on the blade with diameters (3 mm, 6 mm, 9 mm and 12 mm), all had a consistent depth 3 mm. The tests were carried out for two rotation speeds; 250 and 360 rpm. The results showed that PCA of vibration based condition monitoring is a promising technique because it contains information on all the components of the wind turbine contained in the vibration signal. The crest factor was calculated for the PCA residual matrix. The novel approach successfully differentiated the signals from healthy system and system containing cracks in a turbine blade.**

Keywords- Principal Components Analysis (PCA), crack, Residual Matrix.

I. INTRODUCTION

The need to use renewable energy sources has recently become very important due to growing awareness of climate change. Among these sources, wind energy gains importance and a priority in many countries. It is expected that 10% of world consumed electricity would be supplied by the wind by 2020 [1]. Hence, availability and reliability of these machines is essential. Although damage can occur on any component or part of the wind turbine, the most common type is rotor or blade damage. Therefore, special attention should be given to the structural health of blades as they are the key elements of a wind power generation system, and also because of the cost of the blades can account for 15–20% of the total turbine cost [2]. These types of structural failure could be caused by excessive stress, fatigue, material properties, load and environmental factors.

Many of studies were conducted on wind turbine blades after production progress to diagnose and determine defects, whilst a lot of defects are happening during their transfer or assembly on the site; however these studies have led to important observations on the nature of blades design and are contributed to avoid early failure of blades and to invest their quality. Although blade design methods have improved significantly in the last decade there is still much more for improvement in the area of dynamic load control and cost reduction. Many and extensive study of wind turbine maintenances have been conducted experimentally and numerically. Some of these studies have been conducted to minimize failure of wind turbine.

As known the wind energy converters are based on rotational components. Therefore, a highly nonlinear and non-stationary vibration signals are generated due to wind turbine operation conditions, these signals are very complicated, so in this regard Xueli et al. [3] are proposed a fault diagnosis model of a direct-drive wind turbine based on back propagation neural network parameters of the horizontal vibration and the vertical vibration of the wind turbine main shaft are comprehensively considered. It has been known for some time through both analytical and experimental investigations that some machine faults can be directly related to acoustic and vibration harmonics [4]. Yang et al. [5] stated that the wavelet transform (WT) is the suitable and effective technique can be used to monitor generator electrical and drive train mechanical faults. Because of the drive signals are noise rich and difficult to remove it by using conventional filters with fixed cut-off frequencies, the discrete wavelet transforms (DWT) has been applied out for noise cancellation, whilst Continuous Wavelet Transforms (CWT) is then used for feature extraction. Tsai et al. [6] proposed a complex continuous wavelets transform (CWT)-based entropy method which has been applied to distinguish between the healthy structure and the impaired one of the turbine blade to enhance the damage-detection capability of wind turbine blades. Jundert [7] used two different acoustic techniques for blade inspection; those were local resonance spectroscopy and audible sound. The results showed that information about the internal structure of the inspected area can be obtained using features extracted from these signals. Sajauskas et al. [8] used secondary longitudinal surface acoustic waves (LSAW II) to detect surface defects on the inaccessible inner surface of sheet products and showed that this method was particularly efficient in the investigation of regular shape defects (cracks) with predictable orientation. Ghoshal et al. [9] studied four different algorithms for detecting damage on a wind turbine blade based on the vibration response of the blade: transmittance function,

resonant comparison, operational deflection shape and wave propagation. Park et al. [10] studied the linear vibration analysis of a rotating wind-turbine blade to obtain its vibratory characteristics, and proposed a computational algorithm based on variations in blade stiffness due to the centrifugal inertia forces.

II. PRINCIPAL COMPONENT AND RESIDUAL MATRIX APPROACH

Multivariate statistical analysis (i.e. PCA) has been used in many areas of science and engineering to detect abnormalities in the structure of data sets. Its operation can be thought of as extracting from the data those parameters which best explains the variability in the data. PCA works by computing a compact and optimal description of the observed or experimental data set, reducing the number of dimensions of the data set while retaining as much relevant information as possible. It is assumed that the different parameters are uncorrelated with each other, that is the signals from different faults can be discerned from each other. PCA is a useful technique for discerning variables that explain the observed trends in a process.

PCA describes the dispersion of an array of n points in p-dimensional space by introducing a set of principal components. The first principal component is chosen in such a way that is accounts for as much of the variance in the data set as possible. The second principal component is, in mathematical terms said to be orthogonal to the first, uncorrelated with it, that is in reality it would be an independent fault. This second principal component is chosen to account for as much of the remaining variance as possible. The process then proceeds with each succeeding component accounting for as much of the remaining variance as possible. The process continues until a suitable termination is reached depending on the accuracy required or limits of computation.

Consider n samples of actual data collected from m processes and placed in the matrix $X \in \Re^{nxm}$. The first step in calculating the PCA is to normalise this matrix to unit variance and zero mean using scale parameter vectors s and x as the variance and mean vectors respectively. The next step is to determine the covariance matrix R:

$$R = \frac{1}{n-1} X^T X \qquad (1)$$

The third step is to perform Single Value Decomposition (SVD) on R:

$$R = V \Lambda V^T \qquad (2)$$

Where Λ is a diagonal matrix with zero entries everywhere except the leading diagonal, which contains the eigenvalues of R in descending order ($\lambda_1 \geq \lambda_2 \geq .. \geq \lambda_m \geq 0$). Columns of matrix V are the eigenvectors of R. The transformation matrix $P \in \Re^{mxa}$ is generated choosing a eigenvectors or columns of V corresponding to a principal eigenvalues. The purpose of P is to reduce the dimension space of the measured variables.

$$T = XP \qquad (3)$$

The elements of matrix T are called scores, these are the original data (measured values) after being transformed into the reduced dimension space. The columns P are called loadings. Of course the relation shown in Equation (3) can be manipulated to transform the scores back into the original space:

$$X = TP^T \qquad (4)$$

E, the residual matrix is defined as:

$$E = X - X \qquad (5)$$

It follows that the original data space can be calculated as:

$$X = TP^T + E \qquad (6)$$

In Equation (6) E is the variability due to process noise and TP^T is the principal sources of variability in the process [11]. It is very important to choose the number of principal components a, because TP^T represents the principal sources of variability in the process and E represents the variability corresponding to process noise.

The proposed technique is to determine wind turbine blade faults based on the principal component residual matrix analysis (PCRMA) and the algorithm is shown graphically in Fig. 1.

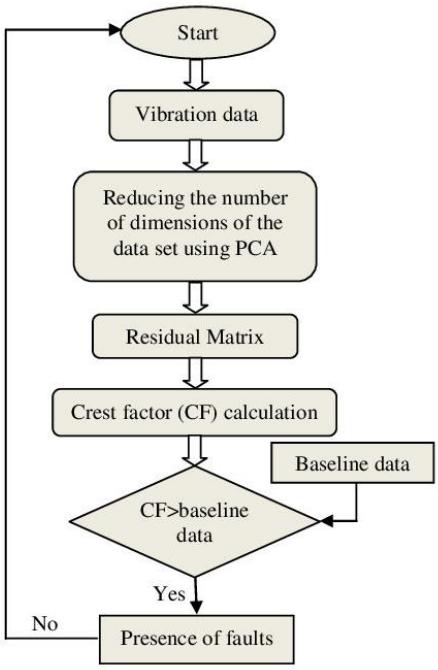

Figure 1 Illustration of the PCA based proposed technique

III. EXPERIMENTAL WORK

The three bladed horizontal-axis wind turbine designed and manufactured in the Manchester Metropolitan University Mechanical Laboratory. The instrumentation: e.g. accelerometers and associated charge amplifiers were used to collect data from wind turbine system. The accelerometers were B&K type 4371 with sensitivity of 10mV/g and suitable for vibration measurements within a range of 1Hz to 12 kHz. Before the accelerometer signals were fed to the analogue-to-digital converter NI USB 9233 card, they passed through a B&K type 2635 charge amplifier to condition the signal. The charge amplifier converts the accelerometer high impedance, low charge (in the range of Pico-coulomb) signal into low impedance and high voltage (in the range of mV) and the cut off frequency for initialising filter was set to 10 kHz. The developed Labview based system allowed the user to monitor and store machine variables, and subsequently a Matlab code was used for further signal processing. The accelerometer was mounted vertically on the nacelle of the wind turbine.

Figure 2 represents wind turbine, it consists of a three airfoil blades; each blade has a length of 32 cm. The wind turbine was located about 1 meter in front of the wind tunnel. The experimental work was carried out with two healthy blades and a single blade with a crack introduced. The seeded cracks were simulated on the blade with diameters; 3 mm, 6 mm, 9 mm and 12 mm, they had a consistent 3 mm depth

Figure2 Wind turbine used in experimental work

IV. RESULT AND DISCUSSION

The collected vibration signal from a wind turbine for the healthy blade case is shown in Figure 3. These were analysed using statistical method such as Kurtosis, RMS and CF.

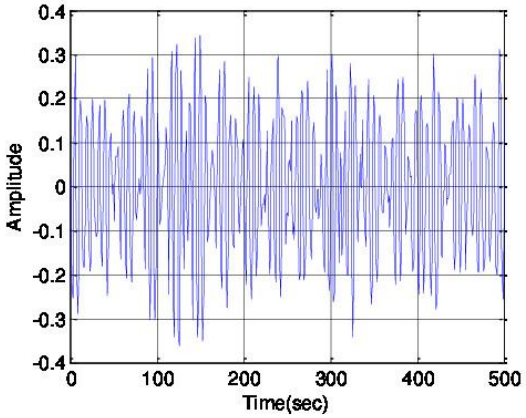

Figure 3 Healthy vibration signal from wind turbine

Figure 4 illustrates statistical analysis for wind turbine vibration signal under different conditions; h is healthy, fault 1 (f1) is a3 mm crack, fault 2 (f2) is a 6 mm crack, fault 3 (f3) is a 9 mm crack and fault 4 (f4) is a 12 mm crack. From Figure 5 it can be seen that the results show no clear trend, which means the method cannot be used to diagnose system defects.

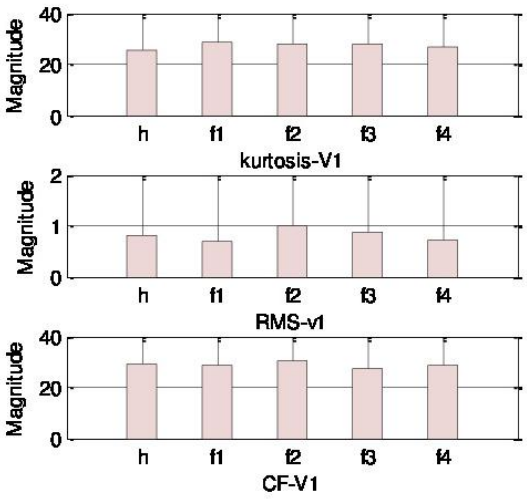

Figure 4 Statistical parameters of vibration signal

PCA is a method for reducing what may be considered a contaminated signal into a series of manageable data sets. Every set contains its principal components (PCs), which are interpretations of the original data. Data were collected and analyzed using PCA method as shown in Figures 5, 6 and 7. Figure 5 shows eigenvalues vs PCs. From theory each PC contains a proportion of the total variance and the eigenvalues represent that amount. Thus the eigenvalues are a measure the

relative importance of each PC in reconstructing the real signal.

As shown from the eigenvalues plot healthy and faulty cases were studied for different fault conditions, but the change in shape of the curves is not sufficiently clear to detect and identify the seeded faults.

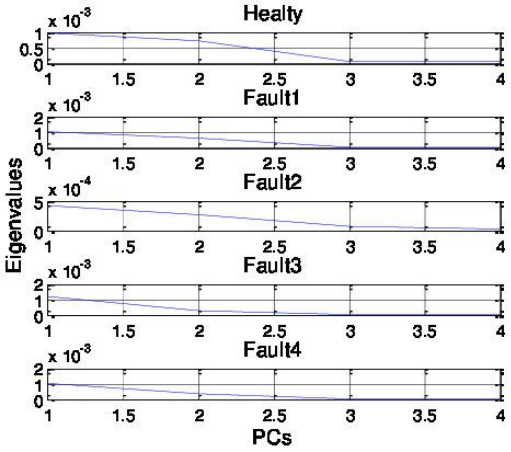

Figure 5 Eigenvalues as a function of Principal Component at rotation speed 360 rpm

Figure 6 shows score plot of healthy and faulty cases, in this case the first plot is a healthy condition and can be used as a guide for the faulty cases. This plot contains certain characteristics such as size, spread and clusters in the data. From the plot there is no clear trend between healthy and faulty cases, which means that it is not sensitive enough to small changes in the vibration signal to detect initial faults.

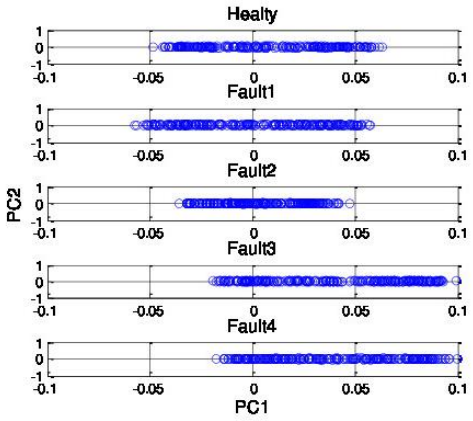

Figure 6 Score plot at rotation speed 360 rpm for the first Principal Component

The main use of PCA is to reduce the dimensionality of a data set and it is assumed that the first few PCs contain most of not all the necessary relevant information contained with the original data. Thus it follows that the remaining PCs should contain mostly noise from the original data. According to PCA theory these PCs can be contained in a separate matrix called the Residual Matrix, which is constructed in the same way as the original data matrix except using only the irrelevant PCs and their respective weightings.

Actually, the relevant scores (PCs) are used to calculate the Residual Matrix. The Residual Matrix contains the information which has been removed from the analysis and the errors are found using this matrix. The sum of the error in each column of the matrix is calculated and squared to give a positive result which it is plotted. The residual errors (matrix) plots for healthy and faulty cases are showed in Figure 7. From this figure, there is a difference between healthy and faulty cases which means the condition of the wind turbine was varying. But to classify the cases between healthy and faulty was difficult.

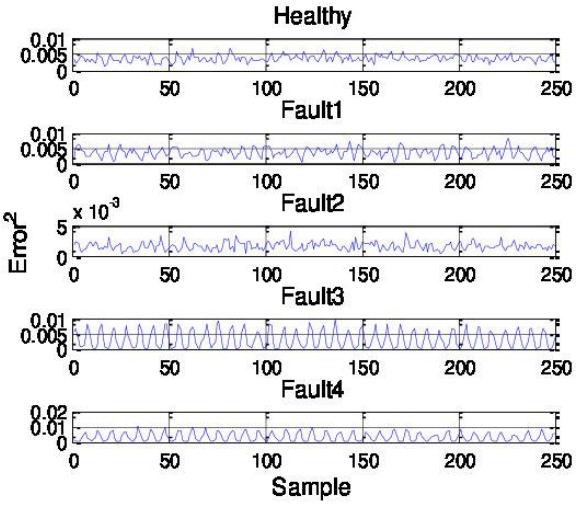

Figure 7. Residual error plot at rotation speed 360 rpm

Figures 8 and 9 represent crest factor values for the residual matrix of wind turbine blades signal for three healthy blades and when the four faults were seeded into one of the blades. It can be seen that the value of crest factor increased with fault level which suggest that the proposed method may have advantages over the other statistical techniques when used with PCA.

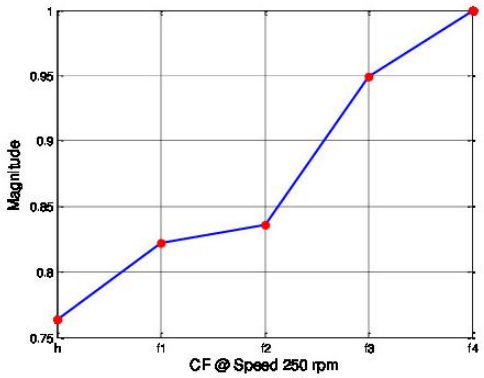

Figure 8 Crest Factor at rotation speed 250 rpm

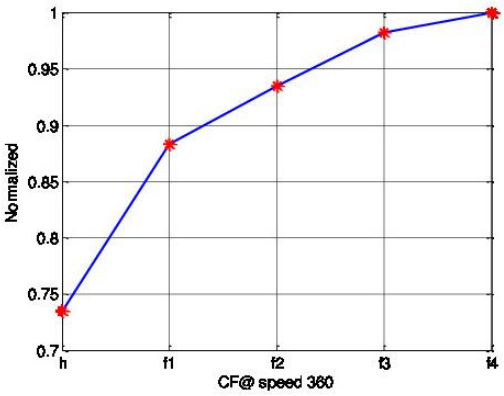

Figure 9 Crest Factor at rotation speed 360 rpm

V. CONCLUSIONS

The vibration signals are collected from wind turbine considered as noise-contaminated signal that simple statistical parameters are not sufficient for fault detection. This study has introduced a promising new approach to detect cracks in wind turbine blades. PCA was used to extract the residual matrix which contains the information removed from the analysis and the errors from the vibration signal. Then the crest factor was applied to the residual matrix. It has been found such a technique has shown great promise in detecting cracked blades on a wind turbine.

REFERENCES

[1] Joselin Herbert GM IS, Sreevalsan E, Rajapandian S. A review of wind energy technologies. Renew Sustain Energy Rev 2007:11(6) 1117.

[2] Ciang C.C. LJ-R, Bang H.-J. Structural health monitoring for a wind turbine system: A review of damage detection methods Measurement Science and Technology 2008;19

[3] Xueli A, Dongxiang J, Shaohua L. Application of back propagation neural network to fault diagnosis of direct-drive wind turbine. World Non-Grid-Connected Wind Power and Energy Conference (WNWEC), 2010, p.1.

[4] Singh G. SAAS. Induction Machine drive condition monitoring and diagnostic research- a survey. Electric Power systems Research 2003;64,145-158.

[5] Yang W, Tavner PJ, Wilkinson MR. Condition monitoring and fault diagnosis of a wind turbine synchronous generator drive train. Renewable Power Generation, IET 2009;3:1.

[6] Tsai CS, Hsieh CT, Lew KL. Detection of wind turbine blades damage by spectrum-recognition using gaussian wavelet-entropy. Anti-counterfeiting, Security, and Identification in Communication, 2009. ASID 2009. 3rd International Conference on, 2009, p.108.

[7] Jüngert A. Damage Detection in wind turbine blades using two different acoustic techniques. The NDT Database & Journal (NDT) 2008.

[8] Sajauskas S, Valinevičius A, Mieżutavičiūtė L. Non-destructive testing of sheet product inner surfaces using longitudinal surface acoustic waves. Ultrasound 2005: P. 12.

[9] Ghoshal A, Sundaresan MJ, Schulz MJ, Frank Pai P. Structural health monitoring techniques for wind turbine blades. Journal of Wind Engineering and Industrial Aerodynamics 2000;85:309.

[10] Jung- Hun Park H-YP, Seok- Yong Jeong, Sang-Il leee, Yoyng-Ho Shin, Jong-Po Park. Linear vibration analysis of rotating wind-turbine blade. current Applied Physics 2009;3.

[11] D. Garc´ıa-A´ lvarez Fault detection using Principal Component Analysis (PCA) in a Wastewater Treatment Plant (WWTP). 2010.

Appendix G: Poster

Manchester Metropolitan University

Coherence Analysis of Wind Turbine Induced Air-borne acoustics and Vibration Signals

Advanced Industrial Diagnostics Research Group

Abdelnasser Abouknik aboukni@yahoo.com Supervisor: Dr. Alhussein Albarbar

1. Abstract:

PZT accelerometers measure the dynamic changes in rotating machinery for vibration control and diagnostic purposes. This type of vibration measuring system is expensive and need to be mounted on the machine itself which introduces other concerns like accessibility and temperature limitations. Microphones offer remote approach of measuring sounds emitted by rotating machinery however, the measured sound is contaminated by background noise. It also contains all sound emitted by different sources which cause overlapping, amplitude and frequency modulations within the measured spectrum. In this work a thorough investigation is carried out to study the visibility of using air-borne acoustic measurements as a potential candidate to provide information similar to those contained within wind turbine vibration signals. The reverberation problems associated with acoustics measurements were also eliminated using special eggs carton box around the condenser microphone used for recording the wind turbine emitted sound signals. Coherence analysis is carried out to compare the information contents of both vibration and sound signals of three bladed horizontal wind turbine. Interestingly, this study show good coherence at frequency bands of rotating speed, gear missing frequencies and fan passing frequency. More important, sound data was found to contain more pronounced information within wider spectrum compared with the acceleration measurement. The achieved results pave the path to carry out more investigation into the capabilities of air-borne acoustic based monitoring techniques and probably lead to fully adoption by the wind turbine control and diagnostics industry.

2. Research Aim:

This work aims at critically assessing wind turbine air-borne acoustic signals information contents compared with their measured vibrations.

3. The proposed method of assessment:

The condition related information contents of wind turbine air-borne acoustic signals is studied using coherence analysis techniques. The coherence is defined as :

$$Coh(\tau) = \frac{\left| S_{xy}(\omega) \right|^2}{S_{xx}(\omega) \, S_{yy}(\omega)}$$

Where $S_{xy}(\omega)$ is the cross-power spectrum density at angular frequency (ω). While $S_{xx}(\omega)$ is the power spectral density of vibration signal and $S_{yy}(\omega)$ is the power spectral density of acoustic signal. In coherence's calculation the signal is squared, thus producing values from 0 to 1. Coherence was calculated and plotted for all expected frequencies from 0 to the highest frequency

4. Experimental setup

The vibration and air-borne acoustic data was collected from a purposely designed and implemented test rig as shown in Figure 1. A piezoelectric accelerometers were B&K type 4371 with sensitivity of 10mV/g mounted on the wind turbine nacelle was used for vibration measurements. For air-borne acoustic measurements; a condenser microphone, type YG-201, frequency response from DC to 20kHz. The microphone was located 50 cm away from the nacelle. A National Instruments data acquisition card (NI USB 9233) was used for data collection and the signal processing algorithms written in MatLab.

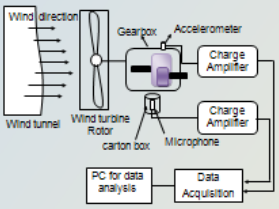

Fig.1. Test rig and instrumentation

5. Experimental Results

Datasets of airborne acoustic and vibration signals were analysed offline using MatLab program. Figure (2-a) represents the time waveform of the airborne acoustic signal for the healthy case, while the time waveform of the vibration signal for the same condition is shown in figure(2-b).

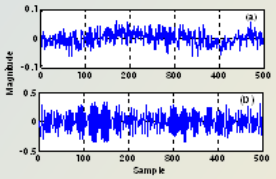

Figure 2 wind turbine time domain signals; (a) airborne acoustic, (b) vibration

Both signals exhibit complex sinusoidal signals superimposed on each other with substantial amount of noise. Clearly not much information could be extracted from such signals; therefore FFT algorithm was used to show them in frequency domain. The measurements were taken at rotation speed 250 rpm, thus the shaft frequency is 4.1 Hz, while the wind turbines blade pass frequency (BPF) is 12.5 Hz. BPF vary with number of blades and rotational speed and can be expressed as:

$$BPF = nx/60$$

where BPF is Blade Pass Frequency (Hz), n is rotation speed (rpm) and x is number of blades. Whilst meshing frequency is 125 Hz. which is can be calculated as follows:

$$f_m = \omega_p N_p = \omega_g N_g$$

Where Np, Ng = number of teeth on pinion and gear respectively and ω_p, ω_g are rotational speeds of the pinion and gear respectively. FFT was applied on both signals and the results as shown in figure 3. As can be seen although the acoustic signal is contaminated more than the vibration but BPF is clearly shown for both signals at 12.5 Hz as well as for the meshing frequency at 125 Hz.

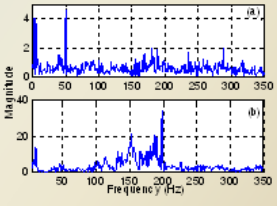

Figure 3 wind turbine frequency domain signals; (a) airborne acoustic, (b) vibration

Thus the coherence will be mostly studied at those frequencies. The cross power spectral density function, defined as the Fourier transform of the cross covariance function, can be used similarly in the spectral domain. The cross power spectral density (cpsd) preformed for two signals. Both signals have 1000 samples long, the same number of sampling the Hanning window full width; and the amount of overlap in the subseries and the result is shown in figure 4.

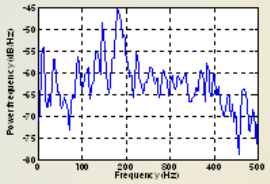

Figure 4 Welch Cross Power Spectral Density Estimate.

As can be seen in figure (5-a), there is change in coherence and values differ from zero to the highest value around 1; a large change. Both signals have a common wave component with different frequencies. The coherence seen in the frequencies 12.5 Hz which generated by blade pass frequency, 37.5 Hz is associated with second harmonic of the blade pass frequency, while 125 Hz is associated with meshing frequency, whilst the large value which gives good coherence is 180 Hz and is likely due to environmental noise, such as wind tunnel noise.

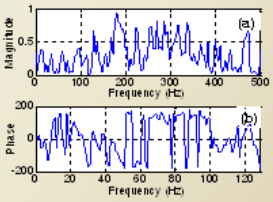

Figure 5 (a) Coherence Estimate via Welch, (b) Coherence phase

The result shows that the values of coherence are greater than zero and less than 1, thus both signals are partially linearly related. From other side figure (5-b) shows coherence phase . The minimum phase coherence between both signals is -180 rad at the frequency 129 Hz. while the maximum phase coherence between the signals is 178.7 rad at 88 Hz.

6. Conclusion

This research investigates the visibility of using microphones to provide information similar to those contained within wind turbine vibration signals

this study show good coherence at frequency bands of rotating speed, gear missing frequencies and fan passing frequency. More important, sound data was found to contain more pronounced information within wider spectrum compared with the acceleration measurement.

The achieved results pave the path to carry out more investigation into the capabilities of air-borne acoustic based monitoring techniques and probably lead to fully adoption by the wind turbine control and diagnostics industry.

Advanced Industrial Diagnostics Research Group

School of Engineering ,Manchester Metropolitan University, Oxford Road, Manchester M1 5GD

Advanced Industrial Diagnostics Research Group

Appendix H: Paper4

International Scholarly Research Network
ISRN Mechanical Engineering
Volume 2012, Article ID 715893, 7 pages
doi:10.5402/2012/715893

Research Article

Novel Approach to Rotating Machinery Diagnostics Based on Principal Component and Residual Matrix Analysis

A. Abouhnik, Ghalib R. Ibrahim, R. Shnibha, and A. Albarbar

School of Engineering, Manchester Metropolitan University, Manchester M1 5GD, UK

Correspondence should be addressed to A. Abouhnik, abouhnik@yahoo.com

Received 6 November 2011; Accepted 21 December 2011

Academic Editor: K. Yasuda

Rotating machinery such as induction motors and gears driven by shafts are widely used in industry. A variety of techniques have been employed over the past several decades for fault detection and identification in such machinery. However, there is no universally accepted set of practices with comprehensive diagnostic capabilities. This paper presents a new and sensitive approach, to detect faults in rotating machines; based on principal component techniques and residual matrix analysis (PCRMA) of the vibration measured signals. The residual matrix for machinery vibration is extracted using the PCA method, crest factors of this residual matrix is determined and then machinery condition is assessed based on comparing the crest factor amplitude with the base line (healthy) level. PCRMA method has been applied to vibration data sets collected from several kinds of rotating machinery: a wind turbine, a gearbox, and an induction motor. This approach successfully differentiated the signals from healthy system and systems containing gear tooth breakage, cracks in a turbine blade, and phase imbalance in induction motor currents. The achieved results show that the developed method is found very promising and Crest Factors levels were found very sensitive for machinery condition.

1. Introduction

Detection of faults in rotating machinery remains a big challenge especially for complex mechanical systems. Despite substantial advances in sensing and signal processing technologies, many difficulties remain to the successful detection of faults at an early stage of their development to avoid catastrophic failure [1, 2]. It has been known for some time through both analytical and experimental investigations that some machine faults can be directly related to acoustic and vibration harmonics [3].

With wind turbines, Jüngert [4] used two different acoustic techniques for blade inspection; those were local resonance spectroscopy and audible sound. The results showed that information about the internal structure of the inspected area can be obtained using features extracted from these signals. Sajauskas et al. [5] used secondary longitudinal surface acoustic waves (LSAW II) to detect surface defects on the inaccessible inner surface of sheet products and showed that this method was particularly efficient in the investigation of regular shape defects (cracks) with predictable orientation. Ghoshal et al. [6] studied four different algorithms for detecting damage on a wind turbine blade based on the vibration response of the blade: transmittance function, resonant comparison, operational deflection shape, and wave propagation. Park et al. [7] studied the linear vibration analysis of a rotating wind-turbine blade to obtain its vibratory characteristics and proposed a computational algorithm based on variations in blade stiffness due to the centrifugal inertia forces.

Parey et al. [8] used empirical mode decomposition (EMD) to analyse nonstationary and nonlinear signals in order to detect localized tooth defects in gears. Kar and Mohanty [9] applied advanced signal-processing techniques, such as the discrete wavelet transform (DWT) and a corrected multiresolution Fourier transform (MFT), to investigate the vibration and current transients in a multistage gearbox under transient load. Endo et al. [10] proposed a differential diagnostic technique to investigate two kinds of localized gear tooth defects, a crack and spall in the tooth of a gear. A set of digital filters filtered the signal to separate the diagnostic information (fault impulses) from the complex

mixture of signals measured with the sensor placed on the gearbox casing. Ibrahim and Albarbar [11] presented a comparison between empirical mode decomposition (EMD) and smoothed pseudo-Wigner-Ville distribution (SPWVD) methods based on the vibration signature and energy calculation procedure, for monitoring gearbox systems. The results showed that the calculation of energy using EMD techniques offers a more effective way to detect early faults than computations using the SPWVD method, and that the computation of energy using the EMD technique is faster than the calculations done using the SPWVD method.

Induction motors are critical components for many industrial processes and frequently integrated in commercially available equipment and industrial processes. Early fault detection would eliminate consequential damages of motors and reduce outage time and costs of repairs.

Several diagnosis techniques for the identification and localisation of the faults have been proposed. Acosta et al. [12] combined motor current signature analysis (MCSA) and extended Park's vector approach (EPVA) for fault detection and diagnosing induction motor stator and rotor-related faults. Antonino-Daviu [13] have proposed a method for rotor bar failure detection based on the stator current during startup using the discrete wavelet transform (DWT). A novel approach to induction motor current signature analysis based on wavelet packet decomposition (WPD) of the stator current was presented by Ye et al. [14]. The feature coefficients extracted using WPD were then used to detect rotor bar breakage and air-gap eccentricity faults. Liang et al. [15] showed that both current spectra and vibration spectra are able to reveal broken rotor bar faults.

2. Principal Component and Residual Matrix Approach

Multivariate statistical analysis (i.e., PCA) has been used in many areas of science and engineering to detect abnormalities in the structure of data sets. Its operation can be thought of as extracting from the data of those parameters which best explains the variability in the data. PCA works by computing a compact and optimal description of the observed or experimental data set, reducing the number of dimensions of the data set while retaining as much relevant information as possible It is assumed that the different parameters are uncorrelated with each other, that is, the signals from different faults can be discerned from each other. PCA is a useful technique for discerning variables that explain the observed trends in a process.

PCA describes the dispersion of an array of n points in p-dimensional space by introducing a set of principal components. The first principal component is chosen in such a way that accounts for as much of the variance in the data set as possible. The second principal component is in mathematical terms said to be orthogonal to the first, uncorrelated with it, that is, in reality it would be an independent fault. This second principal component is chosen to account for as much of the remaining variance as possible. The process then proceeds with each succeeding component accounting for as much of the remaining variance as possible. The process continues until a suitable termination is reached depending on the accuracy required or limits of computation.

Consider n samples of actual data collected from m processes and placed in the matrix $X \in \Re^{n\times m}$. The first step in calculating the PCA is to normalise this matrix to unit variance and zero mean using scale parameter vectors s and x as the variance and mean vectors, respectively. The next step is to determine the covariance matrix R:

$$R = \frac{1}{n-1} X^T X. \tag{1}$$

The third step is to perform single-value decomposition (SVD) on R:

$$R = V \Lambda V^T, \tag{2}$$

where Λ is a diagonal matrix with zero entries everywhere except the leading diagonal, which contains the eigenvalues of R in descending order ($\lambda_1 \geq \lambda_2 \geq \cdots \geq \lambda_m \geq 0$). Columns of matrix V are the eigenvectors of R. The transformation matrix $P \in \Re^{m\times a}$ is generated choosing a eigenvectors or columns of V corresponding to a principal eigenvalues. The purpose of P is to reduce the dimension space of the measured variables

$$T = XP. \tag{3}$$

The elements of matrix T are called *scores*, and these are the original data (measured values) after being transformed into the reduced dimension space. The columns P are called *loadings*. Of course, the relation shown in (3) can be manipulated to transform the scores back into the original space

$$\hat{X} = TP^T. \tag{4}$$

E, the residual matrix, is defined as

$$E = X - \hat{X}. \tag{5}$$

It follows that the original data space can be calculated as

$$X = TP^T + E. \tag{6}$$

In (6), E is the variability due to process noise, and TP^T is the principal sources of variability in the process [16]. It is very important to choose the number of principal components a, because TP^T represents the principal sources of variability in the process, and E represents the variability corresponding to process noise.

The proposed novel technique is to determine rotating machinery faults based on the PCRMA algorithm shown graphically in Figure 1.

3. Experimental Work

The experimental work was carried out in the Mechanical Laboratory of the Manchester Metropolitan University using several different kinds of rotating machinery: a wind turbine,

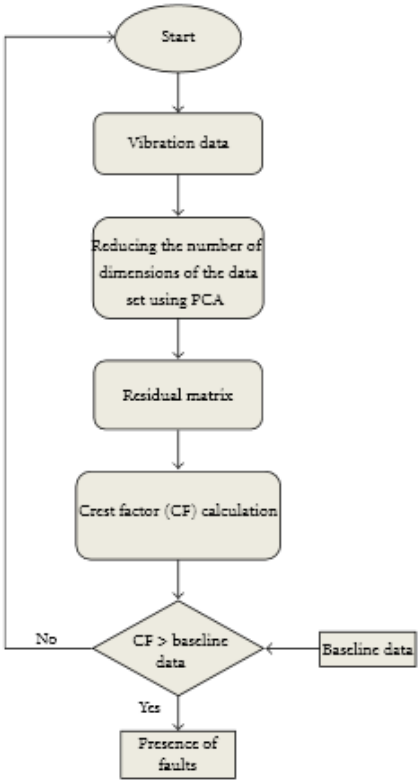

Figure 1: Illustration of the PCA-based proposed technique.

a gearbox, and an induction motor. The same instrumentation, for example, accelerometers and associated charge amplifiers were used to collect data from all three systems. The accelerometers were B and K type 4371 with sensitivity of 10 mV/g and suitable for vibration measurements within a range of 1 Hz to 12 kHz. Before the accelerometer signals were fed to the analogue-to-digital converter NI USB 9233 card, they passed through a B and K type 2635 charge amplifier to condition the signal. The charge amplifier converts the accelerometer high-impedance, low-charge (in the range of Pico-coulomb) signal into low impedance and high voltage (in the range of mV), and the cut-off frequency for initialising filter was set to 10 kHz. The developed Labview-based system allowed the user to monitor and store machine variables, and subsequently, a Matlab code was used for further signal processing. The accelerometer was mounted vertically on the gearbox housing, on the nacelle of the wind turbine, and on the induction motor.

Figure 2 represents wind turbine test rig, and it consists of a six airfoil blades; each blade has a length of 32 cm. The wind turbine was located about 1 meter in front of the wind tunnel for two wind speeds: 4.7 and 5.3 m/s. The experimental work was carried out with five healthy blades

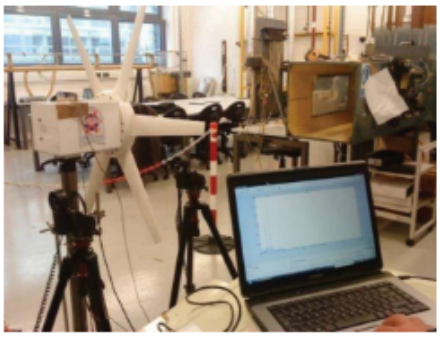

Figure 2: Wind turbine test rig.

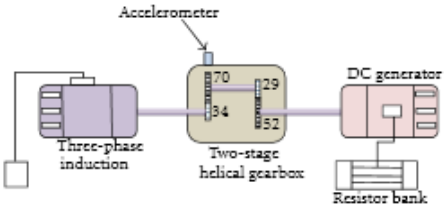

Figure 3: Schematic layout of the gearbox test.

and with a single blade with a crack introduced. The seeded crack was of three lengths: 15 mm, 25 mm, and 40 mm, and it had a consistent 3 mm width and 2 mm depth.

The gearbox used as a second machinery test consists of a two-stage, 11 kW, helical gearbox driven by a three-phase induction motor and connected to a DC generator and resistor banks as shown in Figure 3. Tests were carried out using a healthy pair of gears and the first drive pinion suffering from a tooth breakage of three magnitudes: fault 1 (25% tooth removal), fault 2 (50% tooth removal), and fault 3 (75% tooth removal). The drive pinion at the first stage had 34 teeth meshing with a 70-tooth wheel. The pinion gear at the second stage had 29 teeth meshing with 52-tooth wheel. The vibration signals were collected using an accelerometer mounted vertically on the gearbox housing for a drive speed 90% of full speed and a load of 40% cent of maximum load.

A third rotating machinery test used a 3 kW, 220 V induction motor, and a DC generator with a resistor bank to act as a load. A schematic diagram of the test rig is shown in Figure 4. The motor was tested at 0%, 25%, 50%, 75%, and 100% load in a healthy condition and then under two different phase imbalance voltages of 20 and 40 V.

4. Result and Discussion

The collected vibration data from a wind turbine for the healthy blade case is shown in Figure 5. These were analysed using statistical method such as Kurtosis, RMS, and CF. Figure 6 illustrates statistical analysis for wind turbine vibration signal under different conditions: h is healthy,

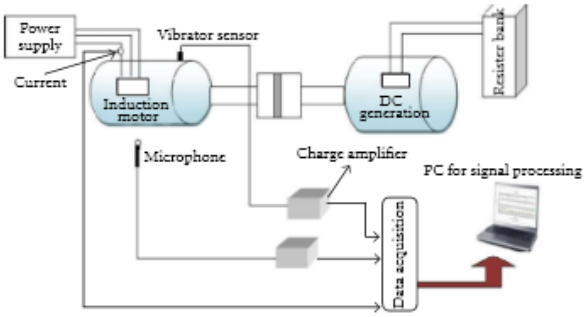

Figure 4: Schematic diagram of induction motor test rig.

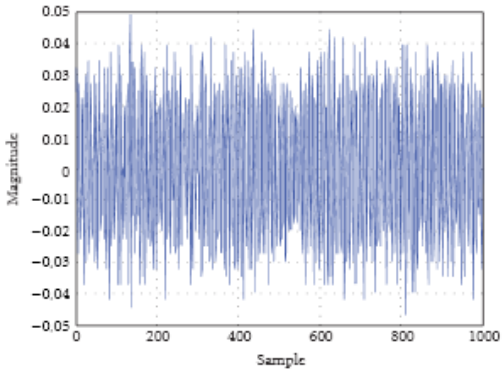

Figure 5: Healthy vibration signal from wind turbine.

fault1 (f1) is a crack 15 mm long, fault2 (f2) is a crack 25 mm long, and fault3 (f3) is a crack 40 mm long. From Figure 5, it can be seen that the results show no clear trend, which means that the method cannot be used to diagnose system defects.

PCA is a method for reducing what may be considered a contaminated signal into a series of manageable data sets. Every set contains its principal components (PCs), which are interpretations of the original data. Data were collected and analyzed using PCA method as shown in Figures 7, 8, and 9. Figure 7 shows eigenvalues versus PCs. From theory each PC contains a proportion of the total variance, and the eigenvalues represent that amount. Thus, the eigenvalues are a measure of the relative importance of each PC in reconstructing the real signal.

As shown from the eigenvalues, plot healthy and faulty cases were studied for different fault conditions, but the change in shape of the curves is not sufficiently clear to detect and identify the seeded faults. Figure 8 shows score plot of healthy and faulty cases; in this case, the first plot is a healthy condition and can be used as a guide for the faulty cases. This plot contains certain characteristics such as size, spread, and clusters in the data. From the plot, there is no clear difference between healthy and faulty cases, which means that this method is not sensitive enough to small changes in the vibration signal to detect initial faults.

The main use of PCA is to reduce the dimensionality of a data set, and it is assumed that the first few PCs contain most of, not all, the necessary relevant information contained with the original data. Thus, it follows that the remaining PCs should contain mostly noise from the original data. According to PCA theory, these PCs can be contained in a separate matrix called the residual matrix, which is constructed in the same way as the original data matrix except using only the irrelevant PCs and their respective weightings.

Actually, the relevant scores (PCs) are used to calculate the residual matrix. The residual matrix contains the information which has been removed from the analysis, and the errors are found using this matrix. The sum of the errors in each column of the matrix is calculated and squared to give a positive result which is plotted. The residual errors plots for healthy and faulty cases are showed in Figure 9. From this figure, there is a difference between healthy and faulty cases which means that the condition of the wind turbine was

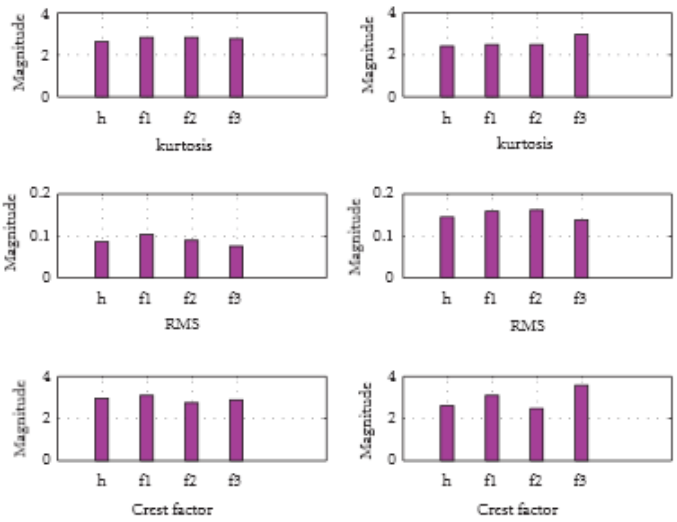

Figure 6: Magnitude of kurtosis, RMS, and crest factor vibration signal from wind turbine with healthy blades and one faulty blade with the fault of three different degrees of severity.

varying. But to classify the cases between healthy and faulty was difficult.

Developing a new way of thinking about this analysis could provide an effective method of evaluating the signals obtained from condition monitoring to determine incipient faults. A PCA-based technique was applied to the measured data for each of the three test systems. The CF was calculated for the residual signal for each of the three systems for each fault seeded into the system.

To test this novel approach, the proposed technique was applied to different data sets. Figures 10 and 11 represent crest factor values for the residual error for wind turbine blades signal for six healthy blades and when the three faults were seeded into one of the blades. It can be seen that the value of crest factor increased with fault level which suggests that the proposed method may have advantages over the other statistical techniques when used with PCA. Secondly, the new approach was used to analyse gearbox signals collected under healthy conditions and for the three tooth faults: fault 1 (25% tooth removal), fault 2 (50% tooth removal), and fault 3 (75% tooth removal). The test was carried out for a load that was 40% of the total load, and the speed was 1350 rpm. Figure 12 shows the results using a PCA-based technique applied to the measured vibration signal. The results showed that there was a clear trend with the value of the CF of the residual error plot increasing with severity of the fault. It is concluded that there is advantage to using the proposed technique.

Finally, the new technique was applied to data collected from an induction motor under different conditions. The motor was tested at 0%, 25%, 50%, 75%, and 100% load in a healthy condition and then under two different single-phase imbalance voltages of 20 and 40 V.

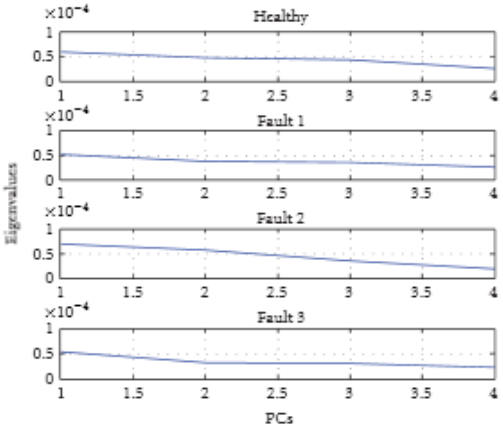

Figure 7: Eigenvalues as a function of Principal Component for healthy and faulty blade at wind speed of 4.7 m/s.

In this case, the CF was also used as a statistical feature extracted from the raw vibration signal, but no adequate, reliable information related to the condition of the motor was observed. To detect the phase imbalance, the PCA method was applied to the measured vibration signals. Crest factor values for the residual error based on PCA were calculated, and in Figure 13, it can be seen that there is a clear relationship between the fault severity and the crest factor for all loads tested. The approach developed here was able to detect changes of the phase imbalance.

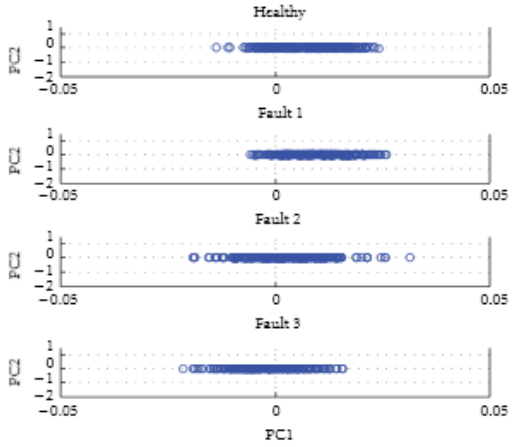

Figure 8: Score plot for healthy and faulty blade at wind speed of 4.7 m/s for the first principal component.

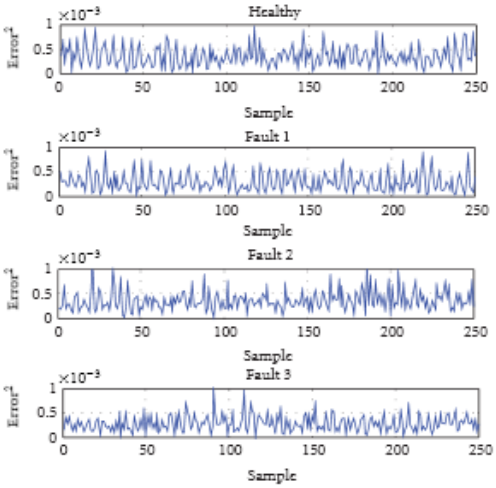

Figure 9: Residual error plot for healthy and faulty blade at wind speed 4.7 m/s.

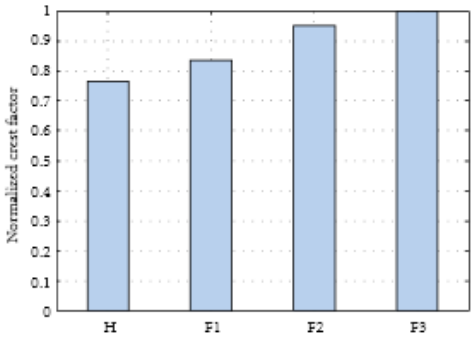

Figure 10: Crest factor for healthy and faulty turbine blade at wind speeds of 4.7 m/s.

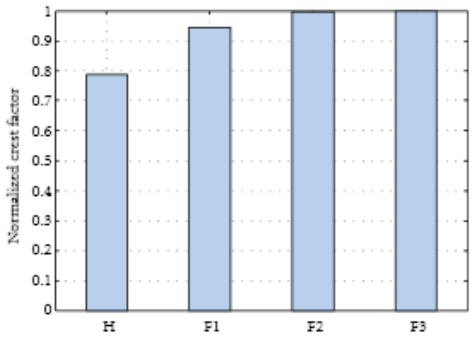

Figure 11: Crest factor for healthy and faulty turbine blade at wind speeds of 5.3 m/s.

5. Conclusion

The vibration signals collected from rotating machinery are often so contaminated that simple statistical parameters are not sufficient for fault detection. This study has introduced a promising new approach to detect faults in different rotating machines. PCA was used to extract the residual matrix which contains the information removed from the analysis and the errors from the vibration signal. Then the crest factor was applied to the residual matrix. It has been found that such

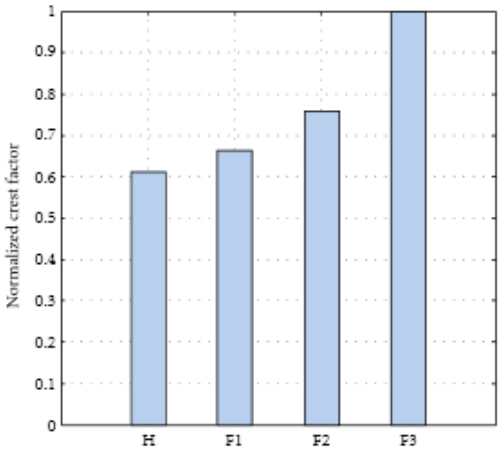

Figure 12: Crest factor plot for healthy gearbox and gearbox with three tooth faults introduced (40% full load and 90% full speed).

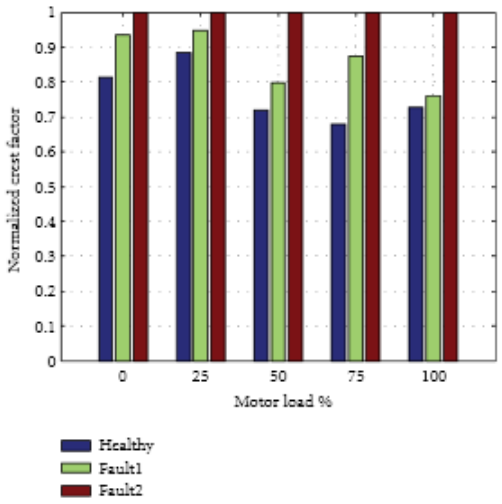

Figure 13: Crest factor of residual error for healthy and faulty induction motor.

a technique has shown great promise in detecting voltage imbalance in an induction motor, gear teeth breakage in a gearbox, and cracked blades on a wind turbine.

References

[1] T. Reilly and T. Proulx, *A Review of Signal Processing and Analysis Tools for Comprehensive Rotating Machinery Diagnostics, Rotating Machinery, Structural Health Monitoring, Shock and Vibration*, vol. 5, Springer, New York, NY, USA, 2011.

[2] Y. Lu, J. Tang, and H. Luo, "Wind turbine gearbox fault detection using multiple sensors with feature level data fusion," in *Proceedings of the ASME Turbine Technical Conference & Exposition*, 2011, GT2011-46538.

[3] G. K. Singh and S. A. S. Al Kazzaz, "Induction machine drive condition monitoring and diagnostic research—a survey," *Electric Power Systems Research*, vol. 64, no. 2, pp. 145–158, 2003.

[4] A. Jungert, "Damage Detection in wind turbine blades using two different acoustic techniques," *NDT Database & Journal of Nondestructive Testing*, 2008.

[5] S. Sajauskas, A. Valinevičius, and L. Miežutavičiūtė, "Non-destructive testing of sheet product inner surfaces using longitudinal surface acoustic waves," *Ultrasound*, pp. 12–16, 2005.

[6] A. Ghoshal, M. J. Sundaresan, M. J. Schulz, and P. F. Frank Pai, "Structural health monitoring techniques for wind turbine blades," *Journal of Wind Engineering and Industrial Aerodynamics*, vol. 85, no. 3, pp. 309–324, 2000.

[7] J. H. Park, H. Y. Park, S. Y. Jeong, S. I. Lee, Y. H. Shin, and J. P. Park, "Linear vibration analysis of rotating wind-turbine blade," *Current Applied Physics*, vol. 10, no. 2, supplement, pp. S332–S334, 2010.

[8] A. Parey, M. El Badaoui, F. Guillet, and N. Tandon, "Dynamic modelling of spur gear pair and application of empirical mode decomposition-based statistical analysis for early detection of localized tooth defect," *Journal of Sound and Vibration*, vol. 294, no. 3, pp. 547–561, 2006.

[9] C. Kar and A. R. Mohanty, "Vibration and current transient monitoring for gearbox fault detection using multiresolution Fourier transform," *Journal of Sound and Vibration*, vol. 311, no. 1-2, pp. 109–132, 2008.

[10] H. Endo, R. B. Randall, and C. Gosselin, "Differential diagnosis of spall vs. cracks in the gear tooth fillet region: experimental validation," *Mechanical Systems and Signal Processing*, vol. 23, no. 3, pp. 636–651, 2009.

[11] G. R. Ibrahim and A. Albarbar, "Comparison between Wigner-Ville distribution- and empirical mode decomposition vibration-based techniques for helical gearbox monitoring," *Journal of Mechanical Engineering Science*, vol. 225, no. 8, pp. 1833–1846, 2011, Proceedings of the Institution of Mechanical Engineers C.

[12] G. G. Acosta, C. J. Verucchi, and E. R. Gelso, "A current monitoring system for diagnosing electrical failures in induction motors," *Mechanical Systems and Signal Processing*, vol. 20, no. 4, pp. 953–965, 2006.

[13] J. Antonino-Daviu, M. Riera-Guasp, J. Roger-Folch, F. Martínez-Giménez, and A. Peris, "Application and optimization of the discrete wavelet transform for the detection of broken rotor bars in induction machines," *Applied and Computational Harmonic Analysis*, vol. 21, no. 2, pp. 268–279, 2006.

[14] Z. Ye, B. Wu, and A. Sadeghian, "Current signature analysis of induction motor mechanical faults by wavelet packet decomposition," *IEEE Transactions on Industrial Electronics*, vol. 50, no. 6, pp. 1217–1228, 2003.

[15] B. Liang, B. S. Payne, A. D. Ball, and S. D. Iwnicki, "Simulation and fault detection of three-phase induction motors," *Mathematics and Computers in Simulation*, vol. 61, no. 1, pp. 1–15, 2002.

[16] D. García-Álvarez, "Fault detection using principal component analysis (PCA) in a wastewater treatment plant (WWTP)," in *Proceedings of the International Student's Scientific Conference*, 2009.

Appendix I: Paper5

Energy Conversion and Management 64 (2012) 606–613

Contents lists available at SciVerse ScienceDirect

Energy Conversion and Management

journal homepage: www.elsevier.com/locate/enconman

Wind turbine blades condition assessment based on vibration measurements and the level of an empirically decomposed feature

Abdelnasser Abouhnik, Alhussein Albarbar*

Advanced Industrial Diagnostics Centre, Faculty of Science & Engineering, Manchester Metropolitan University, Manchester M1 5GD, United Kingdom

ARTICLE INFO

Article history:
Available online 24 August 2012

Keywords:
Empirically decomposed feature intensity level (EDFIL)
Wind turbine vibration
Turbine blade crack
Finite element method (FEM)

ABSTRACT

Vibration based monitoring techniques are well understood and widely adopted for monitoring the condition of rotating machinery. However, in the case of wind turbines the measured vibration is complex due to the high number of vibration sources and modulation phenomenon. Therefore, extracting condition related information of a specific element e.g. blade condition is very difficult.

In the work presented in this paper wind turbine vibration sources are outlined and then a three bladed wind turbine vibration was simulated by building its model in the ANSYS finite element program. Dynamic analysis was performed and the fundamental vibration characteristics were extracted under two healthy blades and one blade with one of four cracks introduced. The cracks were of length (10 mm, 20 mm, 30 mm and 40 mm), all had a consistent 3 mm width and 2 mm depth. The tests were carried out for three rotation speeds; 150, 250 and 360 r/min.

The effects of the seeded faults were revealed by using a novel approach called empirically decomposed feature intensity level (EDFIL). The developed EDFIL algorithm is based on decomposing the measured vibration into its fundamental components and then determines the shaft rotational speed amplitude. A real model of the simulated wind turbine was constructed and the simulation outcomes were compared with real-time vibration measurements. The cracks were seeded sequentially in one of the blades and their presence and severity were determined by decomposing the measured vibration signal into its main components and evaluating the intensity level at the main shaft rotating speed.

The application of the developed monitoring approach on empirical vibration data gave reasonable results and was in good agreement with the simulation predicted levels.

1. Introduction

Recognition of the need to increase the use of renewable energy sources has recently become widespread due to growing awareness of climate change. Among such sources wind energy is gaining importance and it is expected that 10% of world electricity could be supplied by wind power by 2020 [1]. Hence, availability and reliability of wind turbines is essential. Although damage can occur to any component or part of the wind turbine, the most common type is rotor or blade damage and tower damage. Thus, special attention should be given to the structural health of blades because they are the elements of a wind power generation system most likely to be damaged and the cost of the blades can account for 15–20% of the total turbine [2]. Blade failure can be caused by excessive stress, fatigue, material properties, load and environmental factors.

Wind turbines are a rotating machine designed to perform certain functions, so this monitoring technique aims to ensure that it performs the required functions such as generating the power output as planned. When there is little knowledge about the types of faults and the time of fault occurrence, no maintenance actions can be planned in advance. With increased knowledge and experience of the nature of the faults, some actions may be organized routinely or prepared well before the occurrence of the fault.

Park et al. [3] have studied a rotating wind turbine blade to obtain its vibratory characteristics, they derived a computational algorithm based on blade stiffness variation due to centrifugal inertia forces. Jündert [4] used two different acoustic techniques for wind turbine blade inspection; local resonance spectroscopy and audible sound. Both methods were found to give information about the internal structure of the area being inspected. Ultrasound has also been used to check the bonding areas beneath thick glass fiber reinforced plastics (GFRPs) laminates. An ultrasonic air-coupled technique (non-contact and frequency 290 kHz) was applied to detect two different sizes of internal defects (19 mm and 49 mm) in the wind turbine blade by Raisutis et al. [5]. Acoustic emission has successfully been used for monitoring damage development and fault location during a full scale test of a 25 m long wind turbine blade [6]. Sajauskas et al. [7] used secondary longitudinal surface

* Corresponding author.
E-mail address: a.albarbar@mmu.ac.uk (A. Albarbar).

0196-8904/$ - see front matter © 2012 Elsevier Ltd. All rights reserved.
http://dx.doi.org/10.1016/j.enconman.2012.06.008

acoustic waves (LSAWs II) to detect surface defects on the inaccessible inner surface of sheet products and showed that this method was particularly efficient in the investigation of regular shape defects (cracks) with predictable orientation. Ghoshal et al. [8] studied four different algorithms for detecting damage on a wind turbine blade based on the vibration response of the blade: transmittance function, resonant comparison, operational deflection shape and wave propagation.

Yang et al. [9] stated that they developed a new method to deal with non-stationary and non-linear signals. Empirical mode decomposition (EMD) was used to analysis the feature intensity level power signals which is measured from the terminals of 3-phase wind turbine induction generator. The result showed that the intrinsic mode functions (IMFs) are always able to give an obvious indication of change of machine running condition. In another study Yang et al. [10] used bivariate empirical mode decomposition (BEMD) to detect both incipient mechanical and electrical faults. The result showed the proposed BEMD-based technique is convenient for processing shaft vibration signals. Ghalib and Albarbar [11] proposed a computational algorithm based on EMD to detect the gear related fault presence within a 5.5 kW transmission gearbox. The modal characteristics were determined and the vibratory characteristics of healthy and faulty gears were investigated through equations of motion, this work shows that the proposed method is useful to predict the vibratory behavior of a two stage helical gearbox. Furthermore, the developed EMD based algorithm was found more reliable than time–frequency analysis methods. In another recent research paper, Abouhnik et al. [12] investigated the possibility of extracting wind turbine blades health related information based on EMD for a small scale, six bladed wind turbines. Abouhnik et al. [13] presented a new and sensitive approach, to detect faults in rotating machines; based on principal component techniques and residual matrix analysis (PCRMA) of the vibration measured signals. PCRMA method has been applied to vibration data sets collected from several kinds of rotating machinery using accelerometers. The proposed approach successfully differentiated the signals for healthy and faulty conditions. Abouhnik et al. [14] used principal components analysis technique (PCA) to reduce noise from original vibration signals and then to study the effect of damage in wind turbine blade by extracting wind turbine blades related information for, three bladed wind turbines.

This paper presents a novel method based on applying EMD to the measured signal and then calculating the intensity level contained within certain frequency bands; particularly the rotor frequency and its sideband zones. The developed method is supported by simulation study and validated using real-time vibration measurements taken from an operational wind turbine.

2. Wind turbine theoretical simulation

2.1. Wind turbine vibration sources

Understanding the construction and working principles of wind turbines is essential for designing and implementing effective condition monitoring (CM) systems and maintenance strategies. Wind turbines can be affected by the different types of vibration generated by such components as blades, generator, gears, bearings and tower see Fig. 1.

Within the wind turbine the drive train will generate significant and sometimes substantial vibration levels. Essentially the drive train consists of the drive, gears, bearings and shafts and the major excitation will take place at the gear mesh frequency, f_{gm}:

$$f_{gm} = Z \cdot N_{gear} \quad (1)$$

where Z is the number of teeth on the gear and N_{gear} is its rotational speed (in Hz).

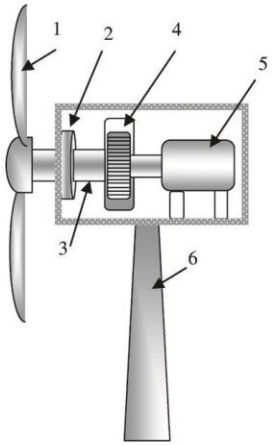

Fig. 1. Schematic of wind turbine: 1. blade, 2. Bearing, 3. Shaft, 4. Gearbox, 5. Generator, 6. Tower.

So-called bearing frequencies, each of which originates from a particular type of bearing vibration, are widely used for CM of bearings [15].

The generator may be a source of excitation for the drive train at higher frequencies due to:

- –the notch passing frequency of the stator in the generator which is normally equal to the number of poles multiplied by the rotational speed of the rotor, and
- –controlling the frequency of a generator indirectly coupled to the grid, with possible higher harmonics in the electric voltage. Vibration due to the rotating blades can be of large magnitude and has been a major cause of failure in wind turbines. Thus there is much research effort directed at determining reliable methods for measuring and assessing this vibration [16]. The wind turbine blade pass frequency, the frequency at which the blades pass a fixed position (BPF) is obviously the number of blades multiplied by the rotational speed:

$$\mathrm{BPF} = n \cdot x/60 \quad (2)$$

where n is the speed of rotation of the turbine blades in r/min, and x is the number of blades.

The vibration signal at any measurement point on a wind turbine will be a mix of many components at different frequencies, different amplitudes and different phases, thus it needs special techniques to analysis the obtained signal. Because the vibration signal will vary with time it should be treated as non-stationary. To better understand the sources and nature of the signals a 3D finite element model was created to predict blade vibration signatures.

2.2. FEM modeling and simulation

A model to simulate the wind turbine, described in Section 3, was created in the ANSYS program, to simulate the real wind turbine used in the Laboratory. The model simulated healthy blades and a blade suffering from cracks. The cracks were of length (10 mm, 20 mm, 30 mm and 40 mm), all had a consistent 3 mm width and 2 mm depth. The tests were carried out for three rota-

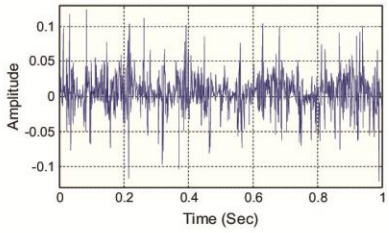

Fig. 2. Simulation vibration signal for healthy conditions.

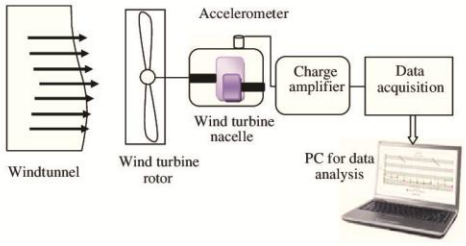

Fig. 3. Schematic diagram of the proposed wind turbine monitoring system.

tion speeds; 150, 250 and 360 r/min. Vibration signals were extracted and the time waveform of the simulation signal for healthy case is shown in Fig. 2. Each signal for both the healthy and faulty conditions was analyzed using EMD; as explained in Section 6.

3. Experimental test

A three bladed wind turbine with 32 cm long airfoil was designed and manufactured in the Manchester Metropolitan University, Advanced Industrial Diagnostics Laboratory. The wind turbine comprises one stage spur gearbox and 12 V DC permanent magnet generator. The experimental work was carried out in the Laboratory and the wind turbine was placed about 1 m in front of the wind tunnel normal to (in line with) the airflow. The accelerometers were B&K type 4371 with sensitivity of 10 mV/g and were mounted on the nacelle of the wind turbine. A B&K type 2635 charge amplifier was used to convert the output of the accelerometer to mV. A National Instruments data acquisition card (NI USB 9233) was connected between a PC and the charge amplifier to collect data, see Fig. 3. Fig. 4 represents the time waveform of the experimental vibration signal for the healthy case. Measured vibration signals for both healthy and faulty conditions were analyzed using EMD, as shown in Section 6.

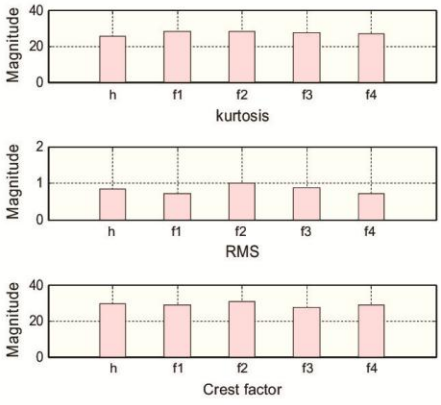

Fig. 5. Selected statistical parameters for healthy and four fault conditions.

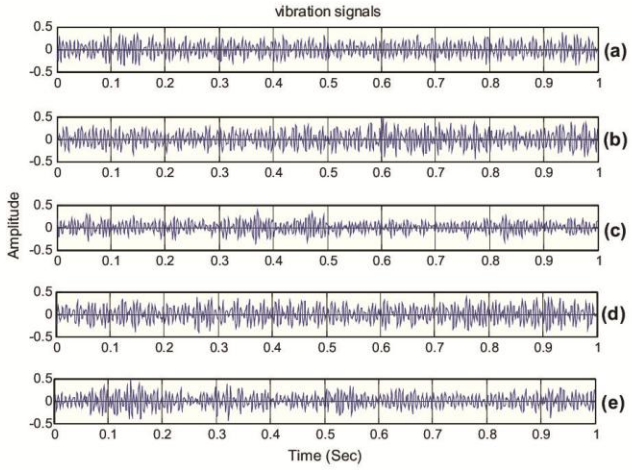

Fig. 4. Experimental vibration signal: (a) healthy case, (b) fault1, (c) fault2, (d) fault3, (e) fault4.

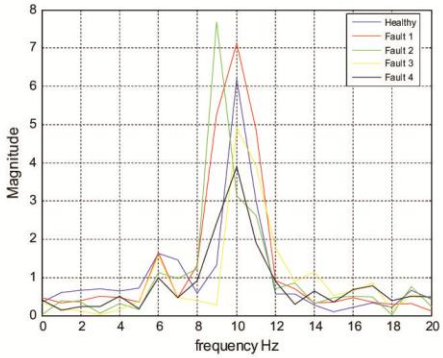

Fig. 6. Frequency spectrum 0–20 Hz for wind turbine vibration signal obtained by FFT, healthy condition and four faulty conditions.

4. Vibration analysis techniques

Vibration analysis is probably the most widely used CM technology for rotating equipment such as gearboxes, bearings and wind turbines. Features extracted from signals which can

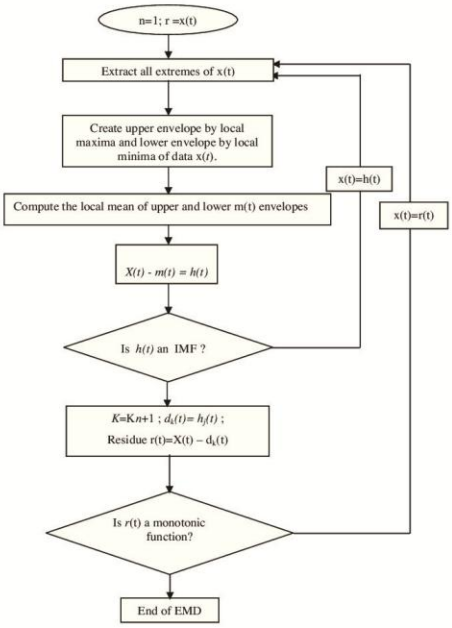

Fig. 7. Flowchart of empirical mode decomposition algorithm [18].

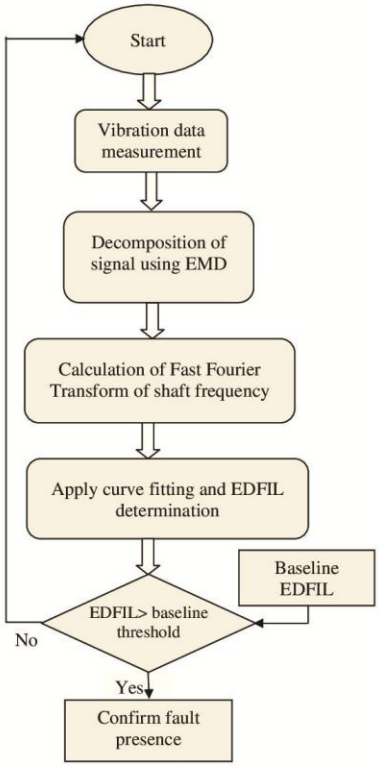

Fig. 8. Flowchart of the proposed EMD and FIL based monitoring technique.

sensitively reflect the characteristics of machinery conditions are very much sought after. Statistical methods including Kurtosis, Root Mean Square and Crest Factor are commonly used to assess the severity of any damage. These parameters were extracted from vibration signals for different conditions and at three different shaft speeds, 150 r/min, 250 r/min and 360 r/min. As can be seen from Fig. 5, which shows three sets of results for comparison, there are fluctuations both within and between healthy and faulty signals so that these measures cannot be used to accurately detect changes in wind turbine blade structure and cannot be used to diagnose wind turbine blade defects. Thus these statistical parameters at least are not suitable for use with non-stationary signals. In order, the faults f1, f2, f3 and f4 were cracks of lengths 10 mm, 20 mm, 30 mm and 40 mm.

The fast Fourier transform (FFT) is a commonly used technique to transform signals from the time to the frequency domain and is often applied to vibration signals where the signal may be considered stationary, but the FFT is not a useful tool for non-stationary signals. Fig. 6 shows the results of the transform over the frequency range from DC to 20 Hz, when the shaft speed was 360 r/min. However, there were no clear trends in the signals probably because the frequency content of the signal changes with time and due to the substantial amount of noise present.

Wind turbines require more advancing monitoring techniques to deal with noise-contaminated and non-stationary signals. In this paper EMD is used to remove noise and decompose data to extract shaft frequency from the original signals.

5. Empirical mode decomposition

The EMD is defined by a process called sifting. It decomposes a given signal $X(t)$ into a finite set of signals called IMFs, to give K modes $d_k(t)$ and a residual term $r(t)$ [17]:

$$X(t) = \sum_{k=1}^{K} d_k(t) + r(t), \quad (3)$$

$$k = 1, 2, \ldots, K$$

The EMD algorithm is summarized by the following steps:

1. Start with the signal $d_1(t)$, $k = 1$. Sifting process $h_j(t) = d_k(t)$, $j = 0$.
2. Identify all local extrema of $h_j(t)$.
3. Compute the upper and the lower envelopes (EnvMax and EnvMin respectively) by cubic spline line interpolation of the maxima and the minima.
4. Calculate the mean of the lower and upper envelopes:

$$m(t) = 1/2[EnvMin(t) + EnvMax(t)] \quad (4)$$

5. Extract the detail $h_{j+1} = h_j(t) - m(t)$
6. If $h_{j+1}(t)$ is an IMF, go to step 7, else, iterate steps 2–5 upon the signal $h_{j+1}(t)$, $j = j + 1$
7. Extract the mode $d_k(t) = h_{j+1}(t)$.
8. Calculate the residual.

$$r_k(t) = X(t) - d_k(t) \quad (5)$$

9. If $r_k(t)$ has less than 2 minima or 2 extrema, the extraction is finished $r(t) = r_k(t)$, else iterate the algorithm from step 1 upon the residual $r_k(t)$, $k = k + 1$. Fig. 7 shows the flowchart of the EMD algorithm.

6. The proposed method

The proposed method starts by measuring the wind turbine nacelle vibration, decomposes the measured signal into its fundamental frequency components and calculates the shaft speed signal intensity level. It then compares it with the threshold amplitude of the baseline data. It uses curve fitting for the FFT spectrum in the region of the shaft frequency and its sideband zones, see Fig. 8.

If the fitted curve for the signal is $p(f)$ the feature intensity level (FIL) of the signal in the frequency band from f_1 to f_2, can be expressed as:

$$FIL = \int_{f_1}^{f_2} p(f)df \quad (6)$$

where f_1 and f_2 are upper and lower frequencies of the frequency band.

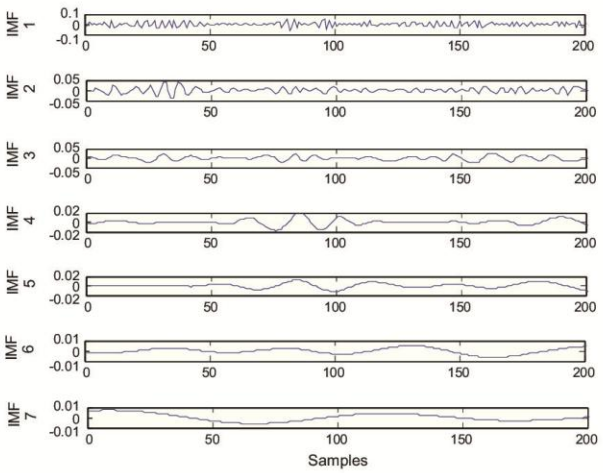

Fig. 9. Decomposition of simulated vibration signals for healthy turbine at 250 r/min.

Digitally using the discrete FFT, the feature intensity level (FIL) of the signal in the frequency band from f_1 to f_2, can be expressed as:

$$FIL = \sum_{f_2}^{f_1} 1/2[p(f_i) + p(f_{(i+1)})]df \quad (7)$$

where $df = f_{(i+1)} - f_i$, $p(f_i)$ = amplitude of signal at f_i and $p(f_{(i+1)})$ = amplitude of signal at $f_{(i+1)}$.

The integration may be done for the whole range of frequencies obtained using the FFT. In this study the area the area contained between adjacent points on the spectral envelope was calculated using the trapezoidal rule via MATLAB.

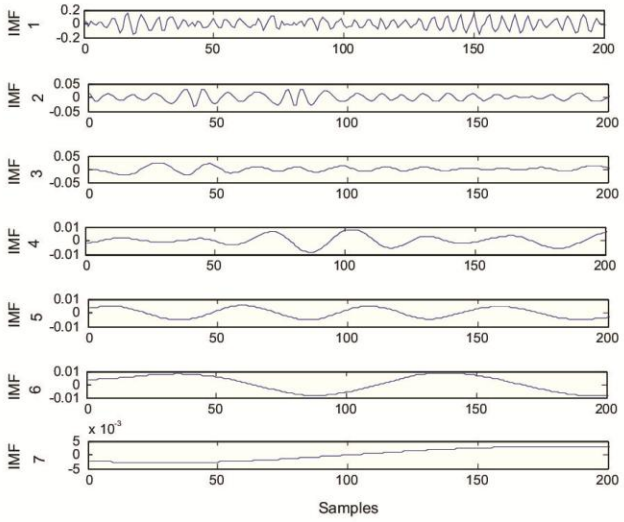

Fig. 10. Decomposition of experimental vibration signals for healthy turbine at 250 r/min.

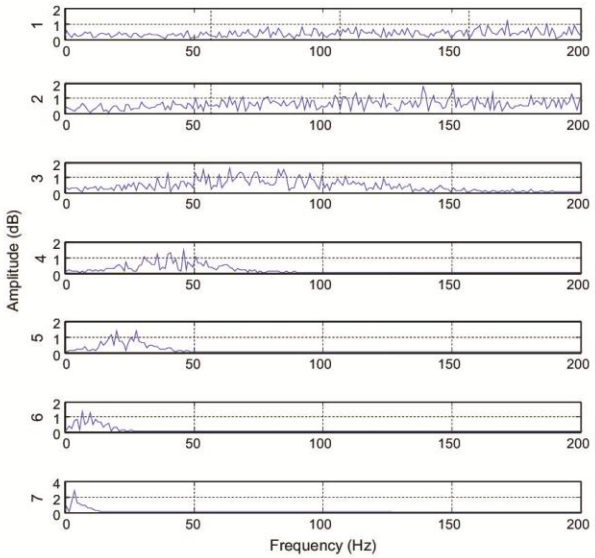

Fig. 11. Fast Fourier spectra from the IMFs obtained from simulation signal.

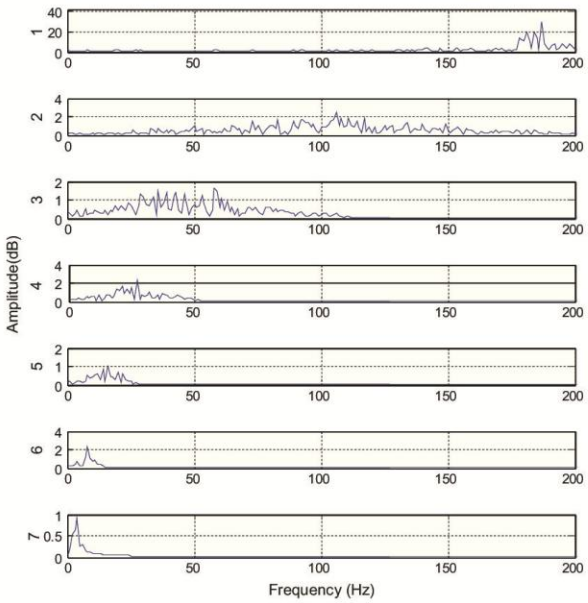

Fig. 12. Fast Fourier spectra from the IMFs experimentally obtained.

7. Result and discussion

The time-domain vibration signals collected from wind turbine were analyzed using statistical methods and the results showed that the faults can be hard to detect as explained in Section 4. The EMD can be used to decompose vibration signals into a finite set of signals and then the intensity level contained within certain frequency bands of interest calculated. These bands were around the rotor frequency and its local sideband zones. The decomposition of the simulation and experimental vibration signals for the healthy case at rotation speed 250 r/min are shown in Figs. 9 and 10, respectively.

Each IMF represents a different vibration source. The FFT was applied to each IMF in turn to produce the spectra shown in Figs. 11 and 12. The spectra corresponding to Mode IMF7 contains a spectral peak in the region to the shaft frequency. The spectra corresponding to the first IMFs are relatively high frequency and originate from such sources as the bearing and gears. The shaft frequency for the simulation work also appears in mode IMF7. Thus for these cases, mode IMF7 was adopted to compute feature intensity level.

Figs. 13 and 14 represent feature intensity level for healthy blades (h – healthy condition) and blades suffering from cracks f1 = 10 mm length, f2 = 20 mm length, f3 = 30 mm length and f4 = 40 mm length at three rotation speeds 150 r/min, 250 r/min and 360 r/min for both simulation and experiment.

For the experimental and simulation results; it is notable that the rate of increase of normalized FIL increases with shaft speed.

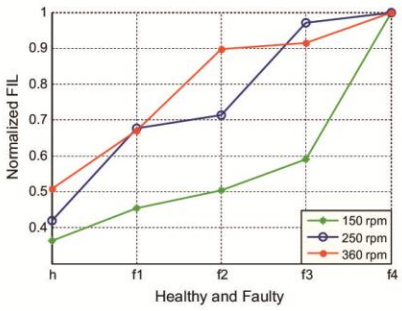

Fig. 13. Normalized feature intensity level contained in simulation signals.

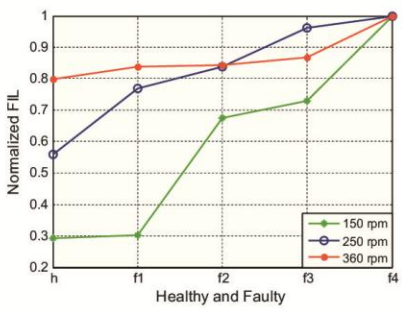

Fig. 14. Normalized feature intensity levels of experimental signals.

This is promising because it suggests that the rate of increase of normalized FIL will be significant for practical applications.

8. Conclusion

In this paper a 3D finite element model of a wind turbine with three blades was created using ANSYS and simulated vibration signals produced for a wind turbine with three healthy blades and with two healthy blades and one blade suffering from one of four different cracks. Experimental vibration signals for healthy and faulty blades were collected and compared with the simulated vibration signals using MATLAB software.

This paper proposes the combination of feature intensity level and EMD as a useful approach to predictive maintenance and CM of wind turbine blades. Feature intensity level and EMD were used to detect the presence and severity of cracks in a wind turbine blade and so help to avoid catastrophic damage. EDFIL and EMD obviously can give an indication of change in the wind turbine running condition. This method appears to provide the possibility of online CM of wind turbines which could be an optimal maintenance strategy for detecting crack initiation. The results showed that the feature intensity level and EMD is suitable and sensitive for diagnosing the given faults.

References

[1] Joselin Herbert GM, Iniyan S, Sreevalsan E, Rajapandian S. A review of wind energy technologies. Renew Sustain Energy Rev 2007;11(16):1117–45.
[2] Ciang CC, Lee J-R, Bang H-J. Structural health monitoring for a wind turbine system: a review of damage detection methods. Meas Sci Technol 2008:19.
[3] Park J-H, Park H-Y, Jeong S-Y, Lee S-II, Shin Y-H, Park J.P., Linear vibration analysis of rotating wind-turbine blade. Curr Appl Phys 2010:10:332–334.
[4] Jüngert A. Damage detection in wind turbine blades using two different acoustic techniques. NDT Data J (NDT) 2008.
[5] Raisutis R, Jasiuniene E, Zukauskas E. Ultrasonic NDT of wind turbine blades using guided waves. Ultrasound Kaunas: Technologija 2008;63(1):7–11.
[6] Borum KK, Mc Gugan M, Brondsted P. Condition monitoring of wind turbine blades. In: Proceedings of the 27th Riso international symposium on materials science. Polymer composite materials for wind power turbines. Denmark; 2006. p. 139–45.
[7] Sajauskas S, Valinevičius A, Miežutavičiūtė L. Non-destructive testing of sheet product inner surfaces using longitudinal surface acoustic waves. Ultrasound 2005:12–6.
[8] Ghoshal A, Sundaresan MJ, Schulz MJ, Frank Pai P. Structural health monitoring techniques for wind turbine blades. J Wind Eng Ind Aerodynam 2000;85:309–24.
[9] Yang W, Jiesheng J, Tavner PJ, Crabtree CJ. Monitoring wind turbine condition by the approach of empirical mode decomposition. In: International conference on electrical machines and systems, ICEMS 2008; 2008. p. 736–40.
[10] Yang WC. Richard Tavner, Peter J. Crabtree, Christopher J. Bivariate empirical mode decomposition and its contribution to wind turbine condition monitoring. Journal of Sound and Vibration 2011;330:3766–82.
[11] Ibrahim GR, Albarbar A. Comparison between Wigner–Ville distribution- and empirical mode decomposition vibration-based techniques for helical gearbox monitoring. J Mech Eng 2011.
[12] Abouhnik A, Ibrahim GR, Shnibha R, Albarbar A. Wind turbine blade fault detection using the empirical mode decomposition method; numerical simulation and experimental testing. In: The third international renewable energy congress, Hammamet, Tunisia; 2011.
[13] Abouhnik A, Ibrahim GR, Shnibha R, Albarbar A. Novel approach to rotating machinery diagnostics based on principal component and residual matrix analysis. ISRN Mechanical Engineering 2012, Article ID 715893, 2012. 7 p. doi: http://dx.doi.org/10.5402/2012/715893.
[14] Abouhnik A, Ibrahim GR, Albarbar A, Mohammed sh-eldin. Wind turbine blades fault detection based on principal component analysis. In: International conference on applications and design in mechanical engineering (icadme 2012) Perlis, Malaysia; 27–28, February 2012.
[15] Peeters. Simulation of dynamic drive train loads in a wind turbine. ISBN 90-5682-728-6, Katholieke Universiteit Leuven: Faculteit Ingenieurswetenschappen Arenbergkasteel-B-3001 Heverlee, Belgium; 2006.
[16] Al-Bedoor BO, Ghouti L, Adewusi SA, Al-Nassar Y, Abdlsamad M. Experiments on the extraction of blade vibration signature from the shaft torsional vibration signals. J Qual Maint Eng 2003;9(2):144–59.
[17] Huang N, Shen Z, Long S, Wu M, Shih H, Zhen Q, et al. The empirical mode descomposition and the Hilbert spectrum for nonlinear and non-stationary time series analysis. Proc Roy Soc London A 1998;454:903–95.
[18] Trnka P, Hofreiter M. The empirical mode decomposition in real-time. In: Fikar M, Kvasnica M, editors. Proceedings of the 18th international conference on process control, Tatranská Lomnica, Slovakia; 2011. p. 284–9.